RUSSIAN ACADEMY OF SCIENCE
FERSMAN MINERALOGICAL MUSEM

volume 44

New Data on Minerals

FOUNDED IN 1907

MOSCOW
2009

ISSN 5-900395-62-6

New Data on Minerals. Volume 44. Moscow: Altum Ltd, 2009. 112 pages, 26 photos, 62 drawings and schemes. Editor: Margarita I. Novgorodova, Doctor in Science, Professor.
Publication of Institution of Russian Academy of Science, Fersman Mineralogical Museum RAS.

This issue contains description of rare pyrope-majorite garnet found in kersantite and spessartite dykes of Chetlas Kamen', Central Timan, Te-bearing fahlores and similar phases from various deposits and phases with composition similar to fahlores, enargite, and luzonite from deposits of Bulgaria; problems concerning recalculation of chemical analyses of these minerals are discussed. Carbonaceous matter and its mineral assemblages in pegmatites of various formations, mineralogical features of multimetal deposits of Russia, Central Asia, and Kazakhstan are reported; role of sorbent minerals for concentration of metals in the supergene zone of these deposits are discussed. Results of experimental study of species of Au, Ag, and Pt-Pd-Sn intermetallic compounds at crystallization of Cu-Fe sulfide melt are given.

Part "Mineralogical Museums and Collections" introduces a collection of mosaic arts from funds of Fersman Mineralogical Museum. In "Mineralogical Notes", a problem of horizontal isomorphic substitutions of chemical elements is discussed. Part "Discussion" contains paper, which continues essay on fundamental and genetic mineralogy published in previous issue and uses the eudialyte group minerals to illustrate a problem of typomorphic features of minerals.

This issue is of interest to mineralogists, geochemists, geologists, researchers of Natural History museums, collectors and amateurs of stone.

Authorized for printing by Institution of Russian Academy of Science, Fersman Mineralogical Museum RAS

Published by
Institution of Russian Academy of Science,
Fersman Mineralogical Museum RAS
Bld. 18/2 Leninskii Prospekt
Moscow 119071 Russia
Phone +7(495) 952-00-67; fax +7(495) 952-48-50
e-mail: mineral@fmm.ru
www.fmm.ru

Altum Ltd
Box 71 Moscow 117556
Phone/fax +7(495) 629-48-12
e-mail: minbooks@online.ru
www.minbook.com

Circulation 300 copies
Printed in Russia

CONTENT

New Minerals and Their Varieties, New Finds of Rare Minerals, Mineral Paragenesis

GARNET OF THE PYROPE–MAJORITE SERIES FROM LAMPROPHYRES OF CENTRAL TIMAN

Natalya I. Bryanchaninova, Alexander B. Makeyev
Institute of Geology of Ore Deposits, Petrography, Mineralogy and Geochemistry (IGEM) RAS, Moscow,
ni@igem.ru, abmakeev@igem.ru

In kersantite and spessartite dikes of Chetlas Kamen' among accessory garnets, that are rather rare in lamprophyres, there was discovered few and for the first time high-majorite pyrope garnet with majorite minal $Mg_3Fe_2[SiO_4]_3$ (26 – 42%), similar to majorite garnet originating from a meteorite. Majorite discovered in Coorara meteorite (Mason *et al.*, 1968; Smith, Mason, 1970) is very rare in the terrestrial rocks. It is shown, that high-majorite pyrope to variable degree is associated with diamond. On the one hand, it occurs as inclusions in diamond crystals, on the other hand, in rocks, where such garnet is found, microcrystalline diamond is established . Pyrope-majorite garnet in lamprophyres testifies to superdeep origin of lamprophyre magma.
2 tables, 2 figures, 14 references.
Keywords: majorite, pyrope, lamprophyre, Timan, inclusions in diamonds, superdeep mineral paragenesises.

Accessory garnets in the Timan lamprophyre attributted to a number of microminerals and occur in autoliths, mantle xenoliths, in olivine and pyroxene phenocrysts, and in the matrix of the rock are very rare and irregular distributed. In chemical composition, garnets from lamprophyre can be divided into three series: grossular-almandine, occasionally containing few pyrope component, andradite-grossular, and pyrope-majorite (Table 1, Fig. 1, 2). Chemical composition of the minerals was determined with a GEOL-733 Superprobe electron microprobe (Vernadsky Institute of Geochemistry and Analytical Chemistry RAS) and JSM-5610LV electron microscope equipped with EDS (Institute of Geology of Ore Deposits, Petrography, Mineralogy and Geochemistry RAS). The results are similar in duplicate measurments. In heavy fractions, content of garnet ranges from a few signes to 0.5%. Yellowish-brown and pinkish pyrope-majorite has rhombo- and pentagon-dodecahedron habit and varies from 0.005 to 0.05 mm in size. Grains of other garnet varieties reach 1.6 mm. Iron-calcium garnets and pyrope-majorite are predominant in lamprophyre of Chetlas Kamen' (Fig. 2).

The garnets from fresh matrix (grossular-almandine, andradite, andradite-grossular) are euhedral, whereas in serpentine-chlorite-calcite and epidote-calcite aggregates, they are significantly corroded and surrounded by kelyphytic rims of variable thickness and composition. These features is favourable for the early deep-seated formation of these garnets. The pyrope with high content majorite component $Mg_3Fe_2[SiO_4]_3$ (26 – 42%), similar to that described only from meteorites and as small inclusions in super-deep diamonds (Kaminsky *et al.*, 2001), was found in several samples from three dikes of the kersantite-spessartite series.

Majorite garnets and their mineral assemblages

Majorite garnets were described as inclusions in diamonds (Table 2) from various diamond-bearing provinces worldwide: Juin fields at Brazil, Snap-Lake, Canada, Yakutia province, Russia, Kankan placers, Guinea (Kaminsky *et al.*, 2001; Pokhilenko *et al.*, 2001; Sobolev *et al.*, 2004; Stachel *et al.*, 2000; Moore *et al.*, 1991), and in alnöite lavas of the Malaita Island, Solomon Islands (Collerson *et al.*, 2000). In aforementioned papers, majorite is considered as garnet, in which according to microprobe data SiO_2 is in excess, i.e., there are non-stoichiometry between cations and Si excess at tetrahedral site. Findings of "majorite" garnet are attached much importance , relating its formation to ultrahigh pressure environment in transitional zone of mantle.

According to modern systematics of garnets, ideal formula of majorite is expressed as $Mg_3Fe_2[SiO_4]_3$ (Back, Mandarino, 2008). Majorite end-member is not found in nature. Recalculated microprobe data of majorite grains found in Australian meteorite, give 66% of of majorite component and the remainder of pyrope.

The majorite was firstly described from the Coorara meteorite in 1970. Its formula $Mg_3(Fe_{1.2},Al_{0.6},Si_{0.2})_2[SiO_4]_3$, calculated on the basis of electrone microprobe data, suggested partial incorporation of Si at octahedral site.

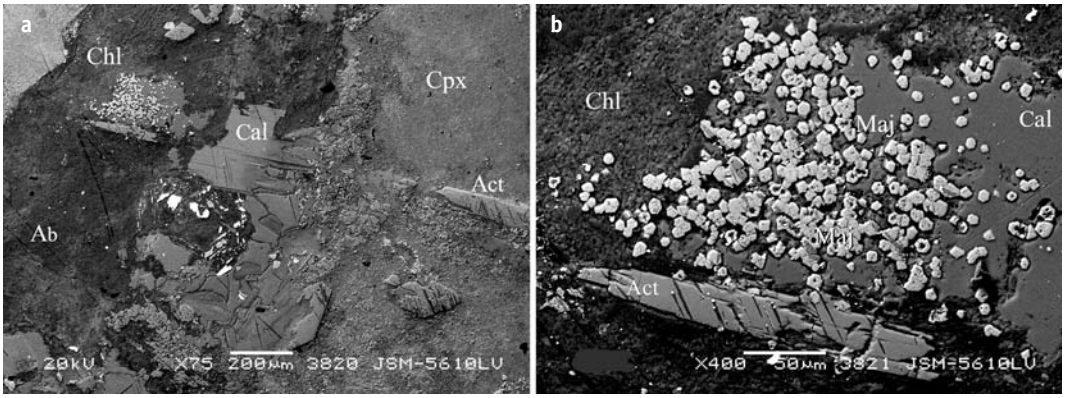

Fig. 1. Scanning-electron microscope image of polished section of lamprophyre-kersantite (spec. 38/180, Kos'yusk Field, Central Timan, Russia. Pyrope-majorite-andradite, andradite, andradite-grossular, and andradite-pyrope-grossular garnets are associated with augite(Cpx), actinolite (Act), chlorite (korundophylite) (Chl), calcite (Cal), albite (Ab). Rhombododecahedral crystals of garnet (Maj) range from 5 to 15 microns. Magnification (a) 75^x,(b) 400^x.

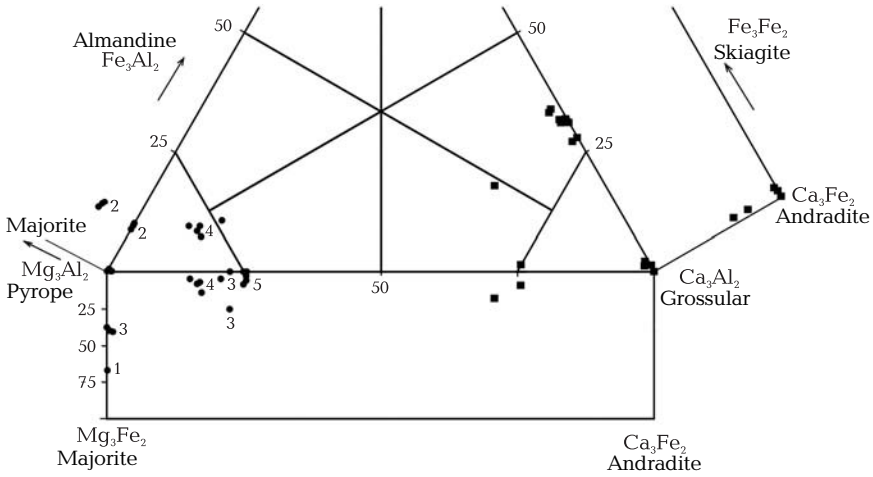

Fig. 2. Composition of garnets plotted on the evolvent of minals majorite-andradite-skiagite-pyrope-grossular-almandine trigonal prism: 1 — majorite from the Coorara meteorite (the first composition, approved by CNMNC IMA), 2 — garnets from diamond inclusions in diamonds from kimberlite pipes the Juin Field (Brazil), 3 — from lamprophyres of the Middle Timan (Russia), 4 — from inclusions in diamonds from kimberlite pipes of the region Snap-Lake (Canada), 5 — from xenoliths in alnöite lavas of the Malaita Island (Solomon Islands). Solid squares denote iron-calcium garnets from lamprophyres studied here (Table 1) and associated with the pyrope-majorite.*
** — skiagite — hypothetical garnet minal $Fe_3Fe_2(SiO_4)_3$.*

No special X-ray structural study was carried out to support incorporation of Si at octahedral sites of trivalent cations in garnets. Non-stoichiometry and excess of silica in composition of real garnets of minute inclusions (which size rarely exceeds 1—20 microns), most likely could be caused by technical problems of electron microprobe measurments or inhomogeneous sample resulted from microingrowths of pyroxene in garnet. Currently, the latter is received fact. In natural pyrope from garnet-bearing xenoliths of diamond-bearing kimberlites, Haggerty and Sautter (1990) and Sautter *et al.* (1991) described omphacite, diopside-jadeite solid solution, , and showed, that with the clinopyroxene content in garnet of 20 and 30%, SiO_2 was 44—45.5 wt.% and crystallochemical coefficients of Si^{4+} calculated on the basis of 12 O, were 3.14—3.24 (Haggerty, Sautter, 1990; Sautter *et al.*, 1991).

For comparison of majorite garnets from variuos regions, we calculated available chemical data of the pyrope-majorite garnets by the same way, implying that majorite is the phase $Mg_3Fe_2[SiO_4]_3$, as it was approved by the International Mineralogical Association for the garnet group minerals (Back, Mandarino, 2008).

Table 1. **Chemical composition (wt.%) and components (%) of garnets from the lamprophyre of the Central Timan, associated with majorite-bearing pyropes**

№№	38/180		Chp-025		116/33				116/43.5		116/47		Chp-036c		Chp-036d	
	1	2	1	2	1	2	3	4	1	2	1	2	1	2	1	2
SiO_2	35.39	36.80	36.92	38.78	38.98	38.81	38.78	38.98	38.81	38.71	38.91	39.32	38.64	38.83	38.75	38.84
TiO_2	1.94	1.10	0.05	0.00	0.00	0.00	0.00	0.00	0.00	0.00	0.00	0.00	0.05	0.00	0.00	0.00
Al_2O_3	5.97	7.35	8.03	21.97	22.05	21.97	21.97	22.05	21.97	21.94	22.05	18.57	21.87	22.00	21.95	22.00
Cr_2O_3	0.00	0.00	0.06	0.00	0.00	0.00	0.00	0.00	0.00	0.00	0.00	0.48	0.19	0.00	0.00	0.00
Fe_2O_3	23.01	21.76	20.12	0.00	0.00	0.00	0.00	0.00	0.00	0.00	0.00	5.30	0.00	0.00	0.00	0.00
FeO	0.84	1.20	1.34	14.00	13.47	14.67	14.00	13.47	14.67	15.29	11.92	7.85	13.77	13.71	14.25	13.40
CaO	31.74	26.01	33.25	25.25	24.62	23.96	25.25	24.62	23.96	23.60	27.12	23.29	25.19	24.89	24.89	25.57
MnO	0.46	0.00	0.24	0.00	0.00	0.07	0.00	0.00	0.07	0.00	0.00	0.00	0.28	0.17	0.08	0.05
MgO	0.64	5.79	0.00	0.00	0.88	0.52	0.00	0.88	0.52	0.46	0.00	5.19	0.00	0.39	0.08	0.15
Sum	100.00	100.00	100.00	100.00	100.00	100.00	100.00	100.00	100.00	100.00	100.00	100.00	99.99	99.99	100.00	100.01
Si^{4+}	2.904	2.939	2.998	3.001	3.002	3.001	3.001	3.002	3.001	2.999	2.998	3.001	2.993	3.000	3.000	3.000
Ti^{4+}	0.119	0.066	0.003	0.000	0.000	0.000	0.000	0.000	0.000	0.000	0.000	0.000	0.003	0.000	0.000	0.000
Al^{3+}	0.577	0.691	0.768	2.001	1.999	2.000	2.001	1.999	2.000	2.001	1.999	1.668	1.994	2.000	2.000	2.000
Cr^{3+}	0.000	0.000	0.004	0.000	0.000	0.000	0.000	0.000	0.000	0.000	0.000	0.029	0.012	0.000	0.000	0.000
Fe^{3+}	1.419	1.306	1.227	0.000	0.000	0.000	0.000	0.000	0.000	0.000	0.000	0.304	0.000	0.000	0.000	0.000
Fe^{2+}	0.058	0.080	0.091	0.905	0.866	0.947	0.905	0.866	0.947	0.989	0.767	0.500	0.891	0.884	0.921	0.864
Ca^{2+}	2.791	2.225	2.893	2.093	2.031	1.985	2.093	2.031	1.985	1.959	2.239	1.905	2.091	2.060	2.065	2.116
Mn^{2+}	0.032	0.000	0.016	0.000	0.000	0.005	0.000	0.000	0.005	0.000	0.000	0.000	0.018	0.011	0.005	0.003
Mg^{2+}	0.078	0.688	0.000	0.000	0.101	0.060	0.000	0.101	0.060	0.053	0.000	0.590	0.000	0.045	0.009	0.017
Pyr	2.6	**22.9**	0	0	3.4	2.0	0	3.4	2.0	1.7	0	17.9	0.6	1.5	0.3	0.6
Alm	1.9	2.7	3.0	**30.1**	**28.9**	**31.6**	**30.1**	**28.9**	**31.6**	**33.0**	**25.5**	**16.7**	**29.7**	**29.4**	**30.7**	**28.8**
Gros	**23.5**	9.1	**34.9**	**69.9**	**67.7**	**66.2**	**69.9**	**67.7**	**66.2**	**65.3**	**74.5**	**48.8**	**69.7**	**68.7**	**68.8**	**70.5**
Andr	**71.0**	**65.3**	**61.4**	0	0	0	0	0	15.2	0	0	0	0	0	0	0

Note: original analyses were normalized to 100%. Content of bivalent and trivalent iron in microprobe analyses is divided on the basis of stoichiometry

Calculation of end-member composition. Formula coefficients (f.c.) are calculated according to standard procedure. Electron microprobe data providing only total iron are corrected: total Fe is redistributed between FeO и Fe_2O_3 taking into account coefficient 1.11 conversing FeO to Fe_2O_3. In this case, stoichiometry between sums of bivalent and trivalent cations is 3.000:2.000. Firstly, spessartine end-member $Mn_3Al_2[SiO_4]_3$ is calculated: 100 (f.c. Mn^{2+})/3 = Spessartine (%). Secondly, almandine end-member $Fe_3Al_2[SiO_4]_3$ is calculated: 100 (f.c. Fe^{2+})/3 = Almandine (%). In the third place, andradite component $Ca_3Fe_2[SiO_4]_3$ linking Fe^{3+} with Ca is calculated: 100 (f.c. Fe^{3+})/2 and 100 (f.c. Ca^{2+})/3; an amount of Andradite is deteremined by the lesser value. In the fourth place, with presence of Cr and Ca excess, uvarovite component $Ca_3Cr_2[SiO_4]_3$ is calculated. The fifth calculated end-member is knorringite $Mg_3Cr_2[SiO_4]_3$: 100 (f.c. Cr^{3+})/2 − "Uvarovite" = Knorringite (%). This component may be absent at high Ca. In this case, Cr is included into uvarovite end-member. Grossular $Ca_3Al_2[SiO_4]_3$ is the sixth calculated component: 100 (f.c. Ca^{2+})/3 − "Andradite" − "Uvarovite" = Grossular (%). The seventh end-member is majorite $Mg_3Fe_2[SiO_4]_3$: 100 (f.c. Fe^{3+})/2 − "Andradite" = Majorite (%). Finally, pyrope $Mg_3Al_2[SiO_4]_3$ is calculated : 100 (f.c. Al^{3+})/2 − "Almandine" − "Grossular» − «Spessartine"= Pyrope (%). Only such succession of calculation allow estimation majorite content. Majorite end-member estimated from virtual excess of SiO_2 in garnets is invalid.

According to calculation results given in Table 2 and plotted on evolvent of trigonal prism (Fig. 2), not all of described garnets with majorite component really contain it in fair quantity. Pyropes with 26−42% of majorite component from the Central Timan lamprophyre and pyrope inclusions with 24−26% of majorite in diamonds from the Juin Field, Brazil

are the closest to majorite from the the Coorara meteorite. These garnets and majorite from the Coorara meteorite are Cr- and Ca-free. Majorite component in all other garnets is lesser and ranges from from 2 to 15%, but they are Cr- and Ca-bearing. All described garnets are distinguished by high content of magnesium components (pyrope, knorringite and majorite), i.e., Mg# varies from 75 to 100%. It is apparent that this value is an indicator of high-pressure conditions of formation of mineral assemblage. It should be noted, that in diamond-bearing rocks, majorite component is found in garnets of ultramafic assemblage and does not documented in garnets of the eclogite one.

Majorite garnets reported from spinel and garnet-spinel xenoliths and megacrysts from alnöites of the Malaita Island, Solomon Islands are attributed to the high-pressure mineral assembalge of, where Ca and Mg perovskite, Al silicate phases, and dimond microcrystal are also involved (Collerson *et al.*, 2000). Neal *et al.* (2001) considered this information as untimely and criticized formula coefficients of Si more than 3 calculated on the basis of 12 O. These researchers correctly suggest that most mentioned analyses characterize admixtures of pyroxenes and amphiboles rather than garnets , and they should not assigned to garnets without X-ray diffraction study. We also consider that among analyses of majorite garnets, given by Collerson *et al.* (2000), not all of them correspond to garnet, and among garnets not all correspond to majorite garnet. However, in

Table 2. **Chemical composition (wt.%) and components (%) of majorite-bearing garnets**

Components	Coorara	Brazil			Lamprophyre of the Central Timan				Snap-Lake, Canada					Alnöites Malaita Island		
		108a	108b	108c	102/25	116/33	116/47	38/180	SL_5-5	SL_3-12	SL_3-30	SL_3-31	SL-133	161	159	CRN136
SiO_2	43.90	42.46	41.46	40.98	42.28	41.68	41.80	40.74	42.00	41.30	42.30	42.20	41.20	41.03	40.56	40.97
TiO_2	0.00	1.83	1.95	2.36	0.00	0.00	0.00	0.00	0.06	0.13	0.06	0.19	0.05	3.20	4.09	3.10
Al_2O_3	6.98	17.22	18.82	18.03	14.71	13.90	13.39	11.55	17.20	15.20	9.46	12.30	16.70	16.00	15.60	14.99
Cr_2O_3	0.00	0.10	0.12	0.07	0.00	0.00	0.00	0.00	8.37	10.20	12.80	11.80	7.71	0.01	0.05	0.00
Fe_2O_3	21.88	10.00	10.00	9.00	14.70	15.60	16.25	17.93	1.65	2.20	4.95	3.30	2.20	10.73	11.96	11.47
FeO	0.00	3.59	4.37	5.20	0.00	0.00	0.44	0.00	4.56	4.50	3.14	3.52	5.38	0.00	0.00	0.00
CaO	0.00	0.00	0.00	0.00	0.00	0.28	0.67	8.61	3.73	4.76	5.11	4.68	5.70	9.75	9.45	9.81
MnO	0.00	0.23	0.30	0.25	0.00	0.37	0.34	0.00	0.28	0.32	0.33	0.32	0.33	0.16	0.16	0.16
MgO	27.61	24.48	24.16	24.00	28.31	28.18	27.10	21.17	22.20	21.10	21.20	21.10	20.00	14.54	14.27	14.90
Sum	100.37	99.81	101.18	99.89	100.00	100.00	100.00	100.00	100.05	99.71	99.35	99.41	99.27	95.42	96.14	95.41
Si^{4+}	3.176	3.013	2.920	2.930	2.998	2.976	2.998	3.003	3.012	3.008	3.132	3.092	3.010	3.013	2.972	3.022
Ti^{4+}	0.000	0.098	0.103	0.127	0.000	0.000	0.000	0.000	0.003	0.007	0.003	0.010	0.003	0.176	0.225	0.172
Al^{3+}	0.594	1.438	1.560	1.517	1.228	1.168	1.130	1.002	1.452	1.303	0.824	1.061	1.436	1.383	1.345	1.301
Cr^{3+}	0.000	0.006	0.007	0.004	0.000	0.000	0.000	0.000	0.474	0.586	0.748	0.683	0.445	0.001	0.003	0.000
Fe^{3+}	1.189	0.533	0.529	0.483	0.783	0.837	0.876	0.993	0.089	0.120	0.275	0.182	0.121	0.592	0.659	0.636
Fe^{2+}	0.000	0.213	0.257	0.310	0.000	0.000	0.027	0.000	0.273	0.274	0.194	0.215	0.328	0.000	0.000	0.000
Ca^{2+}	0.000	0.000	0.000	0.000	0.000	0.021	0.051	0.68	0.287	0.371	0.405	0.367	0.446	0.767	0.742	0.775
Mn^{2+}	0.000	0.014	0.018	0.015	0.000	0.023	0.021	0.000	0.017	0.020	0.021	0.020	0.020	0.010	0.010	0.010
Mg^{2+}	2.974	2.586	2.534	2.555	2.988	2.996	2.894	2.322	2.370	2.288	2.337	2.302	2.176	1.589	1.557	1.636
Pir	33.3	65.0	65.0	65.0	60.9	57.5	54.6	50.0	62.7	54.4	40.2	45.5	59.5	69.0	67.0	65.0
Knor	0.0	0.0	0.0	0.0	0.0	0.0	0.0	0.0	12.7	17.2	23.8	21.7	7.5	0.0	0.0	0.0
Maj	**66.6**	**27.0**	**26.0**	**24.0**	**39.1**	**41.1**	**42.1**	**26.4**	**4.5**	**6.0**	**14.0**	**9.1**	**6.0**	**4.0**	**8.5**	**6.0**
Uvr	0.0	0.0	0.0	0.0	0.0	0.0	0.0	0.0	9.6	12.3	13.7	12.2	15.0	0.0	0.0	0.0
Alm	0.0	7.0	9.0	10.0	0.0	0.0	0.9	0.0	9.0	9.0	6.3	7.3	11.0	0.0	0.0	0.0
Spes	0.0	0.3	0.7	0.7	0.0	0.7	0.7	0.0	0.7	0.7	0.7	0.7	0.7	0.3	0.3	0.3
Andr	0.0	0.0	0.0	0.0	0.0	0.7	1.7	22.6	0.0	0.0	0.0	0.0	0.0	26.0	25.0	26.0

Note: garnets from lamprophyre of the Central Timan are our data, the remaider taken from the following publications: Coorara meteorite (Smith & Mason, 1970); inclusions in diamonds, Juin region, Brazil (Kaminsky et al., 2001); inclusions in diamonds, Snap-Lake, Canada (Pokhilenko et al., 2001); alnöite, Malaita Island, Solomon Islands, Pacific Ocean (Collerson et al., 2000)

separate pyrope-andradite grains of there is a small amount of majorite component (according to our calculations 4−8.5%).

Formation conditions of mineral assemblage *Ca,Mg−perovskite + "majorite" + diamond* were estimated by Collerson *et al.* (2000) through empiric barometer using formula coefficient of Si in garnet formula, which is resulted in very high pressure of 22 GPa and consequently , depth of crystallization of this mineral assemblage of 400−670 km. These calculated data are consitent with experiments for Al-free iron-magnesium garnets. According to Kato (1986), majorite is stable at 2000±200°C and 20 GPa .

Discussion

Non-stoichiometry and excess of SiO_2 in composition of tiny garnet inclusions (size infrequently exceeds 20 microns) in diamond crystals could be caused by: (1) error of microprobe analysis and (2) microinclusions of pyroxenes in garnets. The errors of microprobe analysis might arise due to micrograins of garnets being studied in pyroxene matrix displaying higher Si content in comparison with garnet.

Microinclusions of pyroxenes in garnets are more interesting case. Pyroxene clusters in garnet might be so small that they cannot be detected by conventional techniques and therefore, SiO_2 content can exceed real concentration in garnet. Oriented inclusions of pyroxenes in garnets, which in turn are enclosed in diamond crystals from Brazil and South Africa, are described by many researchers (Moore *et al.*, 1991; Haggerty, Sautter, 1990; Sautter *et al.*, 1991). Experimental study (Ringwood, 1967) suggest that oriented pyroxene inclusions found in natural garnets are resulted from exsolution of hypothetical mantle Fe-Mg-silicate. However, it does not follow that homogeneous phase enriched in pyroxene component should be mineral with the cubic garnet structure. Findings of tetragonal almandine-pyrope phase (TAPP) included in diamonds from the San-Luis placers, Juin district, Brazil (Stachel *et al.*, 2005) support this conclusion. It should be noted that according to cited papers, both tetragonal phases and garnets, containing oriented ingrowths of pyroxenes, are close to almandine-pyrope in composition.

In addition, all the quoted compositions of so called "majorite" with Si excess are characterized by significant Ca, which is not characteristic of original majorite. That is, these unique pyroxene-garnet assemblages are not related to garnet $Mg_3Fe_2[SiO_4]_3$, for which the International Mineralogical Association approved the name "majorite". Therefore, garnet with Si excess should not be attributted to majorite based only on this feature, in order to avoid dual interpretation of the term majorite.

Conclusions

Majorite was found in nature only in the Coorara meteorite. Similar pyrope with high content of the majorite component $Mg_3Fe_2[SiO_4]_3$ (24−27%) was described as tiny inclusions in superdeep diamonds of Brazil (Kaminsky *et al.*, 2001). We identified further higher content of majorite component in pyropes (up to 42%) in several samples of lamprophyres from the kersantite and spessartite dikes in the Central Timan. These are the highest content of the majorite component in the terrestrial garnet.

Inclusions of pyrope-majorite in diamonds associated with ferripericlase, perovskite and manganese ilmenite indicate ultrahigh pressure of formation of the garnet. Mantle xenoliths with the pyrope-majorite garnet in volcanic rocks can be served as indicator of deep origin of such rocks. Thus, pyrope with high content of majorite component discovered in the Central Timan lamprophyre for the first time is testimony to superdeep origin of lamprophyre magma, which could be genetically related to primary sources of the Timan diamonds.

Findings of so called tetragonal almandine-pyrope phase suggest that mineralogists are standing at the threshold of discovery of a new mineral species (with lower symmetry than that of garnet or higher, with respect to pyroxene). This mineral in the transformation series pyroxene to garnet would take place similar to wadsleite in the transformation series olivine through wadsleite to ringwoodite.

References

Back M.E., Mandarino J.A. Fleischer's Glossary of Mineral Species 2008. The Mineralogical Record Inc. Tucson. **2008**. 344 p.

Collerson K.D., Hapugoda S., Kamber B.S., Williams Q. Rocks from the Mantle Transition Zone: majorite-bearing xenoliths from Malaita, Southwest Pacific // Science. **2000**. V. 288. P. 1215−1223.

Haggerty S.E., Sautter V. Upperdeep (Greater 300 kilometers), ultramafic upper mantle

xenoliths // Science. **1990**. V. 248. P. 993–996.

Kaminsky F.V., Zakharchenko O.D., Davies R. et al. Superdeep diamonds from the Juina area, Mato Grosso State, Brazil // Contrib. Mineral. Petrol. **2001**. V. 140. P. 734–753.

Kato T. Stability relation of (Mg,Fe)SiO_3 garnets, major constituents in the Earth's interior // Earth Planet. Sci. Lett. **1986**. V. 77. P. 399–408.

Mason B., Nelen J., White J.S.Jr. Olivine-garnet transformation in a Meteorite // Science. **1968**. V. 160. P. 66–67.

Moore R.O., Gurney J.J., Griffin W.L., Shimisu N. Ultra-high pressure garnet inclusions in Monastery diamonds: trace element abundance patterns and conditions of origin // Eur. J. Mineral. **1991**. N 3. P. 213–230.

Neal C.R., Haggerty S.E., Sautter V. "Majorite" and "Silicate Perovskite" mineral composition in xenoliths from Malaita // Science. **2001**. V. 292. P. 1015.

Pokhilenko N.P., Sobolev N.V., Mak-Donal'd J.A. et al. Crystalline inclusions in diamonds from kimberlites from the Snap-Lake region (craton Slave, Canada): new evidences of anomalous structure of the lithosphere // DAN. **2001**. V. 380. № 3. P. 374–379.

Ringwood A.E. The pyroxene-garnet transformation in the Earth's mantle // Earth Planet. Sci. Lett. **1967**. V. 2. P. 255–263.

Sautter V., Haggerty S.E., Field S. Upperdeep (> 300 kilometers) ultramafic xenoliths: petrological evidence from the Transition Zone // Science. **1991**. V. 252. P. 827–830.

Smith J.V., Mason B. Pyroxene-garnet transformation in Coorara meteorite // Science. **1970**. V. 168. P. 832–833.

Sobolev V.N., Logvinova A.M., Zadgemizov D.A. et al. Mineral inclusions in microdiamonds and macrodiamonds from kimberlites of Yakutia: a comparative study // Lithos. **2004**. V. 77. N 1/4. P. 225–242.

Stachel T., Brey G.P., Harris J.W. Kankan diamonds (Guinea) I: from the lithosphere down to the transition zone // Contrib. Mineral. Petrol. **2000**. V. 140. N 1. P. 1–15.

Stachel T., Brey G.P., Harris J.W. Inclusions in sublithospheric diamonds: glimpses of deep Earth // Elements. **2005**. V. 1. N 2. P. 73–78.

CARBONACEOUS MATTERS IN PEGMATITES OF DIFFERENT GENETIC TYPES AND THEIR ROLE IN FORMATION OF MINERAL ASSOCIATIONS

Nikita V. Chukanov
Institute of Problems of Chemical Physics, Chernogolovka, chukanov@icp.ac.ru
Vera N. Ermolaeva
Vernadsky Institute of Geochemistry and Analytical Chemistry, Moscow, cvera@mail.ru
Igor V. Pekov
Lomonosov Moscow State University, Moscow, mineral@geol.msu.ru
Seppo Lahti
Geological Survey of Finland, Espoo, Finland, seppol@mbnet.fi

Comparative investigation of carbonaceous matters from pegmatites of different formations has been performed. These formations are as follows: high alkaline (Khibina and Lovozero massifs, Kola Peninsula), rare metal granitic (Viitaniemi, Finland), granitic of mica type (Northern Karelia), and alkaline granite amazonitic (Western Keyvy, Kola Peninsula). The existence of steady genetic relation between reduced forms of carbon and several characteristic incoherent rare "bitumenphilic" elements (U, Th, *REE*, Zr, Hf, Nb, Ta, W, Sn) and titanium has been shown as well. Possible mechanisms of the formation and the transformation of carbonaceous matters in pegmatites of different genetic types, their structure and role in processes of mineral genesis are discussed.
2 tables, 11 figures and 46 references.
Keywords: pegmatites, rare elements, bitumen, thucholite, carburan, carbocer.

Introduction

Reduced forms of carbon (graphite, amorphous carbon, bitumen matters) are regular accessory components of many late- and post-magmatic paragenesises connected with formations of different types.

In publications there are specific terms "thucholite" and "carburan" for aggregates of carbonaceous matters from granitic pegmatites enriched in radioactive elements. The term "thucholite" (given according to the chemical composition — ThUCHO-lite) was firstly used (Ellsworth, 1928a) for uranium- and thorium-bearing carbonaceous matter from granite-pegmatitic vein intersecting Precambrian gneisses near the village Konger (Ontario, Canada). Thucholite forms there pseudomorphs after uraninite and original aggregates. Afterwards analogous matter was found in several other pegmatites of Canada: on the territory of the Ontario province (Spence, 1930; Jonasson *et al.*, 1977; Stevenson *et al.*, 1990) and Quebec province (Ellsworth, 1928b; Spence, 1940). Occurrence of thucholite in association with zircon (cyrtolite), titanite, allanite, uraninite, rarely with samarskite is typical for these objects. In the granites of Western Sudets (Poland), aggregates of thucholite occur in the areas with thorite and gummite mineralization (Milulski, 2007). Phase heterogeneity of uranium-bearing bituminous matters from different formations of Great Britain, Scandinavia and Southern Africa was investigated in details (Eakin, Gize, 1992). Nowadays the name "thucholite" (in wide sense) is often used for all mineralized carbonaceous matters from granitic pegmatites. Uranium-bearing carbonaceous matter from granite—pegmatitic veins of the Northern Karelia was firstly characterized by A.E. Fersman (1931) and afterwards described under the name "carburan" (Labuntsov, 1939; Zhirov, Bandurkin, 1968). It is a light, brittle and hygroscopic black colored matter containing up to 90 wt.% of carbon and able to fire on air. Its ash residue contains mainly oxides of U and Pb as well as Fe, Th, Y, Nb, Zr, Sr and trace amounts of other elements (Ti, Sn, Be, Ba a.o.). Two varieties of carburan are distinguished: rounded aggregates among rock-forming minerals and pseudomorphs after crystals of uraninite. Carburan occurred in the paragenesis with unchanged uraninite as well as with titanite, allanite, cyrtolite, xenotime, and monazite. S.M. Popov (1957) considers carburan as a product of later pneumatolytic activity. In granitic pegmatites of Norway, carbonaceous matter is formed at the same stage with uraninite, monazite, allanite, thorite, yttrofluorite, and xenotime. In the pegmatitic vein Ytterby (Sweden), carburan type matter occurs in the association with fergusonite, yttrotantalite, gadolinite, cyrtolite, and xenotime (Fersman, 1931). In the Northern Karelia and in the Kola

Peninsula carburan is characteristic to plagioclase—quartz—muscovite pegmatitic veins. The consequence of accessories formation in these pegmatites is as follows: allanite → monazite → xenotime + cyrtolite + uraninite → pyrrotine + carburan → pyrite → chalcopyrite (Zhirov, Bandurkin, 1968).

Organic matters are characterized by a wide distribution in high-alkaline magmatic rocks and their pegmatites (Chukanov *et al.*, 2005, 2006; Nivin *et al.*, 2005). Characteristic feature of bituminous matters from agpaitic pegmatites is their ability to concentrate some rare elements, e.g. Th and *REE*.

Despite a large amount of publications concerning carbonaceous matters, there are several problems connected with their genesis still remaining unsolved. They include the following questions:

— source of carbon (magma or contamination by the matter of enclosing rocks);

— mechanisms of carbon reduction;

— mechanisms of concentration of rare elements;

— role of organic matter in the processes of mineral formation;

— is the affinity of several rare elements to the organic matters a universal characteristics of these ("bitumenphilic", "coalphilic") elements, or it is firstly connected with the geological formation type.

In the present work new data have been obtained on the relationships between organic matters and the processes of mineral formation in pegmatites of different types.

Objects of investigation

Typical specimens from the following pegmatites of different types containing carbonaceous matters were chosen for comparative investigation.

Rare metal granitic pegmatites are represented by specimens of sugar-like and lamellar albite from Viitaniemi, Finland containing spherical inclusions of thucholite (up to 1 cm in diameter), crystals of zircon, tantalite, pyrochlore (Figs 1, 2), fluorite, black tourmaline, amblygonite—montebrasite, lepidolite.

In **alkaline granitic amazonitic pegmatite** of the mountain Plaskaya (Western Keyvy, Kola Peninsula) organic matter is present in the form of microscopic inclusions in crystalline egg-yellow thorite. Thorite occurs as segregations up to 1 cm among sugar-like albite. This thorite is attributed to the late pegmatite minerals (Voloshin, Pakhomovsky, 1986).

Granitic pegmatites of mica type are represented by the specimen from muscovite deposit Lopatova Guba, Chupinsky region, Northern Karelia, Russia. Carbonaceous matter occurs as black fine-grained pseudomorphs after cubic crystals of uraninite (up to 3 mm in size) grown in massive quartz in the core of a big vein pegmatite body. Associated minerals are potassium feldspar, oligoclase, muscovite, biotite, schorl, almandine, fluorapatite, monazite-(Ce), xenotime-(Y), and zircon.

Associations with bitumenosic matters from agpaitic and ultraagpaitic pegmatites of Lovozero and Khibina massifs (Kola Peninsula) have been also investigated.

In the pegmatitic body "Nastrofitovoye" (mountain Alluayv, Lovozero) black tear-shaped segregations with resinous luster (up to 3 mm in size) of bituminous matter associate with natrolite, raite, vinogradovite, and catapleiite.

In the pegmatite "Palitra" (mountain Kedykverpakhk, Lovozero) organic matter occurs as films and segregations of irregular form (up to 1 mm in size) of dark-brown up to black color with dull luster as well as its micro-

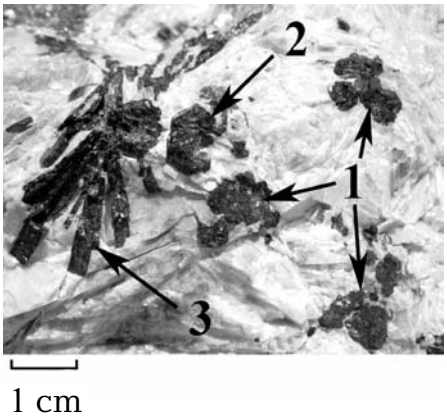

Fig. 1. Association of thucholite (1) with zircon (2) and tantalite (3) in albitite. Viitaniemi, Finland.

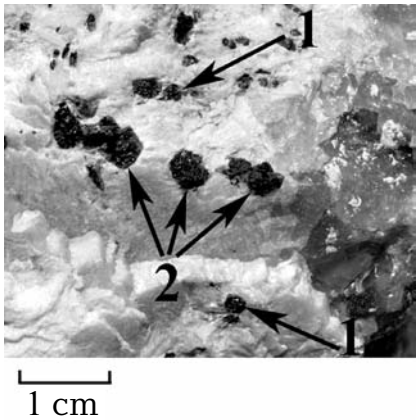

Fig. 2. Association of thucholite (1) with microlite (2) in albitite. Viitaniemi, Finland.

scopic inclusions in grains of X-ray amorphous Na,Th-silikate. The following minerals are tightly associated with organic matter: natrosilite and villiaumite as well as earlier ussingite, kapustinite, kazakovite, lomonosovite, vuonnemite, phosinaite-(Ce), steenstrupine-(Ce) and several high alkaline minerals.

In pegmatite "Koashva-2007/2" (mountain Koashva, Khibiny) big (up to 4 cm in size) spherical segregations of bituminous matter of coaly-black color with submetallic luster at the fracture occur in the hydrothermally altered core where they are intergrown in cavernous aegirine—natrolite aggregates. Associated minerals are astrophyllite, lorenzenite, titanite, burbankite, sphalerite, chlorbartonite and other.

Additionally, bituminous matter ("carbocer") with ingrowths of thorite forming structures of decay in the organic matrix (Chukanov *et al*., 2006) has been used as a reference specimen. This specimen was collected by A.N. Labuntsov in 1930th in rinkite—natrolite vein on mountain Kukisvumchorr, Khibiny (see Labuntsov, 1937) and nowadays is kept in the Fersman Mineralogical Museum of the Russian Academy of Sciences (FMM № 41426).

Methods and results of investigations

Electron-microprobe analysis including obtaining of images of the investigated object in secondary and back-scattered electrons has been performed using the digital scanning electron microscope CamScan MV2300 equipped with YAG-detector of secondary and back-scattered electrons and energy-dispersive X-ray microanalyzer with semi-conductor (Si-Li) detector Link INCA Energy. Time of signal accumulation in every point amounted 500 ms. Investigations were performed under accelerating voltage of 20 kV, current of absorbed electrons at the standard Co specimen of 516 pA, diameter of electron beam at the surface of specimen of 0.157 μm.

All investigated specimens are fine intergrowths of different carbonaceous and mineral microphases. Such structures are characteristic to the products of decay of intermediate complexes of metal cations with organic matter (see Eakin, Gize, 1992).

Contents of elements with atomic number exceeding 10 determined by the microprobe method in the carbonaceous and mineral phases of the specimens under investigation are shown in Tables 1 and 2. In this case carbonaceous matter means homogenous matter where electron microscopy does not detect the presence of other phases, and semi-quantitative X-ray spectroscopic analysis reveals strong predominance (in atomic amounts) of carbon over other elements with atomic numbers exceeding 5. In spite of homogeneity of carbonaceous phases, microprobe analysis constantly reveals the presence of heavy elements (Table 1). In carbocer, calcium is the main trace element with atomic number exceeding 10 (analysis 8 in Table 1; see also Chukanov et. al, 2005, 2006). In other cases carbonaceous phase contains sodium (bituminous matters from granitic pegmatites), uranium and radiogenic (?) lead (carbonaceous matters from alkaline pegmatites), aluminium (thucholite), and other components. Carbonaceous phases of all investigated specimens regardless of their genesis contain sulfur (from 0.39 to 2.41 wt.%).

Table 1. **Chemical compositions of carbonaceous phases (wt.%)**

	Thucholite (Viitaniemi)		Carburan (Lopatova Guba)		Bitumen (Khibiny)		Bitumen (Lovozero)	"Carbocer" (Khibiny)
Number of analysis	1	2	3	4	5	6	7	8
Na	n.d.	n.d.	n.d.	n.d.	1.30	0.54	0.47	n.d.
Ca	3.58	3.86	n.d.	n.d.	n.d.	0.84	n.d.	13.96
Pb	1.02	0.76	11.76	10.39	n.d.	n.d.	n.d.	n.d.
Fe	0.27	0.32	n.d.	n.d.	n.d.	n.d.	n.d.	0.25
Al	3.64	4.17	n.d.	n.d.	n.d.	n.d.	n.d.	n.d.
La	0.10	0.11	n.d.	n.d.	n.d.	n.d.	n.d.	n.d.
Ce	0.04	0.15	n.d.	n.d.	n.d.	n.d.	n.d.	n.d.
U	3.48	2.95	28.34	27.38	n.d.	n.d.	n.d.	n.d.
S	0.93	0.96	1.16	1.54	0.42	0.39	2.41	1.43
P	0.51	0.73	n.d.	n.d.	n.d.	n.d.	n.d.	n.d.
Total	9.53	9.88	35.66	33.97	1.38	1.39	2.76	15.64

Note: n.d. — concentration of the component is below its detection limits by microprobe method

Carbonaceous matters from pegmatites of different types contain different types of mineral inclusions (Table 2). As a rule, mineral inclusions contain intergrowths of carbonaceous phase. The distances between inclusions of carbonaceous phase are often smaller than the size of area excited by electron beam. That leads to the lowering of sums of microprobe analyses.

Original "carbocer" contains inorganic phases presented mainly by thorite and carbonates including rare earth carbonates (Chukanov *et al.*, 2006). Bituminous matters from other pegmatite bodies of the Khibina-Lovozersky complex are characterized by a variety of mineral phases (Figs. 3—5, Table 2).

High-sulfur bitumen from the Lovozero (Fig. 3; analyses 11 and 12 in Table 2) contains numerous inclusions of imperfect isometric crystals (up to 5 μm in size). The habit of some crystals allows assuming tetrahedral symmetry of the mineral. Its composition may be approximately described by the idealized formula $(Th,Ca,Na)_4(Mn,Ti,Nb)_{1-2}(SiO_4)_4(PO_4)\cdot nH_2O$.

In low-sulfur bitumen from the Khibina (Figs. 4, 5) significant amount of inclusions is represented by thorium niobium-silicate (analyses 6—8 in Table 2). The composition of this mineral corresponds to the simplified formula $(Ca,Na)_2\mathit{REE}Th_4(Nb,Ti)_{1+x}Si_{7-8}(O,OH)_y\cdot nH_2O$. Among the other mineral phases in this specimen of bitumen, one may mention high-niobium silicate with Nb:Si ≈ 2:1 (Fig. 4, analysis 9 in Table 2) and strontium-containing fluorite (analysis 10 in Table 2) covering rasvumite grains (Fig. 5).

In thucholite from lamellar albite from Viitaniemi, microprobe analysis shows the presence of very fine (less than 1 μm in size) isometric particles of a phase containing only uranium (presumably, uraninite). More big mineral inclusions (up to 30 μm) contain 62—67 wt.% of uranium and 4—10 wt.% of lead. Constant presence of sulfur (up to 1 wt.%) and low sums of analyses indicates on the possible presence of dissipated carbonaceous matter. In thucholite from the zone of sugar-like albite of the rare metal pegmatite Viitaniemi uranium is distributed between the carbonaceous matter and spherical aggregates of autunite or metaautunite (Fig. 6, analysis 1 in Table 2). Thorium is present only in the mineral phase belonging to the brockite—grayte series (Fig. 7, analysis 2 in Table 2). Carbonaceous matter of thucholite contains Al and Ca. According to the results of electron-microscopic investigation, these elements do not form their own mineral phases.

Contrary to the above mentioned specimens represented by globular aggregates of carbonaceous matter with mineral inclusions and signs of origin and crystallization within the early formed significantly organic phase (Eakin, Gize, 1992), carburan from the Lopatovaya Guba has sure signs of replacement of mineral phase (uraninite) by later introduced carbonaceous matter. Globular aggregates of the carbonaceous matter that do not contain mineral inclusions occur within the multiphase aggregate forming a pseudomorphs after cubic crystal of uraninite (Fig. 8). Mineral phases of carburan are oxides and/or carbonates of U and Pb, silicates of U as well as anglesite (analyses 3—5 in Table 2).

In order to reveal the nature of organic component of carbonaceous matters of peg-

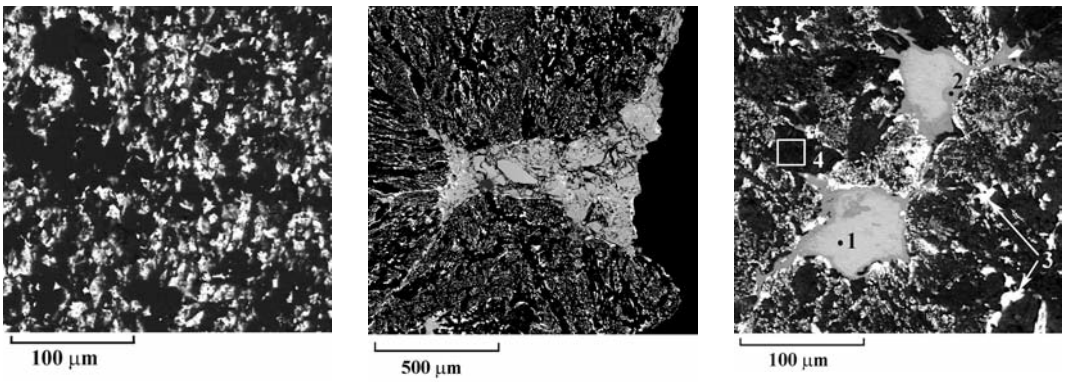

Fig. 3. Decay ingrowths of thorium-calcium silico-phosphate in bitumen. Pegmatite body "Nastrofitovoye", Lovozero, Russia. Image in back-scattered electrons.
Fig. 4. Intergrowth of high-niobium silicate (Nb:Si ≈ 2:1, gray phase in the center) with bitumen containing inclusions of thorium silicate (thorite? — numerous white areas). Khibiny, Russia. Image in back-scattered electrons.
Fig. 5. Rasvumite (1) with edgings of Sr-containing fluorite (2) and ingrowths of thorium niobo-silicate (3) in high-sulfur bitumen (4). Khibiny, Russia. Image in back-scattered electrons.

Table 2. **Chemical compositions of carbonaceous matters of pegmatites (wt.%)**

	Thucholite (Viitaniemi)		Carburan (Lopatova Guba)			Bitumen (Khibiny)					Bitumen (Lovozero)		"Carbocer" (Khibiny)	
Number of analysis	1	2	3	4	5	6	7	8	9	10	11	12	13	14
Na_2O	n.d.	n.d.	n.d.	n.d.	n.d.	0.47	n.d.	1.13	4.31	0.75	n.d.	1.21	n.d.	n.d.
CaO	5.39	7.40	n.d.	n.d.	n.d.	3.03	3.10	2.25	9.29	38.55	2.01	2.42	n.d.	1.18
PbO	0.34	9.68	17.54	6.84	71.33	n.d.	n.d.	n.d.	n.d.	n.d.	n.d.	n.d.	n.d.	n.d.
FeO	1.90	1.14	n.d.	n.d.	n.d.	n.d.	n.d.	n.d.	1.25	1.72	n.d.	n.d.	n.d.	n.d.
Al_2O_3	n.d.	2.62	n.d.	n.d.	n.d.	n.d.	n.d.	n.d.	n.d.	n.d.	0.45	0.96	n.d.	n.d.
La_2O_3	n.d.	0.25	n.d.	n.d.	n.d.	0.71	n.d.	0.48	0.55	n.d.	n.d.	n.d.	n.d.	n.d.
Ce_2O_3	n.d.	0.24	n.d.	1.63	n.d.	4.18	3.15	3.43	1.23	n.d.	n.d.	n.d.	n.d.	n.d.
ThO_2	n.d.	28.23	n.d.	7.61	n.d.	39.19	46.19	44.11	1.65	1.94	31.34	40.51	80.03	75.50
UO_3	64.35	2.98	69.01	41.60	n.d.	n.d.	n.d.	n.d.	n.d.	n.d.	n.d.	n.d.	n.d.	n.d.
TiO_2	n.d.	n.d.	n.d.	n.d.	n.d.	1.31	1.23	1.72	5.60	n.d.	1.84	1.60	n.d.	n.d.
Nb_2O_5	n.d.	n.d.	n.d.	n.d.	n.d.	3.49	3.64	5.51	43.65	n.d.	2.75	1.82	n.d.	n.d.
SiO_2	n.d.	n.d.	n.d.	7.64	n.d.	17.47	18.14	16.94	11.08	n.d.	8.43	12.26	18.52	17.34
P_2O_5	15.34	19.60	n.d.	5.18	n.d.	n.d.	n.d.	n.d.	n.d.	n.d.	2.38	4.10	n.d.	n.d.
SO_3	n.d.	0.28	n.d.	n.d.	25.99	n.d.	n.d.	n.d.	n.d.	n.d.	0.80	0.45	n.d.	0.51
Total	90.42	74.55	86.55	72.68	97.32	72.13	78.47	77.65	79.22	73.72	97.05	98.25	98.55	94.53
						Formula coefficients								
Na	–	–	–	–	–	0.42	–	1.03	0.74	0.03	–	0.65	–	–
Ca	0.89	0.48	–	–	–	1.48	1.55	1.15	0.90	0.85	0.93	0.71	–	0.07
Pb	0.02	0.16	0.98	0.15	0.98	–	–	–	–	–	–	–	–	–
Fe	0.25	0.06	–	–	–	–	–	–	–	–	–	–	–	–
Al	–	0.19	–	–	–	–	–	–	–	–	0.37	0.32	–	–
La	–	0.01	–	–	–	0.12	–	0.08	0.02	–	–	–	–	–
Ce	–	0.01	–	0.05	–	0.71	0.52	0.60	0.04	–	–	–	–	–
Th	–	0.39	–	0.14	–	4.09	4.63	4.73	0.04	0.01	3.07	2.57	0.98	0.99
U	2.08	0.04	3.00	0.69	–	–	–	–	–	–	–	–	–	–
Ti	–	–	–	–	–	0.45	0.41	0.62	0.39	–	0.75	0.33	–	–
Nb	–	–	–	–	–	0.72	0.74	1.17	1.79	–	0.54	0.23	–	–
Si	–	–	–	0.61	–	8.00	8.00	8.00	1.00	–	3.63	3.68	1.00	1.00
P	2.00	1.00	–	0.35	–	–	–	–	–	–	0.87	0.96	–	–
S	–	0.03	–	–	1.00	–	–	–	–	–	–	–	–	0.02
Method of calculation	P_2	P_1	U_3	$(Si,P,As)_1$	S_1	Si_8	Si_8	Si_8	Si_1	1 cation	$(Si,Al)_4$	$(Si,Al)_4$	Si_1	Si_1

Note: n.d. – concentration of the component is below its detection limits by microprobe method. Additionally detected: analysis 1 – SrO 1.23 % ($Sr_{0.11}$), ZrO_2 0.57 % ($Zr_{0.04}$), Sb_2O_5 1.30 % ($Sb_{0.07}$); analysis 2 – TiO_2 0.22 % ($Ti_{0.01}$), SrO 0.86 % ($Sr_{0.03}$), Y_2O_3 0.85 % ($Y_{0.03}$), ZrO_2 0.20 % ($Zr_{0.01}$); analysis 4 – As_2O_5 1.09 % ($As_{0.05}$), Dy_2O_3 1.09 % ($Dy_{0.03}$); analysis 6 – Pr_2O_3 0.80 % ($Pr_{0.12}$), Nd_2O_3 1.48 % ($Nd_{0.24}$); analysis 7 – K_2O 0.74 % ($K_{0.11}$), Nd_2O_3 2.28 % ($Nd_{0.36}$); analysis 8 – Nd_2O_3 2.08 % ($Nd_{0.35}$); analysis 9 – K_2O 0.61 % ($K_{0.07}$); analysis 10 – SrO 7.49 % ($Sr_{0.08}$), F 40.19 % ($F_{1.89}$), -O=F_2 -16.92 %; analysis 11 – MnO 2.05 % ($Mn_{0.75}$), C 38 %, $O_{изб}$ 7 %; analysis 12 – MnO 1.92 % ($Mn_{0.46}$), C 26 %, $O_{surplus}$ 5 %

matites, infra-red (IR) spectroscopy has been used. All organic compounds show resonance absorption of IR radiation in the range 1300—3100 cm^{-1}. In this range silicates, oxides and phosphates do not give strong absorption bands. It makes possible to detect small amounts of organic compounds as admixtures to rock-forming and accessory minerals. IR spectra of carbonaceous matters and associated minerals pressed in the form of tablets with potassium bromide have been obtained using the two-beam spectrophotometer Specord 75 IR in the wavenumber range 400—4000 cm^{-1} with spectral width of slit no more than 2 cm^{-1} for the interval 400—1800 cm^{-1} and no more than 6 cm^{-1} for the interval 1800—3100 cm^{-1}.

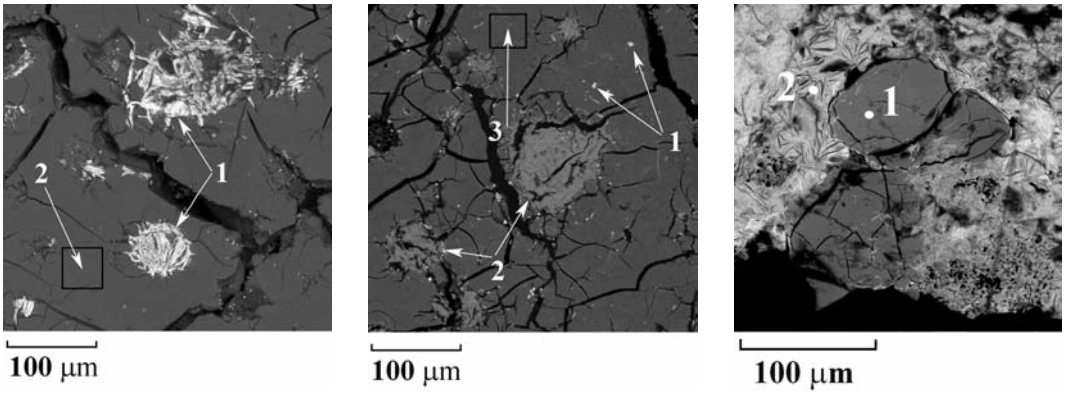

Fig. 6. Aggregates of autinite and/or meta-autinite (1) in thucholite (2). Viitaniemi, Finland. Image in back-scattered electrons.
Fig. 7. Inclusions of mineral grains of the series brockite—grayite (1) and aggregates of nontronite (2) in thucholite (3). Viitaniemi, Finland. Image in back-scattered electrons.
Fig. 8. Aggregates of carbonaceous matter (1) in the U and Pb hydroxide (carbonate?) aggregate (2) from carburan. Lopatova Guba, Russia. Image in back-scattered electrons.

During spectrum recording, analogous tablet of pure KBr was placed in the reference beam. NH_3 (gas) and polysterene were used as standards.

All investigated in the present work carbonaceous matters are characterized by high contents of water and/or hydroxyl groups that show strong wide bands in the frequency range 3100—3600 cm^{-1}. Bitumens from the ultraagpaitic pegmatites of the Khibino-Lovozersky complex (Fig. 9) are characterized by high contents of aliphatic hydrocarbon groups (corresponding C-H stretching vibrations correspond to a series of bands in the range 2800—3000 cm^{-1}) as well as unsaturated organic compounds giving series of bands in the frequency range 1200—1680 cm^{-1}. In the latter interval, bending vibrations of CH_2 and CH_3 groups, stretching vibrations of carboxylate groups and bending vibrations of water molecules are revealed. Their precise detection in this interval is difficult due to the overlapping of bands. High integral intensity of absorbance indicates on the presence of aromatic compounds. Band in the range 1680—1740 cm^{-1} characteristic to IR-spectra of bitumens from pegmatites is attributed to carbonyl groups (C=O stretching vibrations).

IR-spectrum of thucholite from Viitaniemi albitite (Fig. 10) is close to IR-spectra of "carbocers" with low contents of aliphatic hydrocarbon groups (Chukanov *et al.*, 2006): bands of C-H stretching vibrations are weak or are absent, and bands of absorption of aromatic and carboxylate groups are very strong. Spectrum of thucholite also contains bands of carbonyl and uranyl groups (corresponding ranges 1680—1740 and 900—950 cm^{-1}, Fig. 10).

IR-spectrum of carburan does not contain bands that may be for sure related with any organic groups. The strongest bands in the ranges 1400—1550 and 900—950 cm^{-1} presumably correspond to stretching vibrations of ions CO_3^{2-} and UO_2^{2+}, respectively. At the same time microprobe analyses show the presence of uranyl carbonate as well as significant amounts of carbonaceous matter. The latter is characterized by low sums of analyses on elements with atomic numbers exceeding 10 and high (more than 50%) contents of carbon. In total these facts show that significant share of carbon is present in the state characterized by low coefficients of absorption of IR-radiation. Taking into account that coefficient of extinction of stretching vibrations is proportional to the square of the bond-length partial derivative of dipole moment, one may make a conclusion that significant part of the carbonaceous matter of carburan is represented by pure carbon with nonpolar bonds C-C.

Earlier, as a result of investigation of modes of occurrence of bituminous matters in agpaitic pegmatites of the Lovozersky massif a conclusion was drawn that minerals of thorium crystallized at the later stages of pegmatites formation concentrated organic matters in the form of dispersed microscopic inclusions (Chukanov *et al.*, 2005, 2006; Ermolaeva *et al.*, 2007. 2008). Analogous observations were made by us during IR-spectroscopic investigation of minerals of amazonitic pegmatites from Western Keyvy. High concentrations of organic matters have been fixed only in the later thorite ("thorite-II" according to Voloshin, Pakhomovsky, 1986, see Fig. 11). At the Fig. 11, spectrum of Na,Th—silicate from ultraagpaitic

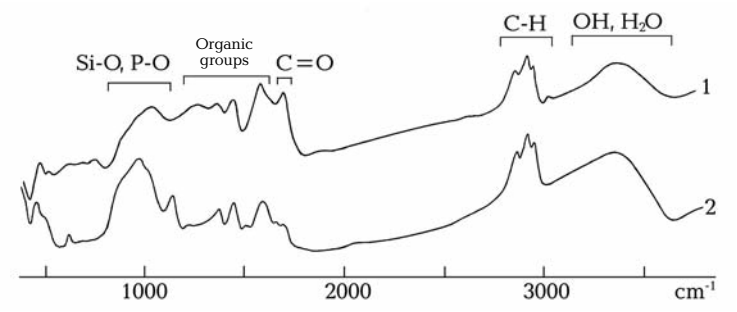

Fig. 9. IR-spectra of bitumens from the pegmatite body "Nastrofitovoye" (1) and from the pegmatite of the Koashva Mountain (2).

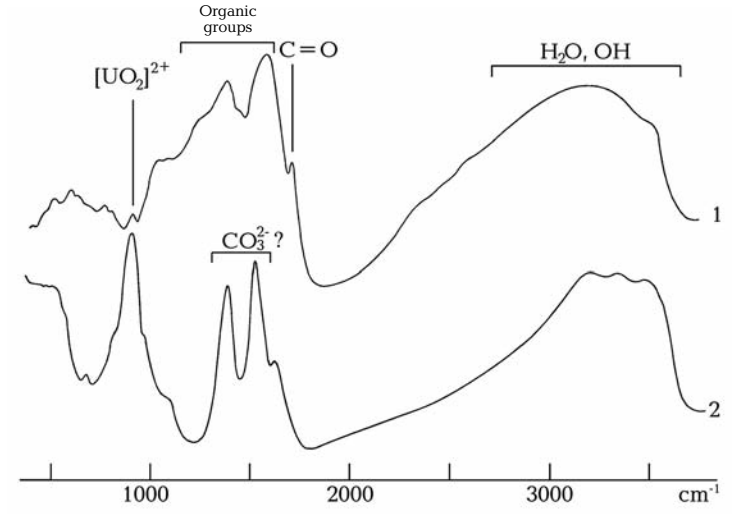

Fig. 10. IR-spectra of thucholite (1 — Viitaniemi) and carburan (2 — Lopatova Guba).

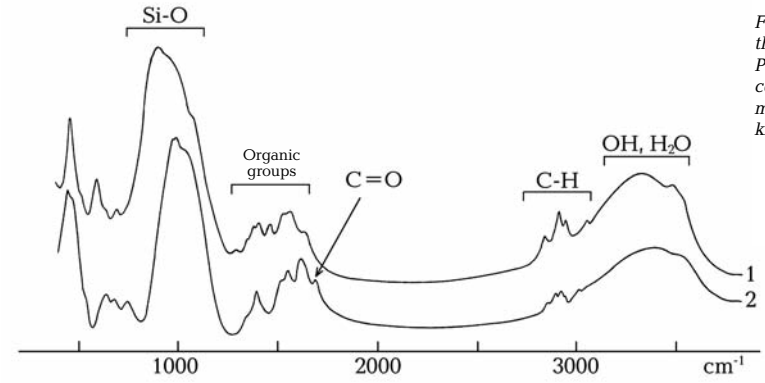

Fig. 11. IR-spectra of thorite (1) from the amazonitic pegmatite (Mountain Ploskaya) and sodium-thorium silicate (2) from the ultraagpaitic pegmatite "Palitra (Mountain Kedykverkhpahk, Lovozero).

pegmatite "Palitra" (mountain Kedykvarpakh, Lovozero) is shown for comparison.

Discussion

As a rule, carbonaceous matters from pegmatites and hydrothermal veins of different genetic types are heterogeneous matters in phase composition. In granitic pegmatites they are often enriched in uranium, thorium and/or rare earth elements. Thucholite (in the wide sense of this term) may contain inclusions of uraninite, or its core consists of uraninite (Spence, 1930; Zhirov, Bandurkin, 1968). Inclusions of thorite and thorianite occur in thucholite enriched in thorium (Parnell, 1988). Rare earth containing thucholite from pegmatite of the Parry Sound region (Canada) contains inclusions of phosphates of *REE* (with lanthanum maximum) and thorium (Parnell, 1990). Specimens investigated in this work were no exception and also were heterophase objects enriched in specific rare elements.

Comparing our results with the data from literary sources we may note that there is a stable general tendency to coexistence of carbonaceous matters and minerals of a row of characteristic incoherent elements (U, Th, *REE*, Zr, Hf, Nb, Ta, Ti, W, Sn). Uplifted concentrations of these elements are connected with definite mineral formation stage. For example, positive correlation of uranium with concentrations of Y, Zr, Nb, Ta, Hf, and *REE* has been revealed in the granitic massif Karkonosze (Poland) where this correlation occurred in miarolitic pegmatites, aplites and quartz veins (Mikulski, 2007). According to A.N. Labuntsov (1939), carburan formation in granitic pegmatites begins at the temperature about 700°C (almost simultaneously with the beginning of crystallization of accessory minerals: titanite, cyrtolite, xenotime-(Y), monazite-(Ce) and uraninite).

Investigation of solid bituminous matters (SBM) from agpaitic pegmatites (mainly by the example of pegmatites of the Khibino-Lovozersky complex) leads to the conclusion of a tight spatial connection of rare metal mineralization with organic matter in postmagmatic differentiates. First of all it concerns to Th, and also to *REE*, U, Ti, Nb, and Zr.

So, from the comparing of data on granitic and alkaline agpaitic pegmatites, one may make a conclusion of existing of a row of "bitumenphilic" elements including the following ones: U, Th, Y, Ln, Zr, Hf, Nb, Ta, Ti, W, Sn, Pb. It is notable that this row almost coincides with the set of coalphilic elements. These elements are distinguished on the basis of a great statistical material accumulated by now in the science of solid caustobioliths and generalized in the recently issued monographs (Yudovich, Ketris, 2006; Arbuzov, Ershov, 2007). In coals most of lithophile rare elements is firstly accumulated in the form of complexes with organic ligands and then partially occurs in concentrated form giving mineral phases. In mature coals mineral forms of these elements may predominate. They may originate authigenically during the decay of their carboxylate salts and other organic forms. It is notable that ash clarkes of lithophile rare elements, as a rule, exceed their concentration in clays from coals. Such elements in coals as Ta, Nb, Zr, Hf, and *REE* may reach industrially significant concentrations (Arbuzov, Ershov, 2007).

Earlier according to the analysis of data on paragenetic correlations between mineral and organic matter in the agpaitic pegmatites we have suggested the following genetical scheme (Chukanov *et al.*, 2005, 2006; Ermolaeva *et al.*, 2007, 2008; Chukanov *et al.*, 2008):

1. Mass crystallization of aegirine at the early stages of pegmatite formation binds greater part of iron in the form of Fe^{3+} that is favorable for the stabilization of the reduced forms of carbon in the residual fluid.
2. Sorption of small carbon-containing molecules (CO, CO_2, CH_4, C_2H_6, C_2H_4 etc.), their polymerization, transformation in aromatic compounds (process of reforming) and selective oxidation occurs at the microporous zeolite-like silicates of Ti, Nb, and Zr playing the role of sorbents and catalysts.
3. Oxygen-containing aromatic compounds with hydrophile functional groups (-OH, -C=O, -COOH, $-COO^-$) act as a complex-forming agents in relation to Th, *REE*, U, Zr, Ti, Nb, Ba, Sr, and Ca. They provide transportation of these ("bitumenphilic") elements in low-temperature hydrothermal conditions in the form of water-soluble macroassociates of the micelle type. Aliphatic bituminous matters, as a rule, are impoverished by oxygen and are less active as complex formation agents.
4. Concentration of Th, *REE* (and to a lesser degree, U, Zr, Ti, Nb) at the later stages of hydrothermal process occurs in the form of microphases that give abundant inclusions in segregations of SBM or in the form of macroscopic segregations of Th and *REE* minerals. In the latter case SBM are captured in the form of inclusions by growing crystal or on the contrary are crowd out to its surface forming outer zones enriched in SBM.
5. At the final stages occurs the decay of homogenous SBM onto organic (partly with Ca, Sr, Ba, and Pb) and mineral (with Th, Ln, Y, Ti, Nb, Ca, Na, K, and Si) microphases.

According to the literature data, tight association of uranium with organic matter may be a result of mobility of hydrocarbons and replacement of uranium minerals by them (Dubinchuk *et al.*, 1977) as well as due to the ability of oxygen ligands to form soluble organic complexes of U^{6+} or as a result of sedimentation of hydrocarbons at the surface of uranium minerals during processes of polymerization caused by radiation (Hoekstra, Fuchs, 1960). Further process at the same time is accompanied by the decay of uranium minerals as well as radiolythic decomposition of organic matters that lead to its dehydration and transformation into the carbonaceous matter of the anthraxolite type.

According to the microscopic investigation of textural peculiar features and electron-microprobe studies, the main genetic-morphology types of uranium-containing bituminous matters are distinguished. Two mechanisms of their formation have been suggested (Eakin, Gize, 1992). During the realization of the first mechanism, formed earlier mineral phases (uraninite, in particular) were later replaced by aggressive organic matter. During this process under the influence of radioactive decay, active organic particles (free radicals and other) may be formed and radiation-induced polymerization of organic molecules occurs. Bituminous matters of the second type were presumably formed in the process of generation of complex compounds of U^{6+} (in lesser degree, Th) with formed before organic matters, further reduction of uranium and decay of the homogenous metal-organic complex onto the organic and mineral (uraninite, coffinite) phases.

Supposition that prolonged radiation of bituminous matter leads to its dehydration, aromatization and polymerization has been repeatedly expressed in earlier publications (Abdel-Gawad, Kerr, 1961; Zumberge *et al.*, 1978; Landais *et al.*, 1987).

According to its mineralogy-morphological characteristics (globular segregations of carbonaceous matter with inclusions of U and Th minerals) and predominating modes of occurrence of carbon (aromatic and carboxylate compounds), thucholite from the Viitaniemi pegmatite is analogous to the Khibina "carbocer". The main differences reflecting geochemical specifity of two formations (rare metal granitic and agpaitic pegmatites) are in the nature of cations of carboxylate salts (alkaline-earth cations in "carbocer", and calcium and aluminium in thucholite) and in the composition of predominating mineral ingrowths (silicates of Th in "carbocer", phosphates and oxides of U and Th in thucholite).

The most likely predecessors of thucholite, as well as carbocer, are hydrocarbon gases primordially present in the residual portions of fluid forming the pegmatite body. In particular, this conclusion was made by authors of the work (Bushev *et al.*, 1997) as a result of investigation of organic compounds of rare metal granitic pegmatite of the Kukurt deposit (Eastern Pamir). According to the gas-chromatography and mass-spectrometer analyses of flying and extracted by chloroform compounds, this pegmatite contains 0.946 cm^3/kg alcans (up to C_8H_{18}), 0.731 cm^3/kg alcens (up to C_7H_{14}) and 44.7 ng/g aromatic hydrocarbons (including polycyclic). Presence of alcens is especially indicative because of their ability for polymerization at catalysts of the Zigler-Natta type under low temperatures. In comparison with thucholite, carburan from the ceramic pegmatites of Karelia is much more mineralized; according to S.M. Popov (1957), its average ash content accounts for more than 35%, and our observations confirm this conclusion.

Origin of carburan in contrast to the thucholite and bitumens of alkaline pegmatites obviously occurred by means of replacement of uraninite crystal by organic matter. Analogous process was reproduced in laboratory conditions (Dymkov *et al.*, 2002) when nasturan interacted with heavy oil under 300°C and 195 atmospheres during 72 hours. As a result, surface of nasturan particles were corroded, and they were overgrown by solid bitumen film.

During the comparison of carbonaceous matters from the granitic and agpaitic pegmatites one can observe that (in spite of the fact that bitumens from the granitic pegmatites were formed under significantly more high temperatures than bitumens from the alkaline pegmatites) in both cases specific mineralization with participation of Ti, Zr, and Nb (for granitic pegmatites also with Ta, Hf, and Sn) is directly preceded by sedimentation of carbonaceous matter. It once more confirms a hypothesis of the catalyst role of the mentioned high-valent transition elements in endogenic processes of formation of organic matters, their polymerization and partial oxidizing up to carbonyl, carboxyl and carboxylate compounds. We may remind that synthetic titanium-silicates and niobium-silicates find a wide application as catalysts of selective partial oxidizing of hydrocarbons in mild conditions (see the review: Chukanov *et al.*, 2004). The ability of transition metals to catalyse polymerization of unsaturated organic compounds in aqueous media and their copolymerization with CO in hydrothermal conditions are also well known (Mecking *et al.*, 2002). For one's turn high-molecular carbonyl, carboxyl and carboxylate compounds have a pronounced affinity with great high-valent cations such as Th^{4+}, U^{4+}, and REE^{3+} and form stable complexes with them. So, all chain of chemical transformations including catalyst formation of high-molecular organic compounds (with participation of Ti, Zr, Nb, Ta, Hf, and Sn), their selective oxidizing, formation of metal-organic complexes with Th^{4+},

U^{4+}, and REE^{3+}, radiolythic decomposition of organic matter and crystallization of minerals of the mentioned rare elements within the organic matrix is regular and caused by physicochemical features of carbon, hydrogen, oxygen and high-valent rare elements. As a result of these processes segregations of mineralized carbonaceous matters are formed. These segregations are natural microreactors with uplifted concentrations, from one side, of elements with high force characteristics (Ti, Zr, Nb, Ta, Hf, and/or Sn), and from the other side, with rare earth elements and/or radioactive elements (Th^{4+}, U^{4+}, *REE*). Mineral phases formed in such microreactors (with predominating silicates including titanium-silicates and niobium-silicates of thorium and lanthanides, see also Chukanov *et al.*, 2005, 2006; Ermolaeva *et al.*, 2007, 2008) are characterized by unique variety. Many of them are unknown in other conditions.

In conclusion let us consider the problem of carbon and carbonaceous matter sources in postmagmatic formations. Most of investigators consider carbonaceous matter of agpaitic magmatic rocks and related pegmatites as a product of natural evolution of magma and not as a result of contamination of enclosing rocks by organic matter (see Labuntsov, 1937; Petersilye *et al.*, 1969; Galimov, Petersilye, 1968; Florovskaya *et al.*, 1968; Loskutov, Polezhaeva, 1968; Nivin, 2002). In favor of this point of view witnesses the fact that in different pegmatite bodies bituminous matters occupy definite position and are connected with the same type paragenesises (and our observations confirm this). At the same time the sources of carbon remains debatable. At the earlier stages of magma evolution carbon is present mainly as a component of volatile components (CH_4, CO, and CO_2). Their mutual transformations are going during the following reactions: $CO + 3H_2 \leftrightarrow CH_4 + H_2O$, $CO_2 + 4H_2 \leftrightarrow CH_4 + 2H_2O$, $2CO + 2H_2O \leftrightarrow CH_4 + CO_2$. Under the hypothesis that in these processes fractionation of carbon isotopes is limited, we have used the data on isotope composition of methane carbon from the rocks and minerals of the Khibiny and Lovozero (δC^{13} from -0.32 to -1.28) for the substantiation of the mantle origin of this carbon (Petersilye *et al.*, 1969). At the same time carbon of bitumens from agpaitic pegmatites was close in isotope composition (δC^{13} from -2.91 to -2.97) to the carbon of carbonaceous chondrites. Afterwards contradictions in the data on isotope composition of hydrocarbon gases from nepheline-syenitic complexes were repeatedly mentioned (Beeskow *et al.*, 2006; Potter, Longstaffe, 2007). On the basis of this it was made a supposition on the possible influx of organic matter (Nivin, 2008).

In our opinion, we ought to regard with great caution to the interpretation of isotope composition of bituminous matters of endogenic origin because such matters are products, as a rule, of catalyst reactions of radical polymerization, disproportioning, reforming and oxidizing (Rudenko, Kulakova, 1986; Chukanov *et al.*, 2005, 2006; Ermolaeva *et al.*, 2007, 2008). In presence of transition metals, free radical polymerization of unsaturated hydrocarbons is possible in conditions analogous to hydrothermal (see the review: Mecking *et al.*, 2002). All these processes may reveal strong spin selectivity that lead to the effective isotope fractionation of ^{12}C and ^{13}C (see the reviews of Buchachenko, 1995; Buchachenko, 2001). Constant tight association of pegmatitic bitumens with radioactive elements (uranium and thorium) results in the formation of radioactive-generated free radicals that is an additional source of spin-selective channels of processes with the participation of organic reagents. In particular, as a result of gamma irradiation, molecules of aromatic carbonyl compounds are transformed into the triplet state and decompose onto fragments forming radical pair. The nucleus of ^{13}C, unlike ^{12}C, has magnetic moment. Due to the hyperfine interaction with such nucleus, uncoupled electrons of the radical pare swiftly transform to the singlet state that makes possible recombination and, as a result, enrichment of original molecules by ^{13}C nuclei. ^{12}C nuclei accumulate in the products of recombination (CO and polycyclic aromatic compounds) (Buchachenko, 2001).

In case of granitic pegmatites the question of the origin of carbon and carbonaceous matter is treated ambiguous. In some works (Ellsworth, 1928a, 1932; Barthauer *et al.*, 1953; Mueller, 1969) hypothesis of magmatic origin of thucholite carbon is proved. But some works contain assumptions on the possibility of contamination of pegmatitic fluid by the bituminous matter of the enclosing rocks. For example, the pegmatite exposed at the Besner mine contains oil-like and asphalt-like bitumens in cross faults of veins, and thucholite occurred in these zones. It was treated as an indication of penetration of oil from above, from the sedimentary suite that is not present now (Spence, 1930). Afterwards this explanation was subjected to criticism (Fersman, 1931). Starting from the presence of a row of oil

occurrences in the Lower Paleozoic of the Ontario region, it was admitted that oil fluid leaked below from the Lower Paleozoic rocks into the underlying Precambrian basement and became polymerized and hardened under the influence of radiation from the closely situated radioactive minerals in the pegmatite. Analogous conclusion was made in the work Steveson *et al.* (1990) based on the results of investigation of organic matter from quartz—calcite (with sulfides) veins of the uranium mine Panel, Canada. This matter practically does not contain Th and U (< 0.5 ppm) in spite of high concentration of uranium in enclosing strata. It was also supposed (Zhirov, Bandurkin, 1968) that graphite from the enclosing metamorphic (originally sedimentary) rocks may serve as the source of carbon for the carburan from the pegmatites of the northern Karelia and Kola Peninsula.

Modes of occurrences of these matters in pegmatites of different types, their microstructure, and connection of their segregations to the specific rare metal mineralization — all these facts are the indications that in most cases bitumens, thucholite and carbocer should be considered as matters formed as a result of natural evolution of pegmatite in tight connection with processes of mineral formation. The presence of carbonaceous matters itself indicates rather low activity of oxygen in the moment of their formation; otherwise, deposition of carbon only in the form of carbonates will occur. In the agpaitic rocks the main channel of oxygen evacuation from the fluid is obviously connected with crystallization of aegirine; as a result of this process iron is bonded mainly in the form of Fe^{3+} (Ermolaeva *et al.*, 2008). In case of granitic pegmatites mechanisms of oxygen evacuation from fluid are less obvious. It is likely that definite role in this process may play crystallization of feldspars (in case of pegmatites from northern Karelia they contain 0.12—0.13 wt.% of Fe_2O_3) as well as muscovite with 1—7 wt.% of Fe_2O_3 and 0.3—0.4 wt.% of FeO (Labuntsov, 1939).

The work was performed with financial support of the Russian Federation Foundation for Basic Research (grant no. 07-05-00130-a).

References

Abdel-Gawad A.M., Kerr P.F. Urano-organic mineral association // Am. Mineral. **1961**. V. 46. P. 402—419.

Arbuzov S.I. and Ershov V.V. Geology of rare elements in coals of the Siberia. Tomsk: D-Print. **2007**. (in Russian).

Barthauer G.L., Rules C.L., Pearce D.W. Investi-gation of thucholite // Am. Mineral. **1953**. V. 38. P. 802—814.

Beeskow B., Treloar P.J., Rankin A.H., Venne-mann T.W., Spangenberg J. A reassessment of models for hydrocarbon generation in the Khibiny nepheline syenite complex, Kola peninsula, Russia // Lithos. **2006**. V. 91. P. 1—18.

Buchachenko A.L. Nucleus-spin selectivity of chemical reactions // Uspekhi khimii. **1995**. V. 9. P. 863—871. (in Russian).

Buchachenko A.L. Magnetic isotope effect: Nuclear spin control of chemical reactions // J. Phys. Chem. A. **2001**. V. 105. P. 9995—10001.

Bushev A.G., Kuz`min V.I., Pen`kov V.F., Novgorodova M.I., Buslaeva E.Yu., and Lobzin E.V. Organic compounds in minerals of pegmatites from Pamir // Geokhimiya. **1997**. V. 35. № 3. P. 348—352. (in Russian).

Chukanov N.V., Pekov I.V., Rastsvetaeva R.K. Crystal chemistry, properties and synthesis of microporous silicates containing transition elements // Usp. Khimii. **2004**. V. 73. № 3. P. 227—246. (In Russian). *Chukanov N.V., Pekov I.V. and Rastsvetaeva R.K.* Crystal chemistry, properties and synthesis of microporous silicates containing transition elements // Russ. Chem. Rev. **2004**. V. 73(1). P. 227—246.

Chukanov N.V., Ermolaeva V.N., Pekov I.V., Sokolov S.V., Nekrasov A.N., Sokolova M.N. Rare metal mineralization connected with bituminous matters in late assembledges of pegmatites of the Khibiny and Lovozero massifs // New data on minerals. **2005**. V. 40. P. 80—95. (In Russian). *Chukanov N.V., Ermolaeva V.N., Pekov I.V., Sokolov S.V., Nekrasov A.N., Sokolova M.N.* Rare metal mineralization connected with bituminous matters in late assembledges of pegmatites of the Khibiny and Lovozero massifs // New data on minerals. **2005**. V. 40. P. 80—95.

Chukanov N.V., Pekov I.V., Sokolov S.V., Nekrasov A.N., Ermolaeva V.N. and Naumova I.S. On the problem of the formation and geochemical role of bituminous matter in pegmatites of the Khibiny and Lovozero alkaline massifs, Kola Peninsula, Russia // Geokhimia. **2006**. № 7. P. 774—789. (In Russian). *Chukanov N.V., Pekov I.V., Sokolov S.V., Nekrasov A.N., Ermolaeva V.N. and Naumova I.S.* On the problem of the formation and geochemical role of bituminous matter in pegmatites of the Khibiny and Lovozero alkaline massifs, Kola Peninsula,

Russia // Geochemistry International. **2006**. V. 44. No. 7. P. 715—728.

Chukanov N.V., Pekov I.V., Ermolaeva V.N. The role of organic matter in peralkaline pegmatites: comparison of minerogenetic and technological processes // Minerals as advanced materials I. Springer Verlag, Berlin-Heidelberg, **2008**. P. 221—229. ISBN: 978-3-540-77122-7.

Dubinchuk V.T., Penkov V.F., Uspensky V.A., Avdonin A.S., Sheuchenko V.N. Replacement of uraninite by kerite and coffinite // Geochem. Int. **1977**. V. 14. P. 182—187.

Dymkov Yu.M., Kunts A.F. and Doynikova O.A. Formation of solid bitumen in the process of interaction between nasturan and oil under 300˚C // Doklady AN SSSR. **2002**. V. 387. № 1. P. 90—94. (in Russian).

Eakin P.A., Gize A.P. Reflected-light microscopy of uranferous bitumens // Mineral. Mag. **1992**. V. 56. P. 85—99.

Ellsworth R.V. Rare-element minerals of Canada // Can. Dep. Mines Tech. Surv. Econ. Geol. **1932**. Ser. 11. P. 268—269.

Ellsworth R.V. Thucholite, a remarkable primary carbon mineral from the vinicity of Parry Sound, Ontario // Am. Min. **1928a**. V. 13. P. 419—442.

Ellsworth R.V. Thucholite and uraninite from the Wallingford mine near Buckingham, Quebec // Am. Min. **1928b**. V. 13. P. 442—448.

Ermolaeva V.N., Chukanov N.V., Pekov I.V. and Shlyukova Z.V. Mineral formation with participation of bituminous matters in pegmatites of the Khibinsky massif: new data // New data on minerals. **2007**. V. 42. P. 33—42.

Ermolaeva V.N., Chukanov N.V., Pekov I.V. and Kogarko L.N. On the role of organic matters in transportation and concentration of thorium and other rare elements in alkaline pegmatites of Lovozersky and Khibinsky ultraagpaitic massifs // Zapiski Vses. Mineral. Obschestva. **2008**. V. 137. № 5. P. 17—33. (In Russian.).

Fersman A.E. Pegmatites, their scientific and practical importance. V. 1. Granitic pegmatites. L.: AN SSSR. **1931**. (In Russian).

Florovskaya V.N., Zezin R.B., Ovchinnikova L.I., Pikovskii Yu.I. and Teplitskaya T.A. Diagnostics of organic matters in rocks and minerals of magmatic and hydrothermal origin. Moscow: Nauka. **1968**. (In Russian).

Galimov E.M. and Petersilye I.A. Isotope composition of carbon from bitumens of igneous and metamorphic rocks // Doklady AN SSSR. **1968**. V. 182. № 1. P. 186—189. (in Russian).

Hoekstra H.R., Fuchs L.H. The origin of thucholite // Econ. Geol. **1960**. V. 55. P. 1716—1738.

Jonasson I.R., Charbonneau B.W., Ford K.L. On the nature and formation of radioactive hydrocarbons from the Ordovician rocks of the Ottawa area // Geol. Surv. Can. Pap. **1977**. V. 77—1B. P. 109—111.

Labuntsov A.N. Pegmatites of northern Karelia and its minerals // Pegmatites of the USSR. V. 2. Moscow: AN SSSR. **1939**. (In Russian.).

Labuntsov A.N. Carbocer. Minerals of Khibinsky and Lovozersky tundra. Moscow-Leningrad: AN SSSR. **1937**. (In Russian).

Landais P., Connan J., Dereppe J.M., George E., Meynier J.D., Monthioux M., Pagel M., Pironon J., Poty B. Alterations of ordanic matter: a clue for uranium ore genesis // Uranium. **1987**. V. 3. P. 307—342.

Loskutov A. V. and Polezhaeva L. I. On the question of the nature of Khibina carbocers // Mater. mineralogy. Kola Peninsula. Leningrad: Nauka. **1968**. № 6. P. 276—281. (In Russian.).

Mecking S., Held A., Bauers F.M. Aqueous catalytic polymerization of olefins // Angew. Chem. Int. Ed. **2002**. V. 47. P. 544—561.

Mikulski S.Z. Metal ore potential of the parent magma of granite — the Karkonosze massif example // Granitoids in Poland. **2007**. № 1. P. 123—145.

Mueller G. Discussion of evidences indicating the extence of petroleums of distinct genetical histories // Rep. 22nd Int. Geol. Congr. (Delhi). **1969**. V. 1. P. 38—63.

Nivin V.A. Gas saturation of minerals in connection with the problem of origin of hydrocarbon gases in the rocks of the Khibinsky and Lovozersky alkaline massifs // Geokhimiya. **2002.** № 9. P. 976—992. (in Russian).

Nivin V.A. Variations of composition of hydrocarbon gases in the Lovozersky massif and possible geological consequences // Petrology and minerageny of the Kola Peninsula. **2008**. Apatity: Izd. KNTs RAN. P. 319—321. (In Russian).

Parnell J. Metal enrichments in solid bitumens: a review // Miner. Deposita. **1988**. V. 23. P. 191—199.

Parnell J. Mineralogy of rare-earth «thucholite», Parry Sound, Ontario // Can. Mineral. **1990**. V. 28. P. 357—362.

Petersilye I.A., Pavlova M.A., Malashkina V.T. New data on the composition of organic matter in rocks and minerals of the Khibinsky massif and character of its change under uplifted temperatures // Mater. mineralogy Kola Peninsula.

Leningrad: Nauka. **1969**. № 7. P. 203—209. (In Russian.).

Popov S.M. Content of water and gases in carburan // Trudy Rad. Inst. **1957**. V. 5, N. 2. P. 256—286. (In Russian).

Potter J., Longstaffe F.J. A gas-chromatograph, continuous flow-isotope ratio mass-spectrometry method for $\delta^{13}C$ and δD measurement of complex fluid inclusion volatiles: Examples from the Khibina alkaline igneous complex, northwest Russia, and the South Wales coalfields // Chemical Geology. **2007**. V. 244. P. 186—201.

Rudenko A.P. and Kulakova I.I. Physicochemical model of abiogenic synthesis of hydrocarbons in natural conditions // ZH.VKhO. **1986**. V. 31. № 5. P. 518—526. (In Russian).

Spence H.S. A remarkable occurrence of thucholite and oil in a pegmatite dyke, Parry Sound, Ontario // Am. Min. **1930**. V. 15. P. 499—520.

Spence H.S. Uraninite and thucholite from Pied des Monts, Charlevoix County, Quebec // Am. Min. **1940**. V. 25. P. 711—718.

Stevenson J., Mancuso J, Frizado J., Truskoski P., Kneller W. Solid pyrobitumen in veins, Panel mine, Elliot Lake District, Ontario // Can. Mineral. **1990**. V. 28. P. 161—169.

Voloshin A.V. and Pakhomovskii Ya.A. Minerals and evolution of mineral formation in amazonitic pegmatites of the Kola Peninsula. Leningrad. **1986**. (in Russian).

Yudovich Ya.E. and Ketris M.P. Valuable trace elements in coals. Ekaterinburg: RIO UrO RAN. **2006**. (In Russian).

Zhirov K.K.and Bandurkin G.A. Mineralogy-geochemical peculiarities of accessory carburans from pegmatites of northern Karelia and Kola Peninsula // Mater. mineralogy Kola Peninsula. Leningrad: Nauka. **1968**. № 6. P. 210—220. (In Russian.).

Zumberge J.E., Sigleo A.C., Nagy B. Molecular and elemental analysis of the carbonaceous matter in the gold and uranium-bearing Vaal-Reef carbon seams, Witwatersrand sequence // Mineral. Sci. Engin. **1978**. V. 10. P. 223—246.

SOME PECULIARITIES OF MINERALOGY OF THE DEPOSITS OF CENTRAL PART OF STRUCTURAL–METALLOGENIC ZONE SREDNA–GORA, BULGARIA

Svetlana N. Nenasheva
Fersman Mineralogical Museum RAS, Moscow, nenashevasn@mail.ru

Results of investigation of samples from the Chelopech deposit are compared with literature data. Minerals are discovered which have very similar optical features and elemental composition to fahlore, enargite and luzonite. However, their formulae are not electroneutral by calculation per 29 atoms in the unit cell or per the fahlore formula. They become electroneutral only by recalculation per larger numbers of atoms in the unit cell (32, 33 and 34 atoms). It is assumed that these are new mineral species similar in optical properties and chemical composition to fahlore, enargite and luzonite. They have following idealized formulae: $Cu^{+}_{11}Me^{2+}_{3}(Te^{4+},\Pi Me^{3+})_4S_{16}$, $Cu^{+}_{11}Me^{2+}_{2}Me^{3+}\Pi Me^{3+}_{4}S_{15}$, $Cu^{+}_{10}Me^{2+}_{3}(Te^{4+},\Pi Me^{3+})_4S_{16}$, $Cu^{+}_{8}Cu^{2+}_{2}Fe^{2+}_{3}As_4S_{15}$, $Cu^{+}_{8}Cu^{2+}_{3}Fe^{2+}_{2}As_4S_{15}$, $Cu^{+}_{2}Cu^{2+}_{3}As_2S_7$ (Me is the metals, ΠMe is the semimetals).
Goldfieldite and Te-tetrahedrite containing more than 24 wt.% tellurium are commonly heterogenous. They contain very small segregations of native tellurium. Moreover, tellurium may enter the sulfur position in their structure.
8 tables, 10 references.
Keywords: fahlore, enargite, luzonite, isomorphism, deposits Chelopech, Radka, Elshitsa.

The copper-pyrite deposits of Chelopech, Radka and Elshitsa are located in the central part of the Sredna-Gora structural-metallogenic zone in the ore region of Panagyurishte. This zone is characterized by the presence of copper- and iron-ore deposits of different genetic types, connected with Late Cretaceous volcanism and Laramide (Upper Cretaceous) intrusions. Copper mineralization is typical for the ore region of Panagyurishte. Two morphogenetic types of deposits are distinguished: copper-porphyritic and copper-pyrite. The Chelopech, Radka and Elshitsa deposits are of the copper-pyrite type. Ore lodes of pyrite composition (Elshitsa deposit), copper-pyrite and polymetallic copper-pyrite compositions (Chelopech and Radka deposits) are distinguished. The deposits were formed in the Late Cretaceous, associated with andesitic dacitic volcanism. They belong to the volcano-hydrothermal type (Bogdanov, 1984). Ore bodies of band-like and stock-like form are steeply dipping and are related to two subparallel volcanic zones striking north-west. They are related to dacitic or andesitic agglomerate tuffs or to contacts of these tuffs with dike-like bodies of rhyodacite. Ore bodies formed in two stages: pyrite (iron pyrite) related to dacitic volcanism, and polymetallic copper-pyrite related to subvolcanic rhyodacite.

According to V.A. Kovalenker *et al.* (1986), the following mineral paragenesises (zones in order of formation) may be distinguished at the Chelopech deposit: chalcopyrite-tennantite-pyrite, chalcopyrite-tennantite, luzonite-enargite-pyrite, and bornite-pyrite. At the Radka deposit, the first zone is eroded and the second and the third zones are exhausted. Only the first zone has been investigated at the Elshitsa deposit. About 50 hypogenic ore minerals were discovered in these deposits (Table 1). Among them there are the rare germanium minerals: briartite $Cu_8(Fe,Zn)_4Ge_4S_{16}$, germanite $Cu^{+}_{10}Me^{2+}_{3,0}Fe^{3+}_{1,0}Ge^{4+}_{2,0}As^{5+}_{1,0}S_{16}$, renierite $Cu^{+}_{10}ZnFe^{3+}_{4}Ge_2S_{16}$, the arsenic analogue of renierite $Cu_{10}Fe_4As_2S_{16}$, and $Cu_{11}Fe_4GeAsS_{16}$. According to L.R. Bernstein (1986), the latter is the end member of the renieritic solid-solution $Cu^{+}_{10}ZnFe^{3+}_{4}Ge_2S_{16} - Cu^{+}_{11}Fe^{3+}_{4}Ge^{4+}As^{5+}S_{16}$. S.N. Nenasheva ($2003_2$) named this mineral "renierite II" $Cu^{+}_{11}Fe^{3+}_{4}Ge^{4+}As^{5+}S_{16}$. Moreover, she assumed that there are three germanites (not one): germanite I $Cu^{+}_{8}Me^{2+}_{3,5}Fe^{3+}_{1.5}Ge^{4+}_{2.5}As^{5+}_{0.5}S_{16}$, germanite II $Cu^{+}_{10}Me^{2+}_{3.0}Fe^{3+}_{1.0}Ge^{4+}_{2.0}As^{5+}_{1.0}S_{16}$ and germanite III $Cu^{+}_{11.0}Me^{2+}_{3.0}Fe^{3+}_{1.0}Ge^{4+}_{3.0}S_{16}$ (Nenasheva, 2003_1). Fahlores of these deposits have their own particular features. Kovalenker *et al.* (1986) presented 50 analyses of fahlores. However, their recalculation showed that formulae from several analyses are non-electroneutral when recalculated per 29 atoms in the unit cell. A formula is considered electroneutral when its balance of valences ($\pm\Delta$ = absolute value of deviation from zero) does not exceed 3%. Formulae from several analyses become electroneutral only when they are recalculated to 32,

Table 1. **Ore minerals of the Radka, Chelopech and Elshitsa deposits by V.A. Kovalenker *et al.* (1986)**

№	Mineral	Deposit			№	Mineral	Deposit		
		Radka	Chelopech	Elshitsa			Radka	Chelopech	Elshitsa
1	Aikinite		+*		25	Marcasite	+	+	+
2	Altaite		+	+*	26	Molibdenite	+*		
3	Arsenosulvanite	+*	+*		27	Mawsonite		+*	
4	Beegerite	+*			28	Nagyagite		+	
5	Betikhtinite	+	+	+	29	Nekrasovite		+*	
6	Bornite	+	+	+	30	Pyrite	+	+	+
7	Briartite	+			31	Renierite	+	+	
8	Vinciennite	+*			32	$Cu^{+}_{10}Fe^{3+}_{4}As^{5+}_{2}S_{16}$	+*		
9	Bismuthine		+		33	$Cu^{+}_{11}Fe^{3+}_{4}Ge^{4+}As^{5+}S_{16}$	+*		
10	Wittichenite	+*	+		34	Rocesite	+*		
11	Galenite	+	+	+	35	Sylvanite		+	+
12	Gallite	+	+		36	Stannite	+	+	
13	Germanite	+			37	Sphalerite	+	+	+
14	Goldfieldite		+*	+*	38	Native tellurium		+	+*
15	Digenite	+	+		39	Tellurobismuthite		+	+
16	Native gold	+	+	+	40	Tennantite	+	+	+
17	Idaite	+	+		41	Tetradymite	+	+	+
18	Cassiterite			+	42	Tetrahedrite	+*	+	
19	Clausthalite		+*		43	Famatinite		+	
20	Covelline	+	+	+	44	Chalcosine	+	+	+
21	Coloradoite		+*		45	Chalcopyrite	+	+	+
22	Colusite	+	+		46	Hemusite		+	
23	Kostovite		+		47	Eucairite		+	
24	Luzonite		+		48	Enargite	+	+	+

Note. + — Minerals firstly discovered at these deposits by V.A. Kovalenker with co-authors (1986). + — Minerals occurring in the ores of these deposits*

Table 2. **Recalculation of fahlore analyses from the Radka, Chelopech and Elshitsa deposits (Kovalenker *et al.*, 1986) to formulae containing different amounts of atoms in the unit cell**

	Radka					Chelopech				Elshitsa		
Association, zone	Number of an. overall	Number of analyses recalculated to 29, 32, 33, 34 atoms				Number of an. overall	Number of analyses recalculated to 29, 32, 33 atoms			Number of an. overall	Number of analyses recalculated to 29 and 33 atoms	
		29	32	33	34		29	32	33		29	33
Bornite-pyrite	15	11	2	1	1	3	2		1	Analyses are abcent. Zone has not been studed		
Luzonite-enargite-pyrite	Analyses are abcent. Zone is exhausted					6	2	2	2	Analyses are abcent. Zone has not been studed		
Chalcopyrite-tennantite	Analyses are abcent. Zone is exhausted					2	2			Analyses are abcent. Zone has not been studed		
Chalcopyrite-tennantite-pyrite	Analyses are abcent. Zone is eroded					7	4	1	2	17	15	2

Note. Depth of zones increases from chacopyrite-tennantite-pyrite to bornite-pyrite zone

33 or 34 atoms in the unit cell (Tables 2, 4—6). It is likely that these are new mineral species. The foregoing induced the author to further investigate fahlores and germanium mineralization from the Chelopech deposit.

Minerals from the Chelopech deposit

Three samples from the luzonite—enargite—pyrite zone (Ch-1, Ch-992, Ch-998) were given to the author by L.A. Pautov, A.A. Agakhanov and V.Yu. Karpenko. Ten microprobe analyses were done (Table 3) using a JEOL JXA-50A electron microprobe equipped with a TRACOR—Xr energy-dispersive spectrometer at a voltage of 20 kV and current of $30x10^{-9}$ nA (analysts L.A. Pautov and A.A. Agakhanov). Calculation of concentrations was done using a ZAF-correction routine. The following standards (analytical lines) were used: ZnS ($Zn_{K\alpha}$ and $S_{K\alpha}$), GaAs ($As_{K\alpha}$), $CuFeSnS_4$ ($Cu_{K\alpha}$, $Fe_{K\alpha}$), synthetic Sb_2S_3 ($Sb_{K\alpha}$).

As a result of the investigation, the following minerals were identified:

1) Enargite (Table 3, analyses Ch-1-1, Ch-992-5, Ch-998-2). In reflected light, it is grayish-blue with very weak double reflection and strong anisotropy (color changes from dark reddish-brown to greenish-yellow). There is no cleavage or twinning. Analyses were recalculated to 8 atoms in the unit cell. $Cu^+Cu^{2+}_2AsS_4$ is idealized formula.

2) Luzonite (Table 3, analyses Ch-1-2, Ch-992-4). In reflected light, the mineral is light-gray to lilac with very weak double reflection and strong anisotropy (color changes from brown-red to green). Polysynthetic twinning is common. Analyses were recalculated to 8 atoms in the unit cell. $Cu^+Cu^{2+}_2AsS_4$ is idealized formula.

3) Tennantite is the blue and isotropic phase (Table 3, analysis Ch-998-1), occurring in association with bornite, chalcopyrite, pyrite and enargite. Recalculation to 29 atoms in the unit cell gives $Cu^+_{10.77}(Fe^{2+}_{0.70}Zn_{0.74})_{1.44}As_{4.07}S_{12.73}$ or $Cu^+_{10.8}(Fe^{2+}, Zn)_{1.4}As_{4.1}S_{12.7}$.

4) An additional phase occurs in association with enargite and luzonite, and has similar optical properties. Three analyses (Table 3, analyses Ch-1-3, Ch-1-4, Ch-1-5) were recalculated to 14 atoms in the unit cell. The average analysis gives $Cu^+_{2.00}Cu^{2+}_{3.13}Fe^{2+}_{0.09}As_{1.83}S_{6.95}$. $Cu^+_2Cu^{2+}_3As_2S_7$ is the ideal formula. We could not obtain an X-ray diffractogram of the mineral because of its intimate intergrowth with enargite and luzonite and of their similar optical characteristics.

5) A bluish isotropic phase (Table 3, analysis Ch-992-1) recalculated to $Cu^+_{8.00}Cu^{2+}_{3.00}Fe^{2+}_{2.00}(As_{4.06}Sb_{0.10})^{3+}_{4.16}S_{14.84}$ with 33 atoms in the unit cell. $Cu^+_8Cu^{2+}_3Fe^{2+}_2As_4S_{15}$ is idealized formula.

6) A grayish-bluish isotropic phase (Table 3, analysis Ch-992-2) was recalculated to $Cu^+_{8.00}Cu^{2+}_{2.44}(Zn_{0.53}Fe^{2+}_{2.23})_{2.76}(As_{3.81}Sb_{0.18})^{3+}_{3.99}S_{15.20}$ with 32 atoms in the unit cell. $Cu^+_8Cu^{2+}_2Fe^{2+}_3As_4S_{15}$ is idealized formula. According to their compositions, phases Ch-992-1 and Ch-992-2 may be the same $Cu^+_8(Cu^{2+},Fe^{2+})_5As_4S_{15}$ composition, but they occur close to each other with a definite boundary between them. Unfortunately, the segregations of the mineral are very small, and we cannot measure its X-ray diffraction pattern.

Phases Ch-992-1 and Ch-992-2 are optically similar to each other and to tennantite.

So, in addition to the minerals established by optical characterization and microprobe analysis: enargite, luzonite, tennantite, pyrite, chalcopyrite, and bornite (analyses of the last three are usual, and are not presented), we obtained analyses of three other phases of the following compositions: $Cu^+_2Cu^{2+}_3As_2S_7$, $Cu^+_8Cu^{2+}_3Fe^{2+}_2As_4S_{15}$, $Cu^+_8Cu^{2+}_2Fe^{2+}_3As_4S_{15}$, all of which are similar to each other (and to fahlore) in optical properties.

Kovalenker *et al.* (1986) presented 18 analyses of fahlores from the Chelopech deposit. Their recalculation to 29 atoms in the unit cell showed that among the fahlores of the chalcopyrite—tennantite—pyrite zone, 4 analyses (Table 4, analyses 3, 4, 5, 9) gave electroneutral formulae. Formulae for analyses 1 and 2 (Table 4) became electroneutral on recalculation to 33 atoms in the unit cell if some tellurium is considered to enter the sulfur position. Analysis 7 (Table 4) was recalculated to a formula with 32 atoms in the unit cell. It is necessary to note that, during recalculation of analyses 1 and 2 (Table 4) to a formula with 33 atoms in the unit cell, tellurium was assigned not only as Te^{4+} at the ΠMe (semimetal) position, but also as Te^{2-} in the S position. The basis for this is the fact that the amount of atoms at the ΠMe position significantly exceeds 4, and the amount of S is low compared to the formulae of complex sulfides of germanium (which are presumably analogues of these antimony-arsenic minerals). Such distribution of tellurium to different positions does not contradict the crystal-chemical features of tellurium. Minerals containing Te^{2-} at sulfur positions (for example, kervelleite $Ag^+_4Te^{2-}S$, aleksite $PbBi_2(Te_2S_2)_{\Sigma 4}$, sedlebakite $Pb_2Bi_2Te_2S_3$, and poubaite $Pb_3Bi_6(Te_4Se_6S_2)_{\Sigma 12}$ and minerals containing tellurium at both cation and anion positions (for example, nagyagite-(Te^{4+}) $Au_{2,5+x}Pb_{22+y}Te^{4+}_6\square_2(S,Te^{2-})_{35,25+0,5x+y}$; (Godovikov, 1997,

Table 3. **Recalculation of analyses of samples from the Chelopech deposit**

№ analysis of mineral phase		Cu	Fe	Zn	As	Sb	S	∑	Mineral
Ch-1-1	wt.%	47.43	0.36	–	18.63	–	32.31	98.72	Enargite
	apfu	2.97	0.03	–	0.99	–	4.01	8.00	
Ch-1-2	wt.%	49.16	0.76	–	20.39	–	33.60	103.92	Luzonite
	apfu	2.94	0.05	–	1.03	–	3.98	8.00	
Ch-1-3	wt.%	47.67	0.46	–	20.03	–	31.84	100	?
	apfu	5.20	0.06	–	1.85	–	6.89	14.00	
Ch-1-4	wt.%	47.14	0.91	–	19.47	–	32.52	100.04	?
	apfu	5.11	0.11	–	1.79	–	6.99	14.00	
Ch-1-5	wt.%	46.82	0.85	–	19.99	–	32.34	100	?
	apfu	5.09	0.10	–	1.84	–	6.96	13.99	
Average from three	wt.%	47.21	0.74		19.83		32.23	100.01	?
preceding analyses	apfu	5.13	0.09		1.83		6.95	14.00	
Ch-992-1	wt.%	43.57	6.94	–	18.95	0.76	29.66	99.88	Bluish,
	apfu	11.00	2.00	–	4.06	0.10	14.84	32.00	isotropic
Ch-992-2	wt.%	41.48	7.79	0.53	17.89	1.38	30.46	99.51	?
	apfu	10.44	2.23	0.13	3.81	0.18	15.20	31.99	
Ch-992-3	wt.%	38.16	10.88	–	17.50	0.83	32.91	100.28	?
	apfu	9.32	3.02	–	3.62	0.11	15.93	32.00	
Ch-992-4	wt.%	47.80	1.48	–	18.36	1.49	32.38	101.52	Luzonite
	apfu	2.94	0.10	–	0.96	0.05	3.95	8.00	
Ch-992-5	wt.%	46.34	2.21	0.46	19.92	–	32.37	101.31	Enargite
	apfu	2.84	0.15	0.03	1.04	–	3.94	8.00	
Ch-998-1	wt.%	46.25	2.62	3.25	20.60	–	27.57	100.29	Tennantite
	apfu	10.77	0.70	0.74	4.07	–	12.73	29.01	
Ch-998-2	wt.%	46.09	0.51	0.46	18.45	–	31.59	97.09	Enargite
	apfu	2.94	0.04	0.03	1.00	–	4.00	8.01	

№ analysis of mineral phase	Formula	Balance of valences, Δ	Δ, %
Ch-1-1	$Cu^{+}Cu^{2+}_{1.97}Fe^{2+}_{0.03}As_{0.99}S_{4.01}$	+7.97 - 8.02 = -0.05	0.6
Ch-1-2	$Cu^{+}Cu^{2+}_{1.94}Fe^{2+}_{0.05}As_{1.03}S_{3.98}$	+8.07 - 7.96 = +0.11	1.4
Ch-1-3	$Cu^{+}_{2}Cu^{2+}_{3.20}Fe^{2+}_{0.06}As_{1.85}S_{6.89}$	+14.07 - 13.78 = +0.29	2.0
Ch-1-4	$Cu^{+}_{2}Cu^{2+}_{3.11}Fe^{2+}_{0.11}As_{1.79}S_{6.99}$	+13.81 - 13.98 = -0.17	1.2
Ch-1-5	$Cu^{+}_{2}Cu^{2+}_{3.09}Fe^{2+}_{0.10}As_{1.84}S_{6.96}$	+13.90 - 13.92= -0.02	0.1
Average from three preceding analyses	$Cu^{+}_{2}Cu^{2+}_{3.13}Fe^{2+}_{0.09}As_{1.83}S_{6.95}$	+13.93 - 13.9 = +0.03	0.2
Ch-992-1	$Cu^{+}_{8.00}Cu^{2+}_{3.00}Fe^{2+}_{2.00}(As_{4.06}Sb_{0.10})^{3+}_{4.16}S_{14.84}$	+30.48 - 29.68 = +0.80	2.6
Ch-992-2	$Cu^{+}_{8.00}Cu^{2+}_{2.44}(Zn_{0.53}Fe^{2+}_{2.23})_{2.76}(As_{3.81}Sb_{0.18})^{3+}_{3.99}S_{15.20}$	+30.37 - 30.40 = -0.03	0.1
Ch-992-3	$Cu^{+}_{8.00}Cu^{2+}_{1.32}Fe^{3+}_{3.02}(As_{3.62}Sb_{0.11})^{3+}_{3.73}S_{15.93}$	+30.89 - 31.86 = -0.97	3.0
Ch-992-4	$Cu^{+}Cu^{2+}_{1.94}Fe^{2+}_{0.10}(As_{0.96}Sb_{0.05})_{1.01}S_{3.95}$	+8.11 - 7.90 = +0.21	2.6
Ch-992-5	$Cu^{+}Cu^{2+}_{1.84}(Fe^{2+}_{0.15}Zn_{0.03})_{0.18}As_{1.04}S_{3.94}$	+8.16 - 7.88 = +0.28	3.4
Ch-998-1	$Cu^{+}_{10.77}(Fe^{2+}_{0.70}Zn_{0.74})_{1.44}As_{4.07}S_{12.73}$	+25.86 - 25.46 = +0.40	1.5
Ch-998-2	$Cu^{+}Cu^{2+}_{1.94}Fe^{2+}_{0.04}Zn_{0.03}As_{1.00}S_{4.00}$	+8.02 - 8.00 = +0.02	0.0

Note. apfu – atoms per formula unit.

Table 4. **Recalculation of fahlore analyses from the Chelopech deposit given by V.A. Kovalenker *et al.* (1986)**

Zone	№	Cu	Fe	Zn	Sb	As	Te	Bi	Se	S	∑
Chp-ten-py	1	39.64	4.06	n.d.	2.01	2.48	26.16	0.34	n.d.	24.79	99.48
	2	40.30	3.87	n.d.	1.45	4.29	24.38	0.21	n.d.	24.90	99.40
	3	43.19	0.41	n.d.	7.50	2.73	17.64	n.d.	1.89	24.91	99.27
	4	45.34	0.51	0.45	2.26	6.42	17.64	0.69	0.19	25.82	99.32
	5	43.67	1.35	5.59	1.95	17.38	1.81	n.d.	n.d.	27.49	99.24
	7	42.08	1.98	6.19	4.52	16.79	n.d.	n.d.	n.d.	29.26	100.82
	9	42.73	1.83	6.21	3.98	17.81	n.d.	n.d.	n.d.	28.52	101.08
Chp-ten	17	42.79	4.87	1.51	9.15	13.87	n.d.	0.53	n.d.	27.67	100.30
	18	42.15	4.66	1.66	11.42	12.14	n.d.	0.44	n.d.	27.56	100.03
Lu-en-py	6	45.18	3.53	0.30	0.43	15.03	n.d.	7.30	0.11	27.40	99.28
	8	47.82	2.83	n.d.	1.77	17.63	n.d.	n.d.	1.74	28.43	100.22
	10	47.90	3.10	0.32	2.16	18.30	n.d.	0,17	0.23	27.94	100.12
	11	47.16	3.70	0.41	0.39	18.79	n.d.	0.64	0.20	29.44	100.73
	12	47.46	3.22	0.32	0.42	18.98	n.d.	n.d.	0.26	28.57	99.23
	13	46.58	3.08	0.11	3.19	19.03	n.d.	n.d.	1.02	27.47	100.48
Bn-py	14	48.04	2.28	1.36	0.47	20.27	n.d.	n.d.	n.d.	29.65	102.07
	15	44.23	3.55	2.30	2.19	17.92	n.d.	1.61	n.d.	28.15	99.95
	16	48.71	1.89	1.04	1.08	20.08	n.d.	n.d.	n.d.	28.54	101.34

Zone	№	n	Formula	Δ, %
Chp-ten-py	1	33	$Cu^{+}_{10}(Cu^{2+}_{1.93}Fe_{1.39})_{3.32}(Sb_{0.32}As_{0.63}Bi_{0.03}Te^{4+}_{3.02})_{4.00}(S_{14.78}Te^{2-}_{0.9})_{15.68}$	0.9
	2	33	$Cu^{+}_{10}(Cu^{2+}_{2.02}Fe_{1.31})_{3.33}(Sb_{0.22}As_{1.08}Bi_{0.02}Te^{4+}_{2.68})_{4.00}(S_{14.72}Te^{2-}_{0.94})_{15.66}$	0.0
	3	29	$Cu^{+}_{10}(Cu^{2+}_{1.43}Fe_{0.12})_{1.55}(Sb_{1.04}As_{0.61}Te^{4+}_{2.32})_{3.97}(S_{13.07}Se_{0.40})_{13.47}$	1.4
	4	29	$Cu^{+}_{11.60}(Fe_{0.15}Zn_{0.11})_{0.26}(Sb_{0.30}As_{1.39}Bi_{0.05}Te^{4+}_{2.25})_{3.99}(S_{13.10}Se_{0.04})_{13.14}$	0.2
	5	29	$Cu^{+}_{10}(Cu^{2+}_{0.40}Fe_{0.35}Zn_{1.29})_{2.05}(Sb_{0.24}As_{3.51}Te^{4+}_{0.21})_{3.96}S_{12.97}$	1.0
	7	32	$Cu^{+}_{8}Cu^{2+}_{2.80}(Zn_{1.54}Fe^{2+}_{0.52})_{2.06}(Sb_{0.60}As_{3.65})_{4.25}S_{14.88}$	2.3
	9	29	$Cu^{+}_{9.96}(Fe_{0.48}Zn_{1.41})_{1.89}(Sb_{0.46}As_{3.52})_{3.98}S_{13.17}$	2.5
Chp-ten	17	29	$Cu^{+}_{10}(Cu^{2+}_{0.23}Fe_{1.32}Zn_{0.35})_{1.90}(Sb_{1.14}As_{2.81}Bi_{0.04})_{3.99}S_{13.11}$	1.7
	18	29	$Cu^{+}_{10}(Cu^{2+}_{0.18}Fe_{1.28}Zn_{0.39})_{1.85}(Sb_{1.44}As_{2.49}Bi_{0.03})_{3.96}S_{13.19}$	3.0
Lu-en-py	6	33	$Cu^{+}_{11}(Cu^{2+}_{1.52}Fe_{0.11}Zn_{0.08})_{1.71}Fe^{3+}_{1.00}(Sb_{0.06}As_{3.53}Bi_{0.62})_{4.21}(S_{15.05}Se_{0.02})_{15.07}$	0.2
	8	32	$Cu^{+}_{8}Cu^{2+}_{3}(Cu^{2+}_{1.28}Fe_{0.83})_{2.11}(Sb_{0.24}As_{3.84})_{4.08}(S_{14.46}Se_{0.36})_{14.82}$	2.8
	10	29	$Cu^{+}_{10}(Cu^{2+}_{1.20}Fe_{0.82}Zn_{0.07})_{2.09}(Sb_{0.26}As_{3.63}Bi_{0.01})_{3.90}(S_{12.95}Se_{0.04})_{12.99}$	0.4
	11	32	$Cu^{+}_{8}Cu^{2+}_{3}(Cu^{2+}_{0.92}Fe_{1.06}Zn_{0.10})_{2.08}(Sb_{0.05}As_{4.03}Bi_{0.05})_{4.13}(S_{14.75}Se_{0.04})_{14.79}$	3.2
	12	33	$Cu^{+}_{11}(Cu^{2+}_{1.57}Fe_{0.35}Zn_{0.08})_{2.00}Fe^{3+}_{0.62}(Sb_{0.06}As_{4.26})_{4.32}(S_{15.00}Se_{0.06})_{15.06}$	1.0
	13	29	$Cu^{+}_{10}(Cu^{2+}_{0.96}Fe_{0.82}Zn_{0.02})_{1.80}(Sb_{0.39}As_{3.80})_{4.19}(S_{12.81}Se_{0.19})_{13.00}$	0.6
Bn-py	14	33	$Cu^{+}_{11}(Cu^{2+}_{1.37}Zn_{0.34})_{1.71}Fe_{0.67}(Sb_{0.06}As_{4.43})_{4.49}S_{15.13}$	1.2
	15	29	$Cu^{+}_{10}(Cu^{2+}_{0.42}Fe_{0.95}Zn_{0.53})_{1.90}(Sb_{0.27}As_{3.58}Bi_{0.12})_{3.97}S_{13.14}$	2.2
	16	29	$Cu^{+}_{10}(Cu^{2+}_{1.21}Fe_{0.49}Zn_{0.23})_{1.93}(Sb_{0.13}As_{3.92})_{4.05}S_{13.02}$	0.1

Note. Here and in the Tables 5 and 6 numbering of analyses is saved as in the work of V.A. Kovalenker with co-authors (1986); n – number of atoms in the unit cell; chp – chalcopyrite, ten – tennantite, py – pyrite, bn – bornite, lu – luzonite, en – enargite; n.d. – not detected

Godovikov and Nenasheva, 2007) are well-known in mineralogy.

Two analyses of fahlores from the chalcopyrite – tennantite zone (Table 4, analyses 17, 18) and two analyses from the luzonite – enargite – pyrite zone (Table 4, analyses 10 and 13) were recalculated to formulae with 29 atoms in the unit cell. Analyses 8 and 11 (Table 4) were recalculated to formulae with 32 atoms in the unit cell. This formula is close to the formula $Cu^{+}_{8}Cu^{2+}_{3}Fe^{2+}_{2}As^{3+}_{4}S_{15}$. Analyses 6 and 12 (Table 4) were recalculated to formulae with 33 atoms in the unit cell, close to the composition $Cu^{+}_{11}Me^{2+}_{2}Fe^{3+}As^{3+}_{4}S_{15}$. Analysis 14 (Table 4) of the mineral from the bornite – pyrite zone recalculates to this formula. Formulae for analyses 15 and 16 (Table 4), belonging to minerals from the same zone, are electroneutral on recalculation to 29 atoms per unit cell.

Fahlores of the Radka and Elshitsa deposits

At the Radka deposit, fahlores occur in three associations (tetrahedrite – tennantite, betekhtinite – bornite – sphalerite – galenite, and renierite – sphalerite – gallite) in ore bodies corresponding to the zone of bornite – pyrite ores at deep horizons of the Chelopech deposit. Other zones at the Chelopech deposit are eroded, or exhausted at the Radka deposit. Nine (of fifteen) analyses of fahlores (Table 5, analyses 1, 2, 5, 8, 9, 10, 13, 14, and 15) were recalculated to formulae with 29 atoms in the unit cell. Analyses 4 and 7 (Table 5) were recalculated to formulae with 32 atoms in the unit cell. Analyses 11 and 12 (Table 5) were recalculated to formulae with 33 and 34 atoms per cell, respectively. The formulae of analyses 3 and 6 (Table 5) are non-electroneutral because they have excess cations.

Seventeen analyses of fahlores from the Elshitsa deposit containing large amounts of tellurium occupy a special position. The formulae of two analyses (Table 6, analyses 14 and 15) are electroneutral on recalculation to the formula of fahlore, i.e. 29 atoms in the unit cell. Seven analyses (Table 6, analyses 1 – 6, 9) recalculate well to the formulae of goldfieldite only by excluding native tellurium in excess of four atoms of semimetals in the formula. The assumption that samples contain very fine inclusions of native tellurium is based on the statement of Kovalenker *et al.* (1986) that tennantite replaces goldfieldite as a result of native tellurium at this deposit. E.M. Spiridonov came to the same conclusion, based on investigation of fahlores from several volcanogenic deposits of Kazakhstan. He noticed that goldfieldite was replaced by tetrahedrite, native tellurium, and chalcopyrite (Spiridonov, 1987). Formulae for six analyses (Table 6, analyses 7, 8, 10 – 13) are electroneutral only after exclusion of native tellurium from the analyses and under the condition that all copper is monovalent. The assumption that all copper in Te-bearing fahlores is monovalent is based on the work of M.I. Novgorodova *et al.* (1978) who assumed that compensation of surplus charge in Te-bearing fahlores arising from the replacement $(As,Sb)^{3+} \rightarrow Te^{4+}$ occurs by vacancy formation. These vacancies are used by Cu^{+} as a path for diffusion. According to Mozgova and Tsepin (1983), a more probable explanation of surplus charge compensation in Te-bearing fahlores is connected with "depolarization at the expense of reduction of Cu^{2+} to Cu^{+} that limits the entrance of divalent metals into fahlores". As the formulae for these analyses are electroneutral under both conditions, one can conclude that all copper in these analyses is monovalent. Fahlores containing more than 24 wt.% tellurium may be recalculated to the same formula if we exclude native tellurium from the analyses. We recalculated a number of tellurium atoms which were excepted from every of analysis into wt.% Te and deducted its amount from total contents of Te. It was found that a tellurium can come into semimetals position up 18.8 to 23.13 wt.% Te, on the average 21.3 wt.%. That is only 21 wt.% Te can come into fahlores as isomorphous impurity. Fahlores isomorphically do not contain more than 21 wt.% tellurium. Formulae for the remaining analyses (Table 6, analyses 16 and 17) are electroneutral only on recalculation to 33 atoms in the unit cell.

Thus, 34 of 50 analyses of fahlore from the Chelopech, Radka and Elshitsa deposits are recalculated to formulae with 29 atoms in the unit cell (to the fahlore formula). Two analyses recalculate to non-electroneutral formulae. Fourteen analyses may be represented as electroneutral formulae with larger numbers of atoms in the unit cell (Table 7). From these analyses, five are recalculated to 32 atoms, eight to 33 atoms, and one is recalculated to 34 atoms in the unit cell. Ideal formulae for five analyses have the following formula $Cu^{+}_{8}(Cu^{2+}_{3}Me^{2+}_{2})_{5}\Pi Me^{3+}_{4}S_{15}$ (where Me is a metal, ΠMe is a semimetal), for two analyses $Cu^{+}_{10}Me^{2+}_{3}(Te^{4+},\Pi Me^{3+})_{4}S_{16}$, for six analyses $Cu^{+}_{11}Me^{2+}_{2}Me^{3+}\Pi Me^{3+}_{4}S_{15}$, and for one analysis $Cu^{+}_{11}Me^{2+}_{3}(\Pi Me^{3+},Te^{4+})_{4}S_{16}$ with 34 atoms in the unit cell.

Results

Formulae of the phases from the Chelopech deposit are compared with non-electroneutral

Table 5. **Recalculation of fahlore analyses from the Radka deposit given by V.A. Kovalenker *et al.* (1986)**

Association	№	Cu	Ag	Fe	Zn	Sb	As	Te	Bi	S	Σ
Tetr-ten	1	41.06	0.70	0.57	6.15	16.26	8.65	0.22	1.35	25.99	100.95
	2	41.00	1.27	1.20	5.97	14.80	9.05	0.57	1.25	26.46	101.57
	3	44.76	0.45	9.61	6.05	11.10	10.48	0.36	0.50	25.40	99.71
	15	42.77	0.45	1.66	6.62	10.84	11.77	n.d.	0.65	26.42	101.18
Bet-bn-sph-ga	4	41.71	n.d.	1.09	7.90	2.09	16.75	n.d.	0,96	29.53	100.03
	5	42.88	0.12	0.51	8.15	2.41	17.58	n.d.	n.d.	27.75	99.40
	6	44.18	n.d.	0.30	8.52	3.00	17.61	n.d.	n.d.	26.62	100.23
	7	41.68	n.d.	1.06	8.10	1.50	18.24	n.d.	0.74	29.72	101.04
	8	43.62	n.d.	0.27	8.35	2.74	18.51	n.d.	n.d.	28.28	101.77
	9	44.47	n.d.	0.28	8.41	2.25	18.77	n.d.	n.d.	28.06	102.24
	10	43.45	n.d.	0.11	7.63	2.98	18.85	n.d.	n.d.	27.98	101.00
	11	43.63	0.14	0.60	7.88	0.80	19.33	n.d.	n.d.	29.43	101.81
	12	42.98	0.13	0.13	8.40	2.45	19.45	n.d.	n.d.	29.09	102.63
	14	43.20	0.18	0.09	8.34	1.38	19.70	n.d.	n.d.	28.47	101.36
Re-sph-gall	13	42.51	0.10	4.06	4.15	0.80	19.60	n.d.	n.d.	28.21	99.43

Association	№	n	Formula	Δ, %
Tetr-ten	1	29	$(Cu^{+}_{9.90}Ag_{0.10})_{10.00}(Cu^{2+}_{0.38}Fe_{0.16}Zn_{1.47}Cd_{0.03})_{2.04}(Sb_{2.12}As_{1.83}Te^{4+}_{0.03}Bi_{0.10}Sn_{0.03})_{4.11}S_{12.85}$	2.9
	2	29	$(Cu^{+}_{9.82}Ag_{0.18})_{10.00}(Cu^{2+}_{0.29}Fe_{0.34}Zn_{1.43}Cd_{0.02})_{2.08}(Sb_{1.90}As_{1.89}Te^{4+}_{0.07}Bi_{0.09}Sn_{0.03})_{3.98}S_{12.95}$	1.3
	3	29	$(Cu^{+}_{9.94}Ag_{0.06})_{10.00}(Cu^{2+}_{1.14}Fe_{0.17}Zn_{1.46}Cd_{0.03}Hg_{0.01})_{2.81}(Sb_{1.43}As_{2.19}Te^{4+}_{0.04}Bi_{0.04}Sn_{0.02})_{3.72}S_{12.46}$	7.0
	15	29	$(Cu^{+}_{10.37}Ag_{0.06})_{10.42}(Fe_{0.46}Zn_{1.56})_{2.02}(Sb_{1.37}As_{2.42}Bi_{0.05})_{3.84}S_{12.70}$	2.2
Bet-bn-sph-ga	4	32	$Cu^{+}_{8}Cu^{2+}_{2.70}(Zn_{1.97}Fe_{0.32})_{2.29}(Sb_{0.28}As_{3.64}Bi_{0.07})_{3.99}S_{15.01}$	0.2
	5	29	$(Cu^{+}_{9.98}Ag_{0.02})_{10.00}(Cu^{2+}_{0.16}Fe_{0.14}Zn_{1.87})_{2.17}(Sb_{0.30}As_{3.53})_{3.83}S_{13.00}$	0.6
	6	29	$Cu^{+}_{10.00}(Cu^{2+}_{0.50}Fe_{0.08}Zn_{1.97})_{2.55}(Sb_{0.37}As_{3.55})_{3.92}S_{12.53}$	6.7
	7	32	$Cu^{+}_{8.00}Cu^{2+}_{2.59}(Zn_{2.00}Fe_{0.31})_{2.31}(Sb_{0.20}As_{3.93})_{4.13}S_{14.97}$	0.8
	8	29	$Cu^{+}_{10.00}(Fe_{0.07}Zn_{1.88})_{1.95}(Sb_{0.33}As_{3.64})_{3.97}S_{12.98}$	0.2
	9	29	$Cu^{+}_{10.26}(Fe_{0.07}Zn_{1.89})_{1.96}(Sb_{0.27}As_{3.67})_{3.94}S_{12.83}$	1.3
	10	29	$Cu^{+}_{10.16}(Fe_{0.03}Zn_{1.73})_{1.76}(Sb_{0.36}As_{3.74})_{4.10}S_{12.96}$	0.1
	11	33	$(Cu^{+}_{11}Ag_{0.02})_{11.02}(Cu^{2+}_{0.32}Zn_{1.99})_{2.31}Fe^{3+}_{0.18}(Sb_{0.11}As_{4.25})_{4.36}S_{15.13}$	3.3
	12	34	$(Cu^{+}_{10.98}Ag_{0.02})_{11.00}(Cu^{2+}_{0.54}Fe^{2+}_{0.04}Zn_{2.19})_{2.77}(Sb_{0.34}As_{4.42})_{4.76}S_{15.46}$	0.3
	14	29	$(Cu^{+}_{9.99}Ag_{0.02})_{10.01}(Fe_{0.02}Zn_{1.88})_{1.90}(Sb_{0.17}As_{3.86})_{4.03}S_{13.05}$	0.8
Re-sph-gall	13	29	$(Cu^{+}_{9.93}Ag_{0.01})_{9.94}(Fe_{1.08}Zn_{0.94})_{2.02}(Sb_{0.10}As_{3.88})_{3.98}S_{13.05}$	0.7

Note. Tetr — tetrahedrite, ten — tennantite, bn — bornite, bet — betekhtinite, sph — sphalerite, ga — galenite, re — renierite, gall — gallite. Including, in analysis 1 — Cd 0.20, Sn 0.22 , in analysis 2 — Cd 0.14, Sn 0.22, in analysis 3 — Cd 0.19, Sn 0,17, Hg 0.14, in analysis 10 — Cd 0.14

formulae of fahlores given in the work of V.A. Kovalenker *et al.* (1986) and recalculated here to electroneutral formulae containing 32, 33 or 34 atoms in the unit cell (Table 8). The analysis of the phase Ch-992-1 and five analyses of fahlores (three from the Chelopech deposit and two from the Radka deposit) may be recalculated to the same electroneutral formulae with 32 atoms: $Cu^{+}_{8}(Cu^{2+}_{3}Me^{2+}_{2})_{5}ΠMe^{3+}_{4}S_{15}$ per unit cell. It is an indication that similar analyses obtained by different authors on different material are not accidental. These analyses may be of some new mineral. Two analyses of minerals from the Chelopech deposit (Table 4, analyses 1 and 2), when recalculated to formulae with 29 atoms in the unit cell have the following valence-balance values: 12.7% and 6.0%, respectively. If they are recalculated to a formula containing 33 atoms in the unit cell, $Cu^{+}_{10}Me^{2+}_{3}(Te^{4+},Sb,As)_{4}S_{16}$, that can be compared with the formula of germanite II, $Cu^{+}_{10}Me^{2+}_{3.0}(Fe^{3+}_{1.0}Ge^{4+}_{2.0}As^{5+}_{1.0})_{4}S_{16}$ (Nenasheva,

Table 6. **Recalculation of fahlore analyses from the Elshitsa deposit given by V.A. Kovalenker *et al.* (1986)**

Zone	№	Cu	Fe	Zn	Sb	As	Te	Bi	S	∑
Chp-ten-py	1	42.48	0.27	n.d.	0.23	4.05	26.44	2.62	25.68	101.77
	2	44.95	0.16	n.d.	0.27	4.32	25.85	0.47	25.43	101.45
	3	43.38	0.39	n.d.	0.23	5.30	25.74	0.10	25.55	100.69
	4	43.62	0.42	n.d.	0.31	5.33	25.64	0.31	25.69	100.32
	5	42.71	0.64	n.d.	0.15	4.75	24.52	3.38	25.25	101.40
	6	42.49	0.55	n.d.	0.38	5.66	24.38	1.38	25.51	100.35
	7	44.72	0.15	n.d.	0.20	5.23	23.97	0.17	26.43	100.87
	8	43.35	0.20	n.d.	0.39	5.04	23.75	0.23	26.13	99.09
	9	43.07	1.03	n.d.	0.16	5.26	23.01	1.30	25.71	99.74
	10	45.15	0.63	0.04	0.20	6.39	22.31	0.14	26.72	101.58
	11	43.83	0.74	n.d.	0.16	6.44	22.07	n.d.	26.14	99.38
	12	44.83	0.13	n.d.	0.36	6.84	21.26	1.49	26.51	101.42
	13	44.47	0.26	n.d.	0.18	5.47	21.24	2.96	26.52	101.40
	14	46.56	0.20	n.d.	0.14	6.84	19.83	0.27	26.35	100.19
	15	46.33	4.76	0.25	n.d.	20.11	1.39	n.d.	29.00	101.84
	16	46.07	4.56	0.26	n.d.	20.04	0.13	n.d.	29.26	100.32
	17	46.17	4.61	0.23	n.d.	20.35	0.23	0.34	30.34	102.27

Zone	№	n	Formula	$Te_{nat.}^{*}$	Δ, %
Chp-ten-py	1	29	$Cu^{+}_{11.30}Fe_{0.08}[(Sb_{0.03}As_{0.91}Bi_{0.21})_{1.13}Te^{4+}_{2.92}]_{4.05}S_{13.54}$	0.57	2.0
	2	29	$Cu^{+}_{11.74}Fe_{0.05}[(Sb_{0.04}As_{0.96}Bi_{0.04})_{1.04}Te^{4+}_{3.01}]_{4.05}S_{13.17}$	0.35	2.4
	3	29	$Cu^{+}_{11.44}Fe_{0.12}[(Sb_{0.03}As_{1.19}Bi_{0.01})_{1.23}Te^{4+}_{2.85}]_{4.08}S_{13..36}$	0.52	0.2
	4	29	$Cu^{+}_{11.44}Fe_{0.12}[(Sb_{0.06}As_{1.19}Bi_{0.02})_{1.27}Te^{4+}_{2.81}]_{4.08}S_{13.35}$	0.53	0.1
	5	29	$Cu^{+}_{11.39}Fe_{0.19}[(Sb_{0.02}As_{1.07}Bi_{0.27})_{1.36}Te^{4+}_{2.71}]_{4.07}S_{13.34}$	0.54	0.3
	6	29	$Cu^{+}_{11.30}Fe_{0.17}[(Sb_{0.05}As_{1.28}Bi_{0.11})_{1.44}Te^{4+}_{2.65}]_{4..09}S_{13.44}$	0.57	1.2
	7	29	$Cu^{+}_{11.40}Fe_{0.04}[(Sb_{0.03}As_{1.13}Bi_{0.01})_{1.17}Te^{4+}_{3.04}]_{4.21}S_{13.35}$	0.00	1.6
		29	$Cu^{+}_{11.48}Fe_{0.04}[(Sb_{0.03}As_{1.14}Bi_{0.01})_{1.18}Te^{4+}_{2.85}]_{4.03}S_{13.44}$	0.21	1.4
	8	29	$Cu^{+}_{11.25}Fe_{0.06}[(Sb_{0.05}As_{1.11}Bi_{0.02})_{1.18}Te^{4+}_{3.07}]_{4.25}S_{13.44}$	0.00	1.1
		29	$Cu^{+}_{11.35}Fe_{0.06}[(Sb_{0.05}As_{1.12}Bi_{0.02})_{1.19}Te^{4+}_{2.84}]_{4.03}S_{13.56}$	0.25	2.6
	9	29	$Cu^{+}_{11.29}Fe_{0.31}[(Sb_{0.02}As_{1.17}Bi_{0.10})_{1.29}Te^{4+}_{2.75}]_{4.04}S_{13.36}$	0.26	0.9
	10	29	$Cu^{+}_{11.33}Fe_{0.18}Zn_{0.01}[(Sb_{0.03}As_{1.36}Bi_{0.01})_{1.40}Te^{4+}_{2.79}]_{4.19}S_{13.29}$	0.00	1.8
		29	$Cu^{+}_{11.41}Fe_{0.18}Zn_{0.01}[(Sb_{0.03}As_{1.37}Bi_{0.01})_{1.41}Te^{4+}_{2.62}]_{4.03}S_{13.38}$	0.19	0.9
	11	29	$Cu^{+}_{11.24}Fe_{0.22}[(Sb_{0.02}As_{1.40})_{1.42}Te^{4+}_{2.82}]_{4.24}S_{13.29}$	0.00	2.4
		29	$Cu^{+}_{11.34}Fe_{0.22}[(Sb_{0.02}As_{1.41})_{1.43}Te^{4+}_{2.60}]_{4.03}S_{13.40}$	0.24	1.2
	12	29	$Cu^{+}_{11.35}Fe_{0.04}[(Sb_{0.05}As_{1.47}Bi_{0.11})_{1.65}Te^{4+}_{2.68}]_{4.31}S_{13.30}$	0.00	1.6
		29	$Cu^{+}_{11.47}Fe_{0.04}[(Sb_{0.05}As_{1.48}Bi_{0.12})_{1.65}Te^{4+}_{2.40}]_{4.05}S_{13.44}$	0.31	2.9
	13	29	$Cu^{+}_{11.36}Fe_{0.08}[(Sb_{0.02}As_{1.18}Bi_{0.23})_{1.43}Te^{4+}_{2.70}]_{4.13}S_{13.42}$	0.00	0.8
		29	$Cu^{+}_{11.41}Fe_{0.08}[(Sb_{0.02}As_{1.19}Bi_{0.23})_{1.44}Te^{4+}_{2.58}]_{4.02}S_{13.48}$	0.13	2.0
	14	29	$Cu^{+}_{11.76}Fe_{0.06}[(Sb_{0.02}As_{1.46}Bi_{0.02})_{1.50}Te^{4+}_{2.49}]_{3.99}S_{13.19}$	0.00	0.15
	15	29	$Cu^{+}_{10}(Cu^{2+}_{0.56}Fe_{1.23}Zn_{0.06})_{1.85}(As_{3.89}Te^{4+}_{0.16})_{4.05}S_{13.10}$	0.00	0.7
	16	33	$Cu^{+}_{11}(Cu^{2+}_{1.01}Fe_{0.35}Zn_{0.07})_{1.43}Fe^{3+}_{1.00}(As_{4.43}Te^{4+}_{0.02})_{4.45}S_{15.12}$	0.00	0.0
	17	33	$Cu^{+}_{11}(Cu^{2+}_{0.79}Fe_{0.34}Zn_{0.05})_{1.18}Fe^{3+}_{1.00}(As_{4.41}Bi_{0.03}Te^{4+}_{0.03})_{4.47}S_{15.35}$	0.00	2.9

Note. $Te_{nat.}^{*}$ *– amount of atoms of tellurium in the formula excluded from the analysis, after it analysis is recalculated. Results of recalculation are presented in the column «Formula»*

Table 7. **Comparison of the formulae of analyses of phases from different deposits that could be recalculated to 32, 33 and 34 atoms per unit cell**

№ table	№	n	Formula	Δ, %
4	8	32	$Cu^{+}_{8}Cu^{2+}_{3}(Cu^{2+}_{1.28}Fe_{0.83})_{2.11}(Sb_{0.24}As_{3.84})_{4.08}(S_{14.46}Se_{0.36})_{14.82}$	2.8
4	7	32	$Cu^{+}_{8}Cu^{2+}_{2.80}(Zn_{1.54}Fe^{2+}_{0.52})_{2.06}(Sb_{0.60}As_{3.65})_{4.25}S_{14.88}$	2.3
4	11	32	$Cu^{+}_{8}Cu^{2+}_{3}(Cu^{2+}_{0.92}Fe_{1.06}Zn_{0.10})_{2.08}(Sb_{0.05}As_{4.03}Bi_{0.05})_{4.13}(S_{14.75}Se_{0.04})_{14.79}$	3.2
5	4	32	$Cu^{+}_{8}Cu^{2+}_{2.70}(Zn_{1.97}Fe_{0.32})_{2.29}(Sb_{0.28}As_{3.64}Bi_{0.07})_{3.99}S_{15.01}$	0.2
5	7	32	$Cu^{+}_{8}Cu^{2+}_{2.59}(Zn_{2.00}Fe_{0.31})_{2.31}(Sb_{0.20}As_{3.93})_{4.13}S_{14.97}$	0.8
4	1	33	$Cu^{+}_{10}(Cu^{2+}_{1.93}Fe_{1.39})_{3.32}(Sb_{0.32}As_{0.63}Bi_{0.03}Te^{4+}_{3.02})_{4.00}(S_{14.78}Te^{2-}_{0.90})_{15.68}$	1.9
4	2	33	$Cu^{+}_{10}(Cu^{2+}_{2.02}Fe_{1.31})_{3.33}(Sb_{0.22}As_{1.08}Bi_{0.02}Te^{4+}_{2.68})_{4.00}(S_{14.72}Te^{2-}_{0.94})_{15.66}$	o.o.
4	6	33	$Cu^{+}_{11}(Cu^{2+}_{1.52}Fe_{0.11}Zn_{0.08})_{1.71}Fe^{3+}_{1.00}(Sb_{0.06}As_{3.53}Bi_{0.62})_{4.21}(S_{15.05}Se_{0.02})_{15.07}$	0.2
4	12	33	$Cu^{+}_{11}(Cu^{2+}_{1.57}Fe_{0.35}Zn_{0.08})_{2.00}Fe^{3+}_{0.62}(Sb_{0.06}As_{4.26})_{4.32}(S_{15.00}Se_{0.06})_{15.06}$	1.0
4	14	33	$Cu^{+}_{11}(Cu^{2+}_{1.37}Zn_{0.34})_{1.71}Fe^{3+}_{0.67}(Sb_{0.06}As_{4.43})_{4.49}S_{15.13}$	1.2
5	11	33	$(Cu^{+}_{11}Ag_{0.02})_{11.02}(Cu^{2+}_{0.32}Zn_{1.99})_{2.31}Fe^{3+}_{0.18}(Sb_{0.11}As_{4.25})_{4.36}S_{15.13}$	3.3
6	16	33	$Cu^{+}_{11}(Cu^{2+}_{1.01}Fe_{0.35}Zn_{0.07})_{1.43}Fe^{3+}_{1.00}(As_{4.43}Te^{4+}_{0.02})_{4.45}S_{15.12}$	0.0
6	17	33	$Cu^{+}_{11}(Cu^{2+}_{0.79}Fe_{0.34}Zn_{0.05})_{1.18}Fe^{3+}_{1.00}(As_{4.41}Bi_{0.03}Te^{4+}_{0.03})_{4.47}S_{15.35}$	2.9
5	12	34	$(Cu^{+}_{10.98}Ag_{0.02})_{11.00}(Cu^{2+}_{0.54}Fe^{2+}_{0.04}Zn_{2.19})_{2.77}(Sb_{0.34}As_{4.42})_{4.76}S_{15.46}$	0.3

Table 8. **Comparison of formulae obtained during investigation of the Chelopech deposit with non-electroneutral formulae of fahlore analyses by V.A. Kovalenker *et al.* (1986) recalculated to electroneutral formulae containing 32, 33 and 34 atoms per the unit cell**

Formula	Amount of atoms in the unit cell	Number of analyses	Minerals, mineral phases
$Cu^{+}_{8}(Cu^{2+}_{3}Me^{2+}_{2})_{5}\Pi Me^{3+}_{4}S_{15}$	32	5	Fahlores, according to V.A. Kova-
$Cu^{+}_{10}Me^{2+}_{3}(Te^{4+},\Pi Me^{3+})_{4}S_{16}$	33	2	lenker with co-authors (1986)
$Cu^{+}_{11}Me^{2+}_{2}Me^{3+}\Pi Me^{3+}_{4}S_{15}$	33	6	Fahlores, according to V.A. Kova-
$Cu^{+}_{11}Me^{2+}_{3}(Te^{4+},\Pi Me^{3+})_{4}S_{16}$	34	1	lenker with co-authors (1986)
$Cu^{+}_{8}(Cu^{2+}_{3}Fe^{2+}_{2})_{5}As_{4}S_{15}$	32	1	Ch-992-1
$Cu^{+}_{8}(Cu^{2+}_{2}Fe^{2+}_{3})_{5}As_{4}S_{15}$	32	1	Ch-992-2
$Cu^{+}_{2}Cu^{2+}_{3}As_{2}S_{7}$	14	3	Ch-1-3, Ch-1-4, Ch-1-5

2003_1), also containing 33 atoms in the unit cell, their valence-balance becomes 1.9% and 1.1%, respectively. These formulae are similar, and $Cu^{+}_{10}Me^{2+}_{3.0}(Te^{4+},\Pi Me^{3+})_{4}S_{16}$ is probably a tellurium analogue of germanite II. Te-bearing fahlores in polished section are very pale pink. Germanite is also pink, and it is no wonder that two analyses of the Te-bearing mineral from the Chelopech deposit recalculate to the fahlore formula. The remaining analyses that are recalculated to the formulae $Cu^{+}_{11}Me^{2+}_{2}Me^{3+}(\Pi Me^{3+})_{4}S_{15}$ (6 analyses), $Cu^{+}_{11}Me^{2+}_{3}(Te^{4+},\Pi Me^{3+})_{4}S_{16}$, $Cu^{+}_{8}Cu^{2+}_{2}Fe^{2+}_{3}As_{4}S_{15}$ and $Cu^{+}_{2}Cu^{2+}_{3}As_{2}S_{7}$ (3 analyses) may be analyses of new minerals.

Conclusions

1. Minerals close in optical properties and elemental composition to fahlore, enargite and luzonite have been discovered in the deposits of the central part of the Sredna-Gora structural-metallogenous zone, Bulgaria. They have non-electroneutral formulae if recalculated to the fahlore formula (29 atoms in the unit cell). They are electroneutral only by recalculation to 32, 33 or 34 atoms in the unit cell. This suggests new mineral species optically and chemically similar to fahlore, enargite and luzonite with the following ideal formulae: $Cu^{+}_{10}Me^{2+}_{3}(Te^{4+},\Pi Me^{3+})_{4}S_{16}$, $Cu^{+}_{8}Cu^{2+}_{2}Fe^{2+}_{3}As_{4}S_{15}$, $Cu^{+}_{8}Cu^{2+}_{3}Fe^{2+}_{2}As_{4}S_{15}$, $Cu^{+}_{11}Me^{2+}_{2}Me^{3+}\Pi Me^{3+}_{4}S_{15}$, $Cu^{+}_{11}Me^{2+}_{3}(\Pi Me^{3+},Te^{4+})_{4}S_{16}$, $Cu^{+}_{2}Cu^{2+}_{3}As_{2}S_{7}$.

2. The tellurium analogue of germanite II may have been discovered — $Cu^{+}_{10}Me^{2+}_{3}(Te^{4+},Sb,As)_{4}S_{16}$.

3. Goldfieldites containing more than 24 wt.% of tellurium are commonly heterogenous. They contain native tellurium as fine admixtures. Formulae from their analyses

become electroneutral only after exclusion of native tellurium in excess of 4 atoms of semimetals in the formula, indicating that this tellurium is present as an admixture.

4. In Te-bearing fahlores (goldfieldite and Te-tetrahedrite), tellurium may enter the cation position (Te^{4+}) as well as the S position (Te^{2-}).

The author is grateful to L.A. Pautov, A.A. Agakhanov and V.Yu. Karpenko for supplying samples from the Chelopech deposit and L.A. Pautov and A.A. Agakhanov for the microprobe analyses.

References

Bogdanov B. Bulgaria // Mineral deposits of Europe. South-Eastern Europe. Moscow: Mir. **1984**. V. 2. P. 294—318. (in Russian).

Godovikov A.A. Structural-chemical systematics of minerals. Moscow: Fersman Mineralogical museum. **1997**. 247 p. (in Russian and English).

Godovikov A.A., Nenasheva S.N. Structural-chemical systematics of minerals. Moscow: ECOST. **2007**. 295 p. (in Russian and English).

Kovalenker V.A., Tsonev D., Breskovska V.V., Malov V.S., and Troneva N.V. New data on mineralogy of the copper-pyrite deposits of central Sredna-Gora of Bulgaria // Metasomatism, mineralogy, and problems of genesis of gold and silver deposits. Moscow: Nauka. **1986**. P. 91—110. (in Russian).

Mozgova N.N. and Tsepin A.I. Fahlores. Moscow: Nauka. **1983**. 279 p.

Nenasheva S.N. On the composition of germanite // New data on minerals. Moscow: ECOST. **2003_1**. Vol. 38. P. 34—40. (in Russian and English).

Nenasheva S.N. Complex sulfides of germanium and their interrelations // Zap. VMO. **2003_2**. Vol. CXXXII. № 5. P. 59—65. (in Russian).

Novgorodova M.M., Tsepin A.I., and Dmitrieva M.T. A new isomorphic row in the fahlores group // Zapiski Vses. Mineral. Obschestva. **1978**. № 1. P. 100—110. (in Russian).

Spiridonov E.M. Typomorphic peculiarities of fahlores of some plutogenic, volcanogenic, and telethermal deposits of gold // Geol. Ore Dep. **1987**. № 6. P. 83—92. (in Russian).

Bernstein L.R. Renierite, $Cu^{+}_{10}ZnFe^{3+}_{4}Ge_2S_{16}$ — $Cu^{+}_{11}Fe^{3+}_{4}Ge^{4+}As^{5+}S_{16}$ a coupled solid solutions series // Amer. Mineral. **1986**. V. 71. P. 210—221.

PECULIARITIES OF COMPOSITION OF Te–BEARING FAHLORES

Svetlana N. Nenasheva
Fersman Mineralogical Museum RAS, Moscow, nenashevasn@mail.ru

The possibility of new mineral species close in optical and chemical features to fahlores is shown in the article. Their idealized formulae, calculated with 32 and 33 atoms in a unit cell, are as follows: $Cu^{+}_{11}Me^{2+}_{1.00}Me^{3+}_{1.00}\Pi Me_{4.00}S_{15}$ and $Cu^{+}_{10}Me^{2+}_{3.00}\Pi Me_{4.00}S_{16}$. It is assumed that they are germanium-free analogues of complex sulfides of germanium (germanite, renierite, briartite). Moreover, the character of tellurium in Te-bearing fahlores from volcanogenic and hydrothermal quartz-sulfide vein deposits of gold – sulfide formation is considered. It is shown that tellurium may enter both cation (Te^{4+}) and anion positions (Te^{2-}) in goldfieldite and Te-bearing tetrahedrite. Goldfieldites containing more than 24 wt.% tellurium are heterogenous as a rule, and contain native tellurium as a very fine admixture. Te-bearing fahlores with a high content of silver (7 – 13 wt.%) may contain admixtures of fine-grained kervelleite Ag_4TeS.
7 tables, 12 references.
Keywords: fahlores, isomorphism, goldfieldite, tetrahedrite, complex sulfides of germanium, kervelleite.

Te-bearing fahlores are characteristic of many volcanogenic and hydrothermal quartz-sulfide vein deposits of gold – sulfide formation. Samples from such deposits were investigated by many researchers: Ransome *et al.* (1909), Frenzel *et al.* (1975), Novgorodova *et al.* (1978), Mozgova and Tsepin (1983), Spiridonov (1987), Spiridonov and Badalov (1983), Sakharova *et al.* (1984), Kovalenker *et al.* (1980, 1986) and Borisova *et al.* (1986). The samples are from the following deposits: Goldfield (Nevada, USA), Calabona (Sardinia island, Italy), Butte (USA), Koch-Bulak (Kuraminsky ridge, Uzbekistan), Kunashir (Kuril Islands, Russia), deposits of the Kamchatka peninsula (Russia), Bulgarian deposits (Chelopech, Radka, Elshitsa). The similarity of geological position and structure of ore bodies of several of the above-mentioned deposits is shown in Table 1.

As was shown during investigation of ore samples from the copper pyrite deposit of Chelopech (see the article of S.N. Nenasheva in this issue), microprobe analyses of optically identified fahlores gave non-electroneutral formulae for recalculation on 29 atoms per unit cell. It is assumed that the average formula of fahlore is $Cu_{12}\Pi Me_4S_{13}$, and that the conventional formula is $Cu^{+}_{10}Me^{2+}_{2}\Pi Me_4S_{13}$ (Mozgova and Tsepin, 1983). Formulae with a balance of valences (Δ – is the absolute value of deviation from zero) not exceeding 3% were considered to be electroneutral. Electroneutrality was obtained only for recalculation on a larger number of atoms in the unit cell, namely 32, 33, 34 (see Table 8 in the article of S.N. Nenasheva in this issue): $Cu^{+}_{8}Cu^{2+}_{2}Fe^{2+}_{3}As_4S_{15}$, $Cu^{+}_{8}Cu^{2+}_{3}Fe^{2+}_{2}As_4S_{15}$, $Cu^{+}_{11}Me^{2+}_{2}Me^{3+}\Pi Me^{3+}_{4}S_{15}$, $Cu^{+}_{11}Me^{2+}_{3}(\Pi Me^{3+}, Te^{4+})_4S_{16}$. Perhaps they are new mineral species. In this connection, literature analyses of Te-bearing fahlores from other deposits (102 analyses altogether) were recalculated. Some of these analyses recalculated to non-electroneutral formulae. Unfortunately, the authors did not give the valence balance. There are two possible explanations of this fact: (1) the authors did not pay attention to valence balance, and so it was not calculated; (2) the authors neglected this data. In my opinion, one can publish only analyses with electroneutral formulae. If a formula is non-electroneutral, it is necessary to explain this phenomenon. Due to the fact that almost all recalculated analyses were given without X-ray characterization, it is possible that these analyses did not belong to fahlores, or the analyzed material was heterogeneous. In some cases during recalculation of formulae and calculation of valence balance, tellurium was assigned not only as Te^{4+} in the position of ΠMe but also as Te^{2-} occupying the position of sulfur. The result of this action is that the amount of atoms at the position ΠMe in these analyses significantly exceeds 4 and the amount of S is very low.

In fahlores (goldfieldite and high-tellurium tetrahedrite) containing more than 20 wt.% tellurium, the distribution of tellurium into different positions does not contradict the crystallochemical features of tellurium. We know the following minerals containing Te^{2-} in the position of sulfur: kervelleite $Ag^{+}_{4}Te^{2-}S$, aleksite $PbBi_2(Te_2S_2)_{\Sigma 4}$, sedlebakite $Pb_2Bi_2Te_2S_3$, and poubaite $Pb_3Bi_6(Te_4Se_6S_2)_{\Sigma 12}$. We also know minerals where tellurium enters both cation and anion positions, for example, nagyagite-(Te^{4+}) $Au_{2.5+x}Pb_{22+y}Te^{4+}_{6}\square_2(S,Te^{2-})_{35.25+0.5x+y}$.

Table 1. **Brief characteristics of the deposits where Te-bearing fahlores occur**

Deposit	Geological setting of deposit	Characteristics of ore bodies
Goldfield, Nevada, USA	Ores are deposited within the Early Tertiary volcanogenic construction of the central type among the silificated dacites	Abundance of sulfides, native gold, tellurides. Fahlores of the tetrahedrite-goldfieldite series are characteristic to the later mineral association
Calabona, Island Sardinia, Italy	Copper porphyric deposit, connected with Post-Triassic Pre-Oligocene dioritic stock within the silificated Triassic limestones	Subvertical intensively weathered lenses of copper ores
Butte, Montana, USA	Hydrothermal quartz-sulfide vein deposit	Sulfide ores contain pyrite, chalcopyrite, chalcocite, fahlores, bornite, enafgite
Kayragach, Kuraminsky ridge, Eastern Uzbekistan	Deposit is located in the caldera of Carboniferous age filled by volcanites connected with secondary quartzites (Spiridonov *et al.*, 1983)	Ore bodies are represented by intersecting calcite-quartz with barite moderate sulfide veins among secondary quartzites
Koch-Bulak, Kuraminsky ridge, Uzbekistan	Ore field is located within one of the satellites of multi-channel central type paleovolcans composed of volcanogenic rocks of andesite and felsite composition	Gold-sulfide-quartz mineralization is connected with the final stage of Lower Triassic acid volcanism procedded after formation of large batholith-like intusions of Middle and Upper Carboniferous age
Deposits of the volcanic belt of Central Kamchatka	Veins and mineralized zones of crushing connected with volcanic structure of Neogene age (Sakharova *et al.*, 1984)	Gold-bearing quartz veins with sulfides and tellurides. Goldfieldite occurs in association with chalcopyrite, pyrite, and native tellurium
Chelopech, Radka, Elshitse, Bulgaria	Copper pyrite deposites are located in the central part of structure-metallogenic zone Sredna Hora. They are formed in the Late Cretaceous in tight connection with andesite-dacititic volcanism. It is attributed to the volcano-hydrothermal type (Bogdanov, 1984)	Ore bodies of band-like and stock-like form are steeply dipping and are connected with dacitic and andesitic agglomerate tuffs. They contain about 50 hypogene ore minerals: besides ordinary sulfides there are fahlores, rare minerals of germanium, tellurides
Oziornoye, Kamchatka	Volcanogenic deposit (Spiridonov, Okrugin, 1985)	Selenium and tellurium bearing fahlore forms metasomatic ingrowths up to 0.1 mm in size in quartz in association with telluroselenides and selenides of Bi and Ag
Gold ore deposit of the East of the USSR	Oligocene and Miocene tuffs of andesites and andesito-basalts with intersecting Early Miocene gabbro-diorites of subvolcanic massif contain ore mineralization (Borisova *et al.*, 1986)	Hydrothermal quartz and quartz-sulfide veins and veinlets with sulfides: sphalerite, galenite, fahlores, and chalcopyrite

Results of recalculation

Recalculated analyses and valence balance of fahlores from the Koch-Bulak deposit are shown in Table 2. These analyses were given by Novgorodova *et al.* (1978). Fifteen of the 32 analyses given in Table 2 (analyses 1, 2, 3, 4, 5, 6, 7, 8, 12, 14, 15, 20, 22, 23 and 27) may be recalculated as electroneutral conventional formula $Cu^{+}_{10}Me^{2+}_{2}\Pi Me_4S_{13}$. Formulae for 5 analyses (analyses 11, 18, 19, 21 and 32) are non-electroneutral. Formulae of analyses from the former list (11, 21 and 32) have valence balance 3.5, 3.1 and 3.2%, and analyses (18 and 19) have 17 and 16.5% valence balance, respectively. They lack S (less than 12 atoms per formula unit) and have much Ag. Attempts to represent Ag as kervelleite, Ag_4TeS, and to recalculate the analyses were unsuccessful. Balance of valences became better, but was 11.4 and 11.7%, respectively, exceeding the norm (3%). The rest of the analyses were recalculated to electroneutral formulae under different conditions: (1) taking some tellurium as Te^{2-} at the S position (analyses 9, 10, 13, 16, 17 and 25). Analysis 17 was recalculated in two ways: (a) tellurium exceeding 4 atoms in the formula at the ΠMe position was assumed to be Te^{2-}, and

Table 2. **Recalculation of analyses of fahlores from the Koch-Bulak deposit given by M.I. Novgorodova *et al.* (1978) to formulae and calculation of their valence balance**

№	Cu	Fe	Zn	Sn	Ag	Sb	As	Te	S	∑
1	42.99	4.01	0.23	1.58	0.20	19.95	7.24	0.07	26.12	102.40
2	38.93	1.13	6.39	0.00	0.28	25.03	3.50	0.11	25.21	100.59
3	43.08	2.95	0.19.	2.42	0.23	20.77	6.68	0.19	25.70	102.21
4	41.13	5.76	0.70	0.43	0.08	19.70	7.66	0.19	26.29	101.94
5	42.79	2.56	0.15	2.81	0.26	21.13	6.52	0.21	25.46	101.88
6	41.13	0.38	6.99	0.00	0.16	16.83	9.19	0.22	26.85	101.86
7	40.17	2.29	4.41	0.00	0.37	25.02	3.50	0.42	25.43	101.61
8	43.65	2.39	0.13	2.95	0.18	19.25	7.43	0.69	25.72	102.38
9	40.46	0.60	5.71	0.00	0.14	25.57	2.69	1.45	24.33	100.95
10	40.84	0.55	5.56	0.00	0.15	24.84	2.75	1.87	24.17	100.73
11	43.48	0.32	4.23	0.00	0.25	15.85	5.30	6.83	25.44	101.70
12	42.59	1.35	1.64	0.00	0.09	17.86	2.76	7.49	24.56	98.34
13	43.02	1.47	1.50	0.00	0.21	17.55	3.56	7.61	24.32	99.24
14	43.91	0.65	3.37	0.00	0.25	12.58	6.44	8.41	26.72	102.23
15	44.46	1.25	1.05	0.00	0.26	16.35	3.15	9.41	25.44	101.37
16	45.41	0.37	1.62	0.00	0.15	15.29	2.64	11.48	25.39	102.35
17	41.80	0.25	1.12	0.00	0.26	14.26	2.53	12.49	23.79	96.50
18	36.53	5.44	1.28	0.00	7.81	10.66	3.23	12.55	22.19	99.69
	36.53	5.44	1.28	0.00	0.00	10.66	3.23	10.24	21.61 + $Te_{nat.}$	88.99
19	37.49	5.40	1.05	0.00	6.34	10.40	3.01	12.81	22.15	98.65
	37.49	5.40	1.05	0.00	0.00	10.40	3.01	10.94	21.68 + $Te_{nat.}$	89.97
20	44.94	0.33	0.29	0.00	0.18	12.88	2.80	14.04	25.57	101.03
21	47.04	0.65	0.00	0.00	0.21	10.99	3.96	14.51	24.52	101.88
22	45.96	0.05	0.11	0.00	0.00	11.63	1.63	14.98	26.03	100.42
23	44.63	2.22	0.15	0.00	0.52	9.06	2.93	15.50	25.70	100.71
24	46.68	0.10	0.16	0.00	0.09	11.00	2.90	15.57	24.98	101.48
25	47.68	0.04	0.00	0.00	0.06	7.76	4.90	16.32	24.54	101.29
26	45.98	0.06	0.05	0.01	0.86	7.93	4.65	16.79	25.36	101.69
27	44.82	0.82	0.00	0.00	0.20	7.97	2.54	19.11	25.63	101.09
28	44.93	0.17	0.00	0.04	0.60	6.87	2.88	21.76	25.32	102.57
29	42.98	0.39	0.06	0.00	1.03	7.15	1.28	22.21	24.52	99.62
30	44.49	0.31	0.00	0.00	0.71	5.23	2.60	23.06	24.34	100.74
31	44.36	0.29	0.00	0.03	0.94	6.32	2.31	23.69	25.25	103.20
32	44.51	0.45	0.00	0.00	1.49	5.40	2.21	24.09	24.41	102.55

№	Formula	$Te_{nat.}$ apfu	Δ, %
1	$(Cu^{+}_{10.65}Ag_{0.03})_{10.68}(Fe_{1.13}Zn_{0.05}Sn_{0.21})_{1.39}(Sb_{2.58}As_{1.52}Te^{4+}_{0.01})_{4.11}S_{12.82}$	0.00	0.6
2	$(Cu^{+}_{10.02}Ag_{0.04})_{10.06}(Fe_{0.33}Zn_{1.60})_{1.93}(Sb_{3.36}As_{0.76}Te^{4+}_{0.01})_{4.13}S_{12.86}$	0.00	2.3
3	$(Cu^{+}_{10.81}Ag_{0.03})_{10.84}(Fe_{0.84}Zn_{0.05}Sn_{0.32})_{1.21}(Sb_{2.72}As_{1.42}Te^{4+}_{0.02})_{4.16}S_{12.78}$	0.00	0.5
4	$(Cu^{+}_{10.14}Ag_{0.01})_{10.15}(Fe_{1.62}Zn_{0.17}Sn_{0.06})_{1.85}(Sb_{2.54}As_{1.60}Te^{4+}_{0.02})_{4.16}S_{12.85}$	0.00	2.4
5	$(Cu^{+}_{10.83}Ag_{0.04})_{10.87}(Fe_{0.74}Zn_{0.04}Sn_{0.38})_{1.16}(Sb_{2.79}As_{1.40}Te^{4+}_{0.03})_{4.22}S_{12.77}$	0.00	1.3
6	$(Cu^{+}_{10.07}Ag_{0.02})_{10.09}(Fe_{0.11}Zn_{1.66})_{1.77}(Sb_{2.15}As_{1.91}Te^{4+}_{0.04})_{4.10}S_{13.03}$	0.00	0.3
7	$(Cu^{+}_{10.23}Ag_{0.06})_{10.29}(Fe_{0.66}Zn_{1.09})_{1.75}(Sb_{3.32}As_{0.76}Te^{4+}_{0.05})_{4.13}S_{12.83}$	0.00	2.2
8	$(Cu^{+}_{10.93}Ag_{0.03})_{10.96}(Fe_{0.68}Zn_{0.03}Sn_{0.40})_{1.11}(Sb_{2.52}As_{1.58}Te^{4+}_{0.09})_{4.19}S_{12.76}$	0.00	1.2
9	$(Cu^{+}_{10.54}Ag_{0.02})_{10.56}(Fe_{0.18}Zn_{1.45})_{1.63}(Sb_{3.48}As_{0.59})_{4.07}(S_{12.56}Te^{2-}_{0.19})_{12.75}$	0.00	2.0
10	$(Cu^{+}_{10.66}Ag_{0.02})_{10.68}(Fe_{0.16}Zn_{1.41})_{1.57}(Sb_{3.38}As_{0.61}Te^{4+}_{0.01})_{4.00}(S_{12.51}Te^{2-}_{0.23})_{12.74}$	0.00	1.4
11	$(Cu^{+}_{10.99}Ag_{0.04})_{11.03}(Fe_{0.09}Zn_{1.04})_{1.13}(Sb_{2.09}As_{1.14}Te^{4+}_{0.86})_{4.09}S_{12.75}$	0.00	3.5
	$(Cu^{+}_{10.99}Ag_{0.04})_{11.03}(Fe_{0.09}Zn_{1.04})_{1.13}(Sb_{2.09}As_{1.14}Te^{4+}_{0.77})_{4.00}(S_{12.75}Te^{2-}_{0.09})_{12.84}$	0.00	1.5
12	$(Cu^{+}_{11.25}Ag_{0.01})_{11.26}(Fe_{0.42}Zn_{0.41})_{0.83}(Sb_{2.46}As_{0.62}Te^{4+}_{0.99})_{4.07}S_{12.85}$	0.00	1.6
13	$(Cu^{+}_{11.30}Ag_{0.03})_{11.33}(Fe_{0.44}Zn_{0.38})_{0.82}(Sb_{2.41}As_{0.79}Te^{4+}_{0.80})_{4.07}(S_{12.66}Te^{2-}_{0.2})_{12.86}$	0.00	0.2

14	$(Cu^{+}_{10.86}Ag_{0.04})_{10.90}(Fe_{0.81}Zn_{0.18})_{0.99}(Sb_{1.62}As_{1.35}Te^{4+}_{1.04})_{4.01}S_{13.10}$	0.00	0.9
15	$(Cu^{+}_{11.37}Ag_{0.04})_{11.41}(Fe_{0.36}Zn_{0.26})_{0.62}(Sb_{2.18}As_{0.68}Te^{4+}_{1.20})_{4.06}S_{12.90}$	0.00	0.9
16	$(Cu^{+}_{11.58}Ag_{0.02})_{11.60}(Fe_{0.11}Zn_{0.40})_{0.51}(Sb_{2.03}As_{0.57}Te^{4+}_{1.40})_{4.00}(S_{12.83}Te^{2-}_{0.06})_{12.89}$	0.00	2.3
17	$(Cu^{+}_{11.41}Ag_{0.04})_{11.45}(Fe_{0.08}Zn_{0.30})_{0.38}(Sb_{2.03}As_{0.59}Te^{4+}_{1.38})_{4.00}(S_{12.87}Te^{2-}_{0.32})_{13.19}$	0.00	3.0
	$(Cu^{+}_{11.41}Ag_{0.04})_{11.45}(Fe_{0.08}Zn_{0.30})_{0.38}(Sb_{2.03}As_{0.59}Te^{4+}_{1.57})_{4.17}(S_{12.87}Te^{2-}_{0.13})_{13.00}$	0.00	1.1
18	$(Cu^{+}_{9.89}Ag_{1.25})_{11.14}(Fe_{1.68}Zn_{0.34})_{2.02}(Sb_{1.51}As_{0.74}Te^{4+}_{1.69})_{3.94}S_{11.91}$	0.00	17.0
	$Cu^{+}_{10.57}(Fe_{1.79}Zn_{0.36})_{2.15}(Sb_{1.61}As_{0.79}Te^{4+}_{1.48})_{3.88}S_{12.40}$ + 10.7 мас.% Ag_4TeS	0.00	11.4
19	$(Cu^{+}_{10.20}Ag_{1.02})_{11.22}(Fe_{1.67}Zn_{0.28})_{1.95}(Sb_{1.48}As_{0.69}Te^{4+}_{1.74})_{3.91}S_{11.94}$	0.00	16.5
	$Cu^{+}_{10.76}(Fe_{1.76}Zn_{0.29})_{2.05}(Sb_{1.55}As_{0.73}Te^{4+}_{1.56})_{3.84}S_{12.33}$ + 8.68 мас.% Ag_4TeS	0.00	11.7
20	$(Cu^{+}_{11.59}Ag_{0.03})_{11.62}(Fe_{0.10}Zn_{0.07})_{0.17}(Sb_{1.73}As_{0.61}Te^{4+}_{1.80})_{4.14}S_{13.07}$	0.00	0.08
21	$(Cu^{+}_{12.09}Ag_{0.03})_{12.12}Fe_{0.19}(Sb_{1.47}As_{0.86}Te^{4+}_{1.67})_{4.00}(S_{12.49}Te^{2-}_{0.19})_{12.68}$	0.00	3.1
22	$Cu^{+}_{11.83}(Fe_{0.01}Zn_{0.03})_{0.04}(Sb_{1.56}As_{0.36}Te^{4+}_{1.92})_{3.84}S_{13.28}$	0.00	4.6
	$Cu^{+}_{10.00}(Cu^{2+}_{1.83}Fe_{0.01}Zn_{0.03})_{1.87}(Sb_{1.56}As_{0.36}Te^{4+}_{1.92})_{3.84}S_{13.28}$	0.00	2.3
23	$(Cu^{+}_{11.47}Ag_{0.08})_{11.55}(Fe_{0.65}Zn_{0.04})_{0.69}(Sb_{1.21}As_{0.64}Te^{4+}_{1.97})_{3.82}S_{13.02}$	0.00	0.9
24	$(Cu^{+}_{12.04}Ag_{0.01})_{12.05}(Fe_{0.03}Zn_{0.04})_{0.07}(Sb_{1.48}As_{0.63}Te^{4+}_{1.89})_{4.00}(S_{12.77}Te^{2-}_{0.11})_{12.88}$	0.00	1.2
	$(Cu^{+}_{12.08}Ag_{0.01})_{12.09}(Fe_{0.03}Zn_{0.04})_{0.07}(Sb_{1.49}As_{0.64}Te^{4+}_{1.89})_{4.02}S_{12.81}$ + $Te_{nat.}$	0.11	2.1
25	$(Cu^{+}_{12.27}Ag_{0.01})_{12.28}Fe_{0.01}(Sb_{1.04}As_{1.07}Te^{4+}_{1.89})_{4.00}(S_{12.51}Te^{2-}_{0.20})_{12.71}$	0.00	2.9
26	$(Cu^{+}_{11.77}Ag_{0.13})_{11.90}(Fe_{0.02}Zn_{0.01})_{0.03}(Sb_{1.06}As_{1.01}Te^{4+}_{1.93})_{4.00}(Te^{2-}_{0.21}S_{12.86})_{13.07}$	0.00	1.0
	$(Cu^{+}_{11.85}Ag_{0.13})_{11.98}(Fe_{0.02}Zn_{0.01})_{0.03}(Sb_{1.07}As_{1.02}Te^{4+}_{1.94})_{4.03}S_{12.96}$ + $Te_{nat.}$	0.21	0.6
27	$(Cu^{+}_{11.55}Ag_{0.03})_{11.58}Fe_{0.24}(Sb_{1.07}As_{0.56}Te^{4+}_{2.45})_{4.08}S_{13.10}$	0.00	2.0
28	$(Cu^{+}_{11.58}Ag_{0.09})_{11.67}(Fe_{0.05}Sn_{0.01})_{0.06}(Sb_{0.92}As_{0.63}Te^{4+}_{2.45})_{4.00}(S_{12.93}Te^{2-}_{0.34})_{13.27}$	0.00	1.1
	$(Cu^{+}_{11.72}Ag_{0.09})_{11.81}(Fe_{0.05}Sn_{0.01})_{0.06}(Sb_{0.94}As_{0.64}Te^{4+}_{2.48})_{4.06}S_{13.08}$ + $Te_{nat.}$	0.34	1.6
29	$(Cu^{+}_{11.48}Ag_{0.16})_{11.64}(Fe_{0.12}Zn_{0.02})_{0.14}(Sb_{1.00}As_{0.29}Te^{4+}_{2.71})_{4.00}(S_{12.98}Te^{2-}_{0.24})_{13.22}$	0.00	0.7
	$(Cu^{+}_{11.58}Ag_{0.16})_{11.74}(Fe_{0.12}Zn_{0.02})_{0.14}(Sb_{1.00}As_{0.29}Te^{4+}_{2.74})_{4.03}S_{13.09}$ + $Te_{nat.}$	0.24	2.5
30	$(Cu^{+}_{11.87}Ag_{0.11})_{11.98}Fe_{0.09}(Sb_{0.73}As_{0.59}Te^{4+}_{2.60})_{3.92}(S_{12.87}Te^{2-}_{0.13})_{13.00}$ + $Te_{nat.}$	0.33	2.0
31	$(Cu^{+}_{11.45}Ag_{0.14})_{11.59}Fe_{0.08}(Sb_{0.85}As_{0.51}Te^{4+}_{2.64})_{4.00}(S_{12.92}Te^{2-}_{0.40})_{13.32}$	0.00	0.9
	$(Cu^{+}_{11.61}Ag_{0.14})_{11.75}Fe_{0.09}(Sb_{0.86}As_{0.51}Te^{4+}_{2.69})_{4.06}S_{13.09}$ + $Te_{nat.}$	0.40	2.3
32	$(Cu^{+}_{11.63}Ag_{0.23})_{11.86}Fe_{0.13}(Sb_{0.74}As_{0.49}Te^{4+}_{2.77})_{4.00}(S_{12.64}Te^{2-}_{0.37})_{13.01}$	0.00	3.2

Note. Here and further in the tables Te_{nat} apfu corresponds with amount of Te atoms per formula unit excluded from the analysis, after this operation analysis is recalculated. Result of recalculation is presented in the column "Formula". Δ, % — corresponds with balance of valences.

(b) the amount of Te^{2-} was equal to the number of atoms lacking for 13 in the anion position; (2) deduction of tellurium exceeding 4 atoms per formula in the ΠMe position, assuming it to be an admixture of native tellurium (analysis 30). Formulae for analyses 24, 26, 28, 29 and 31 are electroneutral under both conditions.

Analyses of Te-bearing fahlores from different deposits are presented in Table 3. Besides the usual elements in fahlores, there are some analyses containing Au, Bi and Pb. According to the data of Mozgova and Tsepin (1983), Pb may enter the position of the semimetals. Analyses 1, 3, 6, 7, 9 and 14 calculate to the fahlore formula. Formulae for analyses 5, 8, 10 and 11 are electroneutral assuming some tellurium enters the sulfur position. Two analyses became electroneutral where native tellurium in amounts exceeding 4 atoms per formula was excluded. Analyses 12, 13 and 15 contain much Ag that is not characteristic for goldfieldite. The formulae became electroneutral if all Ag is assumed to be present as kervelleite, Ag_4TeS. This mineral is poorly diagnosed in thin section and resembles fahlore in reflected light (bluish-white with greenish shade, isotropic). This mineral was discovered in 1990 as very thin (about 30 micron) rims around acanthite in hessite, and it is difficult to distinguish from these minerals in polished section. Of course, one cannot say unambiguously that all Ag in Te-bearing fahlores occurs as admixed kervelleite, but there are some grounds for this possibility: (1) analyses 12, 13 and 15 containing more than 10 wt.% of tellurium also contain much copper and silver, much Me^{2+} and less sulfur; (2) the difficulty in identifying kervelleite because of its optical similarity with fahlore. These facts suggest that analyses 12, 13 and 15 were obtained from material with inclusions of some additional mineral, possibly kervelleite.

Analyses of Te-bearing fahlores (Table 4) from the Kayragach deposit (analyses 1—7, Spiridonov and Badalov, 1983) and Oziornoye (analyses 8—11, Spiridonov and Okrugin, 1985) contain Bi, Sn and Se in addition to the regularly occurring elements. If they are recalculated, as proposed by Spiridonov (1987), to

Table 3. **Recalculation of analyses of fahlores given by N.N. Mozgova and A.I. Tsepin (1983) and V.A. Kovalenker *et al.* (1980) to formulae and calculation of their valence balance**

№	Cu	Fe	Zn	Sn	Ag	Sb	As	Te	S	∑	Author, Deposit
1	47.60	–	–	–	–	1.30	8.10	17.00	26.00	100.00	Springer, Butte
2	46.54	0.04	0.76	–	0.30	5.08	7.09	15.59	25.13	100.53	Mozgova *et al.*, 1983 Kunashir
3*	45.39	0.20	0.20		0.02	9.44	3.25	15.48	25.52	100.30	Kovalenker, Kochbulak, 1980
4[2]*	43.15	1.06	0.24	–	0.03	11.66	2.27	15.47	24.39	100.32	Kovalenker, Kochbulak, 1980
5	46.41	0.13	0.58	–	0.56	6.71	5.38	15.45	24.62	99.84	Mozgova *et al.*, 1983 Kunashir
6	47.1	0.3	–	–	–	9.90	3.0	15.2	25.9	101.4	Frenzel *et al.*, 1975
7[3]*	44.85	1.18	0.22	0.04	0.52	13.46	1.67	14.77	25.57	102.14	Kovalenker, Kochbulak, 1980
8[4]*	42.55	1.08	0.64	0.04	–	11.98	3.10	14.71	24.91	100.70	Kovalenker, Kochbulak, 1980
9[5]*	43.94	0.45	0.37	0.04	–	11.35	2.43	14.71	24.90	98.91	Kovalenker, Kochbulak, 1980
10[6]*	42.53	2.60	0.78	0.03	0.05	10.22	3.59	14.62	24.90	101.57	Kovalenker, Kochbulak, 1980
11	46.06	0.04	1.02	–	0.09	7.80	5.41	14.04	24.86	99.32	Mozgova *et al.*, 1983 Kunashir
12[7]*	36.59	4.68	1.14	–	7.76	11.40	2.71	13.48	23.32	101.26	Kovalenker, Kochbulak, 1980
13[8]*	34.91	6.63	1.09	0.27	8.14	9.73	3.35	13.03	22.90	100.63	Kovalenker, Kochbulak, 1980
14	44.17	0.98	1.00	–	0.48	17.00	–	12.10	25.06	100.86	Kovalenker, Kochbulak, 1980
15[9]*	30.05	7.24	1.64	0.11	12.92	11.70	2.46	11.17	20.08	98.96	Kovalenker, Kochbulak, 1980

№	Formula	$Te_{nat.}$ apfu	Δ,%
1	$Cu^{+}_{11.99}(Sb_{0.17}As_{1.73}Te^{4+}_{2.13})_{4.03}S_{12.98}$	0.00	0.9
2	$(Cu^{+}_{11.87}Ag_{0.04})_{11.93}(Fe_{0.01}Zn_{0.19})_{0.20}(Sb_{0.68}As_{1.53}Te^{4+}_{1.98})_{4.19}S_{12.70}$	0.00	4.4
	$(Cu^{+}_{11.95}Ag_{0.04})_{11.99}(Fe_{0.01}Zn_{0.19})_{0.20}(Sb_{0.68}As_{1.54}Te^{4+}_{1.79})_{4.01}S_{12.79} + Te_{nat.}$	0.20	2.4
3	$Cu^{+}_{11.75}(Fe_{0.06}Zn_{0.05})_{0.11}(Sb_{1.28}As_{0.71}Bi_{0.06}Te^{4+}_{2.00})_{4.05}S_{13.09}$	0.00	0.2
4	$(Cu^{+}_{11.45}Au_{0.09})_{11.54}(Fe_{0.32}Zn_{0.06})_{0.38}(Pb_{0.02}Sb_{1.61}As_{0.51}Bi_{0.06}Te^{4+}_{2.04})_{4.22}S_{12.82}$	0.00	5.2
	$(Cu^{+}_{11.54}Au_{0.09})_{11.63}(Fe_{0.32}Zn_{0.06})_{0.38}(Pb_{0.02}Sb_{1.63}As_{0.51}Bi_{0.06}Te^{4+}_{1.84})_{4.06}S_{12.92} + Te_{nat.}$	0.22	2.2
5	$(Cu^{+}_{12.02}Ag_{0.08})_{12.10}(Fe_{0.04}Zn_{0.14})_{0.18}(Sb_{0.91}As_{1.18}Te^{4+}_{1.99})_{4.08}S_{12.63}$	0.00	5.4
	$(Cu^{+}_{12.02}Ag_{0.08})_{12.10}(Fe_{0.04}Zn_{0.14})_{0.18}(Sb_{0.91}As_{1.18}Te^{4+}_{1.81})_{3.90}(S_{12.63}Te^{2-}_{0.18})_{12.81}$	0.00	1.3
6	$Cu^{+}_{11.98}Fe_{0.09}(Sb_{1.31}As_{0.65}Te^{4+}_{1.92})_{3.88}S_{13.05}$	0.00	1.4
7	$(Cu^{+}_{11.48}Ag_{0.08}Au_{0.01})_{11.57}(Fe_{0.34}Zn_{0.05}Sn_{0.01})_{0.40}(Sb_{1.80}As_{0.36}Te^{4+}_{1.88})_{4.04}S_{12.98}$	0.00	1.6
8	$(Cu^{+}_{11.16}Au_{0.14})_{11.30}(Fe_{0.32}Zn_{0.16}Sn_{0.01})_{0.49}(Sb_{1.64}As_{0.69}Te^{4+}_{1.92})_{4.25}S_{12.95}$	0.00	3.9
	$(Cu^{+}_{11.16}Au_{0.14})_{11.30}(Fe_{0.32}Zn_{0.16}Sn_{0.01})_{0.49}(Sb_{1.64}As_{0.69}Te^{4+}_{1.87})_{4.20}(S_{12.95}Te^{2-}_{0.05})_{13.00}$	0.00	2.2
9	$(Cu^{+}_{11.67}Au_{0.06})_{11.73}(Fe_{0.14}Zn_{0.10}Sn_{0.01})_{0.25}(Sb_{1.56}As_{0.54}Te^{4+}_{1.94})_{4.04}S_{13.04}$	0.00	0.8
10	$(Cu^{+}_{11.01}Ag_{0.01}Au_{0.19})_{11.21}(Fe_{0.76}Zn_{0.20})_{0.96}(Sb_{1.38}As_{0.79}Te^{4+}_{1.88})_{4.05}S_{12.77}$	0.00	6.0
	$(Cu^{+}_{11.01}Ag_{0.01}Au_{0.19})_{11.21}(Fe_{0.76}Zn_{0.20})_{0.96}(Sb_{1.38}As_{0.79}Te^{4+}_{1.65})_{3.82}(S_{12.77}Te^{2-}_{0.23})_{13.0}$	0.00	0.9
11	$(Cu^{+}_{11.92}Ag_{0.01})_{11.93}(Fe_{0.01}Zn_{0.26})_{0.27}(Sb_{1.05}As_{1.19}Te^{4+}_{1.81})_{4.05}S_{12.75}$	0.00	3.5
	$(Cu^{+}_{11.92}Ag_{0.01})_{11.93}(Fe_{0.01}Zn_{0.26})_{0.27}(Sb_{1.05}As_{1.19}Te^{4+}_{1.76})_{4.00}(S_{12.75}Te^{2-}_{0.05})_{12.80}$	0.00	2.4
12	$(Cu^{+}_{9.75}Ag_{1.22}Au_{0.01})_{10.98}(Fe_{1.42}Zn_{0.30})_{1.72}(Sb_{1.58}As_{061}Te^{4+}_{1.79})_{3.98}S_{12.32}$	0.00	12.5
	$(Cu^{+}_{10.40}Au_{0.01})_{10.41}(Fe_{1.51}Zn_{0.32})_{1.83}(Sb_{1.69}As_{0.66}Te^{4+}_{1.49})_{3.74}(S_{12.81}Te^{2-}_{0.19})_{13.00} + 10.57$ mas.% Ag_4TeS	0.00	2.9
13	$(Cu^{+}_{9.34}Ag_{1.28}Au_{0.05})_{10.67}(Fe_{2.02}Zn_{0.28}Sn_{0.04})_{2.34}(Sb_{1.36}As_{0.76}Te^{4+}_{1.74})_{3.86}S_{12.14}$	0.00	15.3
	$Cu^{+}_{10.00}(Fe_{2.16}Zn_{0.30})_{2.46}(Sb_{1.45}As_{0.81}Te^{4+}_{1.17})_{3.43}(S_{12.66}Te^{2-}_{0.34})_{13.00} + 11.15$ mas.% Ag_4TeS	0.00	1.4
14	$(Cu^{+}_{11.53}Ag_{0.07})_{11.60}(Fe_{0.29}Zn_{0.25})_{0.54}(Sb_{2.32}Te^{4+}_{1.57})_{3.89}S_{12.96}$	0.00	0.0
15	$(Cu^{+}_{8.58}Ag_{2.17}Au_{0.07})_{10.82}(Fe_{2.35}Zn_{0.45}Sn_{0.02})_{2.82}(Sb_{1.74}As_{0.60}Bi_{0.08}Te^{4+}_{1.59})_{4.01}S_{11.35}$	0.00	24.5
	$(Cu^{+}_{9.68}Au_{0.07})_{9.75}(Fe_{2.65}Zn_{0.51}Sn_{0.02})_{3.18}(Sb_{1.97}As_{0.67}Bi_{0.08}Te^{4+}_{0.34})_{3.06}(S_{12.16}Te^{2-}_{0.84})_{13.0} + 17.32$ mas.% Ag_4TeS	0.00	1.4

*Note. Including in: *) Bi 0.80; [2]*) Bi 0.81, Au 1.03, Pb 0.21; [3]*) Au 0.12; [4]*) Au 1.69; [5]*) Au 0.72; [6]*) Au 2.26; [7]*) Au 0.15; [8]*) Au 0.58; [9]*) Au 0.72, Bi 0.87*

the formula $(Cu,Ag)_{10.00}(Cu^{2+},Fe,Zn)_{2.00}(Sb,As,Te^{4+},Bi,Sn)_{4.00}S_{13.00}$, only two analyses (analyses 1 and 7) have electroneutral formulae. Valence balance of the analyses exceeds 3%. Eight analyses (analyses 3–6, 8–11) have electroneutral formulae if all copper is assumed to be monovalent. The formula for analysis 2 is non-electroneutral; it is deficient in sulfur. According to Spiridonov and Badalov (1983), high arsenious and high bismuth tellurium ores of the Kayragach deposit formed at "specific conditions from hydrothermal solutions rich in tellurium and bismuth with very high activity of sulfur and simultaneously with elevated oxidizing potential".

Recalculation of fahlore analyses from deposits of the volcanic belt of Central Kamchatka (Sakharova *et al.*, 1983) and calculation of valence balance shows that only four analyses (analyses 1, 4, 5, 6) have electroneutral formulae. The formula for analysis 2 became electroneutral by exclusion of 0.14 atoms per formula of native tellurium (i.e., 1.06 wt.%). The formula for analysis 3 is non-electroneutral because of an excess of cations. It becomes electroneutral after the deduction of 0.05 atoms per formula of native tellurium and recalculation of the analysis assigning Te^{2-} to the sulfur position. Goldfieldite in this deposit occurs in quartz veins as small xenomorphic aggregates in association with chalcopyrite, pyrite and native tellurium. Native tellurium forms xenomorphic tear-shaped and veinlet aggregates in chalcopyrite and goldfieldite. The presence of goldfieldite

Table 4. **Recalculation of analyses of fahlores from the Kayragach deposit (analyses 1—7, Spiridonov *et al.*, 1983) and Oziornoye deposit (analyses 8—11, Spiridonov *et al.*, 1985) to formulae and calculation of their valence balance**

№	Cu	Fe	Zn	Sn	Ag	Sb	As	Te	Bi	Ge	S	∑
1	43.86	4.77	0.62	0.04	0.16	14.14	6.91	2.58	1.58	0.13	27.00	101.79
2	40.73	5.01	0.57	0.07	0.17	14.76	6.85	2.73	1.61	0.06	24.95	97.51
3	42.84	3.73	0.71	0.11	1.12	14.63	4.89	5.02	1.74	0.14	25.21	100.24
4	42.13	3.77	0.72	0.15	1.32	13.94	5.33	5.39	3.96	0.14	25.64	102.69
5	41.25	3.82	0.67	0.12	1.27	14.47	5.74	5.59	3.18	0.15	25.76	102.02
6	41.94	3.86	0.50	0.15	2.11	12.88	4.50	6.38	5.78	0.17	25.24	102.50
7	42.18	2.04	0.49	0.16	1.90	12.39	4.12	7.27	5.24	0.18	25.51	101.48
8	44.6	–	–	–	0.1	2.7	6.2	16.2	0.2		20.7	101.0
9	43.6	0.1	0.8	–	0.2	2.9	6.1	16.0	1.2	12.2	20.0	103.1
10	44.4	–	–	–	0.1	3.5	6.0	15.9	0.1	11.5	19.5	101.1
11	44.1	0.1	–	–	–	2.7	7.5	14.7	0.3	9.9	20.1	99.4

№	Formula	Δ, %
1	$(Cu^{+}_{9.98}Ag_{0.02})_{10.00}(Cu^{2+}_{0.74}Fe_{1.33}Zn_{0.15})_{2.22}(Sb_{1.80}As_{1.43}Bi_{0.12}Te^{4+}_{0.31}Ge_{0.03}Sn_{0.01})_{3.70}S_{13.08}$	1.0
2	$(Cu^{+}_{9.97}Ag_{0.03})_{10.00}(Cu^{2+}_{0.66}Fe_{1.49}Zn_{0.14})_{2.22}(Sb_{2.01}As_{1.52}Bi_{0.13}Te^{4+}_{0.35}Ge_{0.01}Sn_{0.01})_{4.03}S_{12.68}$	6.2
	$(Cu^{+}_{10.63}Ag_{0.03})_{10.66}(Fe_{1.49}Zn_{0.14})_{1.63}(Sb_{2.01}As_{1.52}Bi_{0.13}Te^{4+}_{0.35}Ge_{0.01}Sn_{0.01})_{4.03}S_{12.68}$	3.9
3	$(Cu^{+}_{9.83}Ag_{0.17})_{10.00}(Cu^{2+}_{1.13}Fe_{1.08}Zn_{0.18})_{2.39}(Sb_{1.95}As_{1.06}Bi_{0.14}Te^{4+}_{0.64}Ge_{0.03}Sn_{0.01})_{3.83}S_{12.78}$	5.2
	$(Cu^{+}_{10.96}Ag_{0.17})_{11.13}(Fe_{1.08}Zn_{0.18})_{1.26}(Sb_{1.95}As_{1.06}Bi_{0.14}Te^{4+}_{0.64}Ge_{0.03}Sn_{0.01})_{3.83}S_{12.78}$	1.0
4	$(Cu^{+}_{9.80}Ag_{0.20})_{10.00}(Cu^{2+}_{0.84}Fe_{1.08}Zn_{0.18})_{2.10}(Sb_{1.84}As_{1.18}Bi_{0.30}Te^{4+}_{0.68}Ge_{0.03}Sn_{0.02})_{4.05}S_{12.84}$	5.2
	$(Cu^{+}_{10.64}Ag_{0.20})_{10.84}(Fe_{1.08}Zn_{0.18})_{1.26}(Sb_{1.84}As_{1.18}Bi_{0.30}Te^{4+}_{0.68}Ge_{0.03}Sn_{0.02})_{4.05}S_{12.84}$	2.1
5	$(Cu^{+}_{9.81}Ag_{0.19})_{10.00}(Cu^{2+}_{0.65}Fe_{1.10}Zn_{0.16})_{1.91}(Sb_{1.91}As_{1.23}Bi_{0.24}Te^{4+}_{0.70}Ge_{0.03}Sn_{0.02})_{4.13}S_{12.94}$	4.0
	$(Cu^{+}_{10.46}Ag_{0.19})_{10.65}(Fe_{1.10}Zn_{0.16})_{1.26}(Sb_{1.91}As_{1.23}Bi_{0.24}Te^{4+}_{0.70}Ge_{0.03}Sn_{0.02})_{4.13}S_{12.94}$	1.6
6	$(Cu^{+}_{9.68}Ag_{0.32})_{10.00}(Cu^{2+}_{1.12}Fe_{0.84}Zn_{0.12})_{2.08}(Sb_{1.73}As_{0.98}Bi_{0.45}Te^{4+}_{0.82}Ge_{0.04}Sn_{0.02})_{4.04}S_{12.88}$	5.2
	$(Cu^{+}_{10.80}Ag_{0.32})_{11.12}(Fe_{0.84}Zn_{0.12})_{0.96}(Sb_{1.73}As_{0.98}Bi_{0.45}Te^{4+}_{0.82}Ge_{0.04}Sn_{0.02})_{4.04}S_{12.88}$	1.1
7	$(Cu^{+}_{9.71}Ag_{0.29})_{10.00}(Cu^{2+}_{1.20}Fe_{0.60}Zn_{0.12})_{1.82}(Sb_{1.67}As_{0.90}Bi_{0.41}Te^{4+}_{0.94}Ge_{0.04}Sn_{0.02})_{3.98}S_{13.08}$	2.2
8	$(Cu^{+}_{11.89}Ag_{0.02})_{11.91}(Sb_{0.38}As_{1.40}Bi_{0.02}Te^{4+}_{2.15})_{3.95}(S_{10.94}Se_{2.20})_{13.14}$	1.4
9	$(Cu^{+}_{11.59}Ag_{0.03})_{11.62}(Fe_{0.03}Zn_{0.21})_{1.26}(Sb_{0.40}As_{1.38}Bi_{0.10}Te^{4+}_{2.12})_{4.00}(S_{10.53}Se_{2.61})_{13.14}$	0.7
10	$(Cu^{+}_{12.00}Ag_{0.02}Au_{0.01})_{12.03}(Sb_{0.50}As_{1.38}Bi_{0.01}Te^{4+}_{2.13})_{4.02}(S_{10.45}Se_{2.50})_{12.95}$	1.2
11	$Cu^{+}_{11.93}Fe_{0.03}(Sb_{0.38}As_{1.72}Bi_{0.02}Te^{4+}_{1.98})_{4.02}(S_{10.79}Se_{2.15})_{12.94}$	1.6

Note. Analyses 1, 2 from the central part of the grain, analyses 3—5 from the outer part of the grain, analyses 6,7 from the most outer part of the grain. Including in analysis 3: Mn 0.02, Cd 0.03, Co 0.03, V 0.02 wt.%, in analysis 8 – 10.3 wt.% Se, in analysis 9 – 12.2 wt.% Se, in analysis 10 – 11.5 wt.% Se, in analysis 11 – 9.9 wt.% Se, in analysis 10 Au 0.1 wt.%, in analyses 8–11 Hg, Cd, Pb, Sn, Ge are not discovered

in the gold-bearing quartz-sulfide-telluride veins of the volcanogenic belt of Central Kamchatka and the similarity of mineral associations with those from the deposits of Eastern Uzbekistan and Goldfield (Nevada, USA) is evidence that goldfieldite is a typomorphic mineral of gold-telluride deposits in volcanogenic regions. Results of investigation of fahlores from one of the deposits of the eastern part of Russia (Borisova *et al.*, 1986) also proves this conclusion. These authors discovered Te-bearing fahlores that proved to be goldfieldite–tennantites and goldfieldite–tetrahedrites. Their analyses (Table 5, analyses 7–10) are recalculated to a formula with 29 atoms.

Results of investigations of Kovalenker *et al*. (1986) of Te-bearing fahlores from the deposits of the Central Bulgarian Middle Mountains (Table 6, deposits Chelopech and Elshitsa) are interesting. These deposits belong to the same type as described above. Analyses 1 and 2 from the Chelopech deposit and analyses 21 and 22 from the Elshitsa deposit (assumed to be fahlores by V.A. Kovelenker) recalculate to electroneutral formula containing 33 atoms in the unit cell. Only analyses 3–5 and 19, 20 recalculate to electroneutral formula with 29 atoms in the unit cell. Analyses of fahlores from the Elshitsa deposit containing high concentrations of tellurium (analyses 6–18) are special. Seven analyses (analyses 6–11, 14) recalculate to 29 atoms in the formula only if we exclude native tellurium in amounts exceeding 4 atoms in the formula. Supposition that the samples contain very fine-grained inclusions of native tellurium is based on the note of Kovalenker *et al.* (1986) that tennantite in this deposit replaces goldfieldite, with the occurrence of native tellurium. Spiridonov (1987) comes to the same conclusion based on investigation of fahlores from several volcanogenic deposits of Kazakhstan. He noted that goldfieldite was replaced by tetrahedrite, native tellurium and chalcopyrite. Formulae for six analyses (analyses 12, 13, 15–18) become electroneutral after exclusion of native tellurium, and under the condition that all copper is monovalent. As seen from

Table 5. **Recalculation of analyses of fahlores from the volcanic belt of Central Kamchatka (analyses 1—6, Sakharova *et al.*, 1983) and one deposit of the Russian Far East (analyses 7—10, Borisova *et al.*, 1986) to formulae and calculation of their valence balance**

№	Cu	Ag	Fe	Au	Sb	As	Bi	Te	S	Se	Σ
1	43.0	0.1	0.7	0.3	6.5	0.2	7.0	15.2	23.3	1.9	98.2
2	45.3	–	0.1	0.2	6.6	4.4	1.5	16.1	24.5	–	98.7
3	42.9	0.9	2.0	0.9	7.7	2.9	0.8	17.4	24.5	–	100.00
4	45.0	2.3	0.3	0.2	6.8	0.9	0.8	17.6	25.0	–	98.9
5	46.5	–	0.1	0.4	5.4	4.1	0.9	18.2	26.1	–	101.7
6	44.4	0.4	0.1	0.4	5.3	2.3	0.5	20.2	25.3	–	98.9
7	45.8	–	–	Zn	3.8	6.7	1.2	18.0	26.2		101.2
8	44.0	3.0	0.5	0.2	5.6	1.3	0.5	16.6	26.2	0.3	97.3
9	46.4	1.0	0.2	0.5	6.0	3.5	0.3	15.6	25.7	0.3	99.5
10	45.6	1.4	0.1	0.2	6.3	1.3	0.1	17.6	25.5	0.1	98.3

№	Formula	$Te_{nat.}$ apfu	Δ, %
1	$(Cu^{+}_{11.91}Ag_{0.01})_{11.92}(Fe_{0.20}Au_{0.03})_{0.23}(Sb_{0.94}As_{0.05}Te^{4+}_{2.10}Bi_{0.59})_{3.68}(S_{12.73}Se_{0.42})_{13.15}$	0.00	2.8
2	$Cu^{+}_{11.98}(Fe_{0.03}Au_{0.02})_{0.05}(Sb_{0.91}As_{0.99}Te^{4+}_{2.12}Bi_{0.12})_{4.14}S_{12.83}$	0.00	3.6
	$Cu^{+}_{12.03}(Fe_{0.03}Au_{0.02})_{0.05}(Sb_{0.92}As_{0.99}Te^{4+}_{1.99}Bi_{0.12})_{4.02}S_{12.90} + Te_{nat.}$	0.14	1.4
3	$(Cu^{+}_{11.32}Ag_{0.14})_{11.46}(Fe_{0.60}Au_{0.08})_{0.68}(Sb_{1.06}As_{0.65}Te^{4+}_{2.28}Bi_{0.06})_{4.05}S_{12.81}$	0.00	6.0
	$(Cu^{+}_{11.34}Ag_{0.14})_{11.48}(Fe_{0.60}Au_{0.08})_{0.68}(Sb_{1.06}As_{0.65}Te^{4+}_{2.23}Bi_{0.06})_{4.00}S_{12.81} + Te_{nat.}$	0.05	5.3
	$(Cu^{+}_{11.34}Ag_{0.14})_{11.48}(Fe_{0.60}Au_{0.08})_{0.68}(Sb_{1.06}As_{0.65}Te^{4+}_{2.06}Bi_{0.06})_{3.83}(S_{12.83}Te^{2-}_{0.17})_{13.0} + Te_{nat.}$	0.05	1.5
4	$(Cu^{+}_{11.64}Ag_{0.14})_{12.00}(Cu^{2+}_{0.26}Fe_{0.09}Au_{0.02})_{0.37}(Sb_{0.94}As_{0.20}Te^{4+}_{2.32}Bi_{0.06})_{3.52}S_{13.11}$	0.00	1.3
5	$(Cu^{+}_{11.82}Ag_{0.03})_{11.85}(Fe_{0.03}Au_{0.03})_{0.06}(Sb_{0.72}As_{0.88}Te^{4+}_{2.30}Bi_{0.07})_{3.97}S_{13.15}$	0.00	0.4
6	$(Cu^{+}_{11.69}Ag_{0.06})_{11.75}(Fe_{0.09}Au_{0.03})_{0.12}(Sb_{0.73}As_{0.51}Te^{4+}_{2.65}Bi_{0.04})_{3.93}S_{13.20}$	0.00	0.1
7	$Cu^{+}_{11.57}(Sb_{0.50}As_{1.44}Te^{4+}_{2.27}Bi_{0.09})_{4.30}S_{13.13}$	0.00	1.8
8	$(Cu^{+}_{9.54}Ag_{0.46})_{10.00}(Cu^{2+}_{2.15}Fe_{0.17}Zn_{0.06})_{2.38}(Sb_{0.78}As_{0.29}Te^{4+}_{2.20}Bi_{0.03})_{3.30}(S_{13.25}Se_{0.06})_{13.31}$	0.00	0.8
9	$(Cu^{+}_{10.10}Ag_{0.15})_{10.25}(Cu^{2+}_{1.82}Fe_{0.06}Zn_{0.12})_{2.00}(Sb_{0.81}As_{0.76}Te^{4+}_{2.00}Bi_{0.03})_{3.60}(S_{13.08}Se_{0.06})_{13.14}$	0.00	2.8
10	$(Cu^{+}_{10.10}Ag_{0.20})_{10.30}(Cu^{2+}_{1.85}Zn_{0.07}Fe_{0.03}Cd_{0.03})_{2.00}(Sb_{0.87}As_{0.29}Te^{4+}_{2.29}Bi_{0.03})_{3.45}(S_{13.25}Se_{0.03})_{13.28}$	0.00	1.4

Note. In analysis 10 – Au 0.1 wt.%, Cd 0.1 wt.%

Table 6, formulae for four analyses (analyses 12, 13, 15 and 16) recalculated after deduction of native tellurium have better balance of valences. Supposition that all copper in the analyses (analyses 12, 13, 15−18) is monovalent is based on the note of Novgorodova *et al.* (1978) that in Te-bearing fahlores, compensation of surplus charge during replacement (As, Sb)$^{3+}$ → Te^{4+} occurs by means of vacancy formation. Mozgova and Tsepin (1983) consider that surplus charge compensation is most likely due to "depolarization at the expense of reduction of copper to Cu^+ that limits entering of two-valent metals in it". Due to the fact that formulae for the quoted analyses are electroneutral under both conditions, we can conclude that under high content of tellurium (about 10−24 wt.%), all copper in fahlore will be monovalent. Fahlores containing more than 24 wt.% of tellurium may be recalculated to the same formula provided native tellurium is excluded from the analyses. So, not more than 24 wt.% of tellurium can isomorphically enter fahlores. Formulae for the other two analyses (analyses 21 and 22) become electroneutral only if they are recalculated to 33 atoms in the unit cell. Thus, from 22 analyses of Te-bearing fahlores from the Chelopech and Elshitse deposits, 18 analyses (Table 6, analyses 3−20) recalculate to a formula with 29 atoms in the unit cell, and 4 analyses (Table 6, analyses 1,2,21, and 22) recalculate to a formula with 32 and 33 atoms in the unit cell. The idealized formulae are as follows: $Cu^+_{11}Me^{2+}_{1.00}Me^{3+}_{1.00}\Pi Me_{4.00}S_{15}$ and $Cu^+_{10}Me^{2+}_{3.00}\Pi Me_{4.00}S_{16}$.

In Te-bearing fahlores, zoned crystals occur, indicating changing physicochemical conditions (concentrations of solved components, temperature, pressure, redox potential) during growth. Zones are easily visible in reflected light. As a rule, cores of tetrahedrite composition are greenish and the outer rose-colored zone of goldfieldite composition sometimes has fine zonal structure. Pale-rosy fine zones give way to rose-colored zones and vice versa. It is likely that the intensity of the rosy shade in fahlores is caused by an increase in tellurium. Such zoned crystals were investigated by Spiridonov (1987). Recalculation of 13 analyses from this work (Table 7) show that the formulae for nine analyses (analyses 1−7, 11, 13) from different zones of a fahlore crystal from volcanogenic gold-quartz deposit of the Russian Far East are electroneutral. Formulae for two analyses (analyses 6 and 10) are electroneutral if part of the Te^{2-} is placed into the sulfur position. The formula for one analysis (analysis 8) is non-electroneutral. The sum of analysis 12 greatly exceeds 100% (104.36%), and its formula is non-electroneutral (balance of valences is equal to 3.3%). If all Ag is assumed to be kervelleite, the sum of the analysis and balance of valences becomes much better (98.34% and 0.4%, respectively). According to Spiridonov (1987), fahlores with high contents of Te and Ag represent later generations. Kervelleite also occurs at the later stage of ore mineralization.

Comparison of non-electroneutral formulae obtained during recalculation to the conventional formula for fahlores, $Cu^+_{10}Me^{2+}_2\ \Pi Me_4S_{13}$, and also recalculated to electroneutral formulae (Table 2, analyses 11, 18, 19, 21, and 32; Table 4, analysis 2; Table 5, analysis 3; Table 6, analyses 1, 2, 21, and 22; Table 7, analysis 8) shows that five formulae (of twelve) become electroneutral during recalculation with probable Te^{2-} at the sulfur position (Table 2, analysis 11) and recalculation to 33 atoms in the unit cell (Table 6, analyses 1,2, 21, and 22). One formula for an analysis from the deposit of the volcanic belt of Central Kamchatka (Table 5, analysis 3) becomes electroneutral after excluding 0.05 of atoms per formula of native tellurium and recalculation with Te^{2-} at the sulfur position added to give 13 atoms. Three formulae of analyses (Table 2, analyses 21, 32 and Table 4, analysis 2) have balance of valences 3.1, 3.2 and 3.2 accordingly. They are almost electroneutral. Three formulae, corresponding to two analyses from Koch-Bulak (Table 2, analyses 18 and 19) and one analysis from the volcanogenic gold−quartz deposit of the Russian Far East (Table 7, analysis 8), remain non-electroneutral.

The reader may be surprised by this recalculation of analyses, but all recalculations accord with the isomorphism in fahlores and the complicated, often changing, conditions of crystallization that lead to the formation of zoned crystals.

Conclusions

1. Te-bearing fahlores are very similar to fahlores of different chemical composition and physical features. They have a rosy shade in reflected light, and resemble complex sulfide of germanium (germanite). In volcanogenic and hydrothermal quartz-sulfide vein deposits of gold-sulfide formations (Koch-Bulak, Chelopech, and Elshitsa), isotropic minerals were discovered similar in color to germanite, but their analyses did not contain of germanium. They have non-electroneutral formulae by recalculation to 29 atoms in the unit cell (i.e.,

Table 6. **Recalculation of analyses of fahlores from the deposit Chelopech (analyses 1—5) and Elshitsa (analyses 6—22) given by V.A. Kovalenker *et al.* (1986) to formulae and calculation of their valence balance**

№	Cu	Fe	Zn	Sb	As	Te	Bi	Se	S	∑
1	39.64	4.06	n.d.	2.01	2.48	26.16	0.34	n.d.	24.79	99.48
2	40.30	3.87	n.d.	1.45	4.29	24.38	0.21	n.d.	24.90	99.40
3	43.19	0.41	n.d.	7.50	2.73	17.64	n.d.	1.89	24.91	99.27
4	45.34	0.51	0.45	2.26	6.42	17.64	0.69	0.19	25.82	99.32
5	43.67	1.35	5.59	1.95	17.38	1.81	n.d.	n.d.	27.49	99.24
6	42.48	0.27	n.d.	0.23	4.05	26.44	2.62	n.d.	25.68	101.77
7	44.95	0.16	n.d.	0.27	4.32	25.85	0.47	n.d.	25.43	101.45
8	43.38	0.39	n.d.	0.23	5.30	25.74	0.10	n.d.	25.55	100.69
9	43.62	0.42	n.d.	0.31	5.33	25.64	0.31	n.d.	25.69	100.32
10	42.71	0.64	n.d.	0.15	4.75	24.52	3.38	n.d.	25.25	101.40
11	42.49	0.55	n.d.	0.38	5.66	24.38	1.38	n.d.	25.51	100.35
12	44.72	0.15	n.d.	0.20	5.23	23.97	0.17	n.d.	26.43	100.87
13	43.35	0.20	n.d.	0.39	5.04	23.75	0.23	n.d.	26.13	99.09
14	43.07	1.03	n.d.	0.16	5.26	23.01	1.30	n.d.	25.71	99.74
15	45.15	0.63	0.04	0.20	6.39	22.31	0.14	n.d.	26.72	101.58
16	43.83	0.74	n.d.	0.16	6.44	22.07	n.d.	n.d.	26.14	99.38
17	44.83	0.13	n.d.	0.36	6.84	21.26	1.49	n.d.	26.51	101.42
18	44.47	0.26	n.d.	0.18	5.47	21.24	2.96	n.d.	26.52	101.40
19	46.56	0.20	n.d.	0.14	6.84	19.83	0.27	n.d.	26.35	100.19
20	46.33	4.76	0.25	n.d.	20.11	1.39	n.d.	n.d.	29.00	101.84
21	46.07	4.56	0.26	n.d.	20.04	0.13	n.d.	n.d.	29.26	100.32
22	46.17	4.61	0.23	n.d.	20.35	0.23	0.34	n.d.	30.34	102.27

№	Formula	$Te_{nat.}$ apfu	Δ, %
1	$Cu^{+}_{10.48}Fe^{2+}_{1.22}(Sb_{0.28}As_{0.56}Bi_{0.03}Te^{4+}_{3.44})_{4.31}S_{12.99}$	0.00	11.3
1	$Cu^{+}_{10.48}Fe^{2+}_{1.22}(Sb_{0.28}As_{0.56}Bi_{0.03}Te^{4+}_{3.13})_{4.00}(S_{12.99}Te^{2-}_{0.31})_{13.30}$	0.00	5.2
1*	$Cu^{+}_{10}(Cu^{2+}_{1.93}Fe_{1.07})_{3.00}Fe^{3+}_{0.32}(Sb_{0.32}As_{0.63}Bi_{0.03}Te^{4+}_{3.02})_{4.00}(S_{14.78}Te^{2-}_{0.9})_{15.68}$	0.00	1.9
2	$Cu^{+}_{10.56}Fe^{2+}_{1.15}(Sb_{0.20}As_{0.95}Bi_{0.02}Te^{4+}_{2.83})_{4.00}(S_{12.93}Te^{2-}_{0.35})_{13.28}$	0.00	4.1
2*	$Cu^{+}_{10}(Cu^{2+}_{2.02}Fe_{0.98})_{3.00}Fe^{3+}_{0.33}(Sb_{0.22}As_{1.08}Bi_{0.02}Te^{4+}_{2.68})_{4.00}(S_{14.72}Te^{2-}_{0.94})_{15.66}$	0.00	1.1
3	$Cu^{+}_{10}(Cu^{2+}_{1.43}Fe_{0.12})_{1.55}(Sb_{1.04}As_{0.61}Te^{4+}_{2.32})_{3.97}(S_{13.07}Se_{0.40})_{13.47}$	0.00	1.4
4	$Cu^{+}_{11.60}(Fe_{0.15}Zn_{0.11})_{0.26}(Sb_{0.30}As_{1.39}Bi_{0.05}Te^{4+}_{2.25})_{3.99}(S_{13.10}Se_{0.04})_{13.14}$	0.00	0.2
5	$Cu^{+}_{10}(Cu^{2+}_{0.40}Fe_{0.35}Zn_{1.29})_{2.05}(Sb_{0.24}As_{3.51}Te^{4+}_{0.21})_{3.96}S_{12.97}$	0.00	1.0
6	$Cu^{+}_{11.30}Fe_{0.08}(Sb_{0.03}As_{0.91}Bi_{0.21}Te^{4+}_{2.92})_{4.05}S_{13.54} + Te_{nat.}$	0.57	2.0
7	$Cu^{+}_{11.74}Fe_{0.05}(Sb_{0.04}As_{0.96}Bi_{0.04}Te^{4+}_{3.01})_{4.05}S_{13.17} + Te_{nat.}$	0.35	2.4
8	$Cu^{+}_{11.44}Fe_{0.12}(Sb_{0.03}As_{1.19}Bi_{0.01}Te^{4+}_{2.85})_{4.08}S_{13.36} + Te_{nat.}$	0.52	0.2
9	$Cu^{+}_{11.44}Fe_{0.12}(Sb_{0.06}As_{1.19}Bi_{0.02}Te^{4+}_{2.81})_{4.08}S_{13.35} + Te_{nat.}$	0.53	0.1
10	$Cu^{+}_{11.39}Fe_{0.19}(Sb_{0.02}As_{1.07}Bi_{0.27}Te^{4+}_{2.71})_{4.07}S_{13.34} + Te_{nat.}$	0.54	0.3
11	$Cu^{+}_{11.30}Fe_{0.17}(Sb_{0.05}As_{1.28}Bi_{0.11}Te^{4+}_{2.65})_{4.09}S_{13.44} + Te_{nat.}$	0.57	1.2
12	$Cu^{+}_{11.40}Fe_{0.04}(Sb_{0.03}As_{1.13}Bi_{0.01}Te^{4+}_{3.04})_{4.21}S_{13.35}$	0.00	1.6
	$Cu^{+}_{11.48}Fe_{0.04}(Sb_{0.03}As_{1.14}Bi_{0.01}Te^{4+}_{2.85})_{4.03}S_{13.44} + Te_{nat.}$	0.21	1.4
13	$Cu^{+}_{11.35}Fe_{0.06}(Sb_{0.05}As_{1.12}Bi_{0.02}Te^{4+}_{2.84})_{4.03}S_{13.56}$	0.25	2.6
	$Cu^{+}_{11.25}Fe_{0.06}(Sb_{0.05}As_{1.11}Bi_{0.02}Te^{4+}_{3.07})_{4.25}S_{13.44} + Te_{nat.}$	0.00	1.1
14	$Cu^{+}_{11.29}Fe_{0.31}(Sb_{0.02}As_{1.17}Bi_{0.10}Te^{4+}_{2.73})_{4.04}S_{13.36} + Te_{nat.}$	0.26	0.9
15	$Cu^{+}_{11.33}Fe_{0.18}Zn_{0.01}(Sb_{0.03}As_{1.36}Bi_{0.01}Te^{4+}_{2.79})_{4.19}S_{13.29}$	0.00	1.8
	$Cu^{+}_{11.41}Fe_{0.18}Zn_{0.01}(Sb_{0.03}As_{1.37}Bi_{0.01}Te^{4+}_{2.62})_{4.03}S_{13.38} + Te_{nat.}$	0.19	0.9
16	$Cu^{+}_{11.24}Fe_{0.22}(Sb_{0.02}As_{1.40}Te^{4+}_{2.82})_{4.24}S_{13.29}$	0.00	2.4
	$Cu^{+}_{11.34}Fe_{0.22}(Sb_{0.02}As_{1.41}Te^{4+}_{2.60})_{4.03}S_{13.40} + Te_{nat.}$	0.24	1.2
17	$Cu^{+}_{11.35}Fe_{0.04}(Sb_{0.05}As_{1.47}Bi_{0.11}Te^{4+}_{2.68})_{4.31}S_{13.30}$	0.00	1.6
	$Cu^{+}_{11.47}Fe_{0.04}(Sb_{0.05}As_{1.48}Bi_{0.12}Te^{4+}_{2.40})_{4.05}S_{13.44} + Te_{nat.}$	0.31	2.9
18	$Cu^{+}_{11.36}Fe_{0.08}(Sb_{0.02}As_{1.18}Bi_{0.23}Te^{4+}_{2.70})_{4.13}S_{13.42}$	0.00	0.8
	$Cu^{+}_{11.41}Fe_{0.08}(Sb_{0.02}As_{1.19}Bi_{0.23}Te^{4+}_{2.58})_{4.02}S_{13.48} + Te_{nat.}$	0.13	2.0
19	$Cu^{+}_{11.76}Fe_{0.06}(Sb_{0.02}As_{1.46}Bi_{0.02}Te^{4+}_{2.49})_{3.99}S_{13.19}$	0.00	0.15
20	$Cu^{+}_{10}(Cu^{2+}_{0.56}Fe_{1.23}Zn_{0.06})_{1.85}(As_{3.89}Te^{4+}_{0.16})_{4.05}S_{13.10}$	0.00	0.7
21	$Cu^{+}_{10}(Cu^{2+}_{0.56}Fe_{1.19}Zn_{0.06})_{1.81}(As_{3.89}Te^{4+}_{0.01})_{3.90}S_{13.29}$	0.00	4.7
21*	$Cu^{+}_{11}(Cu^{2+}_{1.01}Fe_{0.35}Zn_{0.07})_{1.43}Fe^{3+}_{1.00}(As_{4.43}Te^{4+}_{0.02})_{4.45}S_{15.12}$	0.00	0.0
22	$Cu^{+}_{10}(Cu^{2+}_{0.36}Fe_{1.18}Zn_{0.05})_{1.59}(As_{3.87}Bi_{0.02}Te^{4+}_{0.01})_{3.90}S_{13.49}$	0.00	7.4
22*	$Cu^{+}_{11}(Cu^{2+}_{0.79}Fe_{0.34}Zn_{0.05})_{1.18}Fe^{3+}_{1.00}(As_{4.41}Bi_{0.03}Te^{4+}_{0.03})_{4.47}S_{15.35}$	0.00	2.9

Note. Analyses 1 and 2*, 21*, 22* are recalculated to formula with 33 atoms in the unit cell, the remaining analyses are recalculated to 29 atoms in the unit cell.*

the formula of the fahlore). The formulae become electroneutral only during recalculation to 32 or 33 atoms in the unit cell. The formulae of complex sulfides of germanium contain the same number of atoms, suggesting that a new mineral species exists that is optically and chemically similar to fahlore with the idealized formulae $Cu^{+}_{11}Me^{2+}_{1.00}Me^{3+}_{1.00}ПMe_{4.00}S_{15}$ and $Cu^{+}_{10}Me^{2+}_{3.00}ПMe_{4.00}S_{16}$. It is possible that they are germanium-free analogues of complex sulfides of germanium (germanite and renierite).

2. Tellurium may enter the Te^{4+} position as well as the sulfur position as Te^{2-} in Te-bearing fahlore goldfieldite and high-tellurium tetrahedrite.

3. Goldfieldites containing more than 24 wt.% of tellurium are, as a rule, heterogenous and contain admixed native tellurium as

Table 7. **Recalculation of analyses of a zoned crystal of fahlore from the gold-quartz volcanogenic deposit of the Russian Far East (Spiridonov, 1987) to formulae and calculation of their valence balance**

№	Cu	Ag	Zn	Fe	Cd	As	Sb	Te	S	Se	∑
1	38.17	0.99	6.32	1.66	0.07	4.20	23.13	Traces	25.33	0.04	99.91
2	39.22	0.90	6.58	0.08	0.33	3.96	23.48	Traces	25.52	0.32	100.39
3	39.46	0.66	6.55	0.07	0.46	3.70	24.09	0.01	25.08	0.35	100.45
4	43.27	1.39	0.84	0.05	0.35	3.28	9.98	14.52	22.89	4.90	101.48
5	42.70	0.94	2.27	0.02	Traces	3.87	15.99	6.77	24.17	2.04	98.78
6	43.46	0.66	0.62	0.07	0.03	1.73	6.39	20.88	22.82	4.14	100.81
7	43.07	1.50	0.99	0.01	0.08	2.97	9.92	14.15	23.49	2.44	98.63
8	43.23	1.85	0.21	0.05	0.36	1.14	4.87	23.08	22.60	3.92	101.36
9	42.94	0.96	2.25	Traces	0.30	3.92	13.32	9.77	23.73	2.44	99.67
10	45.19	0.73	0.65	0.05	0.09	1.28	6.20	21.23	22.70	4.70	102.22
11	42.57	0.92	2.18	0.02	0.05	2.43	12.18	13.35	22.64	4.54	100.90
12	43.32	4.37	0.18	0.15	Traces	2.59	3.15	22.63	23.27	4.66	104.36
12*	43.32	0.00	0.18	0.15	Traces	2.59	3.15	21.34	22.95	4.66	98.34
13	40.79	2.72	2.60	0.39	Traces	2.61	11.63	13.37	23.52	2.54	100.17

№	Formula	Δ, %
1	$(Cu^{+}_{9.82}Ag_{0.15})_{9.97}(Zn_{1.58}Fe_{0.49}Cd_{0.01})_{2.08}(Sb_{3.11}As_{0.92})_{4.03}(S_{12.92}Se_{0.01})_{12.93}$	1.4
2	$(Cu^{+}_{9.79}Ag_{0.14})_{9.93}(Cu^{2+}_{0.29}Fe_{0.02}Zn_{1.64}Cd_{0.05})_{2.00}(Sb_{3.15}As_{0.86})_{4.01}(S_{12.99}Se_{0.07})_{13.06}$	1.7
3	$(Cu^{+}_{9.90}Ag_{0.10})_{10.00}(Cu^{2+}_{0.29}Fe_{0.02}Zn_{1.64}Cd_{0.07})_{2.02}(Sb_{3.25}As_{0.81})_{4.06}(S_{12.84}Se_{0.07})_{12.91}$	1.4
4	$(Cu^{+}_{10.43}Ag_{0.22})_{10.65}(Fe_{0.02}Zn_{0.22}Cd_{0.05})_{0.29}(Sb_{1.38}As_{0.74}Te^{4+}_{1.91})_{4.03}(S_{11.99}Se_{1.04})_{13.03}$	0.6
5	$(Cu^{+}_{11.26}Ag_{0.14})_{11.40}(Fe_{0.01}Zn_{0.58})_{0.59}(Sb_{2.20}As_{0.86}Te^{4+}_{0.89})_{3.95}(S_{12.62}Se_{0.43})_{13.05}$	3.0
	$(Cu^{+}_{9.86}Ag_{0.14})_{10.00}(Cu^{2+}_{1.40}Fe_{0.01}Zn_{0.58})_{1.99}(Sb_{2.20}As_{0.86}Te^{4+}_{0.89})_{3.95}(S_{12.62}Se_{0.43})_{13.05}$	2.3
6	$(Cu^{+}_{11.64}Ag_{0.10})_{11.74}(Fe_{0.02}Zn_{0.16})_{0.18}(Sb_{0.89}As_{0.39}Te^{4+}_{2.78})_{4.06}(S_{12.10}Se_{0.89})_{12.99}$	4.0
	$(Cu^{+}_{11.64}Ag_{0.10})_{11.74}(Fe_{0.02}Zn_{0.16})_{0.18}(Sb_{0.89}As_{0.39}Te^{4+}_{2.72})_{4.0}(S_{12.10}Se_{0.89}Te^{2-}_{0.06})_{13.05}$	2.7
7	$(Cu^{+}_{11.54}Ag_{0.24})_{11.78}(Zn_{0.26}Cd_{0.01})_{0.27}(Sb_{1.39}As_{0.67}Te^{4+}_{1.89})_{3.95}(S_{12.47}Se_{0.53})_{13.00}$	0.2
8	$(Cu^{+}_{11.64}Ag_{0.29})_{11.93}(Fe_{0.02}Zn_{0.05}Cd^{2+}_{0.05})_{0.12}(Sb_{0.68}As_{0.26}Te^{4+}_{3.00})_{3.94}(S_{12.06}Se_{0.85}Te^{2-}_{0.09})_{13.00}$	3.7
9	$(Cu^{+}_{11.32}Ag_{0.15})_{11.47}(Zn_{0.58}Cd_{0.04})_{0.62}(Sb_{1.83}As_{0.88}Te^{4+}_{1.28})_{3.99}(S_{12.40}Se_{0.52})_{12.92}$	0.8
10	$(Cu^{+}_{11.91}Ag_{0.11})_{12.02}(Fe_{0.01}Zn_{0.17}Cd^{2+}_{0.01})_{0.19}(Sb_{0.85}As_{0.29}Te^{4+}_{2.79})_{3.93}(S_{11.86}Se_{1.00})_{12.86}$	4.7
	$(Cu^{+}_{11.91}Ag_{0.11})_{12.02}(Fe_{0.01}Zn_{0.17}Cd^{2+}_{0.01})_{0.19}(Sb_{0.85}As_{0.29}Te^{4+}_{2.65})_{3.79}(S_{11.86}Se_{1.00}Te^{2-}_{0.14})_{13.00}$	1.6
11	$(Cu^{+}_{11.34}Ag_{0.14})_{11.48}(Cd_{0.01}Zn_{0.56}Fe_{0.01})_{0.58}(Sb_{1.69}As_{0.55}Te^{4+}_{1.77})_{4.01}(S_{11.93}Se_{0.97})_{12.92}$	2.3
12	$(Cu^{+}_{11.30}Ag_{0.67})_{11.97}(Zn_{0.04}Fe_{0.04})_{0.08}(Sb_{0.43}As_{0.57}Te^{4+}_{2.94})_{3.94}(S_{12.02}Se_{0.99})_{13.00}$	3.3
12*	$Cu^{+}_{11.70}(Zn_{0.05}Fe_{0.05})_{0.10}(Sb_{0.44}As_{0.59}Te^{4+}_{2.87})_{3.90}(S_{12.28}Se_{1.01})_{13.29}$ + 5.99% Ag_4TeS	0.4
13	$(Cu^{+}_{10.86}Ag_{0.43})_{11.29}(Zn_{0.67}Fe_{0.12})_{0.79}(Sb_{1.62}As_{0.59}Te^{4+}_{1.77})_{3.98}(S_{12.40}Se_{0.54})_{12.94}$	2.6

*Note. Including Mn: in analyses 1, 2, 10, 12 — traces, in analyses 3 and 11 — 0.02, in analyses 4, 5, 6, 7 — 0.01, in analysis 8 — 0.05, in analysis 9 — 0.04 wt.%. *Analysis is calculated under condition that all Ag is attributed at the expense of kervelleite Ag_4TeS. Correspondingly amount of Te is decreased by 1.29% and amount of S by 0.32%*

shown by the following: analyses become electroneutral only if native tellurium is excluded exceeding 4 atoms occupied by atoms of semimetal in the formula.

4. Te-bearing fahlores with a large amount of silver (7—13 wt.%) may contain an admixture of fine-grained kervelleit, Ag_4TeS.

References

Bogdanov B. Bulgaria // Mineral deposits of Europe. South-Eastern Europe. Moscow: Mir. **1984**. V. 2. P. 294—318. (in Russian).

Borisova E.A., Borodayev Yu.S., and Bocharova G.I. Rare varieties of fahlores from one of the gold deposits // Zapiski Vses. Mineral. Obschestva. **1986**. № 3. P. 85—94. (in Russian).

Kovalenker V.A., Troneva N.V., and Dobronichenko V.V. Peculiarities of composition of the main ore-forming minerals from the tube-like ore bodies of the Kochbulaksky deposit // Methods of investigation of ore-forming sulfides and their parageneseses. Moscow: Nauka. **1980**. P. 140—164. (in Russian).

Kovalenker V.A., Tsonev D., Breskovska V.V., Malov V.S., and Troneva N.V. New data on mineralogy of the copper-pyrite deposits of central Sredna-Gora of Bulgaria // Metasomatism, mineralogy, and problems of genesis of gold and silver deposits. Moscow: Nauka. **1986**. P. 91—110. (in Russian).

Mozgova N.N. and Tsepin A.I. Fahlores // Moscow: Nauka. **1983**. 279 p. (in Russian).

Novgorodova M.M., Tsepin A.I. and Dmitrieva M.T. A new isomorphic row in the fahlores group // Zapiski Vses. Mineral. Obschestva. **1978**. № 1. P. 100—110. (in Russian).

Sakharova M.S., Lebedeva N.V. and Chubarov V.M. First discovery of rare minerals of tellurium — goldfieldite, rucklidgeite, and native tellurium // Doklady SSSR. **1986**. V. 278. № 5, P. 1217—1220. (in Russian).

Spiridonov E.M. Typomorphic peculiarities of fahlores of some plutogenic, volcanogenic, and telethermal deposits of gold // Geol. Ore Dep. **1987**. № 6. P. 83—92. (in Russian).

Spiridonov E.M. and Badalov A.S. Evolution of composition of fahlores of the volcanogenic dposit Kayragach in the Eastern Uzbekistan // Geol. Ore Dep. **1983**. № 4. P. 108—114. (in Russian).

Spiridonov E.M. and Okrugin V.M. A new variety of fahlores — selenian goldfieldite // Doklady SSSR. **1985**. V. 280. № 2. P. 476—478. (in Russian).

Frenzel G., Ottemann J., Manhal Al-Tabaqchali, and Huber B. Calabona copper deposit of Alghero, Sardinia // N. Jb. Miner. **1975**. H. 2. S. 107—155.

Ransome E., Emmons W.H. and Carrey G.H. Geology and ore deposits of Goldfield, Nevada // Geol. Surv. Prof. Paper. **1990**. № 66.

MINERALOGICAL FEATURES OF CERTAIN MULTIMETAL DEPOSITS OF RUSSIA, CENTRAL ASIA, KAZAKHSTAN AND ROLE OF MINERAL SORBENTS IN THE CONCENTRATION OF METALS IN THE ZONE OF HYPERGENESIS

Andrey A. Chernikov
Fersman Mineralogical Museum RAS, Moscow, cher@fmm.ru
Victor T. Dubinchuk, Denis O. Ozhogin, Natalia I. Chistyakova
All-Russian Research Institute of Mineral Resources (FGUP VIMS), Moscow, vims@df.ru

There is evidence of genetic proximity by the similarity in distribution of the mineral assemblages in the Onega deposits, Karelia and exogenous infiltration uranium deposits of Central Asia and Kazakhstan. There are many common features of mineralization at the Onega deposits and mineralization of the North Urals and Kodaro-Udokan trough, NW Transbaikalia, where prospects of discovering large precious metal deposits are rather great. The data support the contention (Chernikov, 1977, 2001; Chernikov *et al.*, 2000, 2005, 2007) about the possibility of increasing precious metal reserves associated with uranium-vanadium Onega-type deposits. The role of the mineral sorbents in the concentration of precious and other metals in the supergene zone of deposits in the investigated districts is reviewed.
1 table, 6 figures, 56 references .
Keywords: multimetal deposits, uranium minerals, minerals of precious metals, V and Mo minerals, mineral sorbents, X-ray amorphous matter, supergene zone.

The Onega deposits in Karelia (Middle Padma, Tsarevo, Kosmozero) being large for reserves of complex vanadium ores with a great number of chemical elements: V, U, Pd, Pt, Au, Ag, Mo, Cu, and other (Bilibina *et al.*, 1991; Mel'nikov and Shumilin, 1995) are characterized by certain geological features similar to those of the discordance type deposits (Laverov *et al.*, 1992). At the same time, by association with carbonaceous matter, by number of metals in the ores, and by their restriction to schistose siltstone, they are typical deposits of black schist sequence. The Onega deposits comprise various mineral assemblages that are zoned located in geologic section (Mel'nikov and Shumilin, 1995; Chernikov, 1997, 2001). Copper and molybdenum minerals occur in margins uranium-vanadium mineral assemblages forming ore deposits, and change away from them by albitization and dispersed pyritization of the rocks. Sulfoselenides and selenides are distributed in the frontal part of U-V deposits changed by the zone of hematitized rocks (deep oxidized zone). The modern near-surface oxidized zone displayed as bleached rocks, limonite and Mn oxides follows below surface down to 60–150 m depth, less frequent 250 m limiting U-V deposits from above. The lower part of near-surface oxidized zone, upper levels of cementation zone and deep oxidizing zone of the uranium-vanadium ores are significantly enriched in precious metals.

Such distribution of mineral assemblages in the Onega deposits and their character are similar to those at the exogenous infiltration uranium deposits of Central Asia and Kazakhstan. The differences are mainly in physicochemical features of mineral deposition under deep and near-surface hypergenesis. Albitized and hematitezed rocks characteristic of the Onega-type deposits are absent at stratiform near-surface infiltration uranium deposits of Central Asia and Kazakhstan. However, at these deposits, there is limonitization of permeable rocks forming stratiform near-surface oxidized zone, which as like deep-seated oxidized zone at the Onega-type deposits changes along dip by uranium mineralization, occasionally with vanadium and selenium minerals. Like Onega-type deposits, uranium-vanadium, uranium-selenium or uranium ores frequently grade towards margins into zone of molybdenum minerals (jordesite and molybdenite) occasionally with copper (chalcopyrite). Similar to the Onega-type deposits, molybdenum mineralization alternates along dip by the zone of disseminated pyrite. Such consistence of geo-

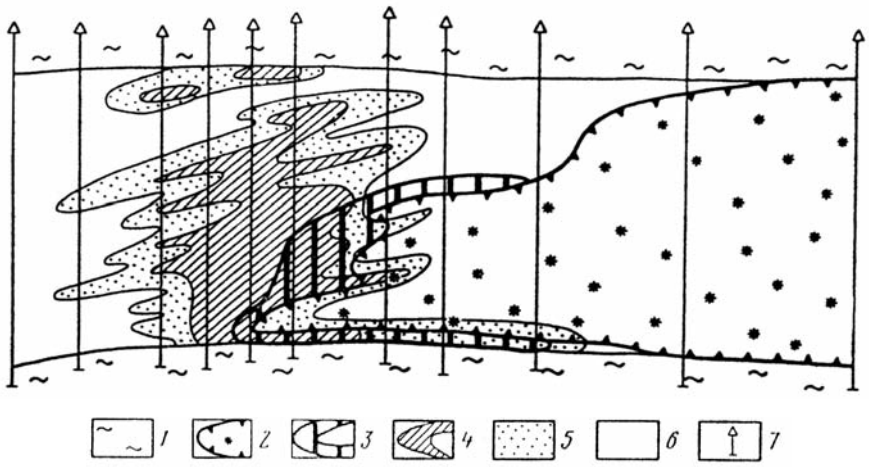

Fig. 1. Distribution of gold in sections of ore-controlling zonning in the Coniacian-Santonian estuary sediments of the Uchkuduk stratiform infiltration uranium deposit. 1 — waterproof aleurolite-clayey rocks (water-permeable sandy rocks between them); 2 — zone of stratum oxidation and front boundary of its distribution; 3 — uranium ores; 4—6 — gold concentration, mg/t: 4 — from 30 to 60, 5 — from 10 to 30, 6 — <10; 7 — drill holes.

chemical and mineralogical zoning of ores of two types of deposits indicates their genetic similarity.

The highest grades of precious metals in the lower part of near-surface oxidized zone of the Onega-type deposits are as follows: few hundred g/t Pd, few ten g/t Au (less frequent Pt), and few thousand g/t Ag. In deep-seated oxidized zone (in hematitized dolomites) out of limits of the uranium-vanadium ores, the highest grade of precious metals is as follows, g/t: 22 Pd , 2.5 Au, 1.1 Pt, and 330 Ag. At the infiltration deposits, the highest grades of the precious metals are characteristic of uranium-coal ores (Kal'djat, Kazakhstan), where the highest Ag is identified at the boundary with oxidized rocks and is in average 12 g/t. Gold grade is lower, but in coals enriched in uranium (with Mo, Re, Ge, V, Sc, Y) it reaches 900 mg/t, less frequent, 1 g/t. In ordinary and low-grade uranium ores, gold content decreases down to 60 mg/t, and that of PGE is further lower. Precious metals are permanently observed in other deposits of stratiformoxidation. It is especially characteristic of gold, whose supergene formation has clearly demonstrated by Chukhrov (1950).

Gold is clear associated with uranium during supergene ore-forming process, although maximum accumulations of these metals do not always agree (Shmariovich *et al.*, 1992). The elevated concentration of Au ranging from 10 to 30 mg/t, ocassionallyto 60 mg/t is found in the zone of stratiformoxidation (Fig. 1). However, the highestt gold grade up to 60 mg/t is more frequently observed in uranium ores. Variation of gold content from 10 to 30 mg/t follows in subsequent zones of molybdenum mineralization and scattered pyritization and in the zone of near-surface oxidation.

Concentration of PGE in these deposits is still lower. Hence, content of precious metals in stratum infiltration deposits is several orders lower than that in the Onega ores. Nevertheless, gold is recovered for decades with underground leaching of uranium at the Uchkuduk-type deposits (Uzbekistan). Grains of native gold from the oxidized zone of the Uchkuduk deposit, near-surface oxidized zone of the Onega-type deposits, and deposits of Southern Kazakhstan (Fig. 2) are similar in X-ray microdiffraction patterns, size of nanoparticles, and shape.

The role of supergene processes to concentrate precious metals at other deposits hosted in metamorphic sequences is not yet estimated and this line of investigation in this direction is rather promissing. For example, Tikhomirova (2006, 2008) reported findings of native gold, silver and copper in the ores of cupriferous sandstone of the Northern Urals. In this case, native gold is observed only in one deposit and one occurrence, whereas native copper and silver are found at all studied objects. Native copper is most common in

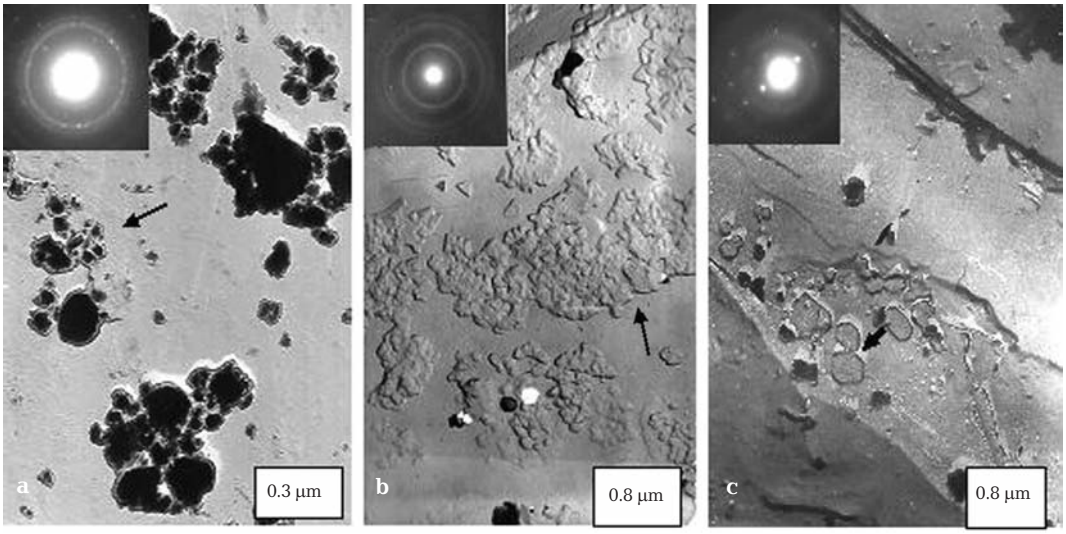

Fig. 2. Replicas with extraction. Segregations of native gold on quartz grains in oxidized zone: a — Onega type; b — Uchkuduk deposit; c — the deposits at Chu-Sorusu depression, Southern Kazakhstan. Arrows show particles, from which were microdifravtion patterns were obtained.

strong leached ores in association with cuprite. Submicron native silver and other Ag minerals are enclosed in chalcocite, bornite and chalcopyrite. And only in malachite and chrysocolla native, native silver occurs as clusters up to ten microns in size.

More data are available for cupriferous sandstone of the Udokan deposit, Kodaro-Udokan trough, NW Transbaikalia, where near-surface and deep-seated oxidized zones are intense. Therein, variegated deposits with elevated precios metals are widespread. In chalcocite-bornite ore and host sandstone of the Udokan deposit, gold grade ranges from 0.01 to 0.3 g/t, platinum, from below detection limit (bdl) to 0.06 g/t, palladium, from below detection limit to 0.009 g/t (Gongal'skiy *et al.*, 2006).The content of precious metals in oxidized malachite-brochantite ores is slightly higher (according to analytical results of three samples), g/t: 0.01—0.5 Au, bdl — 0.01, and 0.01—0.05 Pt (analyst G.E. Belousov, IGEM RAN, chemical-spectral method). Albitite-type metasomatic rocks with uranium oxides, titanates and molybdates is the characteristic feature of the Kodaro-Udokanskiy trough. Assay analysis has revealed in albitite elevated content of Pd (1.3 g/t) with gold grade 0.2 g/t and higher (Knauf *et al.*, 2000; Tatarinov *et al.*, 2000).

The aforementioned data show, that cupriferous sandstone of the Northern Urals and especially rocks of the Kodaro-Udokan trough, being promissing in significant reserves of precious metals, is very similar in mineralizatio to those of the Onera trough. Unfortunately, in the Onega trough, detailed studies have concerned only an estimation of uranium-vanadium ores. Distribution precious metals of uranium-vanadium ores has no been studied out of the uranium-vanadium ores at the Onega-type deposits. At the same time, the applied complex of the modern high resolution analytical techniques revealed important mineralogical features of various formations at these deposits.

(1) In hydrothermal roscoelite-Cr-bearingceladonite-dolomite veinlets, precious metals occur as selenides, selenide-sulfides, and compounds with bismuth and tellurium.

(2) Sprinklings of Powder of native metals (copper, gold, platinum with palladium) and novel natural phase, palladium analogue of auricupride occur in the near-surface and deep-seated oxidized zones.

(3) Native gold in hydrothermal veinlets of the Onega deposits is not found. Therefore, three analyses (№№ 11—13; Kuleshevich, 2008) of such native gold from the Pedrolampe deposit located at the northwestern boundary of the Onega trough are given

Table 1. **Chemical composition of native gold of the Pedrolampi deposit and from deep-seated and near-surface supergene zones of the Onega deposits (wt.%)**

El/№	1	2	3	4	5	6	7	8	9	10	11	12	13	14	15
Au	85.7	84.5	84.9	86.6	83.0	70.2	70.8	86.4	93.5	77.6	93.27	93.64	86.69	86.5	84.4
Ag	13.8	14.9	14.3	13.1	13.1	28.2	24.9	13.0	6.3	22.0	4.33	5.66	4.45	11.5	10.6
Fe	–	0.1	0.3	0.1	–	0.3	0.1	–	0.2	–	0.6	0.7	2.89	–	0.2
Hg	n.d.	n.d.	n.d.	n.d.	n.d.	n.d.	n.d.	n.d.	n.d.	n.d.	1.19	–	4.98	n.d.	n.d.
Pd	0.3	0.3	0.2	0.3	n.d.	n.d.	n.d.	n.d.	n.d.	n.d.	–	–	–	–	–
Cu	–	–	–	–	–	–	–	–	–	–	–	–	–	1.9	2.4
Σ	99.8	99.8	99.7	100.1	96.1	98.7	95.8	99.4	100.0	99.6	99.99	99.00	99.01	99.9	97.6

Note. (1–10) Deep supergene zone the Onega deposits (Middle Padma and Tsarevo, (11–13) hydrothermal gold-sulfide deposit Pedrolampi, (14, 15) near-surface oxidized zone of the Onega deposits. Analyses 1–10 and 14–15 were performed with a electron microprobe Superprobe-8100, All-Russia Institute of Mineral Resources; analyses 11–13 were performed with a Tescan electron microprobe, Institute of Geology, Karelian Scientific Center, Russian Academy of Sciences

in Table 1, Comparison of these analyses with those from deep-seated (№№ 1–10) and near-surface (№ 14, 15) oxidized zones of the Onega deposits show that hydrothermal gold appreciably differs from supergene gold in composition. It is characterized by high fineness (Au content 86.69–93.64 wt%), whereas supergene gold is of lower fineness (Au content 70.2–86.6 wt%). Hydrothemal gold contains Fe (0.6–2.89 wt%) and Hg (1.19–4.98 wt%), whereas maximum Fe content in supergene gold is 0.3 wt% Fe. At the same time, Ag concentration ranges from 4.33 to 5.66 wt% in hydrothermal gold and from 6.3 to 28.2 wt%, in supergene gold. In addition, Cu was occasionally detected in supergene gold (1.9 and 2.45 wt%) and Pd (0.2–0.3 wt%).

(4) Gold in near-surface oxidized zone containing less than 10 g/t of precious metals occurs as irregular-shaped cloddy particles up to 0.1 microns in size.

(5) In the upper deep-seated oxidized zone, gold occurs as broken spindle-shaped particles of 2–3 microns in size. Closer to the middle deep-seated oxidized zone, gold is disseminated in polycrystalline blades of native copper of tens microns in size. Therein, segregations of native Pd-bearing platinum were identified.

Thus, the results obtained testify substantial supergene processes at the Onega deposits. In this case, leaching and redistribution of precious metals in the oxidized zone decrease downword, whereas grain size of native metals increases in this direction, that suggest a great concentration of precious metals in the lower part of the deep-seated oxidized zone. In addition to the previous data, this conclusion is an additional criterion, favor possibile large or unique reserves of precious metals, at the first place, near explored U-V deposits (Chernikov, 1997, 2001 *et al.*; Chernikov *et al.*, 2000, 2005, 2007) about.

Role of mineral sorbents and X-ray amorphous matter in concentration of precious and other metals in supergene zone

All rocks of supergene zone as reported by Ginzburg and Rukovishnikova (1951), Chukhrov (1955), Nikitina (1968), Chernikov (1981, 1982), Vitovskaya and Bugel'skiy (1982), Chernikov *et al.* (2006), Savko *et al.* (2007) contain clay minerals, oxides and hydroxides of Fe, Al, Mn, Si, poor crystallized and X-ray amorphous products, which absorb various ore elements. Previously, Chernikov (1992) distinguished five main groups of strong natural sorbents of chemical elements and compounds, which are characteristic of supergene assemblages of the Onega and other deposits. Natural sorbents of these five groups involve numerous mineral and organic matters. Most of them are of crystal structure and minors are X-ray amorphous, opal, allophone, non-crystallized or nanoscaled oxides and hydroxides of Al, Si, Fe and Mn, and abundant in weathering profile of various crystalline rocks and in supergene zone of the aforementioned deposits.

Among crystalline mineral sorbents, which are complex and variable in composi-

tion, the majority has a great sorption capacity. First of all these are montmorillonite-saponite, where interstack cations are easily exchanged and can be varied from simple monovalent – Li^+, Na^+, K^+, NH_4^+ or bivalent Ca^{2+}, Mg^{2+} to complex $[Al(OH)_2]^+$ or RNH_3^+.

Mineral sorbents and poor crystallized, non-crystallized mineral or organic matter of five above mentioned groups are the major components of such prevalent supergene rocks and minerals, as bentonite, bauxite, laterite, zeolite, perlite, sapropel, coal, turf, and bitumen. They were described in numerous Russian and foreign publications.

It must be emphasized that natural sorbents are composed of several, frequently significantly different mineral sorbents, non-crystallized mineral and organic matter, and in many assemblages of weathering profile, soil, and turf, living matter occurs in great number. (Vernadsky, 1926; Study..., 1970; Turf and sapropel deposits, 1982; Shkol'nik *et al.*, 2004; Savko *et al.*, 2007). Biomorphic matter occurs in bauxite, phosphorite, certain manganese, iron, and gold ores. These ores possess a complex of properties characterizing their sorptive features. In particular, most natural sorbents, especially limonite, laterite, and opoka have polymodal character of distribution of pore volume, fissures and channels by sizes and are attributed to mixed-porous. Micropores, mesopores and macropores are distinguished in them. Macropores are the largest arteries, along which material is transported to mesopores and micropores. Matter is predominantly absorbed in micropores (Tarasevich and Ovcharenko, 1975; Kel'tsev, 1984) in production units, whereas mesopores and macropores under natural conditions, in addition to transport functions, play substantial role during chemisorption, desorption, and transformation, because they are unique channels, along which natural solutions circulate; subsurface water percolate incomparably slower than liquid circulation in experimantal unit. Therefore, macropores, channels, and fissures under natural conditions contain the bulk of products of such processes (Fig. 3). Veinlets and ore minerals are formed along them, in this case, uranophane-beta and according to radiography, sorbents, zeolite and clay, are also enriched in uranium.

Mineral sorbents, colloidal particles, organic matter and microbes are enriched in chemical elements due to: (1) coprecipitating sorbent and adsorbed matter, (2) exchange reactions from solutions, percolated through sorbent, and (3) adsorption, absorption, chemosorption, biosorption, and capillary condensation from solutions and gases, with which sorbents are in contact.

During coprecipitation, sorption of chemical elements by colloidal particles and microbed begins in solution. This phenomenon is the most common during sedimentation in oceans, lakes and rivers. In sediments (including iron-manganese nodules), accumulation of Pb, Bi, Th, U, Au, Ag, Ta, Se, Ge, Tl and many other chemical elements are accumulated as a result of coprecipitation. This contention is supported by both experimental data and observation (Perel'man, 1979; Bowen, 1979; Eisler, 1981; Baturin *et al.*, 1989; Gordeev and Oreshkin, 1990; Pertsev *et al.*, 1990).

Exchange reactions and other sorption processes (the second and third methods of extraction of chemical elements and compounds from subsurfacewaters by natural sorbents) have complex relations. Considering just ion exchange makes no sense in such

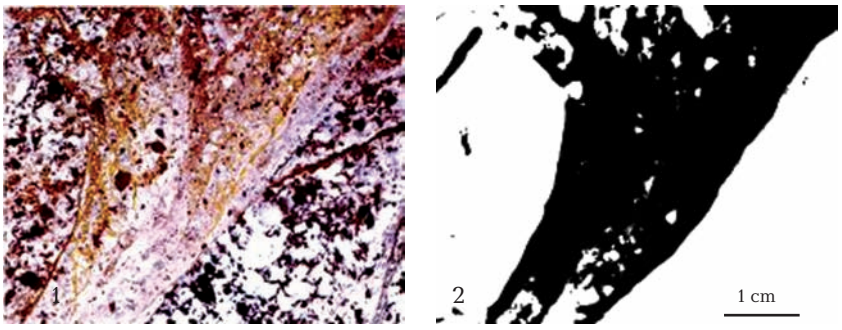

Fig. 3. Segregation of β-uranophane in zeolite-clayey breccia and in zeolitized granite. Yellow spots and veinlets – β-uranophane. Dark-brown spots – gematitized granite. 1 – polished section, 2 – radiography of thin section.

mineral as zeolite and spmectite, which combine different modes of extraction of ions from solutions. It has been just as a result of ionic exchange and other sorption processes, pH, Eh, mineralization, and chemical composition of fissure waters of folded areas and formation water of artesian basin change downward and phyllosilicates through disordered and ordered mixed-layered minerals to chlorites and micas are transformed. Supergene carbonates, sulfates, water-soluble silicates, phosphates and other minerals are formed by the same procedure (Chernikov, 1992, 2001; Chernikov *et al.*, 1994). It should be stressed that poor stable nepheline, major rock-forming mineral of the alkaline massifs, under supergene conditions, suggests its easy transition into supergene silicates as a result of leaching K and Na from tetrahedral aluminosilicates framework transformed into octahedral-tetrahedral aluminosilicates sheet due to water percolated from surface to deep levels of the massifs. Partial leaching of Na and K from nepheline and incorporation H_3O^+ in crystalline lattice lead to the formation of illite or mixed-layered minerals; complete leaching of alkalis from nepheline and saturation by OH^- of the lattice of newly formed mineral result in the precipitation of kaolinite, pyrophyllite, and other claye minerals, which contain only OH^- in their structures In this connection, percolated weak-acidic surface water at the depth of few meters become weak-alkaline and the depth of few hundred meters, occasionally fluorsilicate strong alkaline with pH = 12 (Krainov *et al.*, 1969). Sorption and transformation processes cause the formation of easy soluble gangue minerals as a result of interaction of hosr rocks and subsurface water, during interaction of the alkaline underground waters with host rocks takes place formation of. Formation processes of such minerals were described repeatedly (Dorfman, 1962; Dorfman *et al.*, 1981; Chesnokov *et al.*, 1982; Chernikov *et al.*, 1994; Chernikov, 2001). These are typomorphic minerals formed as a result of deep-seated hypergenesis of alkaline rocks.

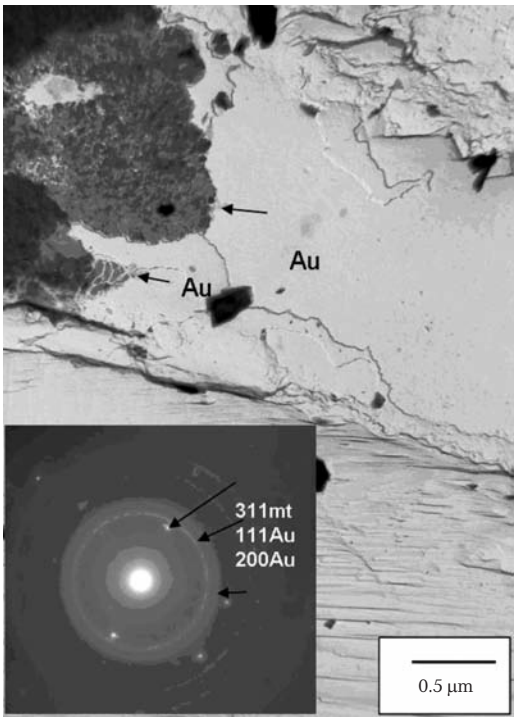

Fig. 4. Film segregations of native gold (shown by arrows) on the surface of jacobsite (Usinsk deposit, Kuznetsky Alatau). Microdiffraction image with reflection circles of native gold and jacobsite (311 mt) is nearby.

An accumulation of gold and other metals in the oxidized zone and weathering profile at the Ural, Altai, Kazakhstan, and Uzbekistan deposits (Shadlun, 1948; Chukhrov, 1950; Golovanov, 1961; Petrovskaya, 1973; Murzin, Malyugin, 1987; Chernikov, 1992) is caused by these processes. Figure 4 shows segregation of native gold on jacobsite, iron-manganese oxide, as result of such process.

At the Olympiada deposit (Enisei Ridge), where large gold and PGE reserves were revealed in weathering profile, native gold as globular segregations of 0.3 to 4.0 microns in size is indentified on the surface metacolloidal nodules of W-bearing tripuhyite (Sergeev & Samotin, 1990). The Native gold most frequently precipitates as fine powder on metacolloidal iron hydroxides (Petrovskaya, 1973). In the gold-bearing weathering crusts, gold is usually hosted in zoned limonite nodules in zones claye minerals. This was observed at the deposits Golden Grove and Coolgardie, Australia, Fasenda Nova, Brazil, Nulambur, India and the weathering profile after quartz-muscovite schist at the Svetlinskiy and Katablinskiy deposits,

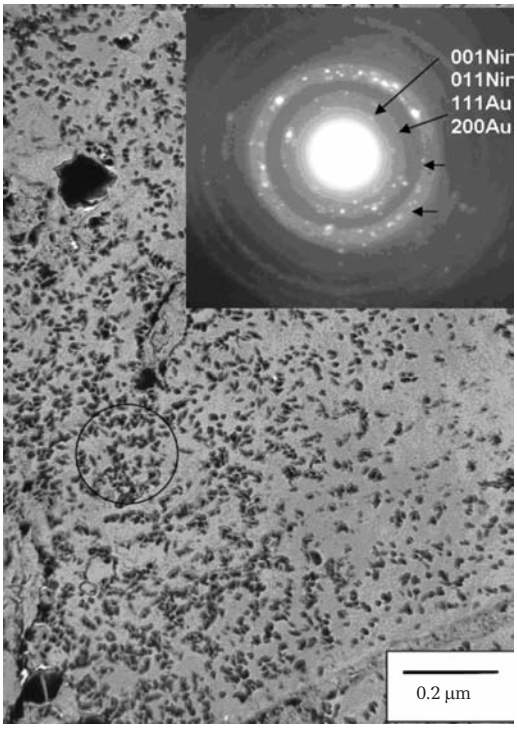

Fig. 5. Fine segregations of native gold and nyngyoite (field of image) on the surface of quartz grain, Khiagda deposit, Vitim Plateau. Microdiffraction image (right upper angle) was obtained from the area marked by circle. It document reflections of native gold (111) and (200) and ningyoite (011).

Urals (Wilson, 1984; Bhaskara *et al.*, 1983; Nair *et al.*, 1987; Kuznetsova, 2000).

Sorption and ion-exchange processes may result in accumulation of other chemical elements and compounds. Chemosorption as well as subsequent transformation and desorption transformation lead to the formation of pitchblende-zeolite, β-uranophane-zeolite (Fig. 3), uranyl phosphate-clayey, schröeckingerite-clayey (Boitsov, Legierski, 1977; Chernikov *et al.*, 1983; Chernikov, 1981, 1992, 2001), silver-clayey, silver-zeolite, silver-goethite, and gold-goethite (Artemenko, 1981; Sakharova *et al.*, 1983; Shilo *et al.*, 1992; Chernikov, 1992; Dvurechenskaya, 2001) ores. At the Khiagda deposit, Vitim plateau, similar processes formed ningyoite segregations with gold and fine-grained associations of native gold and ningyoite on quartz grains (Fig 5).

In addition to known cases of sorption (Ni and Co by goethite and nontronite, uranium and REE by apatite), high concentrations of Au, Pd, Pt, and Ag in iron, manganese, and aluminum oxides were established in weathering crusts in the Urals, Altai, Transbaikalia and other regions of Russia and foreign countries (Chernikov *et al.*, 2006; Savko *et al.*, 2007). At the Nikopol' manganese deposit, Ukraine such segregations of native gold occur on manganese oxides (Fig. 6).

These sorption processes played a major role in the formation of rare metals (Nb, Ta, Be, Zr, TR, Li, Ti) in the weathering crust in several regions of Russia.. There s a good possibility that detailed geological and mineralogical work in these regions will discover economic deposits of uranium, precious, and other metals.

Conclusions

Similar features in the distribution of mineral assemblages and geochemical zoning in the Onega multimetal deposits and the exogenetic infiltration deposits of Central Asia and Kazakhstan testify to their genetic similarity.

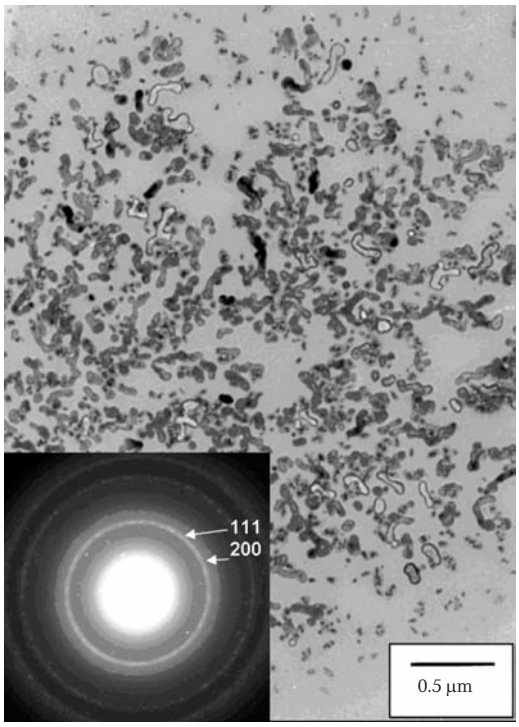

Fig. 6. Segregations of native gold (dark-grey, grey and light-grey) on the surface of manganese oxide (field of image), Nikopol' deposit, Ukraine. Microdiffraction image is at the left lower angle.

Some differences in their mineralogy correspond to physicochemical features of formation at deep and near-surface hypergenesis of these two types. These differences are also in the content of precious metal. In the Onega deposits, which show deep hypergenesis and mineralogical features of different origin, there are higher concentrations of precious metals. The size and character of their distribution in these zones support the contention that it is possible to discover large (and unique) reserves of precious near known uranium-vanadium deposits.

There are close similarities in mineral assemblages in the rocks of the Onega trough, the Southern Urals and the Kodaro-Udokanskiy trough, where prospects of discovering significant reserves of precious metals are good.

Complex of sorption, ion-exchange, and chemisorption processes explain the causes of zoned distribution of typomorphic mineral assemblages and formation of subsurface fluorsilicate waters with high pH in alkaline massifs. Sorption and subsequent transformation and desorption transformation led to important geochemical and mineral assemblages and ores in the zone of hypergenesis of the Ural, Altai, and Transbaikalia deposits in our country and abroad. Consequent geochemical, mineralogical and geological study of the supergene zone of these deposits, occurrences, and anomalies of these regions should result in substantial increase of the reserves of uranium, precious and other metals in our country and abroad. The presence of easily soluble minerals of uranium at the deposits suggests recovery of uranium by underground or heap leaching. Such methods would be economically profitable to work borderline ores (up to 0.01% U) and rocks with low uranium content (possibly, up to 0.005%). Reserves of these ores would increase significantly, even producing large and superlarge deposits. First, this concerns schröeckingerite deposits in Mongolia, Kazakhstan, and possibly, in the USA and other countries with arid climate, as well as β-uranophane-zeolite ores and ores with uranyl minerals associated with clay at the Transbaikalia deposits and other regions of Russia and foreign countries.

References

Artemenko O.V. About mineralogical features of regenerated ore minerals from silver-bearing hydrothermal veins. Vestn MGU. Ser. geol. **1981**. No 6. P. 93–97 [in Russian].

Baturin G.N., Savenko V.S. & Yushina I.G. Associations of chemical elements in oceanic sedimentary cycle. Dokl. AN SSSR. **1989**. V. 309. No 6. P. 1453–1457 [in Russian].

Bhaskara R.A., Barros T.G.C. & Adusumill M.S. Lateritic gold project. **1983**. Ihid. P. 159–176.

Bilibina T.V., Mel'nikov E.K. & Savitskiy A.V. New type of deposits of complex ores in the Southern Karelia. Geol. Ore. Dep. **1991**. V. 33. P. 3–13. [in Russian]

Boitsov V.E. & Legierski Ya. Succession and time of mineral formation at some hydrothermal uranium deposits. Geol. Ore. Dep. **1977**. No 1. P. 39–50 [in Russian].

Bowen N. Environmental geochemistry. L. Etc., Acad. Press. **1979**.

Chernikov A.A. Deep-seated hypergenesis, mineral- and ore formation. Tr. Fersman Mineralogical Museum RAN, Moscow. **2001**. [in Russian].

Chernikov A.A. Natural sorbents, their prospecting-estimation and ecological significance. Izv. RAN Ser. Geologic. **1992**. No 3. P. 118–126 [in Russian].

Chernikov A.A. Relation of weathering crust processes and hypogenic factors during formation of complex (V, Pd, Pt, Au, U) deposits of the Onega type. In: Main geological and commercial types of weathering crusts deposits and placers, technological estimation and exploration. IGEM RAS, Moscow. **1997**. P. 117.

Chernikov A.A. Typomorphism of uranium minerals and its practical significance // Inter. Geol. Rev. **1982**. V. 24. P. 567–576.

Chernikov A.A. Uranium behavior in the zone of hypergenesis. Nedra, Moscow. **1981**. [in Russian].

Chernikov A.A., Dorfman M. & Dvurechenskaya S.S. Specific features of formation of mineral associations of cryogenic and deep-seated hypergenesis // Doklady RAN. **1994**. V. 335. No 4. P. 485–448 [in Russian].

Chernikov A.A., Dubinchuk V.T., Ozhogin D.O. & Chistyakova N.I. Specific features of occurrence and distribution of noble metals in ores and oxidized zone of the Onega uranium-vanadium deposits of Southern Karelia. In: New Data on Minerals. **2007**. V. 42. P.43–49.

Chernikov A.A., Dubinchuk V.T., Chistyakova N.I. et al. New data on vanduim

hematite and micro- and nanocrystals of associated noble metal, copper, zinc and iron minerals New Data on Minerals. **2005**. V. 40. P. 65–71. [in Russian].

Chernikov A., Slukin A., Bugelskiy Yu. & Novikov V. Near-Surface and Deep-Seated Weathering products and large or superlarge ore deposits //12th Quadrenial IAGOD symposium. **2006**. Moscow. 21–24 August 2006. Abstracts. P. 91.

Chernikov A.A., Zenchenko A.A & Shivtorov I.V. Association of uranium minerals with zeolite at new type of uranium deposits. In: Mineralogy of Ore Deposits. Nauka, Moscow. **1983**. P. 5–13 [in Russian].

Chernikov A.A., Khitrov V.G. & Belousov G.E. Role of carbonaceous mattersubstance in formation of large polygenic complex deposits of the Onega type. In: Carbon-bearing Formations in Geological History. KNTs RAN Petrozavodsk:. **2000**. P. 194–199 [in Russian].

Chesnokov B.V., Popov V.A. & Nikondrov S.N. Thenardite – mirabilite mineralization of the Ilmeny and Vishnevye Mountains of the Urals – new type of sulphate mineralization of alkaline massifs. Dokl. AN SSSR. **1982**. V. 263. No 3. P. 693–696.

Chukhrov F.V. Oxidized zone of sulfide deposits of step part of Kazakhstan. AN SSSR, Moscow. **1950** [in Russian].

Chukhrov F.V. Colloids in the Earth's crust. AN SSSR, Moscow. **1955**. [in Russian]

Dorfman M.D. Mineralogy of pegmatite and weathering crust in ijolite-urtite of the Yukspor Mount of the Khibiny massif. AN SSSR, Moscow, Leningrad **1962**. [in Russian].

Dorfman M.D., Goroshchenko Ya.G., Biryuk L.I. & Knyazeva D.N. Interaction of lomonosovite with water solutions of sodium fluoride and carbon dioxide // New Data on Minerals. **1981**. V. 29. P. 149–151 [in Russian].

Dvurechenskaya S.S. Supergene minerals of silver deposits. Tr. TsNIGRI, Moscow. **2001**. [in Russian].

Eisler R. Trace-metal concentration in marine organisms. N.Y.: Etc. Pergam. Press. **1979**.

Ginzburg, I.I. & Rukovishnikova I.A. Minerals of ancient weathering crusts of the Urals. AN SSSR, Moscow, **1951**. [in Russian].

Gongal'sky B.I., Safonov, Yu.G. Safonov, Krivolutskaya et al. Unique Udokan-Chinei ore-magmatic system. In: Large and superlarge ore deposits. V 2. IGEM RAS, Moscow. **2006**. P. 483–509 [in Russian].

Gordeev V.V. & Oreshin V.N. Silver, cadmium, and lead in waters of the Amazonka river, itstributaries and estuary. Geokhimiya. **1990**. No 2. P. 244 – 256 [in Russian].

Kel'tsev N.V. Principles of adsorption technic. M.: Khimiya, Moscow, **1984**. [in Russian].

Knauf V.V., Makar'ev L.B. & Landa E.A. A new type of PGE mineralization. Dokl. Earth Sci. **2000**. V. 371, P. 423–425.

Krainov S.R., Mar'kov A.N & Petrova N.T. et al. Fluor-silicate brines with low alkaline (pH = 12) reaction at the deep levels of the Lovozero massif. Geokhimiya, **1969**. No 7. P. 791–796 [in Russian].

Kuleshevich L.V. Pedrolampi: a Precambrian gold-sulfide deposit, Karelia. Dokl. Earth. Sci. **2008**. V. 423. No 8. P. 1273–1277.

Kuznetsova O.Yu. Mineralogical and geochemical features of formation of gold-bearing weathering crusts of the Urals. Unpub. PhD thesis. IGEM RAS, Moscow. **2000** [in Russian].

Laverov N.P. Velichkin V.I. & Shumilin M.V. Uranium deposits of the Commonwealth countries: The main commercial-genetic types and their distribution // Geology of Ore Deposits. **1992**. V. 34. No 2. P. 3–18 [in Russian].

Mel'nikov E.K & Shumilin M.V. Possible model of formation of uranium-vanadium deposits with noble metals in the Onega region, Karelia. Izv. VUZov, Geol. Expl. **1995**. No 6. P. 31–37 [in Russian].

Murzin V.V.& Malyugin A.A. Typomorphism of gold in the hypergenesis zone. Ural Scientific Center Academy of Sciences of USSR, Sverdlovsk, **1987** [in Russian].

Nair N.G.K. Lateri. Chem. Geol. **1987**. V. 60. No 1/4. P. 309 – 315.

Nikitina A.P. Ancient weathering crust of crystalline basement of the Voronezh anticlise and its bauxite potential. Nauka, Moscow. **1968** [in Russian].

Perel'man A.I. Geochemistry. Vysh. Shkola, Moscow, **1979** [in Russian].

Pertsev N.V., Ul'berg Z.R., Kogan B.S. et al. Mechanism of biogenic concentration of metals at the shelf zones with deficit of geest. Geokhimiya, **1990**. No 1. P. 112–116 [in Russian].

Petrovskaya N.V. Native gold. Nauka, Moscow. **1973** [in Russian].

Savko A.D., Bugel'skiy Yu., Novikov V.M., Slukin A.D. & Shevyrev L.T. Weathering crusts and related mineral resources. Istoki, Voronezh. **2007** [in Russian].

Sakharova M.S., Posokhova T.V. & Artemenko O.V. Typomorphism of native silver. Mineral. Mag. **1983**. V. 3., No 3. P. 3–13.

Sergeev N.B. & Samotin N.D. Typomorphic mineral assemblages and mechanism of mineral formation in gold-bearing ore-forming systems of weathering crusts. In: Exogenous ore-forming systems of weathering crusts. Nauka, Moscow, **1990**. P. 207–215 [in Russian].

Shadlun T.N. Mineralogy of oxidized zone of the Blyava VHMS deposit, South Urals. Tr. IGN AN SSSR, Moscow. **1948**, V. 96. [in Russian].

Shilo N.A., Sakharova M.S., Krivitskaya N.N. et al. Mineralogical features of gold-silver mineralization of the northwestern Pacific framing. Nauka, Moscow. **1992**. [in Russian].

Shkol'nik E.L., Zhegallo E.A., Bogatyrev B.A. et al. Biomorphic structures in bauxites. Eslan, Moscow. **2004** [in Russian].

Shmariovich E.M., Natal'chenko B.I., Brovin K.G. et al. Behaviour of noble metals at the infiltration ore formation. Izv. RAN. Ser. Geol. **1992**. No 9. P. 121–132 [in Russian].

Study of turf raw material and sapropel. Nedra, Moscow. **1970** [in Russian].

Tatarinov A.V., Yalovik L.I., Nikitin S.E. et al. Perspectives for PGE mineralization in Transbaikalia. Razvedka i okhr. nedr. **2000**. No 1. P. 58–61 [in Russian].

Tarasevich Yu.N. & Ovcharenko F.D. Adsorption on clayey minerals. Izd-vo AN USSR , Kiev. **1975**. [in Russian].

Tikhomirova V.D. Native gold and silver in the ores of cupriferous sandstones of the Urals. Proc. All-Russia Conf. Diamonds and noble metals of the Timan-Urals region. Syktyvkar. **2006**. P. 223–224 [in Russian].

Tikhomirova V.D. Mineralogy of oxidized ores in the deposits of cupriferous sandstones in the northern Urals. Geoprint, Syktyvkar. **2008** [in Russian].

Turf and sapropel deposits. Kalinin University, Kalinin. **1982** [in Russian].

Vernadsky V.I. Biosphere. Essays I and II. Nauchno-tekhn. Izd-vo, Leningrad. **1926**. [in Russian].

Vitovskaya I.V. & Bugel'skiy Yu.Yu. Nickel-bearing weathering crusts. Nauka, Moscow. **1982** [in Russian].

Wilson A.F. Origin of quartz-free gold nuggets and supergene gold found in laterites and soils – a review and some new observations. Austral J. Earth Sci. **1984**. V. 31. No 3. P. 203–316.

Crystal Chemistry, Minerals as Prototypes of New Materials, Physical and Chemical Properties of Minerals

EXPERIMENTAL STUDY OF Au AND Ag PHASES DURING CRYSTALLIZATION OF Cu–Fe SULFIDE MELT

Tatyana A. Kravchenko and Elena N. Nigmatulina
Institute of Mineralogy and Petrography, Siberian Branch RAS, Novosibrsk, tanyuk@uiggm.nsc.ru

Species of trace Au and Ag (1 wt.%) in crystallized products of the central part melts of the Cu-Fe-S system have been studied. It has been established that gold of high fineness (80–82 wt.%) and silver (98–99 wt.%) associated with cubic (pc) haycockite $Cu_4Fe_5S_8$ solid solution, bornite Cu_5FeS_4 and pyrrhotite $Fe_{1-x}S$ crystallize from melts containing 47 at.% S, Cu/Fe = 0.93–0.63. Gold of high fineness (84–96 wt.%) and sulfides of the Me_2S type, where Me is up to, at.%: 48 Ag, 23 Au, 18 Cu, 2 Fe, associated with tetragonal chalcopyrite solid solution $Cu_{1-x}Fe_{1+x}S_2$, cubanite $CuFe_2S_3$, talnakhite $Cu_9Fe_8S_{16}$, pyrite FS_2, bornite, and pyrrhotite crystallize from melts of the following composition: 50 at.% S, Cu/Fe = 1–0.43 and 47 at.% S, Cu/Fe = 1.12. It is concluded that the Ag-Au sulfides are formed at temperature higher than 600°C and are resulted from a presence of free sulfur after crystallization of high-temperature cubic (fcc) chalcopyrite solid solution (iss). The relations of the Au-Ag phases and Cu-Fe sulfides in the products of joint crystallization from melts are determined by accumulation of Au-Ag phases during crystallization of iss and fine scattering of Ag as Ag-bearing sulfides are formed.
1 table, 8 figures, 13 references.
Keywords: gold, silver, Cu-Fe-S system.

Introduction

Au and Ag are elements identified in all types of deposits, where they are mainly associated with sulfide ore. Despite numerous studies, the problems concerning mechanism of accumulation and species of these elements in the ore-forming sulfides are unsolved. The magmatic deposits are the least studied. Therefore, the experimental study of Au and Ag behavior during melt crystallization together with sulfides of the Cu-Fe-S system, pyrite FS_2, chalcopyrite $CuFeS_2$, and pyrrhotite $Fe_{1-x}S$, which are major carriers of Au and Ag in sulfide ores is topical. At the same time, the study of crystallization of sulfide melt as probable mechanism of initial gold and silver accumulation is interesting to understand the conditions of formation of Au-Ag deposits of variable genesis.

Many scientists studied the Cu-Fe-S system. The experimental data of phase relations involving pyrite, chalcopyrite, and pyrrhotite (Yund & Kullerud, 1966; Cabri, 1973; Sugaki *et al.*, 1975; Vaughan & Craig, 1978, Tsujmura & Kitakaze, 2004) in general are consistent with the results of study of these minerals (Genkin *et al.*, 1981) in the Noril'sk Cu-Ni magmatic deposit, where up to 150 ppm Ag were detected in chalcopyrite and average 13 ppm Au, in pyrrhotite (Sluzhenikin & Mokhov, 2002). The Au-Ag solid solutions and acanthite Ag_2S are the most abundant proper mineral phases of Au and Ag. These compounds are attributed to the Ag-Au-S system that was completely studied by Barton (1980), who had revealed phase relations, temperatures of phase transitions, and melt temperatures of sulfides. However, available experimental data are insufficient to interpret the conditions of formation of natural sulfide assemblages, where Au and Ag are traces.

The aim of this study is to investigate the behavior of Au and Ag admixture during crystallization from melt together with sulfides of the Cu-Fe-S system, chalcopyrite, pyrite, and pyrrhotite. The features of chemical composition of synthesized phases are not discussed. The focus is on determination of Au and Ag phases depending on composition of synthesized assemblages of Cu-Fe sulfides.

Experimental

The Cu-Fe-S system was used as model macrosystem, where Au and Ag are as microconstituents (traces). In this case, the species of traces are suggested to be determined by physicochemical conditions of crystallization of equilibrium assemblages of Cu-Fe sulfides (macrocomponents). According to

this, the regime of synthesis of phase assemblages of macrosystem was established by melt cooling. Au and Ag (1 wt.%) were introduced in the synthesized samples of macrosystem and regime of synthesis corresponded to that of Cu-Fe sulfide assemblages. Amount of introduced traces is caused by difficult detection of contents below 1 wt.% by microscope and electron microprobe.

The plot of phase relations in the central Cu-Fe-S system constructed by Cabri (1973) was used as basis to select initial melt compositions. This plot is consistent with results of most experimental data on the Cu-Fe-S system and probable high- and low-temperature phase assemblages containing chalcopyrite, pyrite, and pyrrhotite are shown in it. In Fig. 1, the chalcopyrite solid solution field (iss) corresponds to the high-temperature cubic solid solution with face centered (fcc) lattice. It was experimentally established at 800–300°C and named by Merwin & Lombard (1937) as intermediate iss and Yund & Kullerud (1966) called this as chalcopyrite solid solution. Cubanite $CuFe_2S_3$, talnakhite $Cu_9Fe_8S_{16}$, mooihoekite $Cu_9Fe_9S_{16}$, and haycockite $Cu_4Fe_5S_8$ are attributed to the composition field of this solid solution. At the same time, these minerals compose Cu-rich ores of the Noril'sk Cu-Ni deposits. The iss field decreases as temperature drops and its lower boundary corresponds to the 47 at. % S section. The initial compositions of the synthesized samples involving the field of probable phase assemblages of chalcopyrite with pyrite, pyrrhotite, and aforementioned iss crystallized products are shown as black circles 1–9 in Fig. 1. The samples of composition ranging from chalcopyrite to iss with maximum Fe (Cu/Fe 1–0.43) were synthesized along section 50 at.% S and those of composition varying from iss with maximum Cu to iss with maximum Fe (Cu/Fe 1.12–0.63) were synthesized at 300°C along section 47 at.% S. The samples of the Cu-Fe-S system were synthesized from elements: carbonyl iron A-2 (granules), copper B3, and ultrapure sulfur additionally dehydrated by melting in vacuum superfine (pieces). Au and Ag were introduced in the Cu-Fe-S synthesized samples as pieces of Au-Ag alloy (by 50 wt.%). The samples weighted 110–120 mg. All samples were synthesized in vacuum quartz vials by heating up to 1100°C, storage at 1100°C for 12 h, cooling down to 850°C with step 50°C/h, storage at 850°C for 72 h, cooling down to 300°C with step 50°C/h, and cooling down to room temperature at switched off furnace. The rate of melt cooling was selected through experiment for the synthesis of all Cu-Fe-S samples by the same regime and following estimation of gold and silver behavior depending on composition of synthesized assemblages of Cu-Fe sulfides. The sample were cooled from 300°C with

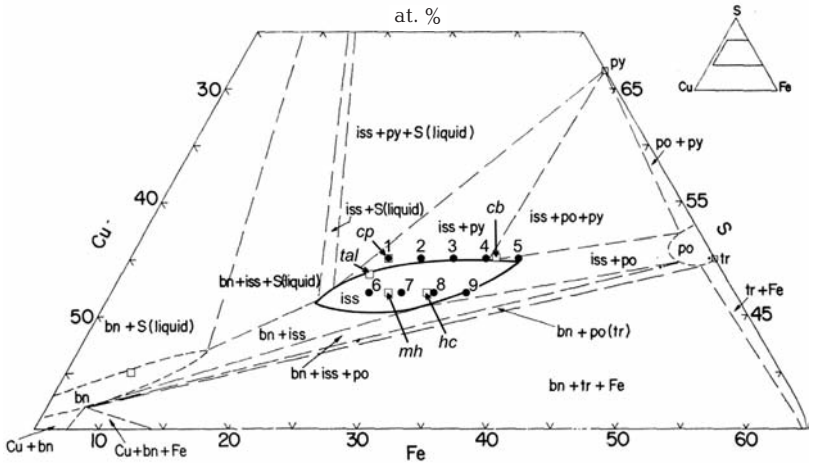

Fig. 1. Phase relations in the central part of the Cu-Fe-S system at 600°C (Cabri, 1973). Squares denote stoichiometric compositions of chalcopyrite $CuFeS_2$ (cp), talnakhite $Cu_9Fe_8S_{16}$ (tal), mooihoekite $Cu_9Fe_9S_{16}$ (mh), haycockite Cu_4Fe5S_8 (hc), bornite Cu_5FeS_4 (bn), cubanite $CuFe_2S_3$ (cb), troilite FeS (tr), and pyrite FeS_2 (py); po – pyrrhotite $Fe_{1-x}S$. Filled circles 1-9 denote initial composition of synthesized samples.

switched off furnace to obtain low-temperature crystallized products of iss rather than hardening.

After synthesis, the crystallized products were studied with optical microscope and X-ray diffraction. Polished sections were prepared from half of each sample (cut through the centre from the top down). The chemical composition of phases and distribution of traces in the sample bodies were detected by a Camebax-Micro electron microprobe according to the RMA-96 universal program (Lavrent'ev & Usova, 1991). The following analytic lines were used: Fe K_α, Cu K_α, S K_α, Ag L_α, Au M_α. In this set, lines are not superimposed. A probable interference of Cu K_{β_1} and Ag L_α in the third order reflection was taken into account by the PLATIN20DEL subroutine built-in RMA-96 program. This subroutine is matrix of delta coefficients taking into account the cross-effect of elements. The following standards were used: $CuFeS_2$, Au, and Ag. Operating conditions are 20 kV, 40 nA, counting time 10 s, and beam diameter 2–3 microns. All components were detected with accuracy of 2 relative percents. The detection limit calculated according to the 2δ test at 99% significance level is as follows, wt.%: 0.04 Cu, 0.03 Fe, 0.01 S, 0.05 Au, 0.04 Ag. BSE images of interrelated synthesized phases were made with JSM 5300 and JSM 6380 LA scanning electron microscopes in Institute of Geology of ore Deposits, Petrography, Mineralogy, and Geochemistry, Russian Academy of Sciences, Moscow, analysts S.F. Sluzhenikin and A.V. Mokhov (Kravchenko *et al.*, 2005; Kravchenko & Nigmatulina, 2007).

Results

The results of investigation of crystallized products of melts containing by 1 wt. % Au and Ag in the central Cu-Fe-S system are given in Table and in Fig. 2. The Cu-Fe-S phases are called master phases, whereas gold and silver phases, impurity phases. In this case, names of mineral analogues are applied to denote the master phases. The Au-Ag alloys of high fineness (> 75 wt.% Au) and silver (98–99 wt.% Ag) are shown as chemical symbols Au and Ag. Other phases containing Au and Ag are denoted as generalized chemical formulas taking into account element whose content is not less than 5 at.%.

The sample 1 matrix is composed of stoichiometric chalcopyrite. Bornite and pyrite occur along margins mainly on the upper surface of ingot (Fig. 2a). The impurity phases crystallize as fine drops and veinlets in the whole body of the sample that hampers their determination. Optical microscopy of great magnification indicates that these phases are characterized by different reflection and are located at the grain boundaries of master phases, in pores and fractures, and on the surface of the sample. The composition of the largest and brightest grains corresponds to gold of high fineness with minor Cu and Fe (Fig. 2b). The grains with less reflection were examined only in the margins of the sample. These are sulfides $(Ag,Au,Cu)_2S$ (Fig. 2c). Variable Ag content (0–0.8 wt.%) was detected in chalcopyrite and bornite both in various grains and within the single grain.

Sample 2 is predominantly composed of chalcopyrite (Fig. 3a). Cubanite $CuFe_2S_3$ as exsolution texture was identified in chalcopyrite being studied at high magnification (Fig. 3d). Like sample 1, gold of high fineness is located between chalcopyrite grains (Fig. 3c). The largest grains of impurity phases occur on the sample surface and are sulfide $(Ag,Cu)_2S$ and Au-Ag alloy (Fig. 3, 3b). In addition to gold, fine white grains with lesser reflection are observed (Figs. 3c, 3d). Analyses of master phases containing such phases are given in Table as (cp + cb)*.

In samples 3 and 4, master phases are chalcopyrite, cubanite, and pyrite (Fig. 4a) and in sample 5, additional pyrrhotite (Fig. 5a). Insignificant bornite occurs on the surface of these samples (Figs. 4c, 5a, 5d). Like sample 5, chalcopyrite and cubanite form exsolution texture, which can be observed only at high magnification (Figs. 4b, 5c). The composition of Au-Ag phases and their relations to Cu-Fe sulfides are similar to those described in sample 1 (Figs. 4b, 4c, 5b, 5d, 5e).

In sample 6, three phase occur as exsolution texture. In composition, these are chalcopyrite, talnakhite, and bornite (Fig. 6a). The grain of Au-Ag alloy whose composition is given in Table is shown in Fig. 6b. Other Au- and Ag-bearing phases were detected

Table 1. **Crystallized products of the Cu-Fe-S melts containing by 1 wt.% Ag and Au**

№	Initial composition: S; Cu; Fe, at.% Cu/Fe	Synthesized phases	Composition: at.%, wt.% Ag	Au	Cu	Fe	S	Total, wt.%
1	50; 25; 25	cp	0.03	0.00	25.03	24.48	50.47	
	1		0.06	0.00	34.48	29.64	35.08	99.26
		py	0.00	0.00	0.087	33.08	66.83	
			0.00	0.00	0.138	46.40	53.80	100.34
		bn	0.39	0.00	49.74	7.86	42.02	
			0.85	0.00	63.77	8.86	27.17	100.65
		Au	7.22	80.72	7.45	4.61	0.00	
			4.50	91.71	2.73	1.49	0.00	100.43
		$(Ag,Au,Cu)_2S$	40.16	12.99	10.20	1.61	35.05	
			50.53	29.84	7.56	1.05	13.11	102.09
		The same	29.45	22.74	5.81	2.41	39.58	
			34.35	48.44	3.99	1.46	13.73	101.97
2	50; 22.5; 27.5	cp	0.09	0.00	23.61	26.22	50.07	
	0.82		0.21	0.00	32.61	31.83	34.89	99.54
		cb	0.14	0.00	18.66	30.38	50.81	
			0.33	0.00	25.99	37.26	35.76	99.34
		Au	4.61	90.46	1.97	2.96	0.00	
			2.68	95.88	0.68	0.89	0.00	100.12
		$(Ag,Cu)_2S$	47.71	0.00	18.24	0.67	32.78	
			66.17	0.00	16.09	0.50	14.13	99.89
		(cp+cb)*	19.83	0.00	16.96	21.20	42.01	
			37.31	0.00	18.80	20.65	23.50	100.26
3	50; 20; 30	cp	0.24	0.00	22.64	27.21	49.92	
	0.67		0.56	0.00	32.78	31.03	34.53	98.90
		cb	0.11	0.00	16.91	32.53	50.45	
			0.26	0.00	23.37	39.52	35.19	98.34
		py	0.00	0.00	0.17	33.41	66.41	
			0.00	0.00	0.27	46.26	52.78	99.31
		bn	0.67	0.00	50.27	8.64	40.42	
			1.43	0.00	62.80	9.48	25.48	99.19
		Au	23.44	71.77	3.11	1.03	0.654	
			14.98	83.77	1.17	0.34	0.124	100.39
		$(Cu,Ag)_3S_2$	18.63	0.84	38.64	0.67	41.22	
			33.54	2.78	40.98	0.62	22.05	99.97
4	50; 17.5; 32.5	cp	0.17	0.00	21.07	28.53	50.23	
	0.54		0.41	0.00	29.03	34.56	34.92	98.92
		cb	0.09	0.00	17.74	31.01	51.16	
			0.28	0.00	25.25	38.00	35.80	99.53
		py	0.00	0.00	0.04	33.33	66.63	
			0.00	0.00	0.06	46.13	52.94	99.14
		bn	0.23	0.00	51.90	7.54	40.33	
			0.49	0.00	64.83	8.27	25.41	99.00
		Au	17.08	78.48	2.81	0.95	0.68	
			10.50	87.84	1.01	0.30	0.12	99.97
		$(Ag,Au,Cu)_3S_2$	27.02	13.09	14.73	1.13	44.03	
			36.72	32.58	11.81	0.78	17.94	99.83
5	50; 15; 35	cp	0.27	0.00	19.54	29.93	50.26	
	0.43		0.63	0.00	27.02	36.37	35.06	99.08

Table 1. **Continuation**

		cb	0.33	0.00	17. 68	31.49	50.50	
			0.77	0.00	24.54	38.40	35.35	99.06
		po	0.00	0.00	0.42	46.05	53,53	
			0.00	0.00	0.62	59.20	39.51	99.33
		py	0.00	0.00	0.12	33.21	66.67	
			0.00	0.00	0.19	46.14	53.17	99.50
		bn	0.44	0.00	52.53	7.14	39.88	
			0.92	0.00	65.54	7.84	25.10	99.40
		Au	6.23	84.55	3.88	4.43	0.92	
			3.72	92.31	1.37	1.37	0.16	98.93
		$(Ag,Au,Cu)_2S$	30.72	13.65	16.17	1.60	37.87	
			40.64	32.97	12.60	1.09	14.89	102.19
6	47; 28; 25	cp	0.00	0.00	25.43	24.71	49.86	
	1.12		0.00	0.00	34.86	29.76	34.48	99.10
		tal	0.00	0.00	27.04	24.12	48.84	
			0.00	0.00	36.68	28.75	33.42	98.85
		bn	0.06	0.00	48.76	11.26	39.92	
			0.12	0.00	62.35	12.66	25.76	100.89
		Au	10.44	82.18	3.79	2.63	0.96	
			6.31	90.74	1.35	0.82	0.18	99.40
		(bn + cp)*	10.33	0.00	34.87	16.65	38.15	
			20.19	0.00	40.13	16.84	22.15	99.31
		(cp + tal)*	13.77	0.00	24.74	21.16	40.13	
			26.24	0.00	28.29	21.77	23.27	99.58
7	47; 25.5; 27.5	hk	0.00	0.00	24.08	28.17	47.76	
	0.93		0.00	0.00	32.81	33.74	32.84	99.39
		bn	0.00	0.00	52.81	9.14	48.05	
			0.00	0.00	67.32	10.24	24.47	102.03
		Au	25.36	66.48	7.39	0.17	0.60	
			16.75	80.15	2.87	0.06	0.12	99.95
		Ag	97.86	0.00	1.44	0.56	0.14	
			97.90	0.00	0.84	0.29	0.04	99.07
8	47; 23; 30	hk	0.00	0.00	23.29	29.19	47.52	
	0.77		0.00	0.00	31.73	34.96	32.68	99.36
		bn	0.00	0.00	49.20	10.85	39.95	
			0.00	0.00	62.87	12.18	25.75	100.80
		Au	19.82	68.39	10.02	1.27	0.49	
			13.12	82.36	3.90	0.44	0.10	99.92
		Ag	98.32	0.00	0.89	0.57	0.22	
			99.52	0.00	0.53	0.30	0.07	100.42
9	47; 20.5; 32.5	hk	0.00	0.00	22.56	30.12	47.32	
	0.63		0.00	0.00	30.75	36.09	32.55	99.39
		bn	0.00	0.00	49.20	10.85	39.95	
			0.00	0.00	62.87	12.18	22.75	100.80
		po	0.00	0.00	1.65	47.85	50.49	
			0.00	0.00	2.37	60.46	36.62	99.46
		Au	20.34	66.92	11.57	1.00	0.17	
			13.54	81.28	4.54	0.35	0.03	99.74
		Ag	98.01	0.00	1.01	0.69	0.29	
			99.10	0.00	0.60	0.36	0.09	100.15

Notes: (cp) chalcopyrite $CuFeS_2$, (py) pyrite FeS_2, (bn) bornite Cu_5FeS_4, (cb) cubanite $CuFe_2S_3$, (tal) talnakhite $Cu_9Fe_8S_{16}$, (hc) haycockite $Cu_4Fe_5S_8$, (po) pyrrhotite ($Fe_{1-x}S$), (*) Cu-Fe sulfides with fine disseminated Ag-bearing phases

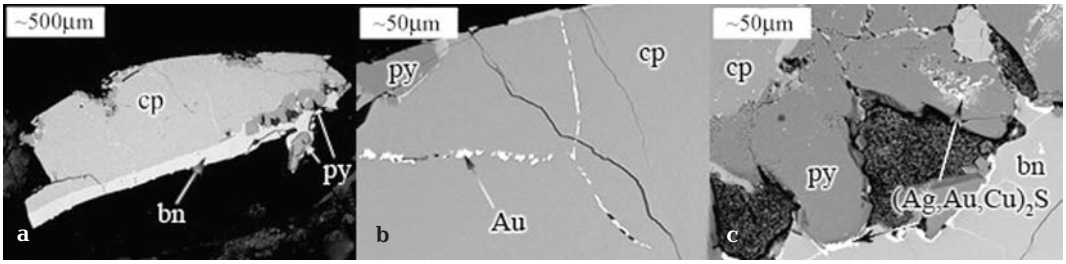

Fig. 2. Sample 1: a — common view of the sample with chalcopyrite (cp), bornite (bn), and pyrite; b — gold between grains of chalcopyrite; c — Ag-Au-Cu sulfides in pyrite and between grains of pyrite and bornite.

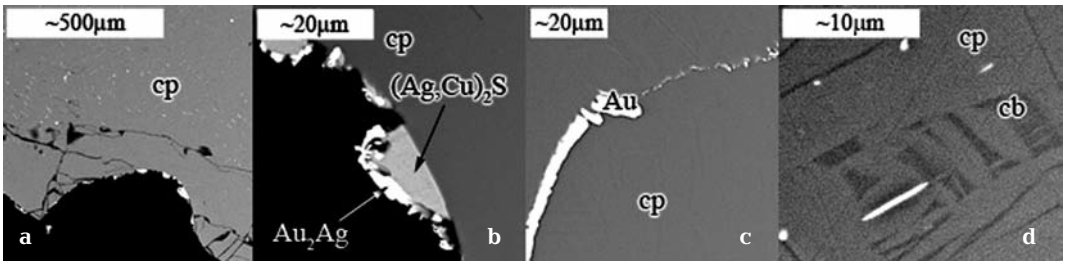

Fig. 3. Sample 2. Au-Ag phases (white) associated with chalcopyrite (cp) and cubanite (cb): a, b — chalcopyrite matrix, $(Ag,Cu)_2S$ sulfides and Au-Ag alloys on the sample surface; c — gold of high fineness between grains of chalcopyrite; d — chalcopyrite-cubanite matrix.

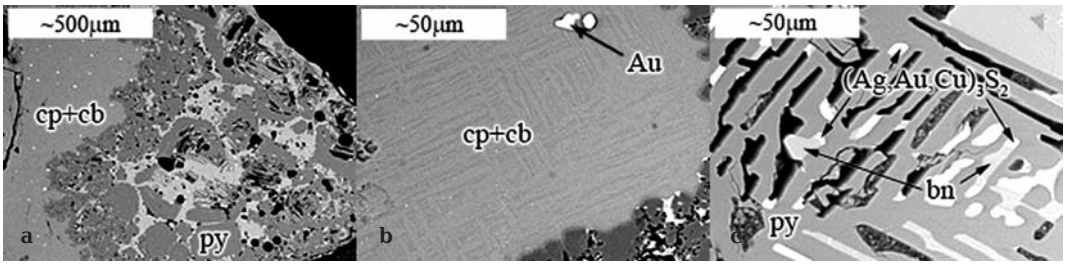

Fig. 4. Sample 4: a — Au-Ag phases (white) associated with chalcopyrite (cp), cubanite (cb), pyrite (py), and bornite (bn); b — gold in chalcopyrite-cubanite matrix; c — Ag-Au-Cu sulfides associated with pyrite and bornite near sample surface.

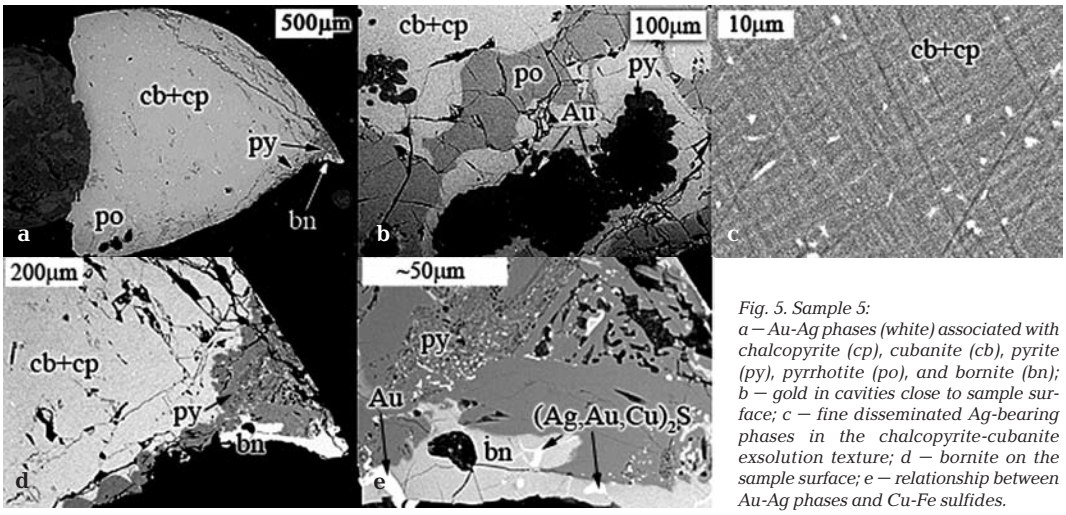

Fig. 5. Sample 5:
a — Au-Ag phases (white) associated with chalcopyrite (cp), cubanite (cb), pyrite (py), pyrrhotite (po), and bornite (bn); b — gold in cavities close to sample surface; c — fine disseminated Ag-bearing phases in the chalcopyrite-cubanite exsolution texture; d — bornite on the sample surface; e — relationship between Au-Ag phases and Cu-Fe sulfides.

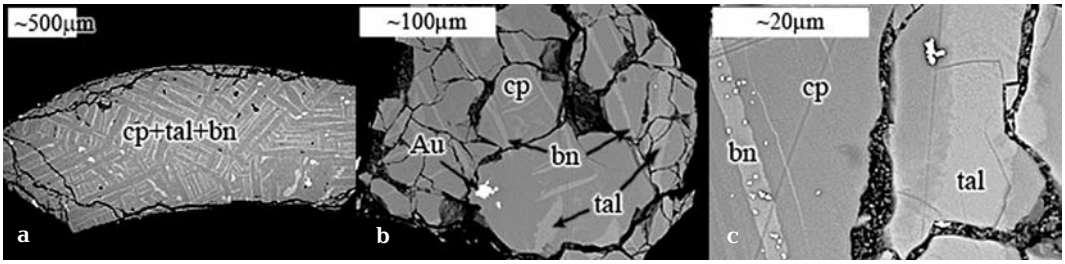

Fig. 6. Sample 6: a — Au-Ag phases (white) associated with chalcopyrite (cp), talnakhite (tal), and bornite (bn); b — gold close near sample surface; c — fine disseminated Ag-beraing phases in chalcopyrite and talnakhite.

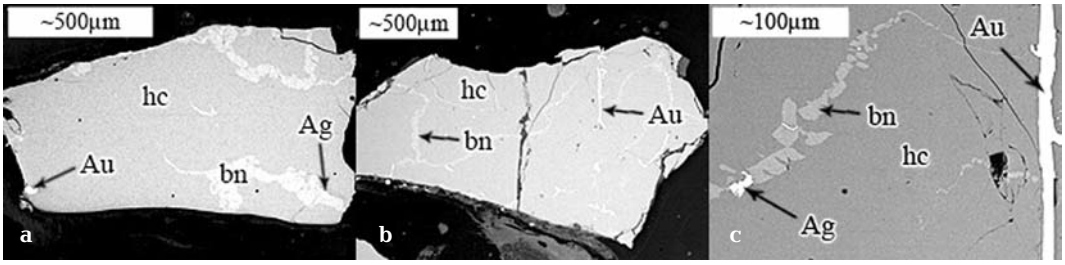

Fig. 7. Gold and silver (white) associated with haycockite (hc) and bornite (bn): a — sample 7; c, d — sample 8.

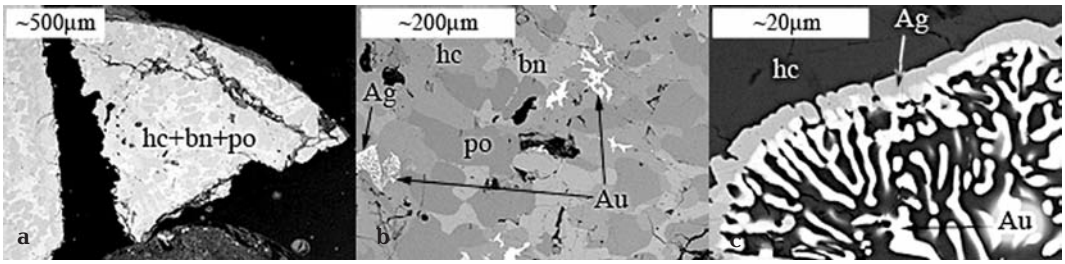

Fig. 8. Sample 9: a — gold and silver (white) associated with haycockite (hc), bornite (bn), and pyrrhotite (po); b — gold and silver between grains of pyrrhotite, haycockite, and bornite; c — Au-Ag zoned grain.

with scanning electron microscope (Fig. 6c). Like aforementioned samples, maximum content of impurities was identified at the grain boundaries of master phases (Table, bn + cp*, cp + tal*).

Samples 7 and 8 consist of bornite, phase of composition close to haycockite, and gold and silver of high fineness (Fig. 7). In sample 9, pyrrhotite occurs along with bornite and haycockite (Fig. 8a). In contrast to above described samples, Au-Ag alloys of samples 7—9 contain higher Ag, and silver crystallize together with them rather than Ag and Au sulfides (Figs. 7, 8). Some Au-Ag grains are zoned (Figs. 8b, 8c). Like samples 1—6, impurity phases occur at the grain boundaries of master phases and on the sample surface.

Thus, the assemblages of Cu-Fe sulfides stable at room temperature and corresponding in composition to initial composition of melts shown in Fig 1 were synthesized: sample 1 — chalcopyrite + bornite + pyrite; samples 2—4 — chalcopyrite + cubanite + pyrite; sample 5 — chalcopyrite + cubanite + pyrite + pyrrhotite; sample 6 — chalcopyrite + talnakhite + bornite; samples 7, 8 — haycockite + bornite; sample 9 — haycockite + bornite + pyrrhotite. The results obtained are consistent with experimental study (Cabri, 1973). At room temperature, chalcopyrite or chalcopyrite with cubanite along section 50 at.% and talnakhite or haycockite along section 47 at.% were synthesized instead of iss (Fig. 1).

Proper phases of Au and Ag are established in all synthesized phases. Gold of high fineness (80—82 wt.%) and silver (98—99 wt.%) crystallize from melts contain-

ing 47 at.% S, Cu/Fe = 0.93–0.63 (samples 7–9). Gold of high fineness (84–96 wt.%) and Ag-Au sulfides of the Me_2S or Me_2S_3 type where Me is Ag (up to 48 at.%), Au (up to 23 at.%), Cu (up to 18 at.%), and Fe (up to 2 at.%) crystallize from the melts containing 50 at.% S, Cu/Fe = 1.0–0.43 and 47 at.%, Cu/Fe = 1.12 (samples 1–6). Extremely fine grains of Ag-Au sulfides prevent exact determination of composition of these compounds. Variable Ag content (0–0.8 wt.%) was detected by electron microprobe in master phases of samples 1–6. In electron microscope, fine disseminated Ag-bearing phases are observed in the master phases. The bulk chemical composition of master phases and impurity phases corresponds to the compositions of mixtures of chalcopyrite with cubanite, bornite, and talnakhite containing up to 37 wt.% Ag (Table, cp + cb*, cp + bn*, cp + tal*).

The fine grains distributed through all samples are characteristic of all Au-Ag phases. In the case, they are predominantly arranged at the boundaries of Cu-Fe sulfide grains, in pores, and on (or close to) the sample surface.

Discussion

According to composition, the synthesized samples can be divided into two groups. The chalcopyrite group (samples 1–6) includes gold of high fineness (84–96 wt.%) and Ag-Au sulfides associated with tetragonal chalcopyrite, cubanite, talnakhite, pyrite, bornite, and pyrrhotite. The haycockite group (samples 7–9) includes gold of high fineness (80–82 wt.%) and silver (98–99 wt.%) associated with haycockite, bornite, and pyrrhotite. Gold of high fineness and products of the iss crystallization were identified in both groups. However, in the chalcopyrite assemblages, Ag-Au sulfides are formed simultaneous with gold, whereas silver crystallizes in the assemblages of haycockite, which is depleted in S in comparison with tetragonal chalcopyrite $CuFeS_2$. It appears from this that crystallization of impurity phases depends on the iss composition and occur during two stages. Gold of high fineness and silver are formed at the first stage. Ag-Au sulfides in the samples of the chalcopyrite group crystallized at the second stage replacing gold and silver of the first stage.

The first stage is characteristic of all samples. Gold and silver are more refractory phases than iss; their alloys crystallize at 1060–960°C. The following crystallization of iss (900–850°C, Yund & Kullerud, 1966) is accompanied with accumulation of most crystallized impurities in residual melt. This is indicated by gold and silver grains at the boundaries of grains of chalcopyrite and haycockite, in pores, and on the sample surface together with pyrite and bornite crystallized after iss at 738° and 568°C (Yund & Kullerud, 1966).

The samples of the chalcopyrite group are enriched in S in comparison with iss. After iss crystallization, they are characterized by phase assemblages iss + S and iss + py + S, which persist in the Cu-rich field of the Cu-Fe-S system at 600°C (Fig. 1). At 568°C, assemblage iss + S in sample 6 changes is replaced by assemblage iss + bn, whereas assemblage iss + py + S in sample 1, by iss + py + bn. It allows concluding that Ag-Au sulfides are formed by the reaction of gold and silver with gaseous sulfur after crystallization of iss but before bornite. This conclusion is supported by the composition and phase relations of synthesized samples. In the chalcopyrite-bearing samples, silver was not identified but fine disseminated Ag-bearing phases which are not in the samples with haycockite were found. In addition, grains of Ag-Au sulfides are close to gold grains of higher fineness (up to 96 wt.%) than in samples with haycockite (up to 82 wt.%). From this it follows that at the formation of Ag-Au sulfides, Au and Ag are redistributed between Au-Ag alloy of high fineness deposited at the first stage and crystallized Ag-Au sulfide ($alloy_1 + S_g \rightarrow alloy_2 +$ sulfide), whereas Ag as sulfides is extremely fine disseminated in the iss. Thus, Ag-Au sulfides are formed at temperature higher than 600°C and are resulted from free sulfur after crystallization of high-temperature cubic (fcc) chalcopyrite solid solution. It is consistent with experimental study of the Ag-Au-S system, where solid solutions of sulfides $(Ag,Au)S_2$ are melted at 838–680°C (Barton, 1980).

Crystallization of Ag sulfides in the samples of chalcopyrite group does not rule out

probable incorporation of Ag into iss and bornite. However, Ag is not detected in the haycockite and associated bornite. It allows concluding that Ag identified in Cu-Fe sulfides of chalcopyrite group occurs as sulfide and incorporate neither iss nor bornite.

Change of phase composition of the samples below 600°C (crystallization of bornite, pyrrhotite and iss exsolution) does not effect on Au and Ag phases in the studied crystallized products of the Cu-Fe-S melts as demonstrated by the identical species of impurities and phase relations within haycockite and chalcopyrite groups of samples.

Despite Au and Ag content in the synthesized samples is higher than bulk concentration of these elements in natural minerals, minimum size of synthesized grains of Au-Ag phases determined by microscope resolution are consistent with results of Au and Ag study in natural mineral assemblages. Au-Ag solid solutions with Ag up to 20 wt.% are the most stable and frequent in nature (Yushko-Zakharova *et al.*, 1986). According to the results obtained, Au-Ag solid solutions of such composition crystallize in all synthesized samples before precipitation of Ag-Au sulfides. In magmatic deposits of the Noril'sk district, proper minerals are the major carriers of Au and Ag (Sluzhenikin & Mokhov, 2002). Solid solutions of gold and silver are the most abundant ranging from gold of high fineness (100%) to nearly admixture-free native silver. In this case, native silver is characteristic of talnakhite and mooihoekite ores and chalcopyrite-pyrite and chalcopyrite-bornite ores contains Ag-Au sulfide in addition to Au-Ag solid solutions. Au-Ag alloys are frequently zoned (Ag content increases toward the grain margins) and patchy (the composition varies in 10–30 wt.%). Like synthesized Cu-Fe sulfides of chalcopyrite group, in chalcopyrite of the Talnakh pentlandite-chalcopyrite ore, vein-let- and irregular-shaped segregations in which Ag reaches 30 wt.% and more are observed in electron microscope.

The results obtained are important to determine Au and Ag phases in the initial magmatic assemblages of Cu-Fe sulfides. However, the study of stability of the Au-Ag synthesized phases and their chemical composition depending on mineral assemblage is required to interpret content of Au and Ag impurities in initial sulfide melt resulting in sulfide ore of the Noril'sk type, their partitioning between phases during melt crystallization and redistribution caused by post-magmatic process.

Conclusions

1. The partitioning of Au and Ag impurities (by 1 wt.%) between phases in the crystallized products of the Cu-Fe-S melts depending on mineralogy of assemblages of Cu-Fe sulfides is identified. Gold of high fineness (80–82 wt.%) and silver (98–99 wt.%) associated with haycockite $Cu_4Fe_5S_8$ cubic (pc) solid solution, bornite Cu_5FeS_4, and pyrrhotite $Fe_{1-x}S$. Gold of high fineness (84–96 wt.%) and Au-Ag sulfides of Me_2S or Me_3S_2 types, in which Me is Ag – up to 48 at.%, Au – up to 23 at.%, Cu – up to 18 at.%, Fe – up to 2 at.%, are associated with tetragonal chalcopyrite solid solution $Cu_{1-x}Fe_{1+x}S_2$, cubanite $CuFe_2S_3$, talnakhite $Cu_9Fe_8S_{16}$, pyrite FeS_2, bornite, and pyrrhotite.

2. Ag-Au sulfides are formed at temperature higher than 600°C and resulted from a presence of free sulfur after crystallization of high-temperature cubic (fcc) chalcopyrite solid solution.

3. The relationship between phases in joint products crystallized from Cu-Fe-S melt is determined by accumulation of Au-Ag phases in residual melt during crystallization of cubic (fcc) chalcopyrite solid solution and fine scattering of Ag at the formation of Ag-bearing sulfides.

Acknowledgements

We thank to S.F. Sluzhenikin and A.V. Mokhov for BSE images of synthesized phases.

This study was supported by the Russian Foundation for Basic Researches (project no. 08-05-233).

References

Barton M.D. The Ag-Au-S system // Econ. Geol. **1980**. 75. P. 303–316.

Cabri L.J. New Data on phase relations in the Cu-Fe-S system // Econ. Geol. **1973**. 68. P. 443–454.

Genkin A.D., Distler V.V., Gladyshev G.D., et al. Sulfide Cu-Ni ores of the Noril'sk deposits. Moscow: Nauka, **1981**. 234 pp. (In Russian.)

Kravchenko T.A., Nigmatulina E.N. Experimental study of fine-dispersed Au and Ag formation in the crystallized products of Cu-Fe sulfide melt // Bull. Earth Sciences. Russian Academy of Sciences. **2007**. No 1. http://www.scgis.ru/russian/cp1251/h-dgggms/1-2007/informbul-1-2007 (In Russian.)

Kravchenko T.A., Pavlyuchenko V.S., Sluzhenikin S.F., Mokhov A.V. Au and Ag behavior during crystallization from melt of phase assemblages of the Cu-Fe-S system with chalcopyrite and pyrrhotite // XV Russian Conference on Experimental Mineralogy. Syktyvkar. Abstr. **2005**. P. 57–59 (In Russian.)

Lavrent'ev Yu.G., Usova L.V. The RMA-89 program for a Camebax-Micro electron microprobe // J. Analyt. Chem. **1991**. 46(1). P. 67–75. (In Russian.)

Merwin H.E., Lombard R.H. The System Cu-Fe-S // Econ. Geol. **1937**. V. 32. P. 203–204.

Sluzhenikin S.F., Mokhov, A.V. Au and Ag in deposits of the Noril'sk destrict // Proc. All-Russia Symp. "Geology, genesis, and mining problems of complete deposits of precious metals". Moscow. **2002**. P. 326–330. (In Russian.)

Sugaki A., Shima H., Kitakaze A., Harada H. Isothermal phase relations in the Cu-Fe-S system under hydrothermal conditions at 350°C and 300°C // Econ. Geol. **1975**. 70. P. 806–823.

Tsujmura T., Kitakaze A. New phase relations in the Cu-Fe-S system at 800°C; constraint of fractional crystallization of sulfide liquid // N. Jb. Miner. Mh. **2004**. 10. P. 433–444.

Vaughan D.J., Craig J.R. Mineral Chemistry of Metal Sulfides. London: Cambridge University Press, **1978**.

Yund R. A., Kullerud G. Thermal stability of assemblages in the Cu-Fe-S system // Jour. Petrology. **1966**. V. 7. P. 454–488.

Yushko-Zakharova O.E., Ivanov V.V., Soboleva L.N. et al. Minerals of precious metals. Handbook. Moscow: Nedra, **1986**. 272 pp. (In Russian.)

Pt–Pd–Sn INTERMETALLIC COMPOUNDS CRYSTALLIZED FROM Cu–Fe SULFIDE MELT

Tatyana A. Kravchenko
Institute of Mineralogy and Petrography, Siberian Branch RAS, Novosibrsk, tanyuk@uiggm.nsc.ru

To understand the formation conditions of Pt-Pd-Fe-Sn minerals in the Noril'sk magmatic Cu-Fe ore they were synthesized by cooling of Fe-Sn-S and Cu-Fe-S melts containing admixtures of Pt, Pd, and Sn (1−2 wt.%) from 1200°C to room temperature. Crystallization of the Fe-Sn-S melts with Fe/Sn 3/1, 1/1 и 1/3 and 50 at.% S leads to the formation of PtSn and $PtSn_2$, which involve the whole Pt (1 wt.%) containing in the melts. The relationship between Pt-Pd phases (by 1 wt.%) and crystallized products of the Cu-Fe-S melts with 50 at.% S and Cu/Fe 1.22−0.25, and 45 at.% S and Cu/Fe 1.44−0.38 has been determined. Isoferroplatinum, Pt_3Fe, has been synthesized in association with cubanite $CuFe_2S_3$ + pyrrhotite $Fe_{1-x}S$, mooihoekite $Cu_9Fe_9S_{16}$ + bornite Cu_5FeS_4, haycockite $Cu_4Fe_5S_8$ + bornite + pyrrhotite, and bornite + pyrrhotite. Pd analogue of isoferroplatinum, Pd_3Fe, has been synthesized in association with cubanite + pyrrhotite. Rustenburgite, Pt_3Sn, atokite, Pd_3Sn, Pd-bearing rustenburgite, $(Pt,Pd)_3Sn$, Fe-bearing niggliite Pt(Sn,Fe), and Sn-bearing solid solutions of the hongshite series (Pt,Pd)(Fe,Cu,Sn) have been synthesized in the crystallization field of isoferroplatinum (50 at.% S, Cu/Fe = 0.25 and 45 at.% S, 1.44 > Cu/Fe ≥ 0.69). Thus, the presence of Sn in the field of stability of Pt-Pd-Fe intermetallic compounds determines the crystallization of their Pt-Pd-Sn analogues. The deficiency of Sn to form Pt-Pd-Sn phases is balanced by Fe and Pt-Pd-Sn-Fe phases crystallize simultaneously. The habit of synthesized phases and phase relationships in the crystallized products studied here are consistent with available published data for relevant natural assemblages.
3 tables, 3 figures, 17 references.
Keywords: chalcopyrite, mooihoekite, haycockite, talnakhite, intermetallic compounds of Pt and Pd.

Introduction

Pt and Pd minerals with Sn from chalcopyrite and chalcopyrite-pyrrhotite ores are unique assemblage at the Noril'sk Cu-Ni deposits. The Sn-bearing Cu-Fe assemblage, in which Sn incorporates into intermetallic compounds with PGE rather than into cassiterite or sulfides, was identified only at the Noril'sk deposits (Nekrasov, 1984). At the other deposits, Pt-Fe alloys, isoferroplatinum, Pt_3Fe and tetraferroplatinum, PtFe are the most abundant, whereas their Pt-Pd-Sn analogues − maslenitskovite, $(Pt,Pd)_3Sn$, rustenburgite Pt_3Sn, atokite, Pd_3Sn, and niggliite, PtSn characteristic of the Noril'sk Cu-Fe ore (Genkin *et al.*, 1981) are sporadic.

The problem of the genesis of Pt-Pd-Sn minerals is attractive due to controversial conclusion of their formation after magmatic crystallization of the major ore-forming sulfides, chalcopyrite, pyrrhotite, and pentlandite (Genkin, 1968; Genkin *et al.*, 1981; Distler *et al.*, 1979, 1988, 1999). Solution of the crystallization sequence problem is primary important because this determines mechanism of accumulation of rare elements. High melting temperature of most Pt-Pd-Sn minerals (> 1200°C) and their close intergrowths with Pt-Fe alloys combined with the data of potential Sn content in the upper mantle (Barsukov & Dmitriev, 1972; Nekrasov, 1984) indicate a probable direct crystallization of Pt-Pd-Fe-Sn intermetallic compounds simultaneously with Cu-Fe sulfides from magmatic melt. However, such crystallization is not studied.

The aim of this study is an experimental modeling of the formation of Pt-Pd-Sn intermetallic compounds during cooling of Cu-Fe sulfide melts relevant to Cu-Fe ores from the Noril'sk Cu-Ni deposits.

Experimental

The Cu-Fe-S and Fe-Sn-S systems are used as model macrosystems, where PGE and also Sn in the Cu-Fe-S system are traces but their amount (not less than 1 wt.%) is sufficient to be detected by optical methods and electron microprobe. In this case, crystallized phases of trace elements are suggested to be determined by physicochemical conditions of crystallization of equilibrium Cu-Fe and Sn-Fe sulfides (macrocomponents). Three runs were carried out.

1. The samples of the Fe-Sn-S system containing 1 wt.% Pt were synthesized. Platinum phases depending on Fe and Sn in initial Fe-Sn sulfide melt were established.

2. The samples of the central Cu-Fe-S system (Fig. 1) corresponding to the composition of the Noril'sk Cu-Fe ores, with which Pt-Pd-

Fe-Sn intermetallic compounds are formed, were synthesized. The relationship between Pt and Pd phases (initial amount 1 wt.%) and assemblages of Cu-Fe sulfides was established and field of stability of the Pt-Fe and Pd-Fe intermetallic compounds was determined.

3. Pt-Pd-Sn intermetallic compounds associated with Cu-Fe sulfides corresponding to the established (item 2) field of stability of Pt-Fe and Pd-Fe intermetallic compounds were synthesized.

Samples (0.2−1 g) of the Fe-Sn-S system were prepared from synthetic FeS and SnS, whereas those of the Cu-Fe-S system, from elements. Carbonyl iron A-2, copper B3, ultrapure sulfur additionally dehydrated by melting in vacuum, ultrapure tin, and metallic platinum and palladium were raw material.

All samples of both systems were synthesized in vacuum quartz vials by cooling of melt from 1200-1150°C to room temperature. The Cu-Fe-S cooled samples were kept at 600°C for couple weeks and at 400°C, for three months. The samples were cooled from 600 and 400°C to room temperature in cold water.

After synthesis, the crystallized products were studied with optical microscope and X-ray diffraction. Polished sections were prepared from half of each sample (cut through the centre from the top down). The chemical composition of phases and distribution of trace elements in the sample bodies were detected by a Camebax-Micro electron microprobe according to the RMA-96 universal program (Lavrent'ev & Usova, 1991). The following analytic lines were used: Fe K_α, Cu K_α, S K_α, Pt M_α, Pd L_α, Sn L_α. In this set, lines are not superposed. The following standards were used: FeS, SnS, $CuFeS_2$, Pt и Pd. Operating conditions are 20 kV, 40 nA, counting time 10 s, and beam diameter 2−3 microns. All components were detected with accuracy of 2 relative percents. The detection limit calculated according to the 2δ test at 99% significance level is as follows, wt.%: 0.05 Cu, 0.03 Fe, 0.02 S, 0.06 Pt, 0.05 Pd, 0.05 Sn.

The conventional names of mineral analogues and generalized chemical formulas taking into account elements whose content is not less than 5 at.% were used to denote synthesized phases.

Platinum phases (1 wt.%) in crystallized products of the Fe–Sn–S melts

The results of investigation of crystallized products of the Fe-Sn-S melts with 50 at.% S and Fe/Sn 3/1, 1/1, and 1/3 containing 1 wt.% Pt are given in Table 1 and in Fig. 2. Most synthesized samples are composed of pyrrhotite, $Fe_{1-x}S$ and herzenbergite that is consistent with experimental study (Moh, 1974). As seen from Table 1, Pt does not incorporate into pyrrhotite and herzenbergite. The isolated Pt-bearing phases were indentified in all synthesized phases. In samples 1 and 2 (Fe/Sn = 3/1 и 1/1), niggliite PtSn was found and $PtSn_2$ was identified in sample 3 (Fe/Sn = 1/3). Thus, in the crystallized products of the Fe-Sn sulfide melts studied here, PtFe compounds were not identified and Pt is associated with Sn.

Platinum and palladium phases in the crystallization products of the Cu–Fe–S melts

The samples of the Cu-Fe-S sytem 50 at.% S, Cu/Fe 1.22−0.25 and 45 at.% S, Cu/Fe 1.44−0.38 with Pt and Pd (1 wt.%) were synthesized. The identical phase composition was established at room temperature in the samples synthesized with different regime of cooling (quenched from 600 or 400°C) (Table 2). The phase relations of Cu-Fe sulfides in the synthesized samples are consistent with experimental data of the Cu-Fe-S system at 600°C (Cabri, 1973) and 400°C (Vaughan & Craig, 1978) (Fig. 1). The primary compositions of the synthesized samples are shown in Fig. 1 as black circles 1−14. The iss field in Fig. 1 corresponds to high-temperature cubic solid solution with face-centered (fcc) unit cell. Cubanite, $CuFe_2S_3$, talnakhite, $Cu_9Fe_8S_{16}$, mooihoekite, $Cu_9Fe_9S_{16}$, and haycockite, $Cu_4Fe_5S_8$ pertain to the compositional field of this solid solution. Together with chalcopyrite, these minerals compose the Noril'sk ore enriched in copper, during deposition of which Pt-Pd-Fe-Sn intermetallic compounds were formed. The synthesized crystallized products of iss are shown in Fig 1b in parenthesizes. These are cubic (fcc) cubanite (samples 3−7) and cubic (pc) phases, which are close in composition to mooihoekite (samples 8 and 9) and haycockite (samples 10 and 11). The synthesized assemblages of Cu-Fe sulfides are given in Table 2. These are chalcopyrite + pyrite + bornite (samples 1 and 2), chalcopyrite + cubanite (samples 3 and 4), chalcopyrite + cubanite + pyrrhotite (samples 5 and 6), cubanite + pyrrhotite (sample 7), mooihoekite + bornite (samples 8 and 9), haycockite + bornite (sample 10), haycockite + bornite + pyrrhotite (sample 11), bornite + pyrrhotite (sample 12), and bornite + pyrrhotite + Cu (samples 13 and 14).

Table 1. **Phases crystallized from the FeS-SnS melts containing 1 wt.% Pt**

№	Initial composition, at.%		Synthesized phases	Composition of synthesized phases, at.% / wt.%				
	FeS	SnS		Fe	Sn	S	Pt	∑
1	75	25	$Fe_{1-x}S$	48.50	0.16	51.34	0.00	
				62.05	0.42	37.71	0.00	100.18
			SnS	0.21	49.75	50.03	0.00	
				0.16	78.14	21.23	0.00	99.53
			PtSn	0.05	49.31	0.25	50.39	
				0.02	37.04	0.05	62.21	99.32
2	50	50	$Fe_{1-x}S$	49.12	0.04	50.84	0.00	
				62.95	0.12	37.41	0.00	100.48
			SnS	0.17	49.89	49.94	0.00	
				0.13	78.52	21.22	0.00	99.87
			PtSn	0.44	49.47	0.24	49.85	
				0.16	37.32	0.05	61.82	99.35
3	25	75	$Fe_{1-x}S$	48.85	0.06	51.09	0.00	
				62.52	0.17	37.54	0.00	100.23
			SnS	0.14	49.92	49.94	0.00	
				0.10	78.50	21.22	0.00	99.82
			$PtSn_2$	0.68	65.99	0.02	33.31	
				0.26	53.73	0.01	44.57	98.57

Table 2. **Phase composition of crystallized products of the Cu-Fe-S melts containing Pt or Pd (1 wt.%)**

№ обр.	Initial composition, at.%			Synthesized phases		
	S	Cu	Fe	Cu-Fe-S	Pt	Pd
1		27.5	22.5	cp + bn + py	$Cu(Fe,Pt)S_4$	PdS
2		25.0	25.0		PtS	
3		22.5	27.5	cb + cp		
4	50.0	20.0	30.0			
5		17.5	32.5	cb + cp + po		
6		15.0	35.0			
7		10.0	40.0	cb + po	Pt_3Fe	Pd_3Fe
8		32.5	22.5	mh + bn	Pt_3Fe + PtS	PdS
9		30.0	25.0		Pt_3Fe	
10		27.5	27.5	hc + bn		
11	45.0	25.0	30.0	hc + bn + po		Pd(Cu,Fe)
12		22.5	32.5	bn + po		
13		20.0	35.0	bn + po + Cu		
14		15.0	40.0		PtFe	

Notes: (cp) chalcopyritem $CuFeS_2$, (bn) bornite (Cu_5FeS_4), (py) pyrite FeS_2, (cb) cubanite $CuFe_2S_3$, (po) pyrrhotite $Fe_{1-x}S$, (mh) mooihoekite $Cu_9Fe_9S_{16}$, and (hc) haycockite $Cu_4Fe_5S_8$.

Platinum and palladium were not detected in sulfides of this macrosystem. In all synthesized samples, they occur as proper phases. According to the results obtained, along section 50 at.% S, Pt and Pd sulfides, malanite, $(Pt,Cu,Fe)S_4$, cooperite, PtS, and vysotskite, PdS were identified in samples 1–6 (Cu/Fe 1.22–0.43), whereas in sample 7 (Cu/Fe 0.25), Pt-Pd-Fe alloys, isoferroplatinum Pt_3Fe and unnamed palladium analogue of isoferroplatinum Pd_3Fe were found. Palladium mineral vysotskite and platinum minerals cooperite

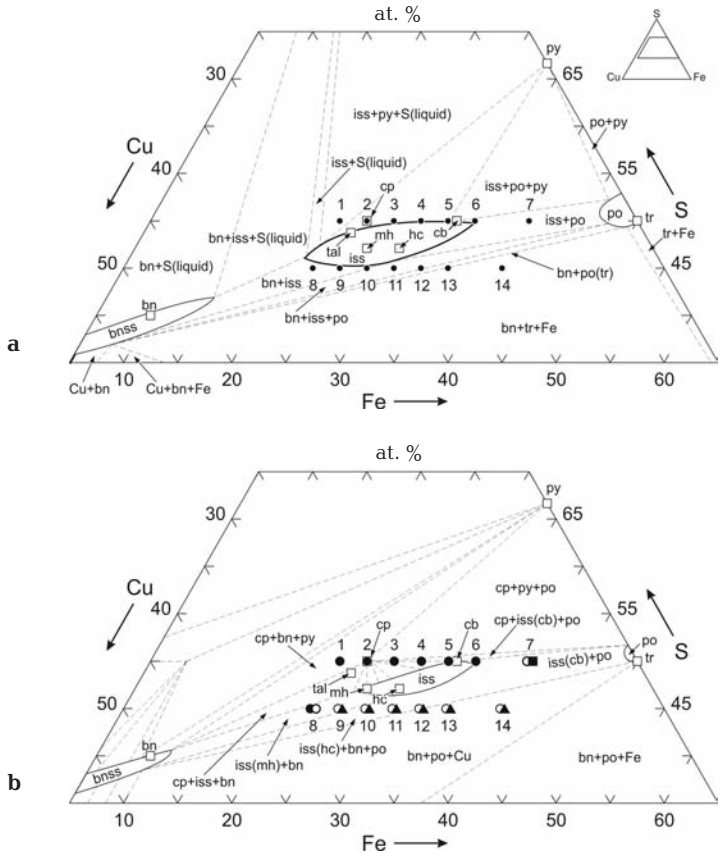

Fig. 1. Phase relations in the central part of the Cu-Fe-S system. (a) at 600°C (Cabri, 1973), (b) at 400°C (Vaughan, Craig, 1978). (iss, bnss, and po) fields of chalcopyrite, bornite, and pyrrhotite solid solutions, respectively. □ – stoichiometric chemical composition of minerals: (cp) tetragonal chalcopyrite $CuFeS_2$, (bn) bornite Cu_5FeS_4, (py) pyrite FeS_2, troilite FeS, and crystallization products of iss: (tal) talnakhite $Cu_9Fe_8S_{16}$, (cb) cubic cubanite $CuFe_2S_3$, (mh) mooihoekite $Cu_9Fe_9S_{16}$, and (hc) haycockite $Cu_4Fe_5S_8$. (1–14) Initial compositions of synthesized samples with admixtures (Fig. 1b) of Pt-Pd phases: ● – (Cu Fe,Pt)S_4, PtS and PdS; ○ – Pt_3Fe, PtFe; ■ – Pd_3Fe; ▲ – Pd(Cu,Fe).

and isoferroplatinum were identified in sample 8 (45 at.% S, Cu/Fe 1.44). The latter minerals crystallize simultaneously. In Pd-bearing samples 9–14 (45 at.% S, Cu/Fe 1.20–0.38), unnamed Pd-Fe-Cu alloys, Pd(Cu,Fe), considered (Nekrasov, 1994) as palladium analogues of hongshite, PtCu, and isoferroplatinum and tetraferroplatinum, PtFe were found in Pt-bearing samples. The same phases were synthesized with both Pt and Pd in primary melt (Kravchenko, 2002, 2006).

Thus, Pt-Fe intermetallic compounds corresponding to the Pt-Fe natural alloys, isoferroplatinum and tetraferroplatinum synthesized in the central Cu-Fe-S system (50 at.% S, Cu/Fe 0.25 and 45 at.% S, $1.44 \geq$ Cu/Fe ≥ 0.40) are associated with cubanite, pyrrhotite, bornite and depleted in S crystallized products of chalcopyrite solid solution – mooihoekite and haycockite. Palladium analogue of isoferroplatinum, Pd_3Fe associated with cubanite and pyrrhotite was synthesized in the same field.

Synthesis of Pt–Pd–Sn intermetallic compounds in the field of stability of their Pt–Pd–Fe analogues in the Cu–Fe–S system

Pt-Pd-Sn intermetallic compounds were synthesized in the Cu-Fe-S system corresponding to the field of crystallization of Pt_3Fe and Pd_3Fe (Table 2, sample 7–12). Electron microprobe data of the synthesized phases, of samples of the macrosystem and of Pt-Pd-Fe phases described above (samples 7–1, 9–1, 11–1, 12–1) are given in Table 3. Samples 7–3, 9–2, 11–2, and 12–2 with admixture of Pt and Sn (Pt/Sn = 3/1), sample 7–4 with admix-

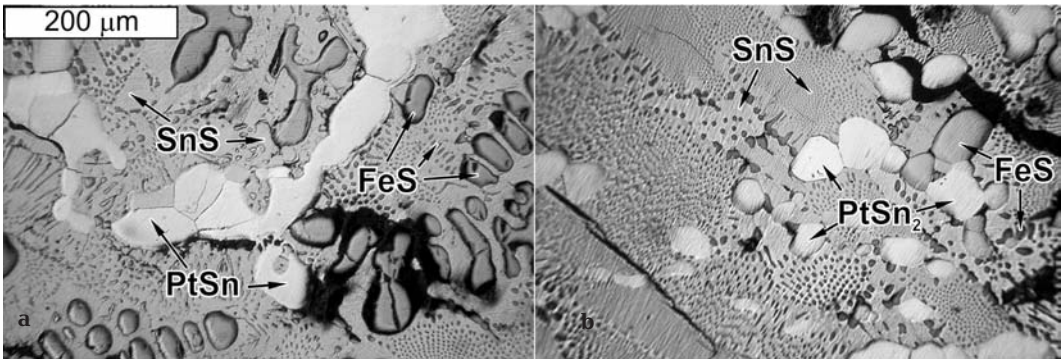

Fig. 2. Platinum phases (1 wt.%) in synthesized samples of the FeS-SnS system. (a) PtSn (Fe/Sn = 3/1 u 1/1), (b) $PtSn_2$ (FeS/SnS = 1/3).

ture of Pd and Sn (Pd/Sn = 3/1) as well as samples 7−5 and 9−3 with Pt, Pd, and Sn (Pt,Pd/Sn = 3/1) were synthesized. In addition, samples 11 and 12 with Pt/Sn = 3/1 and with 1 wt.% Pd were synthesized again (samples 11−3 and 12−3 in the Table 3). The composition of Cu-Fe sulfides and phase relations in the synthesized samples are identical to those in aforementioned Sn-free samples. Both Sn and Pt and Pd are not detected in sulfides of the macrosystem. To estimate the effect of Sn on Pt and Pd species in the synthesized samples, Cu was combined with Pt and Pd in formulas of the Pt-Pd phases with the exception of Sn-bearing solid solution (Pt,Pd)(Fe,Cu,Sn) in sample 12−3. The comparison of results of crystallized Sn-free melts indicates that in all Sn-bearing samples, Pt-Pd-Sn phases, which are analogues of Pt-Pd-Fe phases, were synthesized. In the samples with Pt,Pd/Sn = 3/1, these are rustenburgite, Pt_3Sn, atokite, Pd_3Sn, and palladium rustenburgite, $(Pt,Pd)_3Sn$ containing up to 1 wt.% and 2.5 wt.% Cu. In samples 11−3 and 12−3 with Pt,Pd/Sn > 3/1 (due to Pd in initial samples), Pt-Pd-Sn intermetallic compounds of variable composition were synthesized. These compounds are characterized by zoned grains enriched in Sn and Pt in cores and Pd and Fe, in margins. In sample 11−3, Fe-bearing (up to 3 wt.%) analogues of palladium rustenburgite $(Pt,Pd)_3Sn$ were identified and in sample 12−3, Fe-bearing (up to 4 wt.%) analogues of niggliite PtSn and Sn-bearing (up to 7 wt.%) analogues of the (Pt,Pd)(Fe,Cu) natural solid solutions of hypothetical (Nekrasov, 1994) hongshinite series Pt(Fe,Cu) − Pd(Cu,Fe).

The phase relations in the synthesized samples are shown in Fig. 3. Location of the largest grains on the surface of the samples, in interstices between host sulfide minerals, and in pores and fractures is characteristic feature of the Pt-Pd-Sn synthesized phases. The inclusions of host Cu-Fe sulfides and grains of various shape (well-shaped crystals and crystals with irregularly grown faces, skeletons, veinlets, and irregular shaped grains) are observed within single sample. Similar morphological features are suggested to be features of metacrystals (Genkin, 1968, Genkin *et al.*, 1981). The same phase relations were established for Au and Ag behavior in the studied field of the Cu-Fe-S system (Kravchenko *et al.*, 2005, 2007; Kravchenko & Nigmatulina, this issue).

Thus, in the crystallization field of isoferroplatinum Pt_3Fe in the Cu-Fe-S system (50 at.% S, Cu/Fe 0.25 and 45 at.% S, 1.44 ≥ Cu/Fe ≥ 0.69, Pt,Pd/Sn 3/1), rustenburgite Pt_3Sn, atokite Pd_3Sn, and palladium rustenburgite $(Pt,Pd)_3Sn$ were synthesized and at Pd + Pt/Sn > 3/1, Fe-bearing niggliite Pt(Sn,Fe) and Sn-bearing solid solutions of the hongshinite series.

Conclusions

1. The results obtained indicate that formation of proper phases is mechanism of accumulation of PGE (admixture of Pt and Pd 1−2 wt.%) in the crystallized products of melt in the central Cu-Fe-S system (50 at.% S, Cu/Fe 1.22−0.25 and 45 at.% S, Cu/Fe 1.44−0.38). This results in the absence of PGE admixture in Cu-Fe sulfides. PGE move to the boundaries of crystallized Cu-Fe sulfide grains or cavities, fractures, and sample surface during melt crystallization.

2. The presence of Sn in the field of stability of the Pt-Pd-Fe intermetallic compounds (50 at.% S, Cu/Fe 0.25 and 45 at.% S, 1.44 > Cu/Fe ≥ 0.69) determines crystallization of their Pt-Pd-Sn analogues. In this case, the deficiency of Sn to form Pt-Pd-Sn phases is ba-

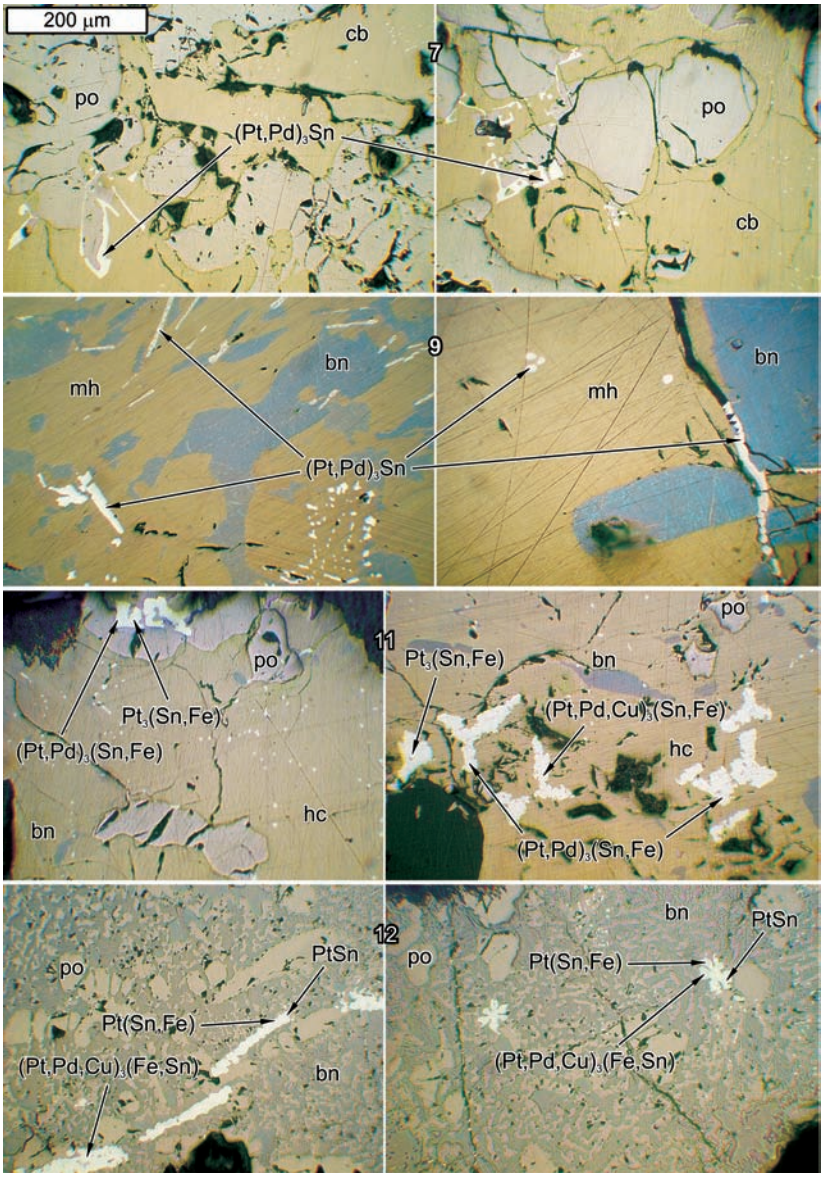

Fig. 3. Pt-Pd-Sn intermetallic compounds (bright white) associated with cubanite (cb), pyrrhotite (po) in sample 7—5, bornite (bn), mooihoekite (mh) in sample 9—3, and haycockite (hc), bornite, and pyrrhotite in sample 11—3, bornite, and pyrrhotite in sample 12—3.

lanced by Fe and Pt-Pd-Sn-Fe phases crystallize simultaneously.

3. Pt-Pd-Fe-Sn intermetallic compounds synthesized from melt along with Cu-Fe sulfides have the same phase relations as typical metacrystals. Thus the phase relations of their natural analogues could not tell us about their formation before or after Cu-Fe sulfides crystallization.

References

Barsukov V.P. & Dmitriev L.V. Upper mantle of the Earth as probable source of ore matter // Geokhimiya. **1972**. No 12. P. 1459—1461. (In Russian).

Cabri L.J. New Data on phase relations in the Cu-Fe-S system. // Econ. Geol. **1973**. 68. P. 443—454.

Distler V.V., Grokhovskaya T.L., Evstigneeva T.L., et al. Petrology of sulfide magmatic ore formation. Moscow: Nauka, **1988**. 232 pp. (In Russian).

Distler V.V., Sluzhenikin S.F., Cabri L.J., et al. Platinum ores of the Noril'sk layered intrusions: magmatic and fluid concentration of noble metals // Geol. Ore Dep. **1999**. 41. P. 214—237.

Table 3. **Phases crystallized from the FeS-SnS melts containing Pt, Pd и Sn**

№	Admixture	Synthesized phase	Composition of phase, at.% / wt.%						∑, wt.%
			Cu	Fe	Pt	Pd	Sn	S	
7		cb	15.25	35.76	0.00	0.00	0.00	48.38	
			21.28	43.84	0.00	0.00	0.00	34.47	99.59
		po	3.60	45.66	0.00	0.00	0.00	50.74	
			5.20	57.96	0.00	0.00	0.00	36.97	100.13
7-1	Pt	Pt_3Fe	1.84	26.17	71.50	0.00	0.00	0.49	
			0.85	9.40	89.71	0.00	0.00	0.10	100.06
7-2	Pd	$(Pd,Cu)_3Fe$	6.56	22.47	0.00	70.85	0.00	0.12	
			4.54	13.68	0.00	82.16	0.00	0.04	100.42
7-3	Pt/Sn = 3/1	Pt_3Sn	2.10	2.69	72.81	0.00	21.98	0.42	
			0.78	0.88	83.05	0.00	15.25	0.08	100.04
7-4	Pd/Sn = 3/1	Pd_3Sn	4.11	2.55	0.00	70.89	22.14	0.31	
			2.47	1.34	0.00	71.24	24.82	0.10	99.97
7-5	(Pt + Pd)/Sn = 3/1	$(Pt,Pd)_3Sn$	2.69	2.91	50.80	19.29	24.00	0.31	
			1.12	1.08	65.63	13.60	18.86	0.06	100.35
9		bn	48.39	12.49	0.00	0.00	0.00	39.11	
			60.88	13.81	0.00	0.00	0.00	24.83	99.52
		mh	25.32	28.39	0.00	0.00	0.00	46.30	
			34.25	33.75	0.00	0.00	0.00	31.60	99.60
9-1	Pt	$(Pt,Cu)_3Fe$	5.08	27.19	67.16	0.00	0.00	0.58	
			2.18	10.24	88.40	0.00	0.00	0.12	100.94
9-2	Pt/Sn = 3/1	Pt_3Sn	3.62	2.70	71.79	0.00	21.89	0.00	
			1.36	0.89	82.69	0.00	15.34	0.00	100.28
9-3	(Pt + Pd)/Sn = 3/1	$(Pt,Pd)_3Sn$	2.70	2.44	51.66	18.90	24.02	0.28	
			1.12	0.90	65.94	13.16	18.66	0.06	99.84
11		bn	56.68	6.85	0.00	0.00	0.00	36.47	
			69.94	7.43	0.00	0.00	0.00	22.70	100.07
		hc	24.15	29.87	0.00	0.00	0.00	45.98	
			32.91	35.78	0.00	0.00	0.00	31.61	100.30
		po	0.67	48.99	0.00	0.00	0.00	50.34	
			0.96	61.95	0.00	0.00	0.00	36.54	99.45
11-1	Pt	$(Pt,Cu)_3Fe$	5.05	27.60	66.72	0.00	0.00	0.64	
			2.16	10.37	87.57	0.00	0.00	0.14	100.24
11-2	Pt/Sn = 3/1	Pt_3Sn	3.42	2.70	71.64	0.00	22.04	0.20	
			1.29	0.90	83.11	0.00	15.56	0.04	100.90
11-3	Pd + Pt/Sn = 3/1	$Pt_3(Sn,Fe)$	3.28	7.53	67.00	2.45	19.46	0.29	
			1.27	2.57	80.01	1.59	14.14	0.06	99.64
		$(Pt,Pd)_3(Sn,Fe)$	3.64	6.77	58.67	10.96	19.67	0.29	
			1.49	2.44	73.77	7.51	15.05	0.06	100.32
		$(Pt,Pd,Cu)_3(Sn,Fe)$	5.57	8.09	46.22	20.46	19.17	0.49	
			2.49	3.18	63.39	15.30	15.99	0.11	100.46
12		bn	54.17	7.14	0.00	0.00	0.00	38.69	
			68.10	7.88	0.00	0.00	0.00	24.54	100.52
		po	2.37	47.59	0.00	0.00	0.00	50.04	
			3.40	59.94	0.00	0.00	0.00	36.18	99.52
12-1	Pt	Pt_3Fe	3.45	29.45	66.65	0.00	0.00	0.45	
			1.48	11.08	87.62	0.00	0.00	0.10	100.28
12-2	Pt/Sn = 3/1	Pt_3Sn	3.35	2.70	71.58	0.00	22.09	0.27	
			1.27	0.90	83.25	0.00	15.63	0.05	101.10
12-3	Pd + Pt/Sn = 3/1	PtSn	1.60	2.04	43.94	3.50	47.80	1.11	
			0.68	0.77	57.58	2.50	38.10	0.24	99.87
		Pt(Sn,Fe)	2.23	10.37	44.89	3.02	39.37	0.13	
			0.98	3.99	60.37	2.21	32.21	0.03	99.79
		(Pt,Pd)(Fe,Cu,Sn)	8.44	33.04	42.32	8.33	7.66	0.20	
			4.30	14.78	66.11	7.09	7.28	0.05	99.61
		$(Pt,Pd,Cu)_3(Sn,Fe)$	8.66	9.64	49.20	11.90	20.37	0.22	
			3.76	3.84	66.99	8.84	16.87	0.05	100.35

Notes: See Table 2 for abbreviations. Only trace phases are given in the synthesized phase column for samples 7-1 — 7-5, 9-1 — 9-3, 11-1 — 11-3, 12-1 — 12-3. The major phases in these samples are identical to those in sample of corresponding number, i.e., 7, 9, 11, 12

Distler V.V., Smirnov A.V., Grokhovskaya T.L., et al. Stratification and subtle layering of differentiated trap intrusions and formation conditions of sulfide mineralization // Conditions of formations of magmatic ore deposits. Moscow: Nauka. **1979**. P. 211–269 (In Russian).

Genkin A.D. Minerals of platinum-group metals and their associations in Cu-Ni ores of the Noril'sk deposit. Moscow: Nauka, **1968**. 106 pp. (In Russian).

Genkin A.D., Distler V.V., Gladyshev G.D., et al. Sulfide Cu-Ni ores of the Noril'sk deposits. Moscow: Nauka, **1981**. 233 pp. (In Russian).

Kravchenko T.A. Experimental study of the Sn role in case of the formation of Pt-Pd phases during crystallization of Cu-Fe sulfide melt // Bull. Earth Sciences. Russian Academy of Sciences. **2002**. No 1. www.scgis.ru/russian/cp1251/h_dgggms/1-2002/informbul-1.htm#term_10. (In Russian).

Kravchenko T.A. Experimental study of crystallization features of Pt-Pd intermetallic compounds from Cu-Fe sulfide melt // Bull. Earth Sciences. Russian Academy of Sciences. **2006**. No 1. www.scgis.ru/russian/cp1251/h_dgggms/1-2006/informbul-1_2006/term-44.pdf (In Russian).

Kravchenko T.A., Nigmatulina E.N. Experimental study of fine-dispersed Au and Ag formation in the crystallization products of Cu-Fe sulfide melt // Bull. Earth Sciences. Russian Academy of Sciences. **2007**. No 1. http://www.scgis.ru/russian/cp1251/h-dgggms/1-2007/informbul-1-2007 (In Russian).

Kravchenko T.A., Pavlyuchenko V.S., Sluzhe-nikin S.F. & Mokhov A.V. Au and Ag behavior during crystallization from melt of phase assemblages of the Cu-Fe-S system with chalcopyrite and pyrrhotite // XV Russian Conference on Experimental Mineralogy. Syktyvkar. Abstr. **2005**. P. 57–59 (In Russian).

Lavrent'ev Yu.G. & Usova L.V. The RMA-89 program for a Camebax-Micro electron microprobe // J. Analyt. Chem. **1991**. 46(1). P. 67–75 (In Russian).

Mihalik P., Hiemstra S.A. & de Villiers J.P.R. Rustenburgite and atokite, two new platinum-group minerals from the Merensky Reef, Bushveld Igneous Complex // Can. Mineral. **1975**. No 13. P. 146–150.

Moh G.H. Tin-containing mineral system I: The Sn-Fe-S-O system and mineral assemblages in orees // Chemie der Erde. **1974**. 33. P. 243–275.

Nekrasov I.Ya. Petrology and platinum content of ring alkali-ultrabasic massifs. Moscow: Nauka, **1994**. 379 pp.

Nekrasov I.Ya. Tin in magmatic and postmagmatic processes. Moscow: Nauka, **1984**. 235 pp. (In Russian).

Vaughan D.J. & Craig J.R. Mineral Chemistry of Metal Sulfides. London: Cambridge University Press. **1978**.

Mineralogical Museums and Collections

MOSAICS IN THE COLLECTION OF THE FERSMAN MINERALOGICAL MUSEUM RAS

Marianna B. Chistyakova
Fersman Mineralogical Museum RAS, Moscow, mineral@fmm.ru

The Fersman Mineralogical Museum RAS possesses a collection of mosaics of different styles dated from the 18th to the 20th century. A description of the exhibits and information on the history of the creation and the artists of some of them is provided.
22 photos and 15 references.
Keywords: Mineralogical Museum, collection, mosaic.

Mosaic is one of the most common examples of ornamental arts and crafts. They are usually made from multi-colored pieces of a hard material placed to form a design, tightly matching each others outlines and fixed with an adhesive to the common base.

Mosaic can be made out of various materials: wood, leather and so on. Most people think of them as a flat image made of stone or colored opaque glass. There are two types of mosaics according to their method of assembly *composite* and *tabular or opus sectile* type.

The first is called *composite* and is assembled from tesserae cubes or short columns of similar size and mostly square in cross-section. This kind of mosaic can be of Roman (or classic) and Byzantine style. The first (Roman) style was used during the time of the rise of the Roman Empire and was usually made with natural stone. The Byzantine style is younger and was usually composed of pieces of colored glass. There are also two basic techniques for the setting of the composite mosaic: direct, and indirect (or Venetian). The direct setting is done by placing tesserae into the cement or putty while the indirect technique is done by gluing the faces of the mosaic onto a paper or a cloth base, then transferring it onto the surface of the piece of art covered with cement and removing the paper or cloth after the cement has set.

The second type of mosaic is the *tabular or opus sectile* type. It is assembled from stone plates of different color, and/or texture, that are cut according to the design. This is also called Florentine for the place where it was the most popular.

There is also a *Russian* sub-type which is found in the *opus sectile* category. Its characteristic feature is the stressing of the natural pattern of the stone rather than having an artistic design. Sometimes general view made more sophisticated due duplication of existing natural stone patterns. The artistic aim of this mosaic is to mimic the texture of a massive natural stone. Flat surfaces are covered with this type of mosaic as well as complex three dimensional shapes. The bases for such complex art forms were made from a soft stone carved with a lathe. They used Pudozh or Putilov limestone for the bases of large carved malachite pieces like vases at the Peterhof Lapidary Factory, where, for the most part, the big malachite masterpieces were made (Fersman, 1961, vol. 2, p. 208). Very big art forms could have a metal base. This type of mosaic was developed to its apex in Russia in the 19th century, therefore it is called Russian mosaic. This technique was also used to make objects from lapis lazuli, banded jasper, agate.

There are also objets d'art made of combined pieces of small sculptures carved from different colored stones. This type of mosaic is called relief or three-dimensional mosaic. This technique was developed and was popular among artists from the Urals in the middle of the 19th century and it was also applied later at Emperor Lapidary Factories.

Mosaic is an ancient art form that was developed during the last several thousands of years. It is possible that this art form could have been invented in prehistoric times, when primitive men attracted to the beauty of colored pebbles made simple ornaments with them.

The Mosaic column from Ur dated 2600–2400 BC was discovered during archaeological excavations in Mesopotamia (now at

the British museum in London). It is decorated with mosaic of shells and lapis lazuli. Also, they discovered mosaic floors at Ur decorated with terracotta wedges made of clays of different colors.

Small household goods from ancient Egypt were decorated with pieces of colored stones. The throne and the wooden table decorated with mosaic of precious colored stones dated 1355–1337 BC were found in the Tutankhamen's tomb.

Supposedly mosaic was mentioned in the Bible in the book of Esther. The feast in the gardens of the Persian king Artaxerxes, who ruled in the period 465–424 BC, was held on a deck paved with green stones, marble, mother of the pearl and black stones.

This form of decorative art migrated from the countries of the Middle East to Greece and developed into a very complex art. The most ancient classic mosaics, dated from the 7–6th centuries BC, were pavements made with river and sea pebbles, so called *opus barbaricum (latin)* and were found in the temples of Artemis in Sparta and the sanctuary of Athena Pronaia in Delphi. Attempts to imitate paintings with mosaic took place starting from the 6th century BC. Existing techniques were not good for that purpose. So, *opus tesselatum (latin)*, a technique that used rectangular pieces of broken pebble, occurred all over the Mediterranean from the 3rd century BC and then throughout all the Greco-Roman territories. Soon tesserae decreased significantly in size and their shapes became more complex, which allowed enhanced artistic effect in the opus vermiculatum (latin). It is believed that then artists started to use pieces of colored glass-like slag along with colored stones.

Opus sectile was another type of mosaic technique which used thin plates of stone cut to a certain shape to fit into the ornament to decorate walls. It was widely used in Alexandria and thus has the name Alexandrian mosaic. It was the most expensive technique. It developed into what now is known as Florentine mosaic widely used in the Renaissance Italy.

The Romans inherited Greek culture and used mosaics widely in the decoration of floors and walls in secular buildings, palaces and houses of the rich. This art also appears in all conquered territories of the Roman time. Beautiful masterpieces were preserved in Pompeii and Herculaneum, Italy from the 4th century BC to the 1st century AD, in Atania, Syria from the 3rd and the 4th centuries, in Madaba, Jordan from the 4th century AD, and in other territories of the Empire.

Christianity followed paganism but used mosaics for different purposes. It was used to depict religious scenes on the walls of churches. The content of mosaic used on walls and apses of churches were determined (established) by the 5th century.

Direct tesserae mosaic and *opus sectile* were both used in the Eastern parts of the Roman Empire. Natural stone tesserae mosaic was used both for walls and floors. For face images on the walls, they used indirect *opus sectile* made of glass cubes and sometimes natural stone. Complex ornaments and scenes were made this way.

Masters of Roman and Byzantine Christian mosaic art used different methods of gaining expression. Mosaic was used in place of fresco and mural paintings in the Medieval West. Artists were forced to increase the color pallette of the glass to match mosaics to paintings. Byzantine mosaic, to the contrary, used fewer colors and had contrasting colors close together. Because the pictures were observed from a distance, the contrast was hidden and it created more vivid impression. For the same reason, images usually had golden and less frequently blue background on Byzantine mosaic.

Roman mosaic art was in it's decline while the Byzantine flourished in the 6th and 7th century. Greek masters of the art traveled to Italy in the 10th century and restored mosaic culture which had almost been lost in the country. Mosaics were used in the decoration of Italian cathedrals until the end of the 14th century.

Paintings replaced mosaics in the building decoration of the Renaissance. Mosaicists, who used to copy fresco brushwork, were forced to mimic paintings in their work and copy masterpieces. Some painters started to make mosaics to completely mimic paintings with it.

A mosaic workshop was established at the Vatican in Rome as early as the beginning of the 17th century. Its main aim was solely the copying of the painting works of the great masters. They developed a pallette of 28,000 colors of glass to render painting colors more precisely. Smaller studios worked along with individual mosaicists in that time.

Mosaic art was cultivated in Venice and Florence as well as in Rome. It was in Florence that opus sectile was developed in the 16th century and that is why the technique was named after the city. Front panels of cathedrals, tabletops and small artifacts with floral ornaments, and images of flowers and animals made of soft and hard natural stones were produced there.

Mosaic art had no such wide development in other European countries. Workshops appeared in various countries from time to time but they did not leave a significant impact in the history of the art.

Mosaics came to Russia from Byzantine following the acceptance of Christianity. The magnificent monument of that time was St. Sophia Cathedral in Kiev built in the 11th century by Yaroslav the Wise. The giant image of Theotokos on a golden background and some smaller fragments of ancient mosaic are preserved in the cathedral.

Production of colored glass was unknown in Russia and it was imported from overseas. Mosaics were not common because the materials and the work of foreign masters were very expensive. It was a forgotten art until the 18th century when Mikhail V. Lomonosov revealed an interest in it. He developed methods of casting and polishing colored glass and created his own technique of assembly. There was a special factory built on the outskirts of Saint Petersburg and they started to train specialists. The first works had been made by M.V. Lomonosov himself. "Poltava battle", the only monumental mosaic of the 18th century, started a whole new genre of historical imaging in Russian art. These works did not find support and monumental *opus sectile* (indirect mosaic) was forgotten for a century after Lomonosov's death in 1765.

Interest in the Roman mosaics revived in Russia at the beginning of the 19th century. It was driven by the desire to use lasting mosaics in the decoration of St. Isaac's cathedral instead of paintings that would easily deteriorate in the humid climate of Saint Petersburg. The Emperor Mosaic Institution was established especially for this purpose in Saint Petersburg in 1847. Professor V. Raffaelly and his brother Pietro came from Italy to supervise development of the colored glass manufacture the following year. Because there were no mosaicists of adequate standards, a temporary mosaic workshop under the lead of master Professor M. Barbery was established in Rome to educate and train Russian artists. Four Russian scholarship artist students of The Emperor Academy of Arts: E.V. Rayev, I.S. Shapovalov, S.T. Fedorov and landscape artist E.G. Solntsev were commissioned to the workshop. They had to master the direct mosaic technique that allowed making the closest match of the original painting. They returned to Saint Petersburg upon finishing their study in 1851. The Emperor Mosaic Institution had been established and there were trained mosaicists by that time (Kuteynikova, 2005, p. 400).

The scholarship students came back to Saint Petersburg accompanied by their teachers J. and L. Bonafede. Their work on mosaics boosted development of Russian direct mosaic which was noted at international art exhibitions starting from the 1860s.

Outstanding mosaic images were also made by masters from the A.A. Frolov private workshop for the cathedral of the Ascension of Christ (Saviour on the Blood) in Saint Petersburg at the end of the 19th century. Frolovs' workshop also decorated civil buildings as well as churches. It was a new step monumental ornamental art in Russian. While the development monumental ornamental art in Russian had its ups and downs, the Florentine mosaic had very gradual and continuous growth. Florentine mosaics started to be made in the time of Empress Elisabeth under the guidance of Italian artist Jacob Martini (Mavrodina, 2007, p. 28). The first Florentine mosaic works produced at Peterhof Lapidary Factory were dated to the 1750s and continued being made until the end of the 19th century.

Mosaic tables and columns made of agate, lapis lazuli and other stones were known from the 1760–1770s. Those rare pieces preserved from that time (dated 1763) were decorated only with carved ornaments, and are not perfectly mastered (Mavrodina, 2007).

The Florentine mosaic in Russia had a big boost in the middle of the 19th century after lapidary master I.V. Sokolov was commissioned to the workshop of Gaetano Biankin in Florence, Italy at the same time as the above mentioned artists. He was sent to master skills in different mosaic technique including glued (lapis lazuli and malachite) and Florentine mosaics, to study how Italian mosaic manufactures were equipped; and what tools and materials were used for mosaic manufacturing and get "the newest" mosaic patterns (Mavrodina, 2007, p. 36, 37).

After I.V. Sokolov returned to Russia, Peterhof Lapidary Factory began to produce mosaic art of very high quality, which attracted attention at international exhibitions.

Emperor Ekaterinburg Lapidary Factory produced pieces of art of high standard. The mosaic map of France was made of various ornamental, precious stones and metals at the factory and had great success at the exhibition in Paris in 1900. This map was a gift to France and was placed in the Louvre after the exhibition (Mostovenko, 2001, pp. 51–54).

The most famous of the Russian mosaicists works are ones of malachite and lapis lazuli. Malachite was used in various ways. At first, it was used as a bright mineral for the Florentine mosaic (opus sectile). Secondly, it was used as a mineral with unique texture to cover big surfaces with small plates of it to obtain the illusion of a massive material. This technique was called the Russian mosaic.

Malachite was first introduced for the interior decoration of the Mikhailovskiy Palace in the late 18th and the beginning of the 19th century. It was used as individual slabs embedded in marble.

Russia became the world center for malachite lapidary processing in the 1820s. This type of mosaic art had its peak in the 1830–1850s. Many workshops produced boxes, snuffboxes, candle holders, and other small items. However, only the work of Ekaterinburg and Peterhof Lapidary Factories brought international fame to Russian malachite items. Giant columns, vases, tables, chandeliers, fireplaces and clocks were manufactured there along with the items mentioned above. It was in those items that the difference between Russian and European masters was clearly shown. It was not only in the size of the things but mainly in the complexity of their shapes and ornament that was much more intricate than natural.

The natural variety of the material textures allowed artists to develop several techniques of assembling malachite slabs on the base in order to form different patterns from simple banded to complex scalloped. These were the five most common assembly methods: 1) "crumpled velvet" assembly with adjacent plates of different in color or pallette made an illusion of crumpled cloth of deep green color. The ornament of the stone pieces did not matter; 2) "banded" or "striated" using pieces with parallel banding and different colors; 3) "radial" or "oculate", sometimes such buds were placed in banded pattern; 4) "on two sides" ; and 5) "on four sides". The last two types were made by placing plates with repetitive ornament symmetrically to one or several crossed planes.

Big lapidary items cost immense sums and their production ceased by the end of the 19th century first with Ekaterinburg Lapidary Factory in 1858 and followed by Peterhof Lapidary Factory.

Popularity of malachite was replaced by lapis lazuli in the 1860s. Lapis lazuli came from Badakhshan deposits and the Baikal region. Items of various sizes from miniature to gigantic were made in glued technique of the Russian mosaic at Peterhof Lapidary Factory. Jasper and rhodonite were also used in items created with such a technique but in much smaller quantities.

The Mosaic workshop at the Academy of Arts was closed in 1918 due to the reorganization of the Academy. The unique world-known collection of smalt containing up to 17,000 shades of colors was destroyed in the process of closing the workshop. Nevertheless, soon it became clear that monumental ornamental art could not fully achieve its de-

corative aim without using mosaics. The project of creating The Russian Institute of Mosaic, Enamel, Decorative Window Panes and Glass was developed at the Academy of Arts in the 1920s. Soon after, mosaics reappeared in the decoration of public buildings: subway stations, conference halls, theaters and so on.

The unique 25 square meter map of the Soviet Union was created at Ekaterinburg Lapidary Factory in 1937 in the Florentine mosaic technique. It was introduced at the Paris and the New York Art Exhibitions in 1937 and 1939.

Russian mosaic art is undergoing a period of transformation at the break of the 21st century. The significance of mosaics in the restoration and construction of churches as well as in the decoration of private houses continues to grow. It is used in the decoration of facades as well as the interior. Private workshops have appeared to satisfy the expectations of amateurs as well as experts. They make monumental works for state projects (subway stations) and churches as well as small items like tabletops, portraits, icons, panels and other. They have started to use ceramics and glass tile along with traditional glass and natural stone.

The Fersman Mineralogical Museum RAS has a small but peculiar collection of mosaic art dated from the 18th to the 20th century. There are some exceptional items among common ones in the collection which were made in Russia and abroad.

The oldest item in the Museum is a pyramidal obelisk decorated with *Roman style* mosaic. It is a collection of all known colored stones from the Urals and made at Ekaterinburg Lapidary Factory. The stone slabs of agate, chalcedony, quarts, amazonite and various jaspers are placed onto the sides of the tall four-sided pyramid. The pyramid rests on four chalcedony spheres and a base. The sides and the top of the base are decorated by the same stones and the bottom part is made of coarse-grained granite. The base and pyramid are gilded in some parts. It was initially supposed been made at the Peterhof Lapidary Factory dated back to 1725, according to the inventory of the Museum. Nevertheless, it was found later that there are numbers engraved on the gilded plates on each stone, which correspond to the numbers of deposits of colored stones in the Urals written in the "General Description of Minerals" of the Urals from 1792–1796 (Semenov, 2001, p. 44). So, according to the investigation of V.B. Semenov and N.I. Timofeyev, the pyramid can be dated to the same period from 1794 to 1799.

Collections of polished colored stones became popular in Russia starting in the 1780s when the popularity of mineralogy was highly recognized at the Court. Such a collection was made for Katherine the Second in 1786 and already had a pyramidal shape. There were other popular shapes along with a pyramidal obelisk: grottoes, fountains, and other intricate compositions. There are only a few collections that have survived and they have immense historical value (Chistyakova, 2007, p. 102).

The small panel of 21x14 cm depicting a white cross on a black background framed with ornament is a more recent item, but is also of high historical value. The panel is not skillfully made: the pieces are not placed evenly to each other and the seams are filled with mastic. It is not the skill of the artist, but the text that is engraved on the back of its copper base that makes it valuable. The text says: "*By the will of the Prince Emperor Nikolay Pavlovich and by the petition of the Prince Grigoriy Petrovich Volkonskiy the Russian Mosaic School was found in Rome. Vasiliy Rayev and Ivan Shipovalov were its first students. This Cross was their first work and had been started by Rayev on June 6, 1847*". Vasiliy Egorovich Rayev was a well known landscape and historical painter, who, with other scholarship students of the Academy of Arts, was commissioned to Rome.

Such scholars' works rarely survived their artists and can be found in collections. This item came to the Mineralogical Museum from the collection of Gatchina and Stroganov's palaces and was mentioned in the common inventory of the museums (the State Hermitage archives. Fund 4, vol. 2, list 14, file 192). It is difficult to say where it was stored. Nevertheless, although it has no artistic value, it tells us about important

efforts made in the training of Russian mosaicists who later decorated St. Isaac's cathedral (Chistyakova, 2005, p. 144).

The Museum has a paperweight with mosaics from Stroganov's heritage collection. It represents an original collection of the most common hard ornamental stones from the Urals. The mosaic was made in the technique of the Roman mosaic with triangular and rhomboidal tesserae that emphasize its beauty. There is eight-point star made of rhomboidal pieces of grayish-green Kalkan jasper with a bright pink rhodonite outline. The background is made with rectangular pieces of various jaspers, jasper agate, aventurine and quartz. This multicolored composition has a frame of malachite, the only soft stone from the Urals presented in the item. The press came to the Museum in 1919 with a big collection from the Stroganov's palace. The name of the workshop where it was made is unknown. Based on the stones used, we suppose, that it was a one from the Urals (Chistyakova, 2007, p. 107).

There is a bigger item, a tabletop of white and patchy marble with a black frame, in the Museum that also represents the Roman technique (photo 1). The origin of it is unknown. It appeared in the Museum in the 1920s at the time when the property of many prominent Russian families was nationalized. The method of assembly and possibly Italian marble used for the tabletop do not help to determine the place where it was made. Italian marble was widely used by Russian mosaicists. The Peterhof Lapidary Factory produced similar tabletops starting from the beginning of the 1800s.

The same technique was used in the very beautiful chess board made of black and patchy Mexican marble (photo 2). The use of the stone from overseas makes us suggest that the board was made in Europe, possibly in a private workshop. Chess boards were not on the list of items produced at the Peterhof Lapidary Factory, and the manufacture in Ekaterinburg used only marble from the Urals.

Another item made in the manner of the Roman mosaic is an Italian clock made in the early 19th century (photo 3). It represents a triumphal arch assembled from various colored stones: marble, lapis lazuli, malachite, labradorite and porphyry. The round clock is at its top along with the bronze decoration. The precise description of the clock and theories of how it ended up in Russia were published in this magazine in 2005 (Chistyakova, 2005, p. 142). Here we direct your attention to two small mosaic panels and the columns of the arch. The panels were made by outstanding Italian mosaicist Giacomo Raffaelli (1753–1836), who was invited by Alexander the First to Russia to organize production of colored glass and a mosaic workshop in the early 1800s. The visit did not take place then because the conditions set by the artist were considered immoderate (Mavrodina, 1999). Nevertheless, he was not forgotten in Russia and became a counselor of the Russian Emperor abroad in 1815. G. Raffaelli invented a method of production and shaping of very small pieces of colored smalt by stretching

Photo 1. Tabletop (marble), 100x60 cm. Inventory from 1927, FMM No PDK-2717, the source is unknown. Photo: from Fersman Mineralogical Museum RAS archive.

Photo 2. Chess board (Mexican and possibly Italian marble), 40x40 cm. Came from the KEPS ш 1925, FMM No PDK-2593. Photo: from Fersman Mineralogical Museum RAS archive.

Photo 3. Clock (marble, malachite, lapis lazuli, labradorite, porphyry, colored glass, gilded bronze), height is 83 cm. Mosaicist G. Raffaelli, Milan, 1814. Came from the State Hermitage in 1926. FMM No PDK-1712. Photo: Michael Leybov.

them in fire. It allowed making very detailed mosaics that simulated painting.

This method of miniature mosaic was used in the decoration of the small mosaic panels on the walls of the arch. They depict suits of armor with a shield featuring the Medusa Gorgon's head the symbol of invincibility. Another agate shield with the Gorgon's head is placed on the top of the clock among with other decoration. Small colored glass tesserae are arranged so artistically that the image looks three dimensional.

The clock of this particular style was so popular that the item from the Museum appeared to be a third copy of the original clock made by G. Raffaelli in 1801, part of which is preserved in the Hermitage. The second copy of the clock was made by Raffaelli in 1804 and was presented by the Pope Pius VII to Napoleon for his coronation. The third copy of the clock has an inscription on the reverse side of the clock says "*Raffaelli Fece Milano 1814*" suggesting that it was made in Milan in 1814, while the first and the second were made in the Vatican workshop.

It is important to note that Raffaelli used the facing technique in the decoration of the columns supporting the entablature of the arch. He artistically glued thin slabs of malachite, rare in Europe then, in the way that later started to be called "the Russian mosaic".

In spite of the fame of Rafffaelli, there is no information in the Museum on the owner of this item or its location from 1814 to 1926. We managed to learn that after the item was finished in 1814 it was shown at the annual exhibition in the Palace of Arts and Science in Palazzo Brera in Milan (M. Alfieri, 2000, p. 263). There is a note that the columns of the clock were made of malachite which confirms that it was the item from our Museum. The clock made in 1801 had jasper and agate columns and the one made in 1804 had amethyst columns.

The Florentine mosaic style is better represented in the Museum than the Roman one. There are small marble plaques that are the earliest items of this type in the collection. We omit their description here because a special article is going to be published.

Photo 4. Cabinet (amboyna wood) with the mosaic panels (marble, lazuli, jasper, labradorite, amazonite, tigers eye, cacholong, pink opal and other stones), height is 160 cm. Peterhof Lapidary Factory, 1885–1888. Came to the Museum from the Laboratory of Stone of the Ministry of Building Materials of the USSR in 1962.
FMM No PDK-5381. Photo: Michael Kalamkarov.

There is a unique cabinet in the Museum made at the Emperor Peterhof Lapidary Factory. It came to the Museum from the Laboratory of Stone at the Ministry of Building Materials of the USSR in 1962. The item is a double door cabinet on top of a table with a small drawer and four legs with a board for the feet (photo 4).

The cabinet was made of the precious unique amboyna wood from Indonesia or, the other source, from the rain forest of South America, and is decorated with gilded bronze. There are panels of Florentine mosaic made of colored stones on its doors and the drawer. The upper board is made from griot, a red marble.

The history of the creation of the cabinet is related to one of the other two similar items placed in the State Hermitage. The research on the subject had been carried out recently and revealed the following history (Mavrodina, 2007, p. 141–157).

Emperor Peterhof Lapidary Factory purchased a single-door red wood cabinet with bronze decoration from Henry Dasson, a Parisian industrialist (Henry Dasson & Co). Dasson supplied the drawings of mosaics that were to be put on the door and the side walls of the cupboard. They planned to decorate the door with the mosaic "Tropical forest on white background" and the walls with the mosaic "Tropical forest with parrots on blue background". In the coarse of intermittent work from 1885 to 1893, they decided to use the mosaics with blue background in the double-door sycamore cabinet made for the order of Empress Maria Fedorovna in 1887. That cabinet and a similar one of amboyna were made by Saint Petersburg cabinet maker A.V. Shutov. Gold and brass master A.Ya. Sokolov did the

metal work for the cabinet in "*all the details matching the sample characters but with the new models and of finer work*" (Mavrodina, 2007, p. 157). The architect N.V. Nabokov who was the supervisor of the order wrote to A.L. Huhn, the director of the manufacture: "*The gilding came out magnificently, but it was a troublesome work*" (Mavrodina, 2007, p. 157). The mosaic panel "Arabesque" was designed by artist Lerish for the amboyna cabinet. Both cabinets, sycamore and amboyna, were finished and sent to an exhibition in Copenhagen in 1889.

All three cabinets were shown on the World's Columbian Exhibition in Chicago in 1893, dedicated to the 400th anniversary of the discovery of the Americas. The Emperor Peterhof Lapidary Factory was awarded a bronze medal and the honorary diploma for the masterpieces.

It is known that the cabinets had appeared as described above in 1910: the amboyna cabinet had "Arabesque" mosaics designed for it and the one of sycamore had the mosaic with parrots on blue background (Mavrodina, 2007, pp. 156–157). It is a mystery when and why the panels were swapped between the cabinets. Obviously, the amboyna cabinet from the Mineralogical Museum has panels "Tropical forest with parrots on blue background" drawn by H. Dasson, which were made for the sycamore cabinet of Maria Fedorovna.

Baron M.P. Klod made watercolor sketches for the mosaics from Dasson's drawings and divided them into separate parts (Mavrodina, 2007, p. 148). This fact was mistakenly taken as if M.P. Klod was the author of the design. The parts were given to several mosaicists and then the completed pieces of the mosaic were assembled on the one panel. The names of the mosaicists are unknown.

The list of the colored stones used in the panels was published by A.E. Fersman (Fersman, 1922, pp. 91–92). He wrote: "*The excellent mosaic was assembled from the following stones: the sky was made from Badakhshan lapis lazuli, water from Siberian lapis lazuli and prasem; flowers were done of quincite (pink opal), cacholong, Orsk variegated jasper, red jasper, and Samara agate; tree trunks were made of petrified wood; leaves and plants of breccia, petrified wood, Kalkan, Italian, banded and dendrite jasper, and Koktebel (Crimea) seabeach pebbles; the butterfly was made of labradorite and tiger's eye; parrots were made of Orsk jasper, Crimean pebbles, head – of glaucolite; wiskers and the beak of jaspers, eye – brick jasper; the tail – petrified wood and jasper*". In addition, Ural amazonite was used for the plants in the center of the picture and famous Italian marble was used in the unevenly colored leafs. Boulders and pebbles of this marble have been collected for centuries on the Mediterranean coast and the banks of Po River.

There is a note by I.P. Andreyev, a fine-art restorer, who worked on stone items at the Hermitage, which states that all three cabinets were sent by the trade company "Russkiye Samotsvety" to Moscow after liquidation of the private collection of Alexander III in Anichkov Palace. Also the note told about stories that were going around at the Peterhof Lapidary Factory in 1919 about Americans who desired to purchase the cabinets and pay with 25 steam engines for each one of them, and about Lenin who banned the deal after looking at the cabinets in Moscow (Mavrodina, 2007, p. 154). There is no information about how and when the cabinet came to the Laboratory of Stone from whence it was given to the Mineralogical Museum.

The amboyna cabinet with "tropical forest on blue background" mosaic was shown at the exhibition in Helsinki in 1989.

There are two tabletops in the Museum with the Florentine mosaics made by a foreign master. One of them is rectangular and represents a massive limestone slab decorated with black marble, possibly Italian, judging by the uneven coloration. Floral ornament and bunches of flowers are placed along the perimeter on a black background with fruits and hummingbirds above them at the corners. The center of the tabletop has a bunch of flowers, bunches of grapes, and butterflies (photo 5). Various ornamental stones are used in the mosaic, the majority of them being soft stones: lapis lazuli, malachite, and turquoise. There are some harder stones as well: cacholong in white flowers, chalcedony, rock crys-

Photo 5. Tabletop (marble, rock crystal, amethyst, cacholong, chalcedony, lazuli, malachite, turquoise and other stones), 120x70 cm. Mosaicist Francesko Belloni, 1851. Came from the Laboratory of Stone of the Ministry of Building Materials of the USSR in 1962. FMM No PDK-5382.
Photo: from Fersman Mineralogical Museum RAS Archive.

tal and amethyst in the grapes, and some types of jasper may be present in the birds feathers and the butterflies wings. The most impressive part of the mosaic is the bunch of grapes made of rock crystal, pale and very bright amethyst. Contrary to the common thin slabs of stone used for the mosaic, the grapes are made of hemispheres sunk into the cement with their round sides down. Underlying foil creates reflection that makes the perfect illusion of three-dimensional grapes.

The tabletop came to the Museum with the cabinet described above from the Laboratory of Stone in 1962. It is possible that it ended up in the laboratory in 1920s before it was moved from Leningrad to Moscow in 1930s. There are Russian malachites of various shades and Baikal lapis lazuli with white spots used in the tabletop. On the reverse side of the board there is harrowed "*Francesko Bello...*" (then illegible) 1851. Obviously, this is the masterpiece by Francesko Belloni (1772–1853), who worked for the Vatican mosaic workshop at the beginning, then from the late 18th century – for the workshop in Paris, patronised by Napoleon, and later – for the French Emperor Court.

The second tabletop is also supposedly of Italian production (photo 6). It is a round polished black thin slab of black Belgian marble fixed on a wood frame. Graceful wreaths of pink, grayish blue and yellow roses are encrusted in the black marble. The leaves and petals are made of multi-colored marble and other carbonates of different origins. The pink petals are most likely made of shell: one can see the characteristic layered structure. Leaves and roses of other colors are carved from unevenly colored marble as in the previous item. Some of the grayish-blue rose petals have a layered structure as in organic matter. At the same time, adjacent details of the same color have large translucent areas of crystalline structure. They are so transparent that we can see the black base through them. It gives the flowers an elegant look. It is possible that an organic material that has suffered partial crystallization was used. The inventory has no information on from where and when it entered the Museum.

The oval carved plate of white marble is among the foreign origin mosaic items in the Museum. Its center is decorated with the blossom of a red poppy surrounded with green leaves (photo 7). The plate came to the Museum in 1926 from the items selected for the Leningrad collection from the collection of either the Gatchina or Stroganov's Palace and was described as a piece of Italian work.

It was a certain mistake because there is a paper sticker on the back of the plate with the printed text "First Class. Price Rs12" and with a pencil inscription "As. Nuthoo Ramsculptor Agra". It is clear even without the inscription that the plate was made in India and resembles widely known items of this kind made by Indian craftsmen. The encrusted parts are made not of softer stones which would polish as well as the marble, but of hard carnelian,

Photo 6. Tabletop (marble, shells on the wood base), diameter is 50 cm. There is no information on the item in the inventory, probably it came in the beginning of 1920s. FMM No PDK-2623. Photo from Fersman Mineralogical Museum RAS Archive.
Photo 7. Carved plate (marble, chalcedony of various colors), 24 x21 cm. Agra, India. Received from the State Museum collection fund in 1925. FMM No PDK-1604. Photo: Michael Leybov.

sard and other colored chalcedony which is characteristic of Indian art.

Florentine mosaic is used in three modern pictures that are on permanent exhibit in the Museum: "Kolomenskoye" made by the mosaicist S.V. Volkov, "The Birds on the Wild Ash Branch" and "Sword Lilies" donated by N.I. Morozov.

"Kolomenskoye" is made of marble of soothing colors, jasper and rhodonite (photo 8). The materials for the different parts of the picture were chosen well. S.V. Volkov used a low quality rhodonite with plenty of manganese oxide dendrites for depicting bushes. Lightcolored rhodonite matches with the soothing shades of the marble. The picture is framed with a thin, almost invisible, aluminum frame.

Multicolored jasper is used for the birds and in the ash berry tree along with coarse-grained marble in the background of the panel "The Birds on the Wild Ash Branch" (photo 9). Translucent aragonite and onyx of mixed colors of white and yellow are used along with marble in the background and jaspers in the leaves and the red flowers on the panel "Sword Lilies". These items feature

Photo 8. Panel "Kolomenskoye" (marble, rhodonite), 33.6 x25.5 cm. Mosaicist S.V. Volkov. Came to the Museum in 1961, written to the inventory in 1997. FMM No PDK-7828. Photo: Michael Leybov.

deep bright colors that make them very spectacular (photo 10).

There is not much information on the artists of these works. It is known that they worked in the mosaic workshop of the Moscow Metrostroy factory (the company that builds subway — translators note) and participated in the creation of mosaics in the halls of the Moscow subway.

S.V. Volkov was one of the artists, who created and restored mosaics in the old halls of

Photo 9. Panel "The Birds on the Wild Ash Branch" (marble, jasper), 56x39 cm. The present of mosaicist N.I. Morozov, 1962. FMM No PDK-5380. Photo: Michael Leybov.

Photo 10. Panel "The Sword Lilies" (marble, jasper, aragonite onyx), 62x27 cm. The present of mosaicist N.I. Morozov, 1962. FMM No PDK-5379. Photo: Michael Leybov.

"Park Kulturi" and "Novokuznetskaya" subway stations and in the hotel "Russia".

N.I. Morozov (1922–1997) was a master of decorative works at the beginning of work for Metrostroy. He worked on the decoration of the halls and stations "Park Kulturi", "Belorusskaya", "Kiyevskaya", "Okhotniy Ryad" and others. As an artist, he decorated administrative and cultural buildings in Moscow and other cities of the Soviet Union. He was awarded with the Order of People's Friendship in the early 1980s. He taught for several years in the Stroganov Moscow State University of Industrial Arts.

The large portrait of Vladimir I. Lenin is among other items of the Florentine mosaic in the Museum. It is made of marble of warm tints (FMM No PDK 6373). The portrait was purchased from the author, L.G. Shteyman, in 1972. The Museum does not have any information on the artist.

Russian mosaic technique is represented in the Museum mostly with items made in Russia of lapis lazuli and malachite and there is also work of the Italian mosaicist in the above mentioned clock.

The small round lapis lazuli column on a rectangular base is probably one of the oldest items decorated with glued on stone slabs in the possession the Mineralogical Museum (photo 11). Baikal lapis lazuli plates are glued in the traditional method of Russian mosaic technique. The whole item is decorated with gilded cast bronze figures. There is a winged female figure on the column's cap. Her left foot rests on a sphere. She has an open book in her left hand and a stylus in her right hand, with which she writes a text starting with the date "December 5th, 1783". We try to find out who is She.

Many of the classic muses and goddesses were depicted with their attributes, such as the muse Calliope, the patron of epic poetry, who was depicted with a writing board and a stylus. Clio, the muse of history, possessed similar objects. Nike, the goddess of victory, was depicted with wings, as well as Fortune, who also had a sphere. It is possible, that the artist had some specific mythological character in his mind, but we cannot distinguish for sure which one. The date written in her book appears to be even more mysterious. We tried to find any significant event in the Russian history on that date as the item was supposedly made in Russia. The only event on the date was the launching of the first hot air balloon but apparently the event had nothing to do with our case.

The date engraved on the item seems to be even stranger in the light of the fact that the Baikal lapis lazuli from which it is made of was discovered only in 1784. Academician E.G. Laksman was the first to discover it on the Sludyanka river and described it in his letter to academician P.S. Pallas, the famous naturalist of that time, in 1784. The first note

Photo 11. Column (Baikal lapis lazuli, gilded bronze; mosaic, casting), height is 84 cm. Entered from the State Museum fund in 1926. FMM No PDK-1620. Photo: Michael Leybov.

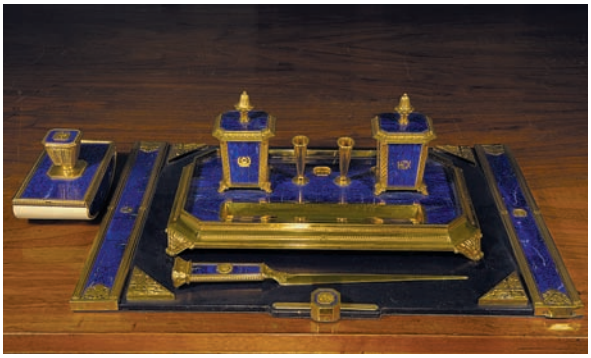

Photo 12. The desk set (Badakhshan lapis lazuli, gold; mosaic, casting), 47x32 cm. The present from the Afghan King Mohammed Zahir Shah to N.S. Khrushchev. Entered the Museum from the Kremlin Armory Chambers in 1985. FMM No PDK-7247-7250. Photo: Michael Leybov.

about the item at the Peterhof Lapidary Factory appeared in 1785 and stated: "the column with pedestal assembled from lapis lazuli on Pudozh stone and decorated with gilded copper figures". The locality of the stone was not mentioned. Only rare things were made of lapis lazuli at the factory starting from the middle of the 1750s and certainly from the stone from Badakhshan. The other six columns "of lazuli stone with bronze bases and capitals" were made in 1800 (Mavrodina, 2007, p. 410) but there is no information on the origin of the ornamental stone that was used. Nevertheless, the description of the items are very similar to the one from the Mineralogical Museum, such an early dating of it seems to be unrealistic. The sufficient exploitation of the Baikal lapis lazuli started only in 1850s. So, the date on the figure most likely corresponds to an event which happened much earlier than its creation. It is also possible that the bronze statue was cast earlier than it was placed on the column and the date can refer to a private family event.

The column came from the State Museum collection fund which does not give any clue to find who the previous owner was. Everything about this item is a mystery.

Another lapis lazuli mosaic piece of art has an exact date. It is a desk set made of Badakhshan lapis lazuli, gold, and leather which was presented by Afghan King Mohammed Zahir Shah to N.S. Khrushchev (photo 12). The set contains six pieces which golden parts have the 375 gold purity identification and brand stamps of the "Garrard & Co Ltd 112 Regent Street London W.1", the English company which manufactured the items. One of the ink-pots has the Afghan emblem and another carries initials HCX (*Cyrillic letters means NSK for Nikita Sergeyevich Khrushchev – translator note*). The desk set came to the Museum from the Kremlin Museums in 1985. Colleagues of Armory Chambers informed us that the item was made in 1955–1956.

Several items manufactured using the glue-on technique were made of malachite. The most significant of them is a big malachite vase. It consists of the round bowl with elaborate and progeoesthetic edge which set on the round neck extending to the bottom and the square base. The outline of the upper part of the neck is decorated with a wreath and belts. Several malachite assembling techniques are used in the vase: "crumpled velvet", "on two sides" and other methods.

The vase came to the Museum from Abamelek-Lazarevs in 1920. Abamelek-Lazarevs is a noble family name which appeared with the union of the two famous Russian families in the 1700s. The last member

Photo 13. Vase (malachite), height is 85 cm. Came from Abamelek-Lazarevs in 1920. FMM No PDK-1713. Photo: Michael Kalamkarov.

Photo 14. Vase (malachite, gilded bronze), height is 51 cm. Came in 1920, the note in the inventory from 1972. FMM No PDK-6372. Photo: Michael Leybov

of the princely family was S.S. Abamelek-Lazarev, an oriental scientist, who was married to M.P. Demidova, the daughter of P.P. Demidov San Donato, the owner of a unique collection of malachite items known in Russia, and Italy as well. It seems that this Museum vase once was one of the prince's family home decoration.

Authentication of malachite items is a difficult issue even for the bigger ones. Multiple private lapidary workshops appeared in the beginning of the 19th century along with Ekaterinburg and Peterhof Lapidary Factory to process malachite. There were rather big companies that supplied works to the Emperor Court (Semenov, 1987, vol. 1, p. 38). The Demidovs had their own lapidary workshop that produced outstanding malachite masterpieces in Petersburg in 1847–1853 (Semenov, 1987, vol. 2, p. 82–84). It is possible that the vase was manufactured in that very workshop. If so, it can be dated between 1847 and 1853. The Demidovs also had Italian mosaicists working for them in the beginning of the 19th century. It is unknown if they produced big items in the workshop.

There are three smaller vases in the Museum. The biggest one is a square vase with progeoesthetic edges and a round neck decorated with a wreath on a square plinth. The base is quite tall and is surrounded with a massive gilded bronze ornamental rim (photo 14). This assemblage of malachite and gold was widely used and added attractiveness to the items.

Photo 14 a. Detail of vase (malachite), shown the way of mosaic assemblage on the plinth of the vase with FMM No PDK-6372. Photo: Michael Leybov.

Different types of mosaic assembling were used in the vase. Malachite was very beautifully assembled on the base with the methods on two and four sides. The neck and the bowl itself have no arranged design assembly. Filling paste is easily noticed in the seams on the bowl which reduces the value of the item.

There is no information on the date and the source of entry of the vase into the Museum. The earliest date that it was recorded in the inventory was 1972. It likely entered the Museum in the 1920s among other stone works and was accidentally missed from the inventory. The very different quality of malachite assembly of the different parts of the item suggests that it was either made in a private workshop or, that the base and the bowl originally belonged to different items.

Another smaller vase made definitely in the 19th century is generously decorated with gilded bronze (photo 15). A gilded bronze rim with egg-shaped bulges intermittent with arrows (egg-and-dart style) decorates the edge of the flattened malachite vase. The plinth, the neck and wreath are made of the gilded bronze and there is a malachite belt between them. The neck widens towards the bottom and is decorated with matted fluting. The ridges between them are polished and shiny. The wide bronze bottom of the neck is covered with floral ornaments and tangled bands. The plinth is the only completely smooth and shiny piece. Judging by the unseen bottom part of the plinth we can assume that there had been a base that is now missing.

The vase entered the Museum from the State Museum Collection Fund. There is no documentation about its previous owners. Judging by the plentiful bronze it could have been made in a private workshop in St. Petersburg, possibly for a private customer.

The Museum has on exhibit a rare malachite vase from the Soviet period. It represents a tall lidded cup (photo 16). Its mosaic is elaborately made with high grade malachite. The banded pattern created using the small slabs of malachite subtly and naturally blends into a radial pattern and a more complex arrangement unfolding onto two or more sides. The gilded bronze or brass plays a big role in the

Photo 15. Vase (malachite, gilded bronze), height is 20 cm. Entered the Museum from the State Museum fund in 1927. FMM No PDK-1623. Photo: Michael Leybov.

Photo 16. Vase (malachite, lapis lazuli, jasper, gilded bronze), height is 130 cm. Made at the Manufacture of Plastic and Carved Stone items in Alma-Ata in 1960. Entered the Museum from the Kremlin Armory Chambers in 1985. FMM No PDK-7246. Photo from Fersman Mineralogical Museum RAS Archive.

Photo 17. Box (malachite), size is 12x7.2x6.3 cm. The item was given by the State. 1983. FMM No PDK-7217. Photo: Michael Kalamkarov.

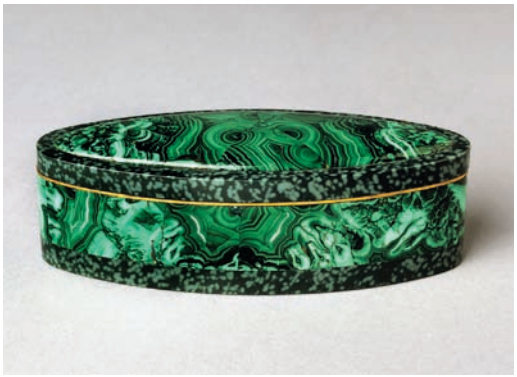

Photo 18. Oval box (malachite, porphyry), length is 13.8 cm. Acquired by the Museum in 1985. FMM No PDK-7270. Photo: Michael Kalamkarov.

decoration emphasizing the velvet tones of the malachite. While the malachite plays a decorative role, the brass carries the meaning. Besides the smooth decorative rims in the deflected upper ridge and in the middle of the item, there are four figures of young builders of socialism: a worker and kolkhoznica (collective farmer), a shepherd, and a folk dancer, each with their own attributes (sheaf, lamb and others). The figures are placed in the steep-roofed arches incorporated into the lower part of the body of the vase. The cup body ends in a bronze sphere with the classic soviet symbols of hammer and sickle, alternating with characteristic Kazakh ornamentation... The malachite neck rests on the base of smooth and decorated bronze. The foundation of the whole structure is placed on the pedestal made of greenish-gray Kalkan jasper. The lid symbolized the northern hemisphere of the Earth. The Florentine mosaic of lapis lazuli depicts the ocean, the map outlines of the Soviet Union is made of bright red jasper, and other countries are shown with different colors. The bronze figure of Vladimir I. Lenin is placed on the North pole.

This vase was made according to the rules of Socialist realism (art tendency of Soviet time) in September of 1960 at the Manufacture of Plastic and Carved Stone items in Alma-Ata and was presented to Nikita S. Khrushchev the same year. A. Shkergin was the author of the design, and he and V.P. Poddubskiy created the metal work, M.S. Shelepov assembled the mosaics. It is possible that the vase was stored among the presents to the government officials in the Kremlin museums. It was sent to the Mineralogical Museum with the desk set in 1985.

Besides the vases, the Museum possesses small malachite boxes decorated with the same facing mosaic technique (photo 17). They all are artworks of a very high standard representing excellent employment and sophistication of the natural stone texture. The most curious is an oval box which has complex blending malachite patterns and is decorated with porphyry along the edge (photo 18).

A shaped stand or, possibly a screen, is another item of malachite in the Museum (photo 19). A thick shaped marble slab acts as its base. The surface is faced with flat malachite slabs assembled in the order of "on four sides" method. "Banded" malachite pattern is used on the sides and carved into the base.

There are several items made with relief (prominent) mosaics. This type of mosaic was developed in Russia in the middle of 1800s. Masters from the Urals were the first to employ the technique. It was utilized at the Emperors Lapidary Factory and private workshops later.

Masters from the Fabergé lapidary workshops made two figures of this type that are well known to the lovers of carved stone: "Ice Carrier" and "Soldier in the reserve regiments uniform of 1914" (photo 20). These items are mentioned by F.P. Birbaum, the main artist of

the company, as the most successful items made with such a technique (Birbaum, 1997, p. 74). Another masterpiece of this type is a snail leaving its shell (photo 21). These items were thoroughly described in an earlier publication (Chistyakova, 2004, p. 130) and were shown in many International Exhibitions besides being on permanent exhibit in the Mineralogical Museum.

There are three paperweights (paper presses) among the decorative objects made with relief mosaic in the Museum. These items were used widely for a long time. The two with berries sculpted of colored stones were most likely made in Ekaterinburg. The third one originates possibly from the Peterhof Lapidary Factory. These desk items were produced by private craftsmen as well as by the state workshops. They were made more than a hundred years ago. The first paper press made at the Peterhof Lapidary Factory was dated by 1805 in the list of the items produced at the factory (Mavrodina, 2007, p. 415). By the middle of the 19th century, they were manufactured in large volumes and from various materials. There is no information as to the time of the appearance of these objects in Ekaterinburg lapidary workshops. A.I. Golomzik states that a private production of paper presses in the Urals appeared also in the beginning of the 19th century (Golomzic, 1983, pp. 114–115). The Emperors Lapidary Factory in Ekaterinburg started to make them later (Pavlovskiy, 1976, p. 90; Semenov, 2003, p. 720).

A paperweight with various berries was donated to the Museum by Moscovite A.N. Kupriyanov in 1959. He stated that the object had been a gift to his grandfather from the Siberian businessman Mikhail Petrov in the 1860s. The other two presses with amethyst bunches of grapes were transferred to the Museum from the Stroganov's Heritage Fund.

Another item is peculiar because its design contains berries and leaves "naturally" placed on the raw intergrowth of morion, albite and microcline. This way of presentation was prompted by V.V. Mostovenko, the director of Ekaterinburg factory. It allowed the reduction of production costs and increased the popularity of the items (Mostovenko, 1919, p. 78, Chistyakova, 2007, p. 106). There are only few items of this kind

Photo 19. Mosaic fragment (malachite), 21x13 cm. Gumeshevsky mine, Sverdlovsk region, Urals. Acquired by the Museum in 1925. FMM No PDK-1898. Photo: Michael Leybov.

Photo 20. Soldier of the reserve regiment of 1914 (multicolored jasper, ophiocalcite, graphic granite, silver), height is 15 cm. Fabergé lapidary workshop. 1915. The design by G.K. Savitskiy, lapidary master P.M. Kremlev. The items were given by the KEPS (Commission for the Studies of the Natural Productive Sources of Russia). 1925. FMM No PDK-2571. Photo: Michael Kalamkarov.

Photo 21. Snail (nephrite, obsidian), 5x3.5 cm. Fabergé lapidary workshop. Entered the Museum from Gatchina Palace, 1926. FMM No PDK-1748. Photo: Michael Kalamkarov.

Photo 22. Paperweight (serpentinite, rock crystal, sard, gypsum selenite, rhodonite, jet coal, coral, marble, jasper), 17x11 cm. Ekaterinburg, earlier than 1860. Donated by A.N. Kupriyanov, 1959. FMM No PDK-4816. Photo: Michael Kalamkarov.

which have survived to the present because of their fragility.

The small collection of the items described here at the Mineralogical Museum contains all types of mosaic art. The collection gives visitors a good chance to see almost full set of mosaic techniques.

References

Alfieri M. New Notes on Giacomo Raffaelli and Michelangelo Barberi // Janette Hanisee Gabriell. The Gilbert Collection. Micromosaics. Trieste: Philip Willson Publishers. **2000**. P. 26.

Birbaum F.P. The History of Fabergė Company. Stonework and Gold-Silver Item Production at Fabergė lapidary workshop // *Fabergė T.F., Gorinya A.S., Skurlov V.V.,* Fabergė and Petersburg Jewelers. Saint-Petersburg, Neva, **1997**, 703 p. (in Russian).

Chistyakova M.B. Fabergė lapidary in the Fersman Mineralogical Museum collection (RAS)// New Data on Minerals. **2004**. V. 39. Pp. 124–140. (in English and Russian).

Chistyakova M.B. What Exhibits are Silent About? // New Data on Minerals. **2005.** V. 40. Pp. 142–144. (in English and Russian).

Chistyakova M.B. Stone-cutting in the Urals. Articles of masters from Ekaterinburg in the Fersman Mineralogical Museum Russian Academy of Sciences // New data on minerals. **2007**. V. 42. Pp. 97–113 (in English and Russian).

Golomzic A.I. Rhodonite. Sverdlovsk, Sverdlovsk book publishers. **1983**, 159 p. (in Russian).

Fersman A.E. Sketches on the History of Stone. Moscow, Academy of Science Publish House. **1961**, 371 p. (in Russian).

Fersman A.E., Vlodavets N.I. The State Peterhof Lapidary Factory. Petrograd, Russian State Academical Printing Works, **1992**, 93 p. (in Russian).

Kuteynikova N.S. Mosaics. Saint-Petersburg, the 18–19th centuries. Saint-Petersburg, Znaki, **2005**, 501 p. (in Russian).

Mavrodina N.M. Family of Raffaelli, the Roman mosaicists // Applied Art of the Western Europe and Russia. Saint-Petersburg, the State Hermitage Publisher, **1999**. Pp. 235–236. (in Russian).

Mavrodina N.M. The Art of Russian Lapidary Artists in the 18–19th Centuries. Saint-Petersburg, the State Hermitage Publisher, **2007**, 599 p. (in Russian).

Mostovenko V.V. My Memories of the Ekaterinburg Lapidary Factory during 1885–1911 //in the book Skurlov, V.V. Jewelers and Lapidary Artists of the Urals, Saint-Petersburg, Liki Rossii, **2001.** Pp. 25–79 (in Russian).

Pavlovskiy B.P. Lapidary Art of the Urals. Sverdlovsk: Sverdlovsk Book Publishers. 1976. 151 p. (in Russian).

Semenov V.B. Malachite. Sverdlovsk: Sredne-Uralsk book Publishers, **1987.** V. 1, 2. (in Russian)

Semenov V.B., Timofeyev N.I. Book of the Carving Art. Ekaterinburg: IGEMMO "Lihica", **2001**, 144 p. (in Russian).

Mineralogical Notes

HORIZONTAL ISOMORPHIC SUBSTITUTIONS OF CHEMICAL ELEMENTS

Eugeny I. Semenov
Fersman Mineralogical Museum RAS, Moscow, mineral@fmm.ru

Horizontal isomorphic substitutions of chemical elements is described.
2 figures, 4 references.
Keywords: isomorphic substitutions, isotopes, neutrons.

According to position of elements in the Periodic table by D.I. Mendeleev, Fersman (1952–1959) distinguished 3 types of isomorphic substitutions (Fig. 1, 2): the most common vertical (Na-K-Rb), horizontal (Fe-Co-Ni) and diagonal (Ti-Nb, Ca-Y, etc.).

The horizontal isomorphic substitutions (Fig. 2) are the widest in the lanthanide group from La № 57 to Lu № 71. The neighbor elements intimately correlate, especially strongly in pairs even-odd lanthanide (for example, Ce and La). Odd lanthanide could be situated in the table to the left of even one (La to unstable Pm) and to the right of even one (Lu paired with Yb). In these seven pairs of lanthanides correlation is frequently caused by the fact that the major isotope of even element (for example, Nd has 7 isotopes) agrees in respect of number of neutrons (82) with single isotope of odd coupled Pr. The agreement of number of neutrons in pair of heavy lanthanides, Dy – Ho (98), Yb – Lu (104), is similar. A shift of isotope spectrum Yb to Lu is characteristic.

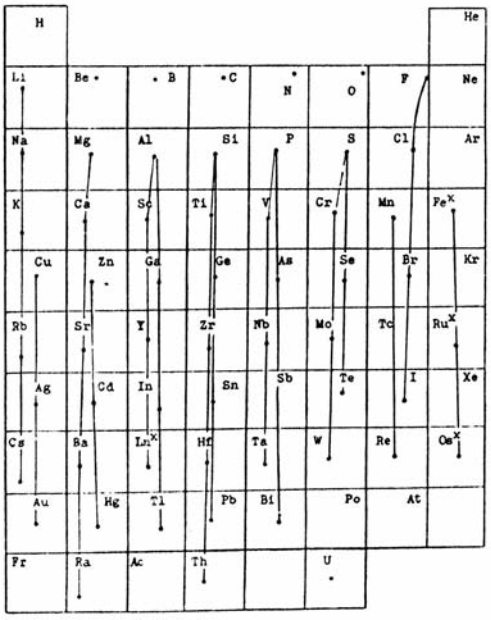

Fig. 1. Scheme of vertical isomorphic substitutions. In squares of the Periodic table are plotted dots according to coordinates: electronegativity of element (increases from left to right along diagonal from 0.7 – Cs to 4 – F) and its ionic radius (from top to bottom from 0.15 Å – N to 2.22 Å – Te).
Fe^x, Ru^x, Os^x, Ln^x are group of elements.

Semenov (1976, 2001) and Galiulin (2007) published the Periodc table with indication of number of neutrons in the major isotope rather than mean atomic weight. Coincidence of number of neutrons of major isotopes in isomorphic pairs Mn-Fe (30), Cu-Zn (34, and for neighboring Ga, 38), Ru-Rh (58, and for neighboring "geochemically alien" Pd, 62) is characteristic. Pair Os-Jr (116) is similar. Horizontal heterovalent isomorphic substitution also is known in pairs Y-Zr ("magic" 50 neutrons) and Pb-Bi (126 neutrons). At vertical (Nb-Ta, Mo-W) and diagonal (Ti-Nb, Sc-Zr) isomorphic substitution, number of neutrons of heavy element is about 2 times more than that of light one (Ti – 26, Nb – 52). On schemes of vertical isomorphic substitutions the distance between vertical lines of related lithophilic and chaecophilic elements is minimal in the central 4th group.

The above data should be kept in mind to distinguish large geochemical groups of elements (s-, p-, d- and f-elements).

References

Galiulin R.V. Crystallography of the Mendeleev table. // Mineral diversity. Sofia, **2007**. P. 53–62.

Semenov E.I. Distribution of rare earths and their position in the Periodic system. Dokl. AN SSSR, **1976**. 231 (2), P. 457–459 [in Russian].

Semenov E.I. Mineralization of rare earths, thorium and uranium. Moscow, Geokart, GEOS, **2001.** 196 p. [in Russian].

Fersman A.E. Selected works. Moscow: Izd. AN SSSR, **1952–1959**. [in Russian].

Fig. 2. Position of major isotopes of elements in the Periodic table, number of neutrons (center of square) and protons (upper part of square). The horizontal line means isomorphic substitution of elements.

Discussion

THE ESSAYS ON FUNDAMENTAL AND GENETIC MINERALOGY: 4. EUDIALYTE–EUCOLITES AND PROBLEMS ON TYPOMORPHISM OF MINERALS

Boris Ye. Borutzky
Institute of Ore Deposit Geology, Petrography, Mineralogy and Geochemistry RAS, Moscow, borutzky@igem.ru

The present paper is a sequel to the previously published (Borutzky, 2008) essay on the minerals of variable composition with variable structure (MVCVS) with an example of eudialyte-eucolites. The characteristic feature of this typical mineral from alkaline complexes is the unique ability to include up to one third of The Mendeleev's Periodic Table of the chemical elements in its composition. This is entailed by a partial realignment of the crystal structure in response to changing chemistry and evolution of the mineral-forming environment with time. According to the author, the detailed typomorphous analysis of eudialyte-eucolites is more informative and useful in terms of genetic mineralogy rather than formal determination of dozens of independent mineral species.
3 tables, 48 references
Keywords: eudialyte-eucolites, minerals of variable composition with variable structure.

What is typomorphism and its issues

«We have to distinguish two types of prospecting features: one is related to the nature of the objects sought for (minerals and elements) that result from ion and lattice structure features. The second is related to an external environment and determine factors due to concentration of the chemical elements»

Alexander E. Fersman

The term "typomorphism of minerals" was first introduced in 1903 by Friedrich Becke (1855–1931), Austrian mineralogist and petrologist, the foreign corresponding member of the Emperor Petersburg Academy of Science. This problem was resumed in Russia in the 1930s by Alexander E. Fersman. In the 1970s the doctrine on typomorphism of minerals was created under the direction of Fedor V. Chukhrov and other outstanding Soviet scientists; and the talks on it were included in the Programme of XI IMA meeting held in Novosibirsk (Scientific foundations.., 1980). The fundamentals of this doctrine lie in observations and revelations of the most typical (typomorphous) minerals, their associations or crystal and mineral morphology (typo-morphous = "typical shape"), typical features of a chemical composition, crystal structure and physical properties of a mineral. All these characteristic features have to correspond with the geological and physical-chemical (including kinetics) conditions of the geological structures formation. In other words, Soviet mineralogy did not aim only to discover new natural chemical compounds, but worked towards determination of the relationship between composition, structure, mineral properties and conditions of formation, i.e. its genetic features in order to use them as the mineralogical indicators for solving problems of rock- and ore-formation.

The investigation of typomorphism is carried out in different ways. Some scientists insist on the universal, global sense of the *typomorphous* features which in this case are the "rules" and not the "particular case". These scientists often consolidate or generalise the geological objects or deposits and rock types without good reason. They are carried away by the "blind" mathematical statistics, create comprehensive world-wide "databases" where only one specimen represents the Khibiny massif in whole, with no indication of the host rocks type, its location and conditions of formation. Such an approach to our point of view is a formal one. This hypertrophied "disadvantage" can be illustrated with the following statement: "nepheline is a typomorphous mineral of the nepheline syenites", which is true but senseless for the further application.

On the other hand, some generalized thesis are quite useful. For example, the occurrence of β-quartz which cannot be formed over 573°C (at normal pressure) or occurrence of microcline which stability field is below 500±50°C – are reliable geo-thermometers applied to judging the temperatures of the rocks and ores formation. The point of inversion $\alpha \rightarrow \beta$ in quartz was widely applied by Alexander E. Fersman for derivation of his

geo-phases. The phase conversion sanidine → microcline[1] has an important significance. The presence of microcline, for instance, make conclusions on the high temperature formation of some microcline-containing agpaitic nepheline syenites, doubtful. Thus, according to the experimental data obtained by Liya N. Kogarko (1977), the average melting temperature of the stratified rock complex of foyaites-lujavrites-urtites from the Lovozero massif is 1070°C in dry conditions or 910°C at P_{H_2O} = 1 kbar. For the rock complex of eudialyte lujavrites these are 990 and 872°C respectively. As microcline crystallisation was impossible at such a high temperatures, it is absolutely obvious that the mineral indicators were ignored. They indicate the post-crystallisation transformations within these rocks, and the possibility of another (rather than direct crystallisation from the melt) interpretation of a genesis of industrial rare-metal agpaitic mineralisation in association with microcline, was not considered.

As pointed out before, the typomorphous features can be not only shapes of the crystals and other mineral formations (proper *typomorphism*), but also peculiarities of the mineral chemical composition *(typochemism)* and crystal structure (*structural typomorphism* which we would like to name similarly "*typostructurism*"). From the critique articles by my opponents (Rastsvetaeva, Chukanov, 2006; Rastsvetaeva, 2007) we find that "*structural* typomorphism is a concept about the close relationship between fine peculiarities of the mineral crystal structure and conditions of its formation – the new and rapidly developing line of geological science". At the XI meeting of the IMA (Scientific fundamentals.., 1980) diverse research papers on structural typomorphism were presented by V.A. Frank-Kamenetsky, V.A. Dritz, B.B. Zvyagin, A.P. Zhukhlistov, S.V. Soboleva, B.M. Shmakin, G.G. Afonina, M.T. Dmitrieva, O.V. Rusinova and V.L. Rusinov. The above mentioned examples of $\alpha \rightarrow \beta$ inversion in quartz and sanidine → microcline transformation, are typical investigations on the structural typomorphism of these minerals, as they reflect exactly "the close relationship between fine peculiarities of the mineral crystal structure and conditions of its formation".

The author in his investigations of mineral typomorphism opposed a "formal" approach but advocated a maximum concrete definition. We called it (apparently poorly) "the concrete typomorphism" or "typomorphism of the minerals from the concrete geological objects". We believe that the factors of the mineral-forming process, both *external* and *internal* (according to the statement by Alexander E. Fersman, see epigraph) are diverse and their combinations within the specific geological objects of different scale are also diverse (Borutzky, 1986; 1988; 1997). Thus, to specify an example with nepheline above, in order to compare different rock types of the Khibiny massif – nepheline syenites, melteigite-urtites, juvites and ristschorrites we shall consider the typomorphous features and difference in the chemical composition of nepheline from the rock-forming nepheline. For comparison of different nepheline porphyres one should consider the composition of nepheline phenocrysts and matrix; and for the small bodies (for instance, individual pegmatite veins or apatite-nepheline ores with different structure etc.) and also consider the changing chemical composition within the crystal growth zones. The *external* and *internal* factors of the mineral-forming process reflect the typomorphous peculiarities of the minerals in a different way. The external factors – geological, thermodynamic and kinetic – determine the relationship of the crystallised mineral with its environment – equilibrium progress, individual mineral growth rules, mineral chemical composition and the number of micro-impurities allowed etc. Also they define the transformation in morphology and properties of the mineral in geological time scale in the post-crystallisation conditions with the changed conditions of the mineral-preserving medium, i.e. the phase transformations within the mineral, metamorphism, metasomatic replacements effected by the late solutions evolved during the change in geological conditions. The *internal* factors – is an ability of the mineral structure, as some sort of a "muzzle", that restrains chemical diversity in the mineral at certain conditions, and (if it is possible) which adjusts to possible chemical and physical-chemical changes of the mineral-preserving

[1] – It is relevant to remind that the high-temperature phases can be metastable crystallised within the low-temperature phases stability fields. But the low-temperature can not be crystallised otherwise. For instance, crystobalite transforms into trydimite at low pressure and 1470°C, trydimite transforms into the high-temperature α-quartz at 870°C, and at 573°C α-quartz transforms into the low-temperature β-quartz. However crystobalite and trydimite often occur in opals as globules. The metastable high-temperature potassium sanidine occurs in alpine veins and other low-temperature hydrothermal formations as adularia. Besides, it is characterised by the less-ordered Si/Al-distribution than sanidine from volcanic rocks.

medium. It is absolutely obvious that these factors should be considered together, in interaction with each other and it is impossible either to contrast them or to consider something alone — typochemism or structural typomorphism. In this scope, it would be logical to speak about the *minerals of variable composition with variable structure (MVCVS)* and eudialyte-eucolites in particular, and also to study their "*structural-chemical*" (crystallochemical) typomorphism.

The features of the *minerals of variable chemical composition with variable structure*

In the previous essay (Borutzky, 2008) the author gave arguments against unwarranted, from his point of view, "multiplication" of eudialyte into several dozens of individual mineral species. Eudialyte is considered as a single mineral species of *a mineral of variable chemical composition with variable structure (MVCVS)*. Its distinctive feature is a zeolite-like complex structure which allows simultaneous occupancy by multiple components (micro-impurities as a rule) in different site positions. However this does not change the individuality of eudialyte in the mineral-forming process, which remains calcium-sodium zirconium silicate with its stability field. Although under substitution there occur interstructure reorganisations: displacements of atomic coordinates, changes of the coordination polyhedra configuration, statistic occupancy of the positions followed by their "splitting" that leads to the changes in the general symmetry. In our opinion this "multiplication" is speculative, although it is based on recommendations accepted by the Commission on New Minerals, Nomenclature and Classification of International Mineralogical Association (CNMNC IMA) that allow the approval of a new mineral if the content of any component within any structural position exceeds 50 rel.% independently of its total content in the mineral (even if it is less than 1—5 wt.%). This formal approach allows one to consider any chemical composition varieties of eudialyte as independent mineral species.

From the point of view of typomorphism all these "new-born" eudialyte minerals are logically to be concerned as the eudialyte varieties. Then there is no need to puzzle over naming *potassium* (or even *potassium-bearing*) *eudialyte* as *rastsvetaevite*, *Nb-bearing eucolite as kentbrooksite, W-bearing as khomyakovite, Sr-bearing as taseqite*. In *Ta-bearing eudialyte* the content of Ta is not dominant in a position with occupancy 3 unlike "lucky" Nb and W that occupy positions with occupancy 1. Also it is worthwhile to mention here that *eucolite* is historically understood as a variety of eudialyte enriched in a number of the heavy multivalent cations which cause maximum distortion of the crystal structure, disappearance of the symmetry centre, increase in density, refractive indices, change of optical sign from positive to negative, appearance of a piezo-effect and change in colour. Natural eucolitization of eudialyte and subsequent eucolite re-crystallisation occur quite often.

Investigations of typomorphism of the minerals should be directed not only to accepting the typical distinctive features but also to the reasons that caused these distinctions. In eudialyte-eucolites, one component is discovered in several different structural positions . For instance, in *kentbrooksite REE* occupy both sodium position *N*(4) and calcium ring *M*(1), and Mn occupies both *M*(1) and "iron" position *M*(2). In *carbokentbrooksite* Mn also occupies positions *M*(1) and *M*(2), and Ca — positions *M*(1), *N*(2) and *N*(3). Why do they so occur? In Table 1 in the previous essay (Borutzky, 2008) we gave several similar examples. On the other hand, the same "iron" position *M*(2) in *low-ferruginoius eudialyte* can be statistically simultaneously occupied by ^{4}Na (Na-"square" Na4b), ^{5}Na (Na-half-octahedron Na4a), $^{5}Fe^{3+}$ and ^{5}Mn (five-end polyhedra), and ^{6}Nb and ^{6}Ti (octahedra). In *alluaivite* the same "iron" position can be occupied by sodium in different coordination polyhedra: ^{4}Na(11) ("square"), ^{7}Na(12) and ^{7}Na(13) (seven-end polyhedra); in *hyper-zirconium eudialyte* — by ^{6}Zr (octahedron); in *Mn,Na-ordered eudialyte* — by $^{4}Fe^{2+}$ ("square"), [^{5}Zr, ^{5}Na] and [^{5}Ti, ^{5}Nb] in two types of the five-end polyhedra *M*(2a) and *M*(2b); in *Ca,Fe-ordered eudialyte* — by ^{4}Zr ("square" *M*(2,4)), ^{5}Mn (five-end polyhedra *M*(2,5a)) and ^{5}Na (five-end polyhedra *M*(2,5b)); in *eudialyte enriched in tantalum* by ^{4}Ta ("square") or ^{6}Ta (octahedra) and ^{5}Fe (five-end polyhedron). Why are such modifications possible? Crystallographers cannot answer these questions and consequently are more tempted to register data arising from structure decoding as a new mineral species.

We assume that in terms of successful *structural* typomorphism (Rastsvetaeva, Chukanov, 2006; Rastsvetaeva, 2007) prior to revealing "the close interrelation of the fine

features of a mineral crystal structure with its formation conditions" one should try to understand and explain the reason for these structural mechanisms. Why such complex compounds as *MVCVS* occur in nature, and why eudialyte-eucolite in particular includes up to one-third of The Mendeleev's Periodic Table of chemical elements without being disintegrated into a number of simple and more equilibrium minerals? We are convinced that the answer to these questions is in the complex approach to the unique eudialyte crystal structure and consideration of eudialyte as a single complex mineral.

The typomorphism of eudialyte–eucolites in the Khibiny massif

Anyway, the variations in the chemical composition of eudialyte-eucolites can be a sensitive indicator for comparison between different types of rocks and other geological formations and help in solving debatable genetic questions. However one should remember that typomorphism investigation is to be undertaken in relation to all geological-petrological-geochemical data on a certain geological object; and both data and conclusions obtained will result in progressing a better understanding of the nature and geological history of the objects studied. We shall consider it as applied to an example of the Khibiny alkaline massif, Kola peninsula.

The very first work on typomorphism of eudialyte-eucolites from Khibiny was fulfilled by the field expeditions by Alexander E. Fersman (Kostyleva, 1929; 1936; Minerals of Khibiny... 1937). The eudialyte from pegmatites within nepheline syenites were studied in detail. It was concluded that sodium eudialyte is typical for khibinite rocks zones, and eucolite enriched in Ca, Fe and Mn — is typical for foyaite zones. The chemical composition of eudialyte was concluded as corresponding to the chemical composition of the host rocks: eudialyte occurs in sodium rocks of the Lovozero massif, and eucolite occurs in the enriched in calcium rocks of the Khibiny massif. This conclusion regarding eudialyte from khibinite rocks and foyaites was later confirmed by Igor P. Tikhonenkov (1963).

Notable progress in typomorphism investigation was made by Vladimir G. Feklichev (1973) who studied distribution of Zr, Hf, Nb, Ta, Sr, *REE*, Be, Ga, Sc, Ba, Li in the Khibiny eudialyte using the detailed geological foundation of detailed zonation of the rocks within the Khibiny massif. According to these data some rare element contents vary widely and irregularly within one and the same rock complex: for example Ta_2O_5 (0.018 ÷ 1.027, in eudialyte from albitites in foyaites the content detected was 1.61%). Other rare elements, such as ZrO_2, HfO_2 and SrO, are distributed equally; and the others are typomorphous for eudialyte from the different rock complexes (Table 1). Thus, the minimum Be content in eudialyte is typical for khibinite rocks; the minimum Nb_2O_5, *REE* and maximum yttrium content are typical for ijolite-urtites and ristschorrites of Poachvumschorr type; the maximum Nb_2O_5, *REE* and maximum cerium content are typical for ijolite and ristschorrites of Yukspor type. The data on *REE* and Y behavior corresponds with ours (Varshal *et al.*, 1967; Borutzky *et al.*, 1975): the maximum content of $\sum REE$ and cerium rare earth were determined in eudialyte from nepheline syenites (more in foyaites rather than in khibinites), and the minimum contents were found in eudialyte from ristschorrites, ijolite-urtites and pegmatites within apatite-nepheline rocks. These variations are inversely proportional to those of yttrium and yttrium rare earth content.

In the region of Bolshoy and Maliy Vudyavr Lakes where most of the Khibiny massif rock types have outcrops, Vladimir G. Feklichev (1975) carried out mineralogical mapping on the basis of typomorphous features of eudialyte: average refractive index $(2n_o + n_e)/3$, optical sign and colour. Among 124 specimens of eudialyte 17 were from the coarse-grained trachytoid knibinites, 50 — from the medium-grained trachytoid knibinites, 9 — from melteigite-urtites, 17 — from ristschorrites

Table 1. **The average content of rare earth elements in eudialyte from Khibiny, after Vladimir G. Feklichev (1973) (wt.%)**

Rocks	Li_2O	BaO	TR_2O_3	TR_Y/TR_{Ce}	Nb_2O_5	Be	Ga	Sc_2O_3
Khibinites	0.001	0.03	0.62	0.069	0.59	0.0001	0.0004	0.003
Ijolite-urtites	0.002	—	0.23	0.260	0.12	0.0001	0.0004	0.001
Ristschorrites of Poachvumschorr type	0.003	0.38	0.25	0.145	0.61	0.0005	0.0006	0.008
Ristschorrites of Yuksporr type	0.001	0.01	2.88	0.041	1.78	0.0024	0.0002	0.004
Foyaites	0.002	0.12	2.24	0.041	1.76	0.0009	0.0008	0.011

and 19 — from foyaites. It was determined that brown eudialyte with increasing refractive index (1.611—1.612) is typical for the coarse-grained khibinites; red eudialyte with lower refractive index (1.609—1.610) is typical for trachytoid knibinites; raspberry-pink eudialyte with the lowest refractive index (1.606—1.608 and less than 1.605) is typical for melteigite-urtites and ristschorrites of Poachvumtschorr type; and brownish-red with medium and high refractive index (1.611—1.614 and over 1.616) is typical for foyaites.

Let us return to the question of the "formal" and "specific" approaches in mineral typomorphism investigation. The maximum specification in the petrological-geochemical research includes comparison of the chemical composition and the structure and features of the mineral from different geological-petrological rocks of a massif complex. During this the most specific details are normally emasculated, as petrologists and geochemists usually disregard mineralogical data. Quite often they made general conclusions or consolidations according to practiced petrogenetic methodology and schemes. Thus, many scientists consider the Khibiny massif as *a single unit*, as an isolated magmatic system which crystallized from its periphery to centre, with crystallization or gravity-crystallization differentiation of the alkali melt (Galakhov, 1975). Describing this system, petrologists calculate the *average* composition of the Khibiny magma prior to its differentiation (Kukharenko *et al.*, 1968), determine the *average* age (Kogarko *et al.*, 1981_1) and speak about the single mineral-forming process within the massive, caused by the sinusoidal change in alkalinity and increasing relative acidity at the end (Khomyakov, 1990). Alexander P. Khomyakov also assumes the integration of the Khibiny and Lovozero massifs into the unit "Khibiny-Lovozero complex".

This all affects the methodology of the eudialyte typomorphism studies. It is especially annoying when mineralogists have been involved. Thus, in the monograph by Viktor N. Yakovenchuk (Yakovenchuk *et al.*, 2005) recently published in English with excellent illustrations, all the types of nepheline syenites from the Khibiny massif were combined into one called *foyaites*, obviously to please petrologists. After that they divided the 30 km radial section through the Khibiny massif into 6 statistic intervals and analyzed correlation of Si/(Si+Nb), Fe/(Fe+Mn) and Ca/(Ca+*REE*) in eudialyte. As a result they formally conclude that from the periphery to the centre of a massif the content of Na, *REE*, Sr, Fe, Nb and Cl decrease; but near "the central arch" the content of Mn, Zr and Nb increase, there eudialyte-Mn, ferrokentbrooksite and ikranite occur; and eudialyte-Fe is typical for urtites and ristschorrites of "the central arch" itself. The reasons for such trends are not discussed.

At present investigations of typomorphism should be fulfilled on the basis of more reliable facts and methods. The behaviour of minerals, as well as rocks, do not end with their crystallisation. As usual, they undergo changes during the long geological history, they can form in several stages, change their chemical composition and structure during changes in the mineral-forming and mineral-preserving medium, undergo metasomatic replacements and post-crystallisation alterations. Eudialyte is not an exception and all this reflects in its typomorphous features.

Liya N. Kogarko (1977) considers eudialyte as a magmatic mineral which crystallised from alkaline agpaitic magma (Kogarko *et al.*, 1980; 1981_2) — the dry one (although her own experiments reveal that in such a melt up to 10% of water can be dissolved), the high-temperature one, 1000—800°C (although the gap between the liquidus and solidus curves can reach several hundreds of degrees), the one occurred in reductive conditions. On the contrary, we consider that eudialyte was formed in a typical paragenesis with aenigmatite, rinkite, lamprophyllite, aegirine (enriched in Fe^{3+}) and microcline (that cannot be formed at temperatures higher than 500—550°C) during the late, auto-metasomatic, relatively low-temperature stage of formation of nepheline syenites and their pegmatites, i.e. with the alkaline solutions involved. Obviously, the process does not end here and later, during the low-temperature stage eudialyte undergoes *eucolitization*. The details of this process were described earlier (Borutzky, 2008).

Igor V. Pekov (2001) postulates the change from sodium conditions of alkalinity to potassium conditions during the final stages of evolution of the agpaitic alkaline rock complexes. Unlike him, we repeatedly showed that at least in the Khibiny massif the high-alkaline paragenesis with adularia-like orthoclase, kalsilite and rare ultra-alkaline accessory minerals were formed during the infiltrating metasomatic effect of the nepheline-syenite magma fluids onto the chemically contrasting basic rocks from "the central arch" (meltei-

gite-urtites) captured within the massif as a huge relic. According to the principle of Dmitry S. Korzhinsky (1955; 1993), the drastically increasing potassium activity is caused by the acidic-basic interaction of the fluids with the matrix being replaced, and is variable depending on the temperature and equilibrium of metasomatic reactions. Giving accord to Alexander P. Khomyakov (1990) opinion on the trend of a sinusoidal change of alkalinity and increasing acidity towards the end of the process, we nevertheless insist on the detailed investigation of this phenomenon in different formations, and show that in the case of eudialyte it leads to distinctive results (Ageeva, 1999; 2002; Ageeva *et al.*, 2002_1; 2002_2; Azarova, 2005).

Discussing one or other specific problems of the Khibiny massif geology, petrology and mineralogy, we constantly face the fact that our concept of its geological history, understanding its nature and its rock-forming process is not adequately known. Most likely it happens because petrologists are unfamiliar with the mineralogical literature or do not realise the validity and reliability of mineralogical indicators as solutions for petrological problems.

We consider Khibiny as a composite *volcanic-plutonic* complex, formed by a succession of caldera subsidences. They were composed of: (1) nepheline-syenite magma with a large quantity of relicts and xenoliths of Archean-Proterozoic frame host rocks, and (2) Paleozoic volcanic rocks (varying in composition from alkaline picrites, augite-porphyres to phonolites and rhomb-porphyres), and also (3) ancient foliated fine-medium-grained stratified melteigite-urtites. The relict and xenolith rocks have more or less undergone metamorphism, syenitisation and fenitisation influenced by the fluids derived from nepheline-syenite magma. These processes were most intensive within the so-called "central arch" of the massif, where the relics of the fine-medium-grained melteigite-urtites were transformed into giant-grained agpaitic metasomatic rocks (fenites) of malignite, urtite, juvite and nepheline-syenite (ristschorrites) composition, considerably enriched in potassium (Mineralogy of Khibiny... 1978; Borutzky *et al.*, 1978; 1980; Borutzky, 1988; 1997). The rocks of "the central arch" are obviously situated in the lowermost, shattered and heated part of the massif and differ from the rocks of "the western arch" by their increased basicity (Table 2) which increases activity of the most basic components in the fluid solutions. The most basic replaced substrate corresponds to the fine-grained urtites dated to the middle part of a section of the stratified rocks. This is exactly how the giant-grained urtites, underlying apatite-nepheline ore bodies, have been formed. The relative potassium enrichment in nepheline indicates the considerable role of this element in the mineral-forming system. During fenitisation the fluid solutions composition evolves into a nepheline syenite one. According to this, the role of silicon is increasing and the leucocratic metasomatic rocks forming, transform in the sequence: urtite → feldspar urtite → juvite → ristschorrite. The melanocratic metasomatic rocks transform in the sequence: feldspar ijolite → malignite. Mineralogically it appears as replacement of nepheline by kalsilite (Ageeva, Borutzky, 2004), and later – replacement of nepheline and pyroxene by structurally disordered adularia-like orthoclase (Mineralogy of Khibiny..., 1978; Borutzky, 1988; 1997).

Thus, returning to the problem of eudialyte-eucolite typomorphism, we see that it is closely related to the change in alkalinity conditions of the mineral-forming solutions and re-distribution of their components according to the principle of acidic-basic interaction by Dmitry S. Korzhinsky (1955; 1993).

The typomorphism of eudialyte in "the central arch" rocks in the Khibiny massif

From the above mentioned publications (Rastsvetaeva, Chukanov, 2006; Rastsvetaeva, 2007) we found out that Alexander P. Khomyakov *et al. determined* that "rastsvetaevite formation in the Khibiny massif was carried out by *the solid-phase transformation* of eudialyte *under potassium metasomatosis conditions*" (italic type – by the author). "At present, along with the rastsvetaevite holotype described, similar high-potassium eudialyte containing over 5–6% K_2O was *discovered* (Khomyakov *et al.*, 2006) in the several regions of the Khibiny massif in the poikilitic nepheline syenites (ristschorrites). This discovery is undoubtedly interesting for the full understanding of the typomorphism of potassium minerals in the Khibiny massif". We were surprised by this statement because we never saw any publications on eudialyte typomorphism by Alexander P. Khomyakov, and he never supported our concept on the metasomatic genesis of ristschorrites from the Khibiny massif (Mineralogy of Khibiny..., 1978; Borutzky *et al.*, 1978; 1980; Borutzky,

Table 2. **Petrochemical formulae of the Khibiny massif rocks and indexes of basicity $\Delta Z^{H_2O}_{298^\circ K}$ calculated, after Alexey A. Marakushev (1979)**

№	Rocks	Formula	$\Delta Z^{H_2O}_{298^\circ K}$
		Nepheline syenites:	
1	Khibinites (40 an.)	$K_{2.44}Na_{5.31}Ca_{0.55}Sr_{0.02}Mg_{0.28}Mn_{0.06}Fe^{2+}_{0.78}Fe^{3+}_{0.51}Ti_{0.24}Al_{7.22}Si_{16.06}P_{0.03}O_{49.87}F_{0.13}$	3.60
2	Lyavotschorrites (32 an.)	$K_{2.34}Na_{5.40}Ca_{0.74}Sr_{0.04}Ba_{0.01}Mg_{0.33}Mn_{0.08}Fe^{2+}_{0.77}Fe^{3+}_{0.42}Ti_{0.32}Nb_{0.03}Al_{7.27}Si_{15.79}P_{0.05}C_{0.11}O_{49.86}F_{0.14}$	3.69
3	Lujaurites (12 an.)	$K_{2.96}Na_{4.79}Ca_{1.15}Mg_{0.73}Mn_{0.06}Fe^{2+}_{1.13}Fe^{3+}_{0.74}Ti_{0.55}Al_{6.32}Si_{15.63}P_{0.04}O_{50.00}$	3.97
4	Foyaites (17 an.)	$K_{2.15}Na_{5.32}Ca_{0.44}Sr_{0.01}Ba_{0.02}Mg_{0.25}Mn_{0.04}Fe^{2+}_{0.51}Fe^{3+}_{0.41}Ti_{0.17}Al_{7.33}Si_{16.30}P_{0.06}C_{0.15}O_{49.93}F_{0.07}$	3.34
		Melteigite-urtites of stratified rock complex of "the central arch":	
	In total (109 an.)*	$K_{1.71}Na_{6.46}Ca_{2.36}Mg_{1.29}Mn_{0.07}Fe^{2+}_{1.02}Fe^{3+}_{1.22}Ti_{0.74}Al_{6.74}Si_{13.79}P_{0.20}O_{50.00}$	4.75
5	Ijolites medium-grained mesocratic from the upper strata (21 an.)*	$K_{1.78}Na_{6.51}Ca_{2.10}Mg_{1.12}Mn_{0.07}Fe^{2+}_{0.93}Fe^{3+}_{1.23}Ti_{0.71}Al_{6.58}Si_{14.00}P_{0.18}O_{50.00}$	4.62
6	Ijolites fine-grained mesocratic from the upper strata (9 an.)*	$K_{1.71}Na_{6.54}Ca_{2.14}Mg_{1.14}Mn_{0.06}Fe^{2+}_{0.96}Fe^{3+}_{1.27}Ti_{0.81}Al_{7.07}Si_{13.49}P_{0.20}O_{50.00}$	4.68
7	Ijolites fine-medium- - grained mesocratic from the middle strata (21 an.)*	$K_{1.62}Na_{6.19}Ca_{2.51}Mg_{1.55}Mn_{0.06}Fe^{2+}_{1.00}Fe^{3+}_{1.18}Ti_{0.61}Al_{6.26}Si_{14.15}P_{0.13}O_{50.00}$	4.67
8	Trachytoidal urtites from - the stratified band from middle strata (16 an.)*	$K_{1.85}Na_{7.23}Ca_{1.86}Mg_{0.84}Mn_{0.05}Fe^{2+}_{0.86}Fe^{3+}_{1.04}Ti_{0.59}Al_{8.20}Si_{13.20}P_{0.16}O_{50.00}$	5.05
9	Melteigites of the stratified band from middle strata (17 an.)*	$K_{0.75}Na_{3.55}Ca_{4.73}Mg_{2.71}Mn_{0.13}Fe^{2+}_{2.39}Fe^{3+}_{2.41}Ti_{1.33}Al_{3.04}Si_{12.70}P_{0.67}O_{50.00}$	3.91
10	Ijolites medium-grained mesocratic from the lower strata (10 an.)*	$K_{1.62}Na_{6.25}Ca_{2.64}Mg_{1.43}Mn_{0.08}Fe^{2+}_{0.91}Fe^{3+}_{1.19}Ti_{0.81}Al_{6.49}Si_{13.73}P_{0.16}O_{50.00}$	4.72
11	Ijolites fine-grained melanocratic with titanite from the lower strata (15 an.)*	$K_{1.75}Na_{6.69}Ca_{2.29}Mg_{1.17}Mn_{0.05}Fe^{2+}_{1.02}Fe^{3+}_{1.04}Ti_{0.79}Al_{7.26}Si_{13.32}P_{0.23}O_{50.00}$	4.57
		Agpaitic metasomatic rocks:	
12	Massive giant-grained urtites (91 an.)*	$K_{1.94}Na_{6.89}Ca_{1.72}Mg_{0.54}Mn_{0.05}Fe^{2+}_{0.67}Fe^{3+}_{0.82}Ti_{0.44}Al_{8.22}Si_{13.48}P_{0.48}O_{50.00}$	4.73
13	Juvites (107 an.)*	$K_{3.4}Na_{5.97}Ca_{1.32}Mg_{0.54}Mn_{0.05}Fe^{2+}_{0.63}Fe^{3+}_{0.76}Ti_{0.48}Al_{7.87}Si_{14.26}P_{0.20}O_{50.00}$	4.73
14	Juvites (39 an.)**	$K_{2.73}Na_{5.96}Ca_{1.16}Sr_{0.03}Ba_{0.01}Mg_{0.43}Mn_{0.04}Fe^{2+}_{0.58}Fe^{3+}_{0.74}Ti_{0.51}Al_{7.90}Si_{14.41}P_{0.14}C_{0.15}O_{49.85}F_{0.15}$	4.42
15	Ristschorrites (46 an.)*	$K_{3.65}Na_{4.63}Ca_{0.51}Mg_{0.31}Mn_{0.04}Fe^{2+}_{0.79}Fe^{3+}_{0.57}Ti_{0.30}Al_{7.65}Si_{15.65}P_{0.07}O_{50.00}$	4.03
16	Ristschorrites (98 an.)**	$K_{4.16}Na_{4.24}Ca_{0.51}Sr_{0.02}Ba_{0.02}TR_{0.02}Mg_{0.27}Mn_{0.03}Fe^{2+}_{0.56}Fe^{3+}_{0.50}Ti_{0.23}Zr_{0.05}Al_{7.84}Si_{15.50}P_{0.05}C_{0.09}O_{49.91}F_{0.09}$	4.15
17	Kalsilite-bearing ristschorrites (epileucitophyres?) (3 an.)	$K_{6.70}Na_{1.96}Ca_{0.22}Sr_{0.00}Ba_{0.00}Mg_{0.06}Mn_{0.01}Fe^{2+}_{0.24}Fe^{3+}_{0.49}Ti_{0.10}Al_{8.32}Si_{15.86}O_{50.00}$	5.64
		Volcanic rocks of "the wester arch":	
18	Picrite-porphyrites (2 an.)	$K_{0.28}Na_{1.56}Ca_{3.36}Sr_{0.02}Mg_{8.91}Mn_{0.06}Fe^{2+}_{3.31}Fe^{3+}_{0.96}Ti_{1.31}Zr_{0.01}Al_{1.75}Si_{13.04}P_{0.22}C_{0.06}O_{49.79}F_{0.21}$	3.81
19	Pyroxenites (2 an.)	$K_{0.68}Na_{0.76}Ca_{4.34}Sr_{0.02}Mg_{8.26}Mn_{0.07}Fe^{2+}_{2.23}Fe^{3+}_{2.15}Ti_{1.31}Zr_{0.01}Al_{1.66}Si_{12.70}P_{0.19}C_{0.06}O_{49.77}F_{0.23}$	3.89
20	Melteigites (2 an.)	$K_{0.86}Na_{1.36}Ca_{5.59}Sr_{0.05}Ba_{0.02}Mg_{5.78}Mn_{0.06}Fe^{2+}_{1.59}Fe^{3+}_{1.93}Ti_{1.29}Zr_{0.01}Al_{2.13}Si_{13.10}P_{0.28}C_{0.10}O_{49.68}F_{0.32}$	4.05
21	Melilitite	$K_{0.41}Na_{1.24}Ca_{9.50}Sr_{0.07}Ba_{0.02}Mg_{4.54}Mn_{0.10}Fe^{2+}_{1.94}Fe^{3+}_{3.84}Ti_{1.75}Zr_{0.01}Al_{1.93}Si_{9.79}P_{0.45}C_{0.07}O_{49.58}F_{0.42}$	5.10
22	Melilititic picrite	$K_{0.18}Na_{1.15}Ca_{6.52}Sr_{0.04}Ba_{0.01}Mg_{11.47}Mn_{0.12}Fe^{2+}_{1.47}Fe^{3+}_{2.92}Ti_{0.72}Al_{1.23}Si_{10.91}P_{0.03}C_{0.08}O_{49.87}F_{0.13}$	5.72
23	Augitite-porphyritites (3 an.)	$K_{0.96}Na_{2.53}Ca_{2.90}Sr_{0.04}Ba_{0.01}Mg_{4.07}Mn_{0.07}Fe^{2+}_{2.25}Fe^{3+}_{1.09}Ti_{1.23}Al_{3.90}Si_{14.12}P_{0.20}C_{0.13}O_{49.58}F_{0.42}$	3.25
24	Nephelinites (2 an.)	$K_{1.12}Na_{5.19}Ca_{2.43}Sr_{0.09}Ba_{0.03}Mg_{2.17}Mn_{0.14}Fe^{2+}_{1.91}Fe^{3+}_{1.05}Ti_{1.22}Al_{5.09}Si_{13.74}P_{0.30}C_{0.11}O_{49.25}F_{0.75}$	3.90
25	Feldspar nephelinites (4 an.)	$K_{1.94}Na_{4.04}Ca_{1.13}Sr_{0.07}Ba_{0.02}Mg_{1.17}Mn_{0.10}Fe^{2+}_{1.64}Fe^{3+}_{0.76}Ti_{0.65}Zr_{0.05}Al_{6.54}Si_{14.85}P_{0.20}C_{0.16}O_{49.60}F_{0.40}$	3.22
26	Nepheline mela-phonolites (3 an.)	$K_{1.35}Na_{5.51}Ca_{0.59}Sr_{0.08}Ba_{0.03}Mg_{0.54}Mn_{0.07}Fe^{2+}_{0.74}Fe^{3+}_{0.53}Ti_{0.33}Zr_{0.04}Al_{7.60}Si_{15.51}P_{0.10}C_{0.15}O_{49.76}F_{0.24}$	3.21
27	Rhomb-porphyry (4 an.)	$K_{2.81}Na_{3.82}Ca_{0.46}Sr_{0.02}Ba_{0.01}Mg_{0.46}Mn_{0.08}Fe^{2+}_{0.59}Fe^{3+}_{0.57}Ti_{0.32}Zr_{0.05}Al_{6.55}Si_{16.60}P_{0.11}C_{0.09}O_{49.81}F_{0.19}$	2.96

Notes: Petrochemical formulae are calculated for 50 atoms of oxygen (O + F).

* — *calculated for the data by A.A. Arzamastsev et al. (1987);* ** — *calculated for our data*

1988; 1997). Now it turned out that Alexander P. Khomyakov *et al. determined* metasomatic genesis of potassium eudialyte in ristschorrites, "disguised" as *rastsvetaevite*.

In as much as the text cited seemed well-known to us, although it has been "paraphrased", we decided to turn to the article on rastsvetaevite (Khomyakov *et al.*, 2006). There we found references to the publications of Olga A. Ageeva (Ageeva, 1999; Ageeva *et al.*, 2002_1) where these ideas were borrowed. Would it be more correct to refer to Olga A. Ageeva Ph.D. thesis (2002) directly, which is totally devoted to the problem of mineral-forming process and typomorphism of the minerals in ristschorrites, as well as to refer to other publications discussing genetic features and typomorphism of the Khibiny eudialyte within "the central arch" rocks (Ageeva *et al.*, 2002_2; Azarova, 2005), rather than "attribute" this conclusion to Alexander P. Khomyakov?

It was mentioned above in the previous chapter that according to our concept, ristschorrites were formed during the last stage of fenitisation, in the following succession: giant-grained urtite → feldspar urtite → juvite → ristschorrite. Mineralogy of accessory minerals in these metasomatic rocks, including eudialyte was studied by Olga A. Ageeva (1999; 2002) in detail. There are two morphological types of the minerals: metasomatically replaced relics of the altered substrate and new formations, i.e. the product of their re-crystallisation. The relict remnants show the non-equilibrium character of the infiltration metasomatosis process, and the speed of advance of the flowing solutions is left behind the equilibrium of the chemical reactions progress. This enables one to trace the development of transformations in eudialyte, to find out its typomorphous features and to explain their character (Ageeva, 1999; 2002; Ageeva *et al.*, 2002_1).

For the initial giant-grained urtites *the sodium* (sodium-ferri-ferrous) eudialyte[2], is typomorphous, for example:

$(Na_{13.4}K_{1.1}Sr_{0.1})_{14.6}(Ca_{5.7}Mn_{0.2}Na_{0.1})_6Fe_{1.4}(Zr_{2.6}Ti_{0.4})_3[Si_{25.8}(Al,Zr,Nb)_{0.2}]_{26}O_{72.0}Cl_{1.6}$,

$K_{alk} = 0.56$, $\Delta Z^{H_2O}_{298°K} = 4.933$.

In ristschorrites it is replaced by eudialyte enriched in potassium — the *potassium-sodium* eudialyte:

$(Na_{12.6}K_{3.8}Sr_{0.6})_{16.9}(Ca_{5.8}Mn_{0.1}REE_{0.1})_6Fe_{0.8}Mn_{0.4}(Zr_{2.8}Ti_{0.2})_3[Si_{26.0}(Zr,Nb)_{0.0}]_{26}O_{73.3}Cl_{1.5}$,

$K_{alk} = 0.63$, $\Delta Z^{H_2O}_{298°K} = 5.737$.

Having no access to structural analysis facilities we therefore group the components logicaly. However, it is clear that the potassium eudialyte is characterized by the higher alkali content (potassium, above all), the higher manganese (due to iron) content, the lower content of titanium and the higher content of strontium and silicon.

During the following hypogenic leaching (obviously due to increasing aqua content in the fluid), the *potassium-sodium* eudialyte, for instance:

$(Na_{13.5}K_{3.3}Sr_{0.4}Ba_{0.1})_{17.3}(Ca_{5.9}Mn_{0.1})_6Fe_{1.0}Mn_{0.1}(Zr_{2.8}Ti_{0.2})_3[Si_{26.0}(Zr,Nb)_{0.0}]_{26}O_{73.0}Cl_{1.9}$,

$K_{alk} = 0.65$, $\Delta Z^{H_2O}_{298°K} = 5.761$,

is replaced by the *potassium-oxonium* eudialyte:

$(Na_{3.3}K_{1.9}Sr_{0.1})_{5.3}(Ca_{5.4}Mn_{0.2})_{5.6}Fe_{1.1}(Zr_{2.7}Ti_{0.3})_3[Si_{25.7}Zr_{0.3}]_{26}O_{72.8}Cl_{1.7} \cdot 8H_3O^+$,

$K_{alk} = 0.21$, $\Delta Z^{H_2O}_{298°K} = 1.970$.

It is obvious that the alkali, calcium and strontium are intensively carried away from the structure, while manganese, titanium and zirconium are less mobile and get relatively accummulated. Potassium is carried away less intensive than sodium (apparently, activity of K in the system is still high), which is replaced by oxonium groupings. The following transformation of the potassium-oxonium eudialyte result in its decomposition and formation of individual grains of the water-containing potassium and potassium-sodium zirconium silicates: paraumbite, potassium gaidonnayite, georgechaoite etc. These processes of the eudialyte transformation within ristschorrites are the principal and fundamental; corresponding to the character of the host rocks transformation — ristschorritization.

However, there are exceptions: in the contact zone of ristschorrites with unaltered urtites (with the intense "soda" mineralisation) and in the so-called *soda horizons* amongst urtites. The titanium-enriched eudialyte and alluaivite are formed under those conditions.

Unlike alluaivite described by Alexander P. Khomyakov in the Lovozero massif (Khomyakov *et al.*, 1990; Rastsvetaeva *et al.*, 1990_2) — individual crystals on eudialyte, the Khibiny alluaivite occurs not only as separate formations but also it forms gradual conversion from the potassium-sodium eudialyte replaced, to the titanium eudialyte (Ageeva *et al.*, 2002_1).

In ristschorrites from Rasvumschorr mountain the *potassium-sodium* eudilayte:

[2] — The analyses of eudialyte were calculated on the basis of (Si+Al+Zr+Ti+Nb+W) = 29 cations, which form the "rigid" frame of the structure containing SiO_4-tetrahedra rings connecting with (Zr,Ti)-octahedra. K_{alk} = (Na+K)/Si (in atomic %) — the relative coefficient of alkalinity. $\Delta Z^{H_2O}_{298°K}$ (kcal) — index of the total basicity of the mineral, after Alexey A. Marakushev (1979).

$(Na_{12.7}K_{3.0}Sr_{0.2})_{15.9}(Ca_{5.7}Mn_{0.2}REE_{0.1})_{6.0}Fe_{1.1}(Zr_{2.8}Ti_{0.2})_3[Si_{25.8}(Zr,Nb,Al)_{0.2}]_{26}O_{72.2}Cl_{1.8}S_{0.03}$,

$K_{щел} = 0.61$, $\Delta Z^{H_2O}_{298°K} = 5.398$,

is replaced by the *titanium* eudialyte:

$(Na_{13.8}K_{1.9}Sr_{0.1})_{15.8}(Ca_{5.0}Mn_{0.4}REE_{0.1})_{5.5}Fe_{0.9}(Zr_{2.1}Ti_{0.9})_3[Si_{25.3}(Zr_{0.4}Al_{0.2}Nb_{0.1})_{0.7}]_{26}O_{72.4}Cl_{0.9}S_{0.13}$,

$K_{alk} = 0.62$, $\Delta Z^{H_2O}_{298°K} = 5.306$.

In this case in the same summary alkalinity, ferriferrous and basicity, potassium is replaced by sodium, strontium is leached, calcium is replaced by manganese, zirconium — by titanium, the number of additional octahedra substituting silicon increases, chlorine content decreases, sulphur content increases. The mineral-forming medium becomes enriched in titanium and we see it in the paragenesis of titanium eudialyte with Ti-bearing aegirine.

For the "soda" horizons among urtites of Rasvumschorr mountain the compositions of the newly-formed alluaivite and associated eudialyte are as follows: *sodium* eudialyte —

$(Na_{14.4}K_{0.2}Sr_{0.4}Ba_{0.1})_{15.1}(Ca_{5.7}Mn_{0.3})_6Fe_{1.2}Mn_{0.4}(Zr_{2.6}Ti_{0.4})_3[Si_{25.9}(Zr,Al,W)_{0.1}]_{26}O_{72.6}Cl_{1.5}S_{0.04}$,

$K_{alk} = 0.56$, $\Delta Z^{H_2O}_{298°K} = 4.941$, *alluaivite* — $(Na_{18.4}K_{0.0}Ba_{0.1})_{18.5}(Ca_{5.2}Mn_{0.6}REE_{0.1})_{5.9}Fe_{0.1}(Ti_{2.4}Nb_{0.6})_3[Si_{25.8}Nb_{0.2}]_{26}O_{73.0}Cl_{0.4}S_{0.59}$,

$K_{alk} = 0.72$, $\Delta Z^{H_2O}_{298°K} = 9.521$.

The primary *sodium* eudialyte here, as with the majority of eudialyte from urtites or their relicts, was sodium-ferriferrous, almost non-potassium and was not affected by ristschorritisation process. As a result of transformation we observe the same trend: the total substitution of potassium by sodium (with enrichment in the latter), calcium by manganese, zirconium by titanium and niobium; leaching of strontium, iron, chlorine and increasing sulphur concentration. It is interesting that in these ultra-alkaline sodium conditions, the sodium-ferriferrous eudialyte and alluaivite move outside the limits of their stability fields and are replaced by zirsinalite $Na_6CaZr[Si_6O_{18}]$ and koashvite $Na_6(Ca,Mn)(Ti,Fe)[Si_6O_{18}]$ respectively, and later transformed into lovozerite $Na_3H_3CaZr[Si_6O_{18}]$ or into tisinalite $Na_3H_3(Ca,Mn)(Ti,Fe)[Si_6O_{18}]$.

Let us have a look at all these varied substitutions in the eudialyte structure in terms of the principle of acidic-basic interaction by Dmitry S. Korzhinsky (1955; 1993).

The structural–chemical typomorphism of eudialyte and the principle of acidic–basic interaction of the components by Dmitry S. Korzhinsky

Trying to explain the multiple variations in the Khibiny eudialyte from the chemical and thermodynamic points of view, we engage the principle of acidic-basic interaction of the components by Dmitry S. Korzhinsky (1955; 1993). In alkali-basic magmatic melts, according to this principle, the *activity* of the most basic components is increasing while the activity of the acidic components is decreasing. This leads to: (1) the expansion of the crystallisation fields of the alkali leucocratic minerals (nepheline, alkali feldspar) due to contraction of the melanocratic minerals (pyroxene, amphibole) and, therefore, leads to the agpaitic sequence of crystallisation; (2) the dissociation of amphoteric components according to the acidic type, after which they function as anions in the crystallising minerals, and which explains the wide diversity of alkaline titanium- and zirconium silicates; (3) the intense absorption of Cs, Rb, K, Na, Li, Ba, Sr, Ca, *REE*, Y, Mn, Nb, Ta, Zr, Hf, Ti, Ga, Th, U as micro-impurities in crystallising minerals; (4) the dissolution of fugitive components: aqua, Cl, F, S, CO_2 in a melt of decreasing temperature that prevents their dissociation. By virtue of alkali mobility in the magmatic process (Korzhinsky, 1946) any local enrichment in them is possible within separate parts of the magma chamber, accumulation within the periphery and dissociation of the alkaline fluids from the magma. Thus, the conditions of acidity-basicity is a considerable factor in the mineral-forming process, and obviously has to be reflected in the components abundance and hence on the structural-chemical isomorphism in the minerals.

According to Alexey A. Marakushev (1979), indexes of basicity $\Delta Z^{H_2O}_{298°K}$, kcal, (affinity with proton) of the components, calculated as oxides, decrease in the following order: Cs_2O (64.248) > Rb_2O (61.114) > K_2O (56.388) > Na_2O (44.910) > Li_2O (30.094) > BaO (28.321) > SrO (26.966) > EuO (24.330) > CaO (21.192) > La_2O_3 (13.715) > MgO (13.680) > Ce_2O_3 (13.025) > Pr_2O_3 (12.817) > Pm_2O_3 (12.651) > Nd_2O_3 (12.145) > MnO (11.558) > Sm_2O_3 (10.953) > Eu_2O_3 (10.881) > Gd_2O_3 (10.813) > Ho_2O_3 (10.593) > Yb_2O_3 (9.869) > Y_2O_3 (9.833) > Tb_2O_3 (9.468) > Dy_2O_3 (9.440) > Tm_2O_3 (9.220) > Er_2O_3 (8.726) > PbO (7.713) > ZnO (6.800) > FeO (6.698) > GeO (6.368) > BeO (4.808) > Sc_2O_3 (4.232) > Al_2O_3 (3.326) > ThO_2 (0.455) > Ga_2O_3 (0.454) > H_2O (0.000) > Cr_2O_3 (-0.008) > Mn_2O_3 (-1.298) > SiO_2 (-1.886) > Fe_2O_3 (-1.958) > B_2O_3 (-2.026) > GeO_2 (-2.197) > Ta_2O_5 (-2.291) > Nb_2O_5 (-2.460) > HfO_2 (-2.674) > H_2S (-2.770) > UO_2 (-2.807) > CO_2 (-2.936) > UO_3 (-3.3) > ZrO_2 (-3.633) > CeO_2 (-3.740) > WO_2 (-4.467) > P_2O_5 (-4.536) > TiO_2 (-4.659) > WO_3 (-5.1) > HF (-18.700) > HCl (-20.410).

Thus, in the following isomorphous pairs numerators contain more basic components and denominators more acidic components: Rb/K, K/Na, Li/Mg, Ba/Sr, Sr/Ca, Ca/*REE*, Ca/Mg, Ca/Mn, Mn^{2+}/Fe^{2+}, Fe^{2+}/Fe^{3+}, Ca/Th, *REE*/Th, Al/Ga, Al/B, Al/Fe^{3+}, Si/Ge^{4+}, Ta/Nb, Hf/Zr, Nb/Ti, Zr/Ti, Fe/Ta, Fe/Nb, Fe/Zr, Fe/Ti, Al/Si, Si/Nb, Si/Zr, Si/Ti, Si/W, S^{2-}/C^{4+}, S^{2-}/Cl, F/Cl. In the line of *REE* of The Mendeleev's Periodic Table of the chemical elements the monotonous succession of decreasing basicity is broken: $La^{3+} > Ce^{3+} > Pr^{3+} > Pm^{3+} > Nd^{3+} > Sm^{3+} > Eu^{3+} > Gd^{3+} > Ho^{3+} > Yb^{3+} > (Y^{3+}) > Tb^{3+} > Dy^{3+} > Tm^{3+} > Er^{3+}$ (excluding Eu^{2+} and Ce^{4+}).

According to Alexey A. Marakushev (1979), the activity ($\log\alpha_{M+}$) of potassium is always higher than the activity of sodium at any temperatures and pH. The values of $\Delta Z^{H_2O}_{1200^\circ K}$, $\Delta Z^{H_2O}_{600^\circ K}$ and $\Delta Z^{H_2O}_{298^\circ K}$ K_2O and Na_2O — are 86.200, 66.332 and 56.388 kcal and 70.000, 53.025 and 44.910 kcal, respectively. In other words, during interaction of the fluids with materially sodium urtite substrate of a higher basicity, activity of potassium has to increase compared to that of sodium; although it will decrease later by cooling. In the process of ristschorritisation of urtites, the nepheline-aegirine-diopside paragenesis is replaced by the kalsilite—aegirine-diopside paragenesis (kalsilite has higher basicity than nepheline) and then — by the orthoclase — aegirine paragenesis (minerals of the lower basicity). Excess sodium is leached from the forming metasomatic rocks, but later "settles" as a "soda" mineralisation and albite veins.

To compare the basicity of the different eudialyte formed we need to compare the ratio of total basic and acidic components, as the more basic components in the structure (alkali, calcium) co-exist with acidic components (silicon, zirconium, titanium, niobium, chlorine). Such a comparison indicates that there is a general trend of enrichment of eudialyte in basic components during increasing alkalinity-basicity of the mineral-forming medium. However, essential deviations in certain structural positions can be observed in the case of pair substitutions. Apparently, the acidic-basic interaction can be shown in one and the same site within the structure.

In the Table 3 we give information on the structural positions in eudialyte with different symmetry and typical for them, isomorphous substitutions. Analysis of these data shows that even during *eucolitisation* of eudialyte the local substitution of the acidic components by the basic ones (for example, iron — by manganese or chlorine — by fluorine) occurs as well as the substitution of the basic components by the acidic components (silicon — by niobium, zirconium, titanium or tin, and sodium — by calcium, strontium, *REE* and manganese) according to the general trend of decreasing alkalinity. As a result of such an inter-compensation of the components the equal site positions related through the centre of symmetry transform into the non-equal positions which leads to symmetry lowering and the "modular" structures appearance. Thus, N_1 is split into $N(1)$ = Na, Ca, *REE* and $N(2)$ = Na, $N4$ — for $N(4)$ = Na, Ca, Sr, Mn, *REE*, H_3O^+, and also K, and $N(3)$ = Na, Sr, Ba, *REE* and K, the "additional" *silicon* position — for $M(4)$ = Si(7) and $M(3)$ = Nb, Zr, Ti, W, and also Al, Mn or Na, *calcium* position — for M(1a) and M(1b), that can be occupied also by Ca and Mn, Y, *REE*; and also Na and Sr, and *iron* position — for M(2,4) by Fe^{2+} and M(2,5) by Fe^{3+}, that can be occupied by Zr, Ti, Nb, Ta, and also Mn, *REE* and Y; and sodium subpositions N_5 and N_6.

In *potassium* eudialyte the effect of the interaction is more definite: potassium (the component of the highest basicity) replaces sodium, iron is replaced by manganese, the content of silicon and strontium is increased, but part of the zirconium is replaced by acidic titanium. Potassium-sodium eudialyte is more basic than sodium eudialyte. The hydratation of eudialyte leads to the abrupt decrease in total basicity and leaching of more basic components — sodium, potassium and calcium. In *titanium* eudialyte the basicity of the isomorphous components is decreased: potassium is replaced by sodium; calcium — by manganese and *REE* and zirconium — by titanium. Besides, the content of silicon is decreasing, although chlorine is partially replaced by the less acidic sulfur. The total basicity decreases. It can indicate that the "sodium" mineralisation in ristschorrites occurs as a result of leaching sodium, which has accumulated locally in separate zones within the rock. The same trend also lasts during the forming of alluaivite, however it is more contradictory: potassium is replaced by sodium, but strontium — by barium, calcium — by manganese and *REE*, zirconium — by titanium. Along with these iron is replaced by sodium, titanium — partially by niobium, chlorine — considerably by sulfur. The silicon content is the maximum possible in minerals with eudialyte structure. Therefore the genuine basicity of alluaivite is extremely high, it is determined by the maximum content of sodium. The acidic-basic interaction in

Table 3. **The character of isomorphic substitutions in different structural positions in eudialyte**

	Positions "splitting"			Typical component in the primary eudialyte	Isomorphic substitutions (components with the higher basicity comparing to the substituted position are marked with the **bold type**, more acidic components — with the regular type)
	Eudialyte $R\bar{3}m$	Eucolite $R3m$	Eucolite $R3$		
N_1	*Na*(1a), *Na*(1b)	*Na*(1a), *Na*(1b)	*Na*(1a), *Na*(1b)	Na	Ca, *REE*
N_2		*Na*(2)	*Na*(2)	Na	—
N_3		*Na*(3a), *Na*(3b)	*Na*(3)	Na	**K**, *REE*, Sr, Ba
N_4	*Na*(4)	*Na*(4)	*Na*(4)	Na	**K**, H_3O^+, Ca, Sr, Mn, *REE*
N_5	*Na*(5)	*Na*(5)	*Na*(5)	Na	—
N_6^*				Na	**K**, Sr
N_7^*				Na	**K**, Sr
M_1	M_1	M_1	*M*(1a), *M*(1b),	Ca	**Na**, Mn, **Sr**, Y, *REE*,
M_2	$M(2,4) = {}^4Fe^{2+}$	$M(2,4) = {}^4Fe^{2+}$	$M(2,4) = {}^4Fe^{2+}$	Fe^{2+}, Fe^{3+}	Fe^{3+}, **Mn, *REE*, Y, Na**,
	$M(2,5) = {}^5Fe^{3+}$	$M(2,5) = {}^5Fe^{3+}$	$M(2,5) = {}^5Fe^{3+}$		Ti, Nb, Ta, Zr
Z	*Z*	*Z*	*Z*	Zr	**Nb**, Ti
$[Si_3O_9]$	*Si*(1)	*Si*(1), *Si*(2)	*Si*(1), *Si*(2)	Si	—
$[Si_9O_{27}]$	*Si*(3), *Si*(3s), *Si*(5)	*Si*(3), *Si*(4), *Si*(5), *Si*(6)	*Si*(3), *Si*(4) *Si*(5a), *Si*(5b), *Si*(6a), *Si*(6b)	Si	—
M_3	*M*(3a), *M*(3b)	*M*(3a), *M*(3b)	*M*3	Si	**Al**, Nb, Zr, Ti, **Mn**, W, **Na**
M_4	*Si*(7), *Si*(7a)	*Si*(7), *Si*(7a)	*Si*(7), *Si*(7a)	Si	—
Oxygen positions	*O*(1-3), *O*(7-9), *O*(13-15), *O*(19-20)	*O*(1-18)	*O*(1-6), *O*(7a), *O*(7b), *O*(8-9), *O*(10a), *O*(10b), *O*(11-12), *O*(13a), *O*(13b), *O*(14a), *O*(14b), *O*(15), *O*(16a), *O*(16b), *O*(17a), *O*(17b), *O*(18-20)		
Anion positions *X*	*X*(1a), *X*(1b), *X*(1c), *X*(1d), *X*(1e), *X*(1f)	*X*(1a), *X*(1b), *X*(1c), *X*(1d), *X*(2a), *X*(2b) *X*(2c), *X*(2d)	*X*(1a), *X*(1b), *X*(1c), *X*(2a), *X*(2b), *X*(2c), *X*(2d)	Cl, **OH**	**F, C, S**

Notes: * *— in the "modular" structures by increasing cell parameter along c-axis up to 60 Å; besides, all the positions in the "modular" structures are getting redoubled:* N_1 *and* N_1^*, N_6 *and* N_6^*, N_7 *and* N_7^*, M_1 *and* M_1^*, *Z and* Z^*, $[Si_9O_{27}]$ *and* $[Si_9O_{27}]^*$ *etc.*

eudialyte of different composition stabilize them within the limits of the stability field of the mineral, and allows us to consider them as varieties of the single mineral species.

Conclusions

In the present paper the author tried to enlighten the current state of the mineral typomorphism problem using eudialyte-eucolite as an example , and to illustrate the possibility of applying typomorphism features data of this mineral as indicators of the mineral-forming processes in the Khibiny alkaline massif, Kola Peninsula. The *structural* typomorphism problem is not as simple as our opponents consider (Rastsvetaeva, Chukanov, 2006; Rastsvetaeva, 2007). In the previous

essay (Borutzky, 2008) we partially examined this problem. The intermediate members of the series eudialyte – alluaivite and potassium eudialyte in the Khibiny massif were formed during metasomatic replacement and later re-crystallization of normal sodium-ferriferrous eudialyte, which is typomorphous of the massive giant-grained urtites, being formed during the early stage of "the central arch" rocks fenitisation, and also their pegmatites and hydrothermal rocks. SEM and EMPA investigations of secondary eudialyte reveal replacement and transformation structures, i.e. relicts of the primary eudialyte. There are reasons to consider that these "relicts" can remain on a structural level. The same was determined by Giovanni Ferraris *et al*. (Ferraris *et al*., 2001) in bornemanite formed during the replacement of lomonosovite; and Peter Nemeth (Nemeth *et al*., 2005) in the structure compiled with epitaxial intergrowths of epistolite, murmanite and shkatulkaite.

Incidentally, in the structure of the zirconium alluaivite from the Khibiny massif (Ageeva *et al*., 2002_2), studied by Sergey V. Krivovichev (personal communication) no regular alternation of zirconium and titanium modules was detected, unlike *dualite* from the Lovozero massif (Rastsvetaeva *et al*., 1999; Khomyakov *et al*., 2007). The duplication of a c-parameter is determined by other reasons. Concerning potassium eudialyte, later named as *rastsvetaevite* (Rastsvetaeva, Khomyakov, 2001; Khomyakov *et al*., 2006) and containing three modules: "eudialyte", "alluaivite" (without titanium) and "barsanovite-kentbrooksite" is direct indication of the "eucolitisation" process beginning with conservation of primary eudialyte relicts in the newly-formed phase. That is why we consider that all diversity of potassium eudialyte in the Khibiny ristschorrites cannot be reduced to the formation of rastsvetaevite only. Moreover, our opponents know very well that after *potassium* eudialyte the *potassium-oxonium* variety is formed (Sokolova *et al*., 1991; Rastsvetaeva *et al*., 19901).

Typomorphism is a scientific issue, and it is not correct to reduce all the diversity of the relationships between the structure of eudialyte and geological conditions of their occurrence, i.e. *structural-chemical* isomorphism, only to the listing of the "new" mineral species. We believe that the structural analysis does not exhaust its potentialities, and we shall learn about the true reasons of the multiple structural-chemical typomorphous features of such a complex structures as the *minerals of variable composition with variable structure.*

References

Ageeva O.A. Transformation of eudialyte during potassium metasomatosis (the Khibiny massif) // Mineralogical society and mineralogical science on the verge of the XXI century. Abstracts. St.-Petersburg: **1999**. P. 201–202.

Ageeva O.A. Typomorphism of accessory minerals and evolution of mineral-forming process within ristschorrite complex rocks (the Khibiny massif). PhD thesis in geology and mineralogy. Moscow: IGEM RAS. **2002**. 180 p.

Ageeva O.A., Borutzky B.Ye., Hangulov V.V. Eudialyte as mineralogical-geochemical indicator of metasomatism during poikilitic nepheline syenite rock forming process (Khibiny massif) // Geochemistry. $\mathbf{2002_1}$. № 10. P. 1098–1105.

Ageeva O.A., Borutzky B.Ye., Chukanov N.V., Sokolova M.N. Alluaivite and genetic aspect of titanium-enriched eudialyte formation in the Khibiny massif // ZVMO. $\mathbf{2002_2}$. № 1. P. 99–106.

Ageeva O.A., Borutzky B.Ye. Kalsilite in the Khibiny massif rocks: morphology, paragenesis, conditions of formation // New data on minerals. **2004**. Vol. 39. P. 40–50.

Azarova Yu.V. Minerals of eudialyte group and products of their alteration as a mineralogical-geochemical indicator of post-magmatic processes during lujavrite-malignite complex formation within the Khibiny massif // Geochemistry. **2005**. № 7. P. 786–792.

Arzamastsev A.A., Ivanova T.N., Korobeynikov A.N. Petrology of ijolite-urtites in Kibiny massif and rules of distribution of apatite deposits within them. Leningrad: Nauka, **1987**. 110 pp.

Borutzky B.Ye. Some aspects of a problem of typomorphism in minerals (by experience of minerals from agpaitic nepheline syenites study) // Typomorphism of minerals and mineral associations. (Abstracts of the III meeting on typomorphism in minerals. Opalikha, 1–3 November 1983). Moscow: Nauka, **1986**. P. 116–124.

Borutzky B.Ye. Rock-forming minerals of the high-alkaline complexes. Moscow: Nauka, **1988**. 215 pp.

Borutzky B.Ye. Typomorphism of minerals from high-alkaline magmatic complexes. Doctor of Science (geology and mineralogy) thesis, scientific lecture. Moscow: IGEM RAS. **1997**. 119 p.

Borutzky B.Ye. Essays on fundamental and genetic mineralogy: 3. Minerals of variable composition with variable structure and problems of species formation in mineralogy. Eudialyte-eucolites. // New Data on Minerals. Moscow: **2008**. Vol. 43. P. 148–173.

Borutzky B.Ye., Varshal G.M., Pavlutskaya V.I., Sokolova M.N., Shlyukova Z.V. Rare earth elements in minerals from the Khibiny massif // Isomorphism in minerals. Moscow: Nauka, **1975**. P. 221–246.

Borutzky B.Ye., Sokolova M.N., Shlyukova Z.V. Typomorphism and conditions of formation of minerals and mineral associations in alkaline rocks of the Khibiny massif // Composition and structure of minerals as indicators of their genesis. Moscow: Nauka, **1978**. P. 76–108.

Borutzky B.Ye., Sokolova M.N., Shlyukova Z.V. Typomorphism of the Khibiny massif minerals; the role of post-magmatic processes in formation of agpaitic mineralisation // Scientific fundamentals and practical application of typomorphism of minerals. Materials of the XI IMA meeting, Novosibirsk, 4–10 September 1978, Moscow: Nauka, **1980**. P. 137–144.

Feklichev V.G. Data on the chemical typomorphism of eudialyte from Khibiny // Ore minerals research. Moscow: Nauka, **1973**. P. 119–132.

Feklichev V.G. Optical-mineralogical mapping in the Khibiny massif with the trend application // Automation in analysis and geological mapping fields. Moscow: IMGRE, **1975**. P. 71–84.

Ferraris G., Belluso E., Gula A., Soboleva S.V., Ageeva O.A., Borutskii B.E. A structural model of the layer tinanosilicate bornemanite based on seidozerite and lomonosovite modules // Canad. Miner. **2001**. P. 1665–1673.

Galakhov A.V. Petrology of the Khibiny alkaline massif. Leningrad: Nauka, **1975**. 256 pp.

Khomyakov A.P. Mineralogy of ultraagpaitic rocks. Moscow: Nauka, **1990**. 196 pp.

Khomyakov A.P., Nechelustov G.N., Arakcheeva A.V. Rastsvetaevite, $Na_{27}K_8Ca_{12}Fe_3Zr_6Si_4[Si_3O_9]_4[Si_9O_{27}]_4(O,OH,H_2O)_6Cl_2$ – new mineral with modular eudialyte-like structure and crystallochemical systematics of eudialyte group // ZRMO. **2006**. № 1. P. 49–65.

Khomyakov A.P., Nechelustov G.N., Rastsvetaeva R.K. Alluaivite, $Na_{19}(Ca,Mn)_6(Ti,Nb)_3Si_{26}O_{74}Cl\ 2H_2O$ – new titanium silicate with eudialyte-like structure // ZVMO. **1990**. Vol. 1. P. 117–120.

Khomyakov A.P., Nechelustov G.N., Rastsvetaeva R.K. Dualite, $Na_{30}(Ca,Na,Ce,Sr)_{12}(Na,Mn,Fe,Ti)_6Zr_3Ti_3MnSi_{51}O_{144}(OH,H_2O,Cl)_9$ – new zirconium-titanium silicate with modular eudialyte-like structure from Lovozero alkaline massif, Kola Peninsula, Russia // ZRMO, **2007**. Vol. 136. № 4. P. 31–42.

Kogarko L.N. Issues of agpaitic magmas formation. Moscow: Nauka, **1977**. 294 pp.

Kogarko L.N., Kramm U., Bleckslandt A. et al. Age and origin of alkaline rocks of the Khibiny massif (Rb and Sr isotopes) // Doklady AN SSSR. **1981**$_1$. Vol. 260. № 4. P. 1001–1004.

Kogarko L.N., Krigman L.D., Lazutkina L.N. Magmatic crystallisation if eudialyte in the nepheline-eudialyte system // Doklady AN SSSR. **1980**. Vol. 255. № 1. P. 170–173.

Kogarko L.N., Krigman L.D., Lazutkina L.N. Phase equilibria in eudialyte-nepheline system // Geochemistry. **1981**$_2$. № 2. P. 233–241.

Korzhinsky D.S. The principle of the alkali mobility during magmatic events // To academician Dmitry S. Belyankin 70th birthday. Moscow: AN SSSR. **1946**. P. 242–261.

Korzhinsky D.S. Essay on magmatic processes // The main issues in the study of magmatic ore deposits. Moscow: AN SSSR. **1955**. P. 335–456.

Korzhinsky D.S. Acidic-basic interaction of fluids with rocks and magma // The fundamentals of metasomatism and metamagmatism. Moscow: Nauka, **1993**. P. 217–221.

Kostyleva E.E. Eudialyte-eucolite isomorphous series from the Khibiny and Lovozero tundras // Proceedings of Mineralogical Museum of Academy of Science of the USSR, **1929**. Vol. 3. P. 169–222.

Kostyleva E.E. Zirconium silicates. // Mineralogy of the Union. Series A. Vol. 6. Moscow: AN SSSR. **1936**. P. 6–35.

Kukharenko A.A., Il'insky G.A., Ivanova T.N. et al. Clarkes of the Khibiny alkaline massif // ZVMO. **1968**. Part 97. Vol. 2. P. 133–149.

Marakushev A.A. Petrogenesis and ore-forming (geochemical aspects). Moscow: Nauka, **1979**. 264 pp.

Mineralogy of Khibiny massif. Under revision of academician Fedor V. Chukhrov. Moscow: Nauka, **1978**. Vol. 1 – Magmatism and post-magmatic alterations. 228 pp. Vol. 2 – Minerals. 586 pp.

Minerals of Khibiny and Lovozero tundras. Under revision of academician Alexander E. Fersman, N.A. Smolyaninov and E.M. Bonstedt. Moscow-Leningrad: AN SSSR, **1937**. 563 pp.

Nemeth P., Ferraris G., Radnoczi G., Ageeva O.A. TEM and X-ray study of syntactic intergrowths of epistolite, murmanite and shkatulkalite // Canad. Miner. **2005**. V. 43. P. 973–987.

Pekov I.V. On the change of conditions of alkalinity from sodium to potassium at the late stages of agpaitic complexes evolution // Alkaline magmatism of Earth. Moscow: GEOKHI RAS, **2001**. P. 55–56.

Rastsvetaeva R.K. Structural mineralogy of the eudialyte group. Overview // Crystallography. **2007**. Vol. 52. № 1. P. 50–67.

Rastsvetaeva R.K., Khomyakov A.P., Chapuis G. Crystal structure and crystal-chemical features of new Ti-rich member of the eudialyte family // Zeitschrift fur Kristallogr. **1999**. Vol. 214. P. 271–278.

Rastsvetaeva R.K., Sokolova M.N., Borutzky B.Ye. Crystal structure of potassium-oxonium eudialyte // Crystallography. **1990**$_1$. Vol. 35. №6. P. 1381–1387.

Rastsvetaeva R.K., Khomyakov A.P. Modular structure of high-potassium eudialyte analogue, with doubled c-period // Crystallography. **2001**. Vol. 40. № 4. P. 715–721.

Rastsvetaeva R.K., Khomyakov A.P., Andrianov V.I., Gusev A.I. Crystal structure of alluaivite // Doklady AN SSSR. **1990**$_2$. Vol. 321. № 6. P. 1379–1383.

Rastsvetaeva R.K., Chukanov N.V. Mineral species or mineral variety? // New data on minerals. Moscow: EKOST, **2006**. Vol. 41. P. 172–183.

Scientific fundamentals and practical application of typomorphism of minerals (Materials of the XI IMA meeting, Novosibirsk, 4–10 September 1978). Under revision of academician A.V. Sidorenko, academician V.S. Sobolev, D.V. Rundkvist, academician F.V. Chukhrov, B.Ye. Borutzky, A.I. Ginzburg, N.Z. Evzikova and L.N. Kogarko. Moscow: Nauka, **1980**. 302 pp.

Sokolova M.N., Borutzky B.E., Arkhipenko D.K., Rastsvetaeva R.K., Vlasova E.V. On potassium-oxonium eudialyte from Khibiny, Kola Peninsula // Doklady AN SSSR. **1991**. Vol. 318. № 3. P. 712–716.

Tikhonenkov I.P. Nepheline syenites and pegmatites in the North-Eastern part of the Khibiny massif; the role of post-magmatic events of their formation. Moscow: AN SSSR. **1963**. 247 pp.

Varshal G.M., Borutzky B.Ye., Sokolova M.N., Shlyukova Z.V. On rare earth elements in minerals of eudialyte-eucolite group from the Khibiny massif // Methods of chemical analysis and chamical composition of minerals. Moscow: Nauka, **1967**. P. 87–101.

Yakovenchuk V., Ivanyuk G., Pakhomovsky Y., Men'shikov Y. The Khibiny. Ed. F. Wall. Apatity: Laplandia Minerals Ltd. **2005**. 468 p.

THE HIGHLIGHTS OF 2009 AT THE FERSMAN MINERALOGICAL MUSEUM RAS

Elena A. Borisova
Fersman Mineralogical Museum RAS, Moscow, mineral@fmm.ru

On the 25 September 2009 the meeting devoted to the 125th anniversary of Alexander N. Labuntsov birth (1884–1963), the discoverer of the Khibiny apatite deposits (Kola Peninsula, Russia), took place at the Fersman Mineralogical Museum. His daughter, Marina A. Labuntsova, PhD in biology, spoke about his hard course of life and his scientific expeditions. On the same day the exhibition on Alexander N. Labuntsov's scientific contribution was launched at the museum. Self-collected mineral specimens, including fersmanite – the new-discovered and named after academician Alexander E. Fersman mineral from Khibiny massif, and also mineral described by Labuntsov and later named as labuntsovite after him by Evgeny I. Semenov & Tatiana A. Burova, were on the display. Among the other exhibits there are published papers, field-notes, personal tools and recently found in the RAS archives Alexander N. Labuntsov's letters to academician Vladimir I. Vernadsky. The exhibition is on until the end of 2010. The detailed description of the display and newly found documents are expected in the next issue of the magazine "New data on Minerals".

During the 4th Moscow Science Festival held on the 9–11 October 2009 Fersman Mineralogical Museum welcomed over 500 visitors. The museum staff gave a number of free guided tours: "Visiting Hostess of a Copper Mountain" – for the kids, and "Treasures of the Planet Earth" – for everyone.

On the 18 November the museum held the competition "Jewellers – for the XXI century" (nomination "Lapidary Art") organised by Gokhran of the Russian Federation and National Collection Centre supported by Ministry of Culture of the Russian Federation and Presidential Culture Council, in commemoration of 290th anniversary of the State Precious Metals and Gemstones Repository of the Russian Federation. Lapidary and carvers from Moscow (Jewellery house "Aristocrat"), St.-Petersburg (Regional association "Art Lapidary Union", "GRINGOR" Ltd., "Petrozoloto", "Russian gems") and Yekaterinburg (Jewellery house "Moiseykin" and Ilya Borovikov Urals lapidary) took part in the competition. The jury noted an art values and fine performance technique of the pieces by masters from St.-Petersburg – Alexander Levental (art-piece "Angel"), Sergey Shimansky ("Time"), Sergey Falkin ("Jazz"), Anton Ananyev ("Desire"), and also interior clocks by "Moiseykin" jewellery house – "Warrior" (lapis and other decorative stones, cut diamonds, rubies set in gold, silver, brass), "Wood-grouse" (different types of jasper, cut diamonds set in gold, silver etc.), and also carved art-pieces by Ilya Borovikov Urals lapidary – soldier of Napoleon army (chess-)figures and Alexander V. Suvorov small sculpture (jasper, chalcedony, cacholong, agate, black nephrite, chrysoprase, precious metals and gemstones; height – 31 cm). The final information on the awards granted will be published on www.investinart.ru.

The new museum book "Art in stone" is to be published in the near future (Moscow: Altum, 2009. 72 pages, 131 colour photographs). The author of a project – Elena L. Sokolova, scientific editor – professor Margarita I. Novgorodova. The colourful album contains articles on the decorative and ornamental stones from the Fersman Mineralogical Museum collection and private collection of Anatoly N. Korobkov, well-known lapidary and carver, the chairman of the stone society. The album is intended for a general public.

FERSMAN MINERALOGICAL MUSEUM OF RUSSIAN ACADEMY OF SCIENCES PUBLICATIONS

EPIGENETIC LOW GRADE METAMORPHISM AND Co–Ni–Sb–As MINERALISATION IN NORILSK ORE–FIELD

By Ernst M. Spiridonov & Yulia D. Gritsenko. 2009. 218 pp. Published by "Nauchny Mir", (in Russian)
The book is dedicated to the problem of regenerated ore concentrations at ore deposits - the problem of interrelations between metamorphism and ore-forming process. The work highlights the origin of the Co-Ni antimony and arsenic mineralisation at Norilsk ore-field that comprehends various types of endogenic mineralisation. It was determined that the parameters of the metamorphic-hydrothermal Co-Ni-Sb-As mineralisation, formed 80-100 Ma later than the trapp formation, corresponds to zeolite facies of metamorphism. This mineralisation together with carbonates, hematite, sulfides of Zn, Pb, Cu, Ni, Mn, Ag, Bi, Cd, Sb, selenides of Pb, Ag, native arsenic, silver, bismuth, uraninite is a miniature five-element formation, first discovered at Norilsk ore-field.

STRUCTURAL–CHEMICAL SYSTEMATIC OF MINERALS

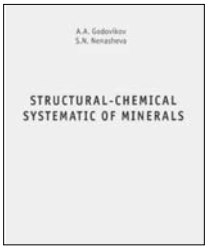

By Alexander A. Godovikov & Svetlana N. Nenasheva. 2007. 196 pp. Published by Fersman Mineralogical Museum.
The classification tables are complemented by the new mineral species that were discovered during 1994—2006. The formulae of some mineral species were corrected and some mineral species were transferred to some taxons according to new data on their chemical composition or crystal structure. The classification tables include nearly 4500 mineral species.

STRUVE COLLECTION: MINERAL DRAWINGS ALBUM

A Treasure of the Fersman Mineralogical Museum RAS
By Nina A. Mokhova, edited by Margarita I. Novgorodova. 2005. 100 pp. Published by Fersman Mineralogical Museum.
The book is the first published of the Album of Drawings of the famous mineral collection which was made by outstanding Russian diplomat Heinrich Christopher Gottfried von Struve (1772—1852).

NEW DATA ON MINERALS. Volumes 41, 42, 43

Three new volumes (vol. 41—43) of the oldest Russian scientific magazine published by Fersman Mineralogical Museum RAS are recommended to everyone interested in mineralogy. They contain articles concerning new minerals discoveries and new finds, new information on the mineral collections and museum exhibitions.

NATURAL MINERAL FORMS

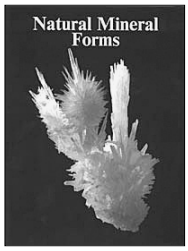

Edited by Margarita I. Novgorodova. 2003. 64 pp. Published by Fersman Mineralogical Museum.
The book includes systematization and description of the various mineral forms known in nature. This is the first published well-illustrated book which tracks evolution of the crystal perfection over different mineral-forming conditions. The crystals range from almost ideal to highly imperfect ones which could be attributed to mineral aggregates as well as single crystals. The shapes of minerals formed in different media (gas, liquid, vicious, solid) are also considered.

To order these publications visit web-site: www.minbook.com or e-mail: minbooks@online.ru